The Dissertation Committee for Christopher Campbell Hadlock Certifies that this is the approved version of the following dissertation:

Quantile-Parameterized Methods for Quantifying Uncertainty in Decision Analysis

Committee:

J. Eric Bickel, Supervisor

Ofodike Ezekoye

Robert Hammond

John Hasenbein

Benjamin Leibowicz

Quantile-Parameterized Methods for Quantifying Uncertainty in Decision Analysis

by

Christopher Campbell Hadlock, B.S.M.E., M.S.E.

Dissertation

Presented to the Faculty of the Graduate School of

The University of Texas at Austin

in Partial Fulfillment

of the Requirements

for the Degree of

Doctor of Philosophy

The University of Texas at Austin

May, 2017

Dedication

To my parents.

Acknowledgements

First, I would like to acknowledge my advisor, J. Eric Bickel, for both his support of this research, and his invaluable mentorship. He sparked my interest in decision analysis with his practical and engaging "in layman's terms" teaching style. Second, he taught me how to do research effectively, by always writing down relevant ideas as if writing a paper, forcing me to formally document my ideas and thematically tie them together in a seamless manner. Third, he improved my writing by advising me to address three questions when developing a formal publication: "What is so? What is new? So, what?". Finally, his example taught me to be respectfully frank and direct, and not fear asking questions or pointing out the limitations of ideas.

I would like to thank Robert Hammond, John Hasenbein, Ofodike "DK" Ezekoye, and Benjamin Leibowicz for serving on my doctoral committee, and for their helpful suggestions. I thank Robert Hammond for his swift and sincere feedback and responses to all my loaded questions, and for his enthusiasm in serving on my committee, despite his continuously-busy schedule at Chevron. I thank John Hasenbein for his patience and availability, and for teaching me to be more precise with technical language. I also thank Benjamin Leibowicz for enthusiastically agreeing to join my committee somewhat last-minute, and despite doing so, for his availability and energetic curiosity in my work. Finally, I thank DK Ezekoye for his patience and interest in my work.

I want to extend a special thank you to Tom Keelin and Brad Powley, whose joint work on quantile-parameterized distributions inspired much of my work herein. Tom Keelin helped greatly improve the quality of the work herein, and the quality of the related publication, "Johnson Quantile-Parameterized Distributions", through his

extensive correspondence and thoughtful feedback. I also thank Tom for the privilege of him joining our panel and jointly presenting our work at the 2016 INFORMS Annual Meeting in Nashville, Tennessee.

I am incredibly grateful for the support of my friends and family, which has been integral in the pursuit of my doctoral degree. I thank my wife, Caroline, for her continual love and support, both of which were essential in carrying me through moments of demoralization. I thank Tom Giles for his characteristic selflessness, and contagious sense of positivity and common sense, which has been a continual source of encouragement throughout my graduate journey.

Quantile-Parameterized Methods for Quantifying Uncertainty in Decision Analysis

Christopher Campbell Hadlock, Ph.D.

The University of Texas at Austin, 2017

Supervisor: J. Eric Bickel

In decision analysis, analysts must often encode an expert's uncertainty of a quantity (e.g., the volume of oil reserves in a proven, but undeveloped oil field) using a probability distribution. This is commonly done by eliciting a triplet of low-base-high percentile assessments, such as the $\{10^{th}, 50^{th}, 90^{th}\}$ percentiles, from the expert, and then fitting a probability distribution from a well-known family (e.g., lognormal) to the assessed quantile-probability (or QP) pairs. However, curve fitting often requires non-linear, non-convex optimization over a distribution parameter space, and the fitted distribution often never honors the assessed QP pairs – reducing both the fidelity of the model, and trust in the analysis. The development of quantile-parameterized distributions (or QPDs), distributions that are parameterized by, and thus precisely honor the assessed QP pairs, is a very important yet nascent topic in decision analysis, and contributions in the literature are sparse. This dissertation extends existing work on QPDs by strategically developing a new smooth probability distribution system (known as J-QPD) that is parameterized by (and honors) assessed QP pairs. J-QPD also honors various natural support regimes – for example: bounded (e.g., fractional uncertainties, such as market shares, are necessarily bounded between zero and one); semi-bounded (e.g., volume of oil reserves is necessarily non-negative, but may have no well-defined upper bound); etc. We

then show that J-QPD is maximally-feasible, highly flexible, and approximates the shapes of a vast array of commonly-named distributions (e.g., normal, lognormal, beta, etc.) with potent accuracy, using a single system. This work also presents efficient, high-fidelity methods for capturing dependence between two or more uncertainties by combining J-QPD with modern correlation assessment and modeling techniques. We then provide an application of J-QPD to a famous decision analysis example, demonstrating how J-QPD facilitates rapid Monte Carlo simulation, and how its implementation can aid actual decisions that might otherwise be made wrongly if commonly-used discrete methods are used. We conclude by noting important tradeoffs between J-QPD and existing QPD systems, and offer several extensions for future research, including a first look at designing new discrete distributions using J-QPD.

Table of Contents

List of Tables

List of Figures

Chapter 1 : Introduction

BACKGROUND

Any decision consists of three components, which Howard (1988a) jointly refers to as the decision basis: alternatives; information; preferences. Alternatives are what a decision maker can do. Information refers to what the decision maker knows (or does not know). Preferences specify what the decision maker wants (or does not want). This dissertation is about the information component of the decision basis, and more specifically, about introducing tools for quantifying uncertainty in decision problems.

Many complex decisions involve the assessment of some uncertain quantity, or *uncertainty*. Uncertainties can be continuous, such as the volume of oil reserves in a proven, but undeveloped oil field, or discrete, such as the presence or absence (yes/no) of hydrocarbons in a newly-explored subsea region. This dissertation focuses on continuous uncertainties. In the absence of historical data (e.g., the monthly returns of the S&P500 over the past twenty years), partial information of an uncertainty is often elicited from an expert in the form of quantile-probability (or QP) pairs, as illustrated in Figure 1.1. In this case, a decision analyst (or analyst) has assessed an expert's {0.1, 0.5, 0.9} quantiles, or {10^{th}, 50^{th}, 90^{th}} percentiles, for the volume of oil reserves in a proven, but undeveloped field to be {2.5, 5, 9} million barrels (MMbbl), respectively.

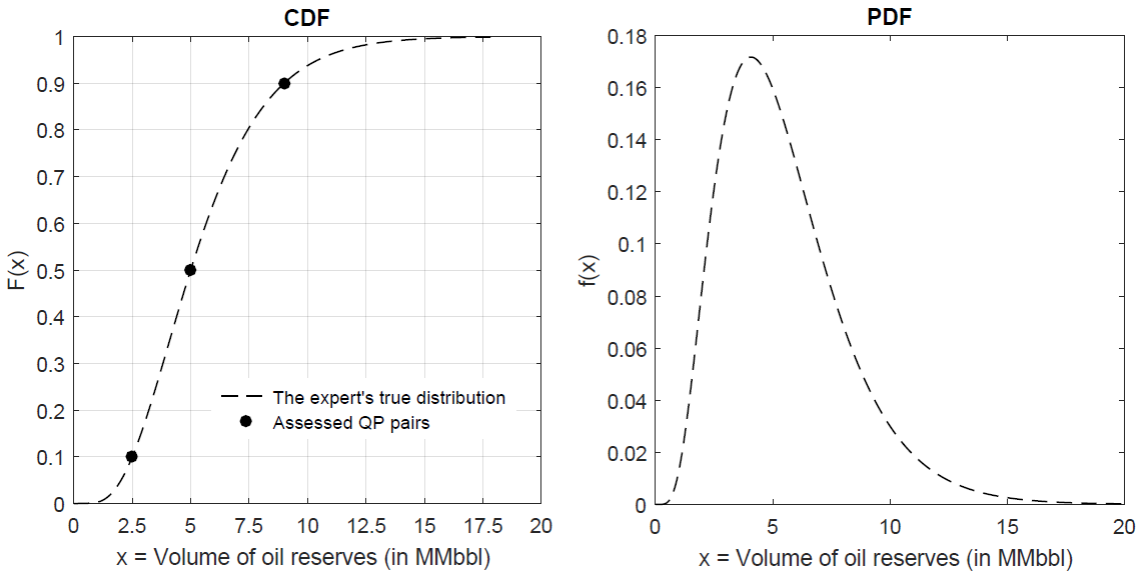

Figure 1.1. An Expert's Distribution for Reserves and Assessed QP Pairs.

As a formal discipline, decision analysis adopts a Bayesian perspective, in which an individual's knowledge, or subjective uncertainty, can be encoded into a probability distribution[1]. In Figure 1.1, the continuous dashed curve is the expert's distribution for the uncertain volume of oil reserves, denoted X. The left (right) curve is the expert's cumulative distribution function (probability density function), or CDF (PDF). Adopting the nomenclature of Howard (1988b), if the expert were a *clairvoyant*, then his probability distribution for X would be a point mass on the actual volume of reserves in the field, having a probability of one, and zero for all other values of X. The fact that Figure 1.1 displays a distribution indicates that the expert is uncertain about the value of X that will be realized upon observation at some future time.

In practice, an analyst obtains information about the expert's distribution for X by assessing several QP pairs, as shown by the points in Figure 1.1. QP pairs are obtained by

[1] For example, see Matheson and Howard (1968).

asking the expert questions like: "What is your[2] probability that X is less than 20?"; or "What value of X is so small, that you believe there is only a 10% chance that the realized value for X will be less than this number?". The first question is referred to as a "fixed value" type question, while the second is referred to as a "fixed probability" type question[3]. The latter question might be used to elicit the expert's response of 2.5 million barrels in the example of Figure 1.1.

The answer to each such question provides the analyst with a new QP pair; i.e., a new point lying precisely on the expert's CDF for X, presuming that there is no *assessment error*. Assessment error corresponds to elicited QP pairs that do not precisely lie on the expert's true CDF, as depicted in Figure 1.2, where the analyst has elicited perfect responses for the expert's $\{10^{th}, 50^{th}, 90^{th}\}$ percentiles (depicted by solid points), but imperfect responses for the 30^{th} and 70^{th} percentiles (depicted by hollow points). In this case, the expert's true $\{30^{th}, 70^{th}\}$ percentiles are {3.81, 6.44} MMbbl, but the expert instead reported these numbers to be {4, 6} MMbbl.

[2] We say "your" (rather than "the") to emphasize probability as a state of belief, and that distributions are expected to be person-specific; e.g., your distribution is probably different from mine. By contrast, "the distribution" is often used in classical statistics, suggesting that there is only one "true" distribution for a given uncertainty, but that it is unknown.

[3] According to Abbas et al. (2008).

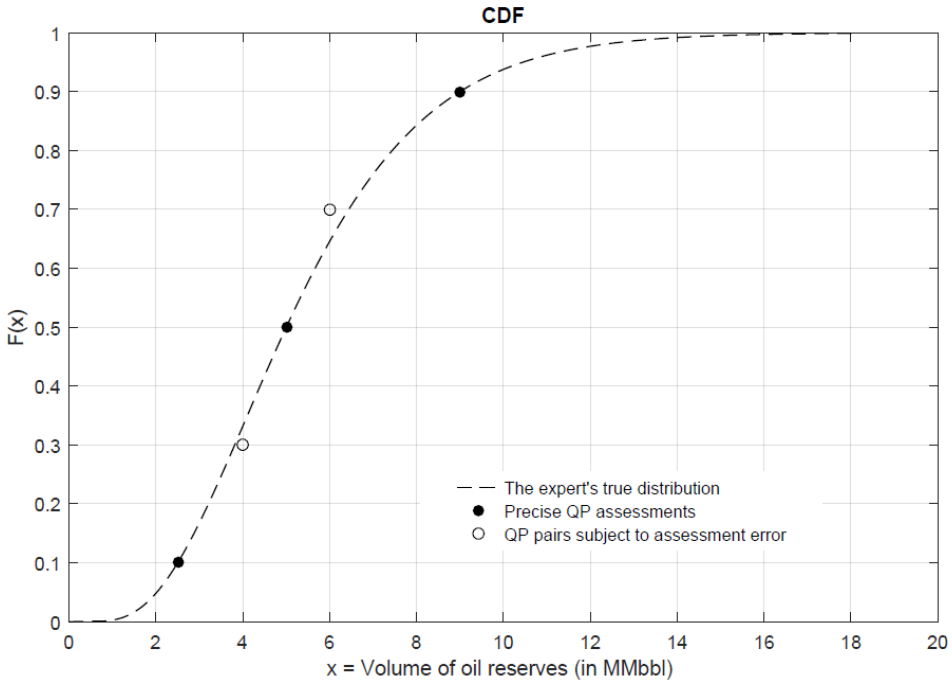

Figure 1.2. Example Involving Assessed QP Pairs Subject to Assessment Error.

Assessment error can arise from *cognitive biases* noted by Tversky and Kahneman (1974), or by *motivational biases* noted by Winkler and Matheson (1976). Such biases can yield sets of QP pairs that Spetzler and Staël von Holstein (1975) refer to as *incoherent* – they do not conform to the axioms of probability. Figure 1.3 provides an example of incoherent QP data. In this case, the assessed QP pairs shown in Figure 1.3 (right) are incoherent since the 30th percentile exceeds the 50th percentile. In the absence of biases, assessment error may still arise simply due to imprecision of the elicited responses with respect to the expert's true values[4]. In this dissertation, unless explicitly noted otherwise, we assume that we have a coherent set of perfectly-assessed QP pairs.

[4] For models quantifying assessment errors due to imprecision, see, for example, Hammond and Bickel (2017) and Wallsten and Budescu (1983).

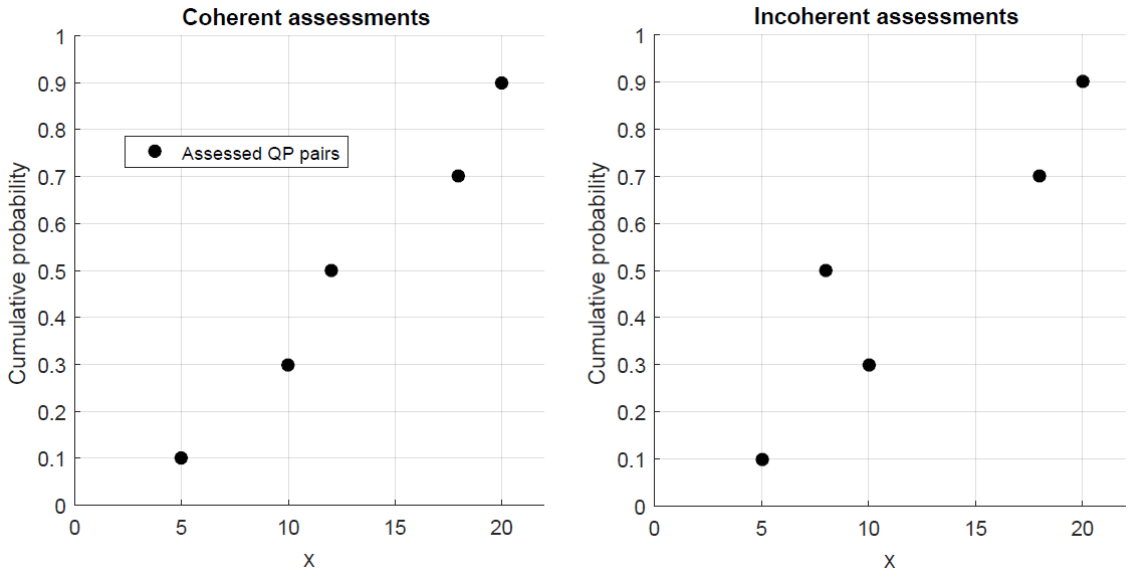

Figure 1.3. Examples of Coherent and Incoherent Assessment Data.

In practice, eliciting authentic QP pairs can be a timely and costly process[5], since special procedures[6] may be needed to eliminate cognitive[7] and motivational biases. Consequently, analysts cannot assess the infinite number of points on an expert's CDF, and are constrained to gathering only a small, finite number of QP pairs for each uncertainty. However, given a set of QP pairs, analysts want a *complete* characterization of the expert's distribution, depicted by the dashed line in Figure 1.2 and Figure 1.4, and must decide how to build some continuous *approximation* (shown by the solid line in Figure 1.4) for the expert's true distribution.

[5] For example, see Merkhofer (1987).
[6] For example, see Selvidge (1980).
[7] For example, see Spetzler and Staël von Holstein (1975).

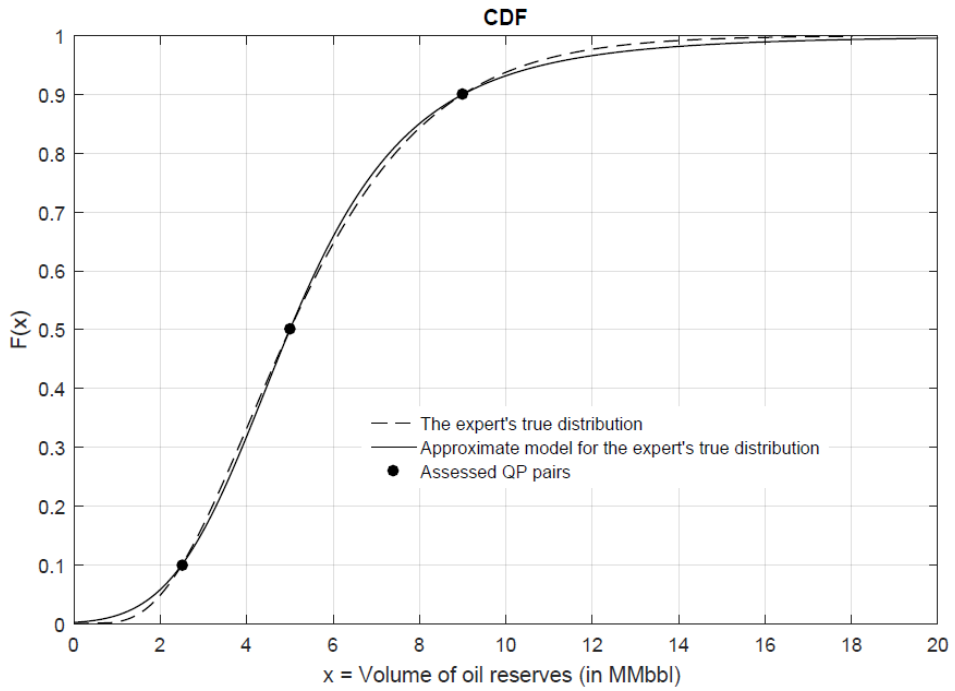

Figure 1.4. Approximating the Expert's True Distribution with a Model.

A simple, but widely-used approach for assigning a distribution to a set of QP pairs is by systematically constraining the uncertainty to a finite number of discrete possible outcomes, and then choosing probabilities to assign to those outcomes – a process known as *discretization*, as illustrated in Figure 1.5. Discretization presents several practical advantages. First, as noted by Bickel et al (2011), and Willigers (2009), discretization can greatly reduce the computational burden faced in problems with increasingly large numbers of uncertainties, by reducing the number of possible outcomes to a few systematically-chosen scenarios. Also, reducing the space of outcomes to several discrete scenarios allows an analyst to easily communicate the problem with decision makers by use of a decision tree, as depicted in Figure 1.6.

In this example, reading the tree from left to right, the decision maker first decides whether to explore. The decision not to explore yields a sure $0 MM in net present value

(NPV), while the decision to explore is subject to a discrete (binary) uncertainty – whether hydrocarbons are present. If hydrocarbons are absent, the decision maker incurs a net loss of $10MM, since money is invested in exploration, but no value is subsequently realized. If hydrocarbons are present, then the decision to explore is subject to a continuous uncertainty upon volume of reserves (represented in Figure 1.1), given the presence of hydrocarbons, which has been discretized into three scenarios: {2.5, 5.0, 9.0} MMbbl, with estimated NPV outcomes of {-$10MM, $20MM, $50MM}, respectively. The discrete scenarios depicted in the tree[8] enable decision makers or laypeople to intuitively visualize risks surrounding a decision.

[8] For more on decision trees, see Clemen (2014), or McNamee and Celona (1990).

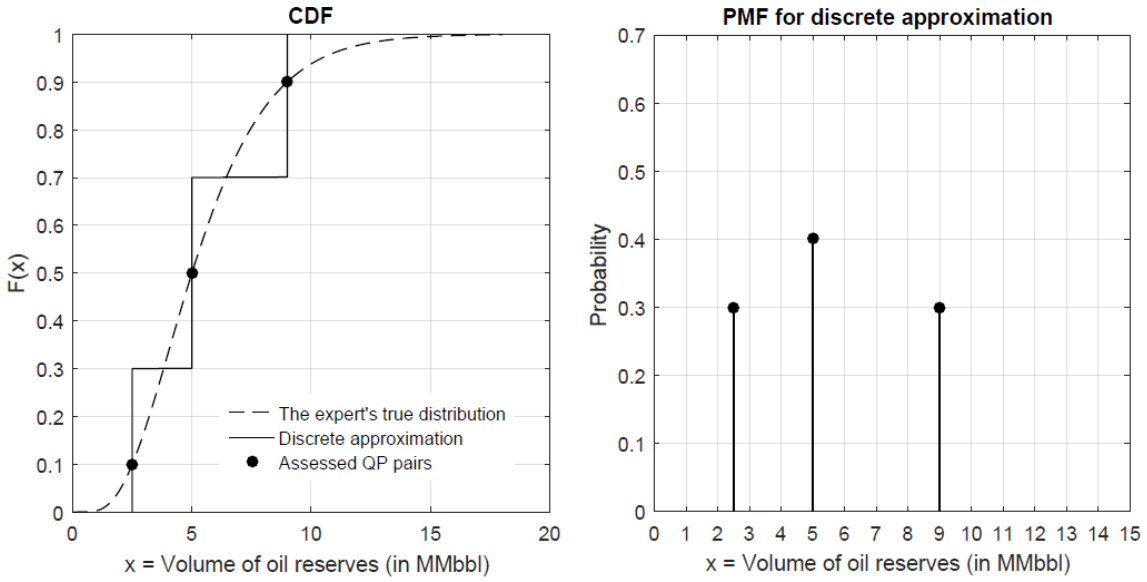

Figure 1.5. A Discrete Approximation for an Expert's Distribution on Reserves.

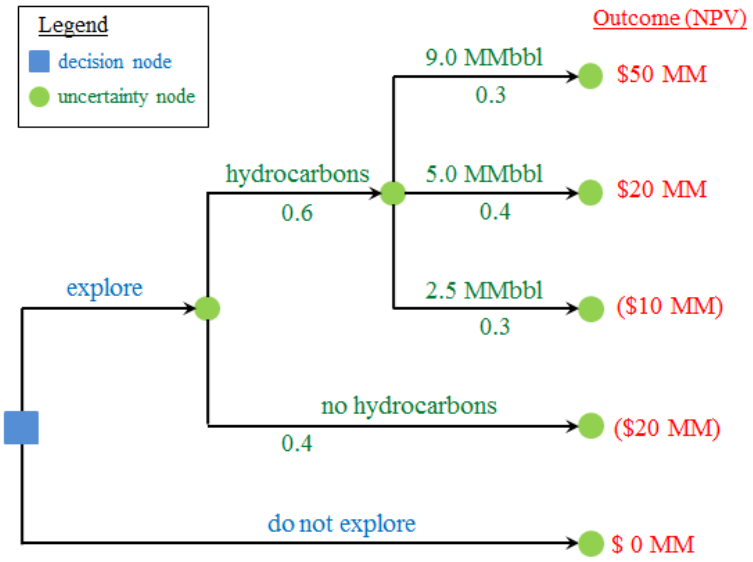

Figure 1.6. A Decision Tree for an Exploration Decision.

The example in Figure 1.5 and Figure 1.6 implements a common discretization method used in the oil and gas industry known as the Extended Swanson-Megill (ESM) shortcut, which assigns probabilities of {0.3, 0.4, 0.3} to the {10^{th}, 50^{th}, 90^{th}} percentiles.

However, the competitive tractability of discretization comes at the cost of potentially large approximation errors, which could misguide decision making. Keelin (2016), for example, illustrates how discretization yields poor decision making in a real-world bidding problem involving a portfolio of real-estate assets. We also demonstrate how discretization can induce poor decision making later in this dissertation using a famous decision analysis example problem. Theoretical treatment of discretization is widely covered in the literature[9], and its applications are pervasive[10]. In this dissertation, however, we focus primarily on methods for assigning continuous distributions to assessed QP pairs, and we briefly cover several extensions to discretization in the concluding chapter.

MOTIVATION

In terms of existing methods for assigning continuous distributions to assessed QP pairs, a common approach is to fit a distribution (e.g., by least-squares) from a well-known family (e.g., beta, gamma, normal, lognormal, etc.), as shown in Figure 1.7, where the solid curve represents a least-squares fit for a normal distribution with respect to the assessed QP pairs. While this gives us a continuous approximation for the expert's true distribution (dashed), two clear limitations of fitting approximations are:

- The fitted distribution usually does not honor (pass through) the assessed percentiles, as illustrated in Figure 1.7, which can reduce model fidelity and trust in the analysis.

[9] For recent contributions, see: Hammond and Bickel (2017); Hammond and Bickel (2013a, b); Bickel et al. (2011); Hammond (2014). Also, see: McNamee and Celona (1990); Miller and Rice (1983); Keefer and Bodily (1983); Smith (1990, 1993); Zaino and D'Errico (1989); Hurst et al. (2000).

[10] For applications, see: Willigers (2009); Hurst et al. (2000); Stonebraker and Keefer (2009); Pflug (2001); Wang and Dyer (2012); Tauchen and Hussey (1991); Stonebraker (2002); Keefer (1995); Keeney (1987), Upadhyay and Ezekoye (2008).

- Least-squares fits require solving an optimization problem for the distribution parameters, which some analysts may find inconvenient or difficult to implement.

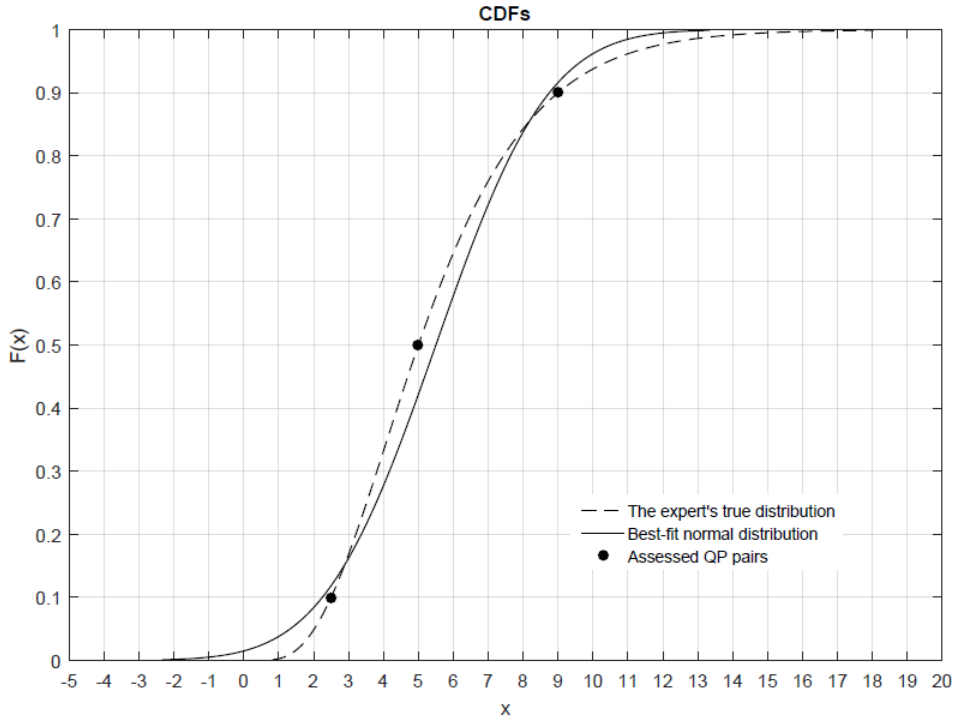

Figure 1.7. A Least-Squares Fit Normal Distribution for the Assessed QP Pairs.

Alternatively, Abbas (2003a and 2003b) assigns distributions by maximizing Jaynes' (1968) entropy, subject to honoring assessed QP pairs, as shown in Figure 1.8, where an expert provides {10^{th}, 50^{th}, 90^{th}} percentile assessments for the peak market share of a new product (if launched) – a quantity which is necessarily bounded between zero and one. For bounded uncertainties, as in Figure 1.8, maximum-entropy assigns a conditional uniform distribution ("straight-line") between adjacent assessments, making it a mathematically-tractable method for approximating an expert's distribution. Also, maximum-entropy distributions honor the assessed QP pairs, unlike least-squares fits. However, if an experts' knowledge changes smoothly (has continuous derivatives) over

its domain, as illustrated by the dashed curves in Figure 1.8, then straight-line poorly-approximates the expert's distribution.

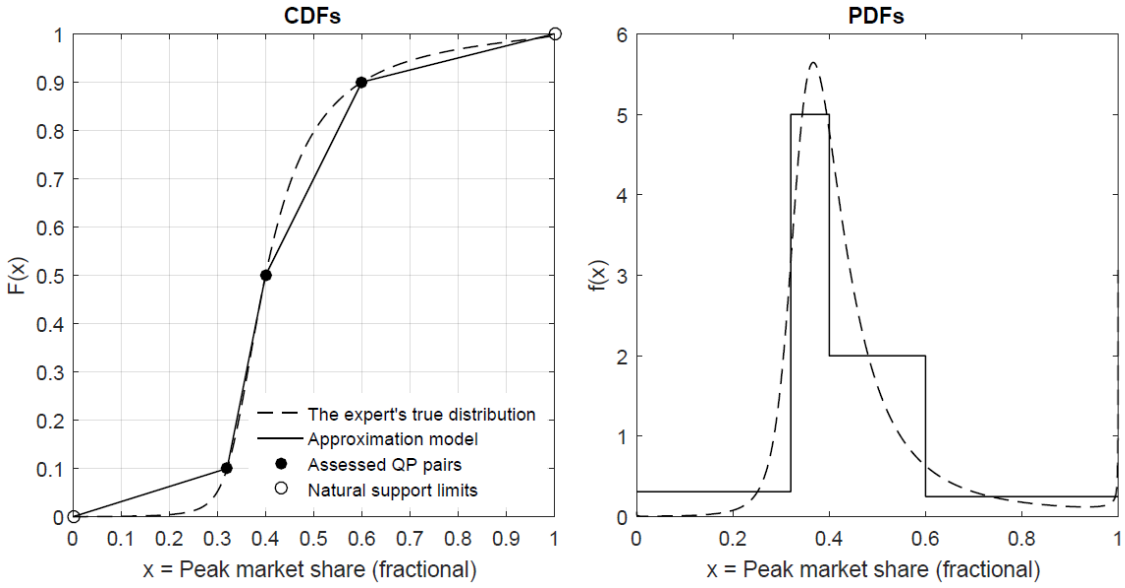

Figure 1.8. A Maximum Entropy Distribution (solid curve) for QP Pairs on [0, 1].

Runde (1997) takes a different approach by using Hermite tension splines to assign distributions to QP pairs. As Powley (2013) notes, however, while this method generates smooth and flexible distributions, it provides little basis for performing subsequent Monte Carlo simulation. In response to these limitations, Keelin and Powley (2011) (KP), Powley (2013), and Keelin (2016) pioneered the notion and development of *quantile-parameterized distributions* (QPDs). QPDs represent a major advance in decision analysis, since they present several key advantages over other existing methods:

- QPDs are parameterized by, and thus precisely honor, a given set of QP pairs, eliminating the need to solve a non-linear optimization problem for distribution parameters, unlike with many curve-fitting procedures. More importantly, however, the QPD passes through the QP pairs, unlike a fitted distribution.

- QPDs can closely approximate many commonly-named distributions, such as normal, lognormal, beta, etc.
- QPDs are characterized by their quantile function, which makes them convenient for subsequent Monte Carlo sampling via inverse-transform-sampling[11].

However, QPDs are subject to several issues, perhaps the most notable of which is *infeasibility*, meaning that there exist many sets of coherent QP pairs for which there exists no valid QPD assignment. We discuss infeasibility in more detail later.

CONTRIBUTIONS

This dissertation makes several contributions to the literature on methods for encoding an expert's knowledge of a given uncertainty, given a set of QP pairs. Like the work of Keelin and Powley (2011), and Keelin (2016), we present a new system, known as "J-QPD", of smooth probability distributions that are directly parameterized by assessed QP pairs. This is incredibly helpful in practice, since it allows an analyst to go directly from a finite set of QP pairs to a complete continuous representation of an expert's knowledge of a given uncertainty, without the need to apply curve-fitting. Unlike the QPDs developed by Keelin and Powley (2011), however, we demonstrate that our new system satisfies our notion of *maximally-feasible*, which means that we can always find a distribution assignment for *any* coherent set of specified QP pairs, and satisfying a specific structure, which we discuss in more detail later.

We also rigorously demonstrate the ability of our new system to closely-approximate a vast set of commonly-named distributions (e.g., beta, gamma, lognormal, etc.) sharing the same set of QP pairs and support, by using four different measures of closeness: the absolute percent difference in means by inter-decile range (APDM);

[11] We discuss quantile functions and touch on inverse-transform sampling in more detail in Chapter 2.

absolute percent difference in variance (APDV), the Kolmogorov-Smirnov (KS) distance; and the cross-entropy or Kullback-Leibler (KL) divergence. The APDV, KS distance, and KL divergence measures of closeness are well-known. However, the APDM measure is a relatively new approach for comparing the mean of two distributions. We demonstrate and justify the use for all four closeness measures. Also, in our analysis of the closeness of J-QPD to well-known families of distributions, we provide a novel and rigorous approach for performing the comparison, inspired by Hammond and Bickel (2013a).

We then demonstrate the flexibility of our new J-QPD system, as depicted in Pearson's well-known moment-ratio space, and generate several additional new probability distribution systems occurring as parametric limiting cases to J-QPD. We then show that one of these new systems, having semi-bounded support, is also maximally-feasible, and capable of capturing heavier-tailed shapes than its parent counterpart.

Finally, we combine J-QPD with existing methods to generate two new approaches for encoding dependence between uncertainties: the *marginal procedure* (MP), and the *conditional procedure* (CP). By augmenting J-QPD assignments with well-known methods for assessing dependence, we demonstrate that MP is an efficient, high-fidelity method for encoding (and simulating from) a continuous joint distribution among a set of dependent uncertainties.

Of integral importance in our concluding observations is our list of strengths and weaknesses of our new J-QPD systems, compared to the QPDs developed by Keelin and Powley (2011), Powley (2013), and Keelin (2016). For example, Keelin and Powley's QPDs are more directly extendible to larger sets of QP pairs, while our J-QPDs specify a prescribed number of QP pairs of a specific structure. However, given our prescribed QP structure, our J-QPD system is maximally-feasible, whereas Keelin and Powley's QPDs cannot handle many sets of coherent QPDs. Also, additional steps are needed to engineer

the support of Keelin and Powley's QPDs, such as by use of transformations, some of which may yield distributions with undefined or infinite moments.

ORGANIZATION

This work is organized as follows. Chapter 2 is a reference chapter, providing background information on the fundamentals of quantile functions, since they serve as a foundation for all subsequent chapters of this dissertation. Chapter 3 reviews the notion of quantile-parameterized distributions (QPDs) pioneered by Keelin and Powley (2011), and its extensions by Powley (2013) and Keelin (2016), since their work most closely relates to, and is the primary motivation for the distribution systems we develop herein. In Chapter 4, we construct our new J-QPD probability distribution systems based on our stated desiderata. In Chapter 5, we show that our new J-QPD systems satisfy our notion of maximally-feasible, and provide a comparative visual depiction of the feasibility span of various commonly-named distributions compared to J-QPD. In Chapter 6, we demonstrate that J-QPD can closely approximate a vast array of commonly-named distributions with potent accuracy, using our four measures of closeness. In Chapter 7, we examine the flexibility of the J-QPD system, as measured by Pearson (1895, 1901, and 1916). Chapter 8 introduces a "logistic version" of our J-QPD systems, which we refer to as "L-QPD", using the logistic distribution in place of the normal distribution as its basis for construction, along with important tradeoffs between the two systems. Chapter 9 provides two separate and detailed methodologies for encoding dependence between uncertainties using J-QPD. In Chapter 10, we partially walk through an illustrative decision analysis example to more comprehensively demonstrate how J-QPD might be implemented in practice, and where existing approaches might fail in place of J-QPD. Chapter 11 concludes with a summary of the main contributions presented in this

dissertation, recommendations and guidelines for practice, and several avenues for future research.

Chapter 2 : Some Basics of Quantile Functions

Most all concepts on quantile functions in this chapter are not new, except where explicitly stated. However, inclusion of this chapter is essential in developing a basic understanding and intuition for quantile functions, particularly since most of our contributions beginning in Chapter 4 largely build on these concepts. This applies to readers across a broad range of experience and education in probability theory, in large part because the quantile function representation of probability distributions generally enjoys much less coverage than do CDFs and PDFs in the teaching of probability theory – see Gilchrist (2000). We hope that this chapter provides great illumination upon the utility of quantile functions for the novice reader in probability, while refreshing interest and basic technical understanding for more advanced readers.

Unless explicitly noted, most all definitions and propositions in this chapter are adopted from Gilchrist (2000) or Powley (2013). For a supplemental overview of quantile functions, along with proofs of some of the propositions stated herein, we refer the interested reader to Powley (2013). For a more detailed and extensive examination of quantile functions, we refer the interested reader to Gilchrist (2000).

DEFINITION OF A QUANTILE FUNCTION

Let $F(x)$ denote the CDF for random variable, X. The quantile function, $Q(p)$, is defined as:

$$Q(p) = \inf\left(x \in \mathbb{R} \mid p \le F(x)\right). \tag{2.1}$$

This definition for a quantile function provides a generalization of the inverse of F, for cases in which the inverse may be undefined[1]. Like a CDF or PDF, a quantile function

[1] This happens, for example, with discrete distributions.

fully characterizes a probability distribution. For many commonly-named distributions (e.g., normal, lognormal, gamma, Weibull, beta, etc.), the quantile function is the inverse of the CDF, which we assume throughout this dissertation, unless explicitly noted otherwise. A given function, $Q(p)$, must meet two attributes to be a quantile function:

(1) It must be defined over the domain: $p \in (0, 1)$.

(2) It must be non-decreasing over this domain.

Figure 2.1 (left) shows the quantile function for the standard normal distribution, while Figure 2.1 (right) shows its inverse, the CDF for the standard normal distribution. Notice that Q takes a percent point in decimal form as input (say $p = 0.2$, denoting 20%), and returns the $100p^{th}$ percentile of the distribution.

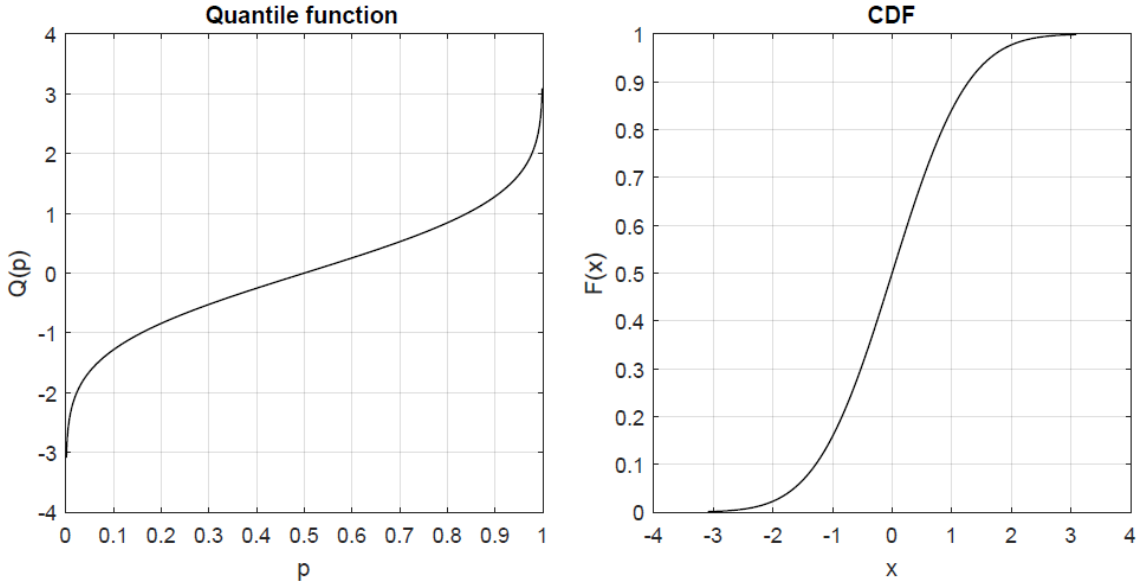

Figure 2.1. Quantile Function and CDF for the Standard Normal Distribution.

For example, in Figure 2.1 (left), $Q(0.2) = -0.8412$ is the 20^{th} percentile for the standard normal distribution. Alternatively, we say that if X has a standard normal distribution, then the probability that X is less than or equal to –0.8412 is 0.2, as conveyed in Figure 2.1 (right). Table 2.1 presents the quantile function characterization for several well-

known elemental distributions. Unless explicitly noted, throughout this dissertation, $\Phi^{-1}(p)$ refers to the quantile function for the standard normal distribution. Now we introduce the concept of transformations upon a quantile function.

QUANTILE FUNCTIONS FOR SOME COMMONLY-NAMED DISTRIBUTIONS

Distribution	Quantile function, Q(p)	Parameters
Normal	$\mu + \sigma \cdot \Phi^{-1}(p)$	$\mu, \sigma > 0$
Uniform	$l + (u - 1) \cdot p$	l, u
Exponential	$-\lambda \cdot \log(1-p)$	$\lambda > 0$
Lognormal	$\exp(\mu + \sigma \cdot \Phi^{-1}(p))$	$\mu, \sigma > 0$
Logistic	$\mu + \sigma \cdot \log\left(\frac{p}{1-p}\right)$	$\mu, \sigma > 0$
Weibull	$\left(-\lambda \cdot \log(1-p)\right)^{a}$	$\lambda > 0, a > 0$

Table 2.1. Quantile Functions for Several Commonly-Named Distributions.

SOME BASIC TRANSFORMATION RULES FOR QUANTILE FUNCTIONS

Q-Transformations

The Q-Transformation Rule: If $T(x)$ is a non-decreasing function of x, and $Q(p)$ is a quantile function, then $T(Q(p))$ is a quantile function. Moreover, suppose X has quantile function, $Q(p)$, and that Y has the quantile function, $T(Q(p))$. Then $Y = T(x)$.

The Q-transformation rule is particularly useful since we often perform many mathematical operations upon uncertain quantities. When the operator T is non-decreasing, the Q-transformation rule provides a simple mapping from the distribution (quantile function) of one random variable (X) to that of the transformed random variable (Y). For example, referencing Table 2.1, the lognormal distribution results from applying the "exp" transformation, $T(x) = e^{x}$, to the quantile function for the normal distribution. Alternatively, the Weibull distribution results from applying the transformation, $T(x) = x^{a}$, to the quantile function for the exponential distribution.

One of the simplest Q-transformations is the positive affine transformation, $T(X) = aX + b$, where $a > 0$. Define the transformed variable: $Y = T(X) = aX + b$. Figure 2.2 provides an illustration showing the quantile function, CDF, and PDF for $Y = 3X + 5$ for the case in which X has a standard normal distribution.

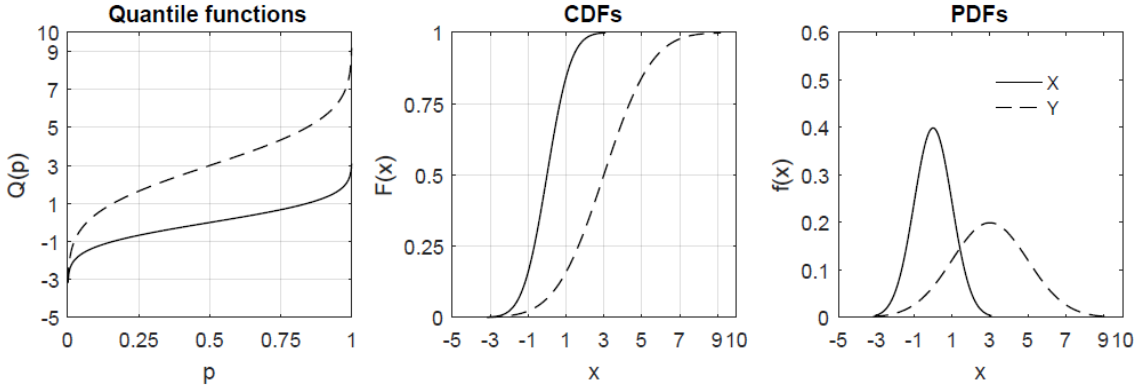

Figure 2.2. Quantile Functions, CDFs, and PDFs for X, and $Y = 3X + 5$.

Notice that the PDF and CDF of X shift to the right by 5 units, and then are scaled (stretched in this case) by a factor of 3. The PDF shortens in height to maintain the Law of Total Probability – the integral of the PDF over its domain must equal one. Thus, the positive affine transformation produces effects on location (with b) and scale (with $a > 0$), but not on shape – the distribution is only shifted or stretched/squeezed.

Notice that the Q-transformation function, T, operates directly on $Q(p)$, which is equivalent to applying the operator directly to X itself, mapping the random variable, X, into the new random variable, $Y = T(X)$. Based on this observation, if X has support on $\{a, b\}$, then Y has support on $\{T(a), T(b)\}$. This fact leads to powerful methods for engineering the support of an uncertainty by use of Q-transformations.

Table 2.2 lists a few well-known Q-transformations for various support scenarios. Note the effect of these transformations on distribution support. For example, if X has a normal distribution, then using the "exp" transformation, $Y = e^X$, induces a lognormal

distribution for Y. This is especially useful if an uncertainty is required to be non-negative. Alternatively, the logit and probit transformations might be useful for modeling a bounded uncertainty, such as market share, which is bounded between zero and one.

Transformation name	$T(x)$	Support of X	Support of $Y=T(X)$
Positive affine	$ax + b$, $a > 0$	$[l, u]$	$[al + b, au + b]$
Exponential ("exp")	e^x	$(-\infty, \infty)$	$(0, \infty)$
Logit	$\frac{e^x}{1+e^x}$	$(-\infty, \infty)$	$(0, 1)$
Probit	$\Phi(x)$	$(-\infty, \infty)$	$(0, 1)$

Table 2.2. Some Well-Known Transformations for Controlling Support.

In addition to affecting support, many Q-transformations, other than simple affine transformations, affect distribution shape. Figure 2.3 (Figure 2.4) illustrates the effects of applying the "exp" (logit) transformation to a random variable, X, having a standard normal distribution. The "exp" transformation maps normal distributions to lognormal distributions, which are known to exhibit varying degrees of right-skew, unlike normal distributions. Alternatively, the probit and logit transformations map distributions on $(-\infty, \infty)$ (such as the normal distribution) to distributions with support on (0, 1).

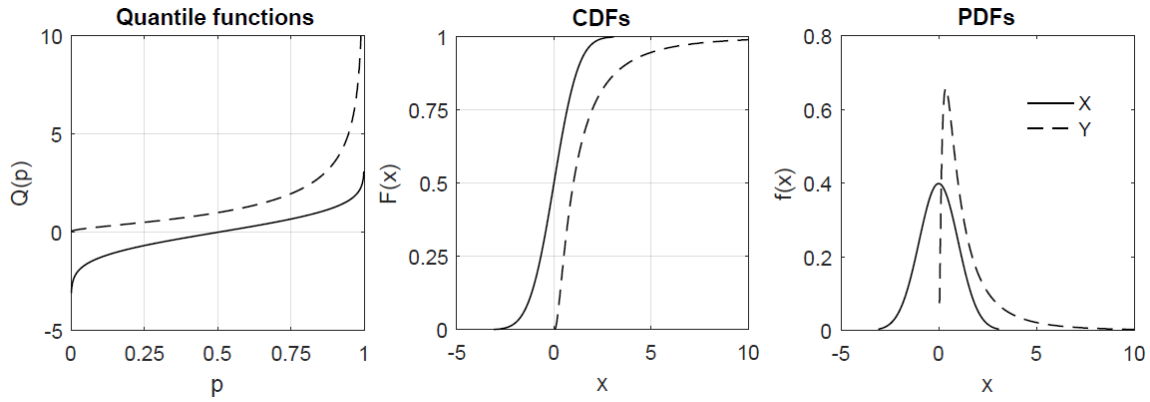

Figure 2.3. Quantile Functions, CDFs, and PDFs for X, and $Y = \exp(X)$.

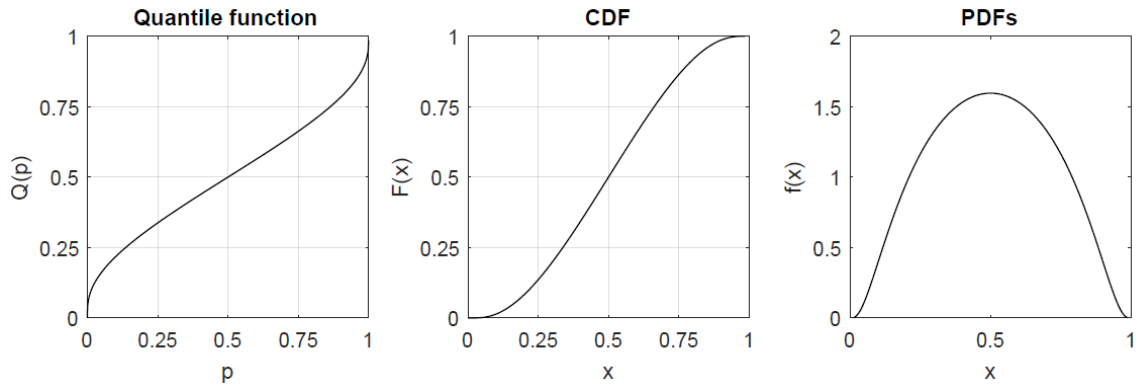

Figure 2.4. Quantile Functions, CDFs, and PDFs for Y=exp(X)/(1+exp(X)).

While the Q-transformation operates directly on $Q(p)$, and thus directly on X, there are other useful types of transformations that manipulate Q in other ways.

The Reciprocal Rule: Suppose X has quantile function, $Q(p)$, and that $Y = 1/X$. The quantile function for Y is $1/Q(1-p)$.

The Uniform Transformation Rule: If U has a uniform distribution on [0, 1], and $Q(p)$ is a non-decreasing function of p, then $X = Q(U)$ has the quantile function, $Q(p)$.

The Uniform Transformation Rule provides a basis for inverse-transform sampling. Specifically, if $\{u_1, u_2, \cdots, u_n\}$ is a random sample of n observations drawn from a uniform distribution on [0, 1], then $\{Q(u_1), Q(u_2), \cdots, Q(u_n)\}$ is a random sample of n

observations drawn from the probability distribution with quantile function, Q. This sampling procedure is the essence of inverse-transform sampling. Figure 2.5 provides an example showing a histogram of 10,000 observations drawn from the exponential distribution. We further implement inverse-transform sampling in conjunction with our new J-QPD probability distributions in subsequent chapters.

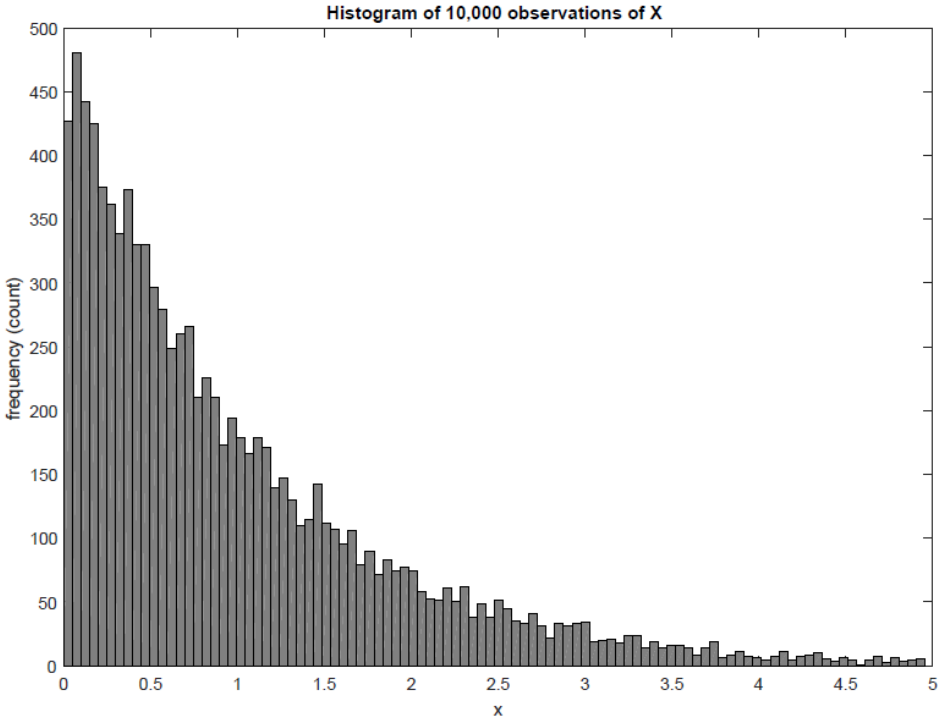

Figure 2.5. Histogram for an Exponential Distribution via Inverse-Transform Sampling.

The Reflection Rule: Suppose X has quantile function, $Q(p)$, and that Y has quantile function, $-Q(1-p)$. Then the PDF of Y is the reflection of the PDF of X about the line, $x = 0$. Figure 2.6 shows an illustration of the reflection rule applied to the exponential distribution. In this case, since the quantile function for the exponential distribution is $Q(p) = -\lambda\log(1-p)$, the reflection rule implies that the quantile function for the reflected exponential distribution is $Q(p) = \lambda\log(p)$. Also, note that under the reflection rule, if the PDF for X is $f(x)$, then the PDF for Y is $f(-x)$.

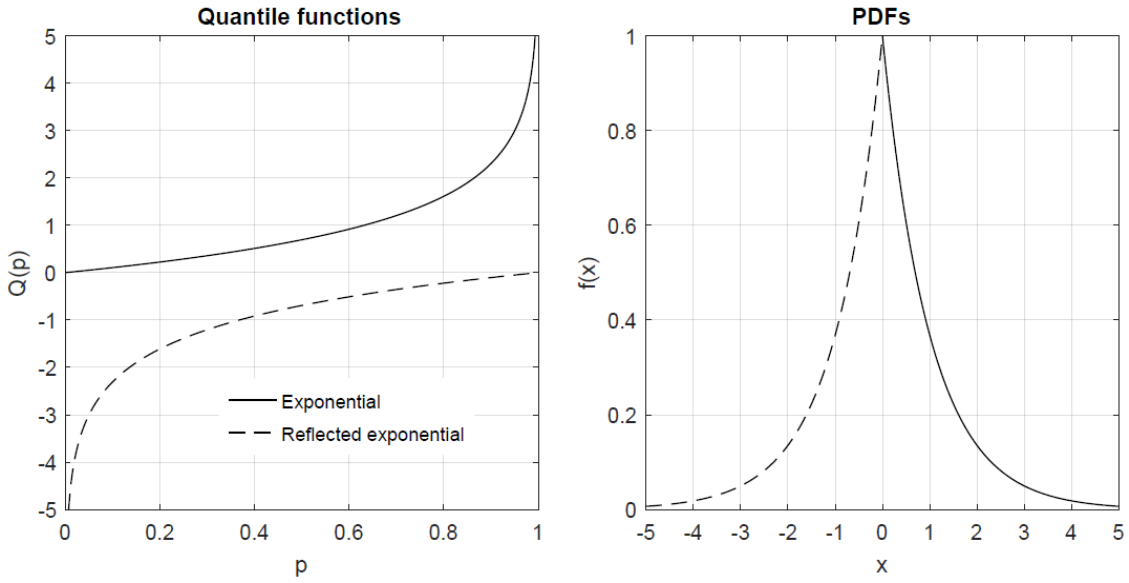

Figure 2.6. QFs and PDFs for the Exponential and Reflected Exponential Distributions.

The Addition Rule: If $Q_1(p)$ and $Q_2(p)$ are quantile functions, then $Q_1(p)+Q_2(p)$ is also a quantile function.

The Linear Combination Rule: If $Q_1(p)$ and $Q_2(p)$ are quantile functions, $a > 0$, and $b > 0$, then $aQ_1(p) + bQ_2(p)$ is also a quantile function.

The *p*-Transformation Rule: If $Q(p)$ is a quantile function, and $a > 0$, then $Q(p^a)$ is a quantile function.

The logistic distribution presented in Table 2.1 results from applying the addition rule to the quantile functions for the exponential distribution and the reflected exponential distribution. That is, the logistic distribution is built from the exponential distribution, the addition rule, and the reflection rule[2]. Although the logistic distribution is symmetrical and similar in shape to a normal distribution, Gilchrist (2000) produces a skewed logistic distribution by applying the linear combination rule to the exponential- and reflected

[2] For more on the logistic distribution, see Balakrishnan (1992).

exponential distributions. Later, we present well-known distributions whose construction involves the *p*-Transformation rule.

COMPUTING MOMENTS USING QUANTILE FUNCTIONS

It is often useful to compute the moments of a probability distribution directly from its quantile function. As with PDFs, computation of moments using quantile functions is straightforward. The k^{th} raw moment for the quantile function, Q, is given by:

$$\mu_k' = \int_0^1 Q^k(p)dp. \tag{2.2}$$

Thus, the mean is given by:

$$\mu = \mu_1' = \int_0^1 Q(p)dp. \tag{2.3}$$

Using this notation, the computation for the k^{th} central moment is given by:

$$\mu_k = \int_0^1 \big(Q(p) - \mu\big)^k \, dp. \tag{2.4}$$

We can use these expressions to build the variance, skewness, and kurtosis of Q, as shown in Table 2.3. Unlike PDFs and CDFs, one advantage of computing moments with quantile functions is that we need not specify lower and upper bounds of support in the integral computations, since the quantile function always ranges from 0 to 1.

Moment	Symbol	Computation
Variance	σ^2	$\int_0^1 \left(Q(p)-\mu\right)^2 dp.$
Skewness	γ_1	$\frac{\int_0^1 \left(Q(p)-\mu\right)^3 dp}{\sigma^3}$
Kurtosis	γ_2	$\frac{\int_0^1 \left(Q(p)-\mu\right)^4 dp}{\sigma^4}$

Table 2.3. Computation of Higher-Order Moments Using Quantile Functions.

Variance is a measure of distribution spread or scale, and is not a measure of shape, since it only involves stretching or squeezing of the distribution. Traditional shape measures of skewness and kurtosis are defined such that they are invariant to affine transformations (shifting or scaling) of a distribution. Specifically, the subtraction of μ in the numerator of these two measures removes location (shifting) effects, while the σ^3 and σ^4 terms in the denominator (respectively) remove the effects of scale (stretching or squeezing). We revisit skewness and kurtosis in Chapter 7, where we evaluate the flexibility of our new J-QPD distribution system.

ADVANCED DISTRIBUTIONS WITH QUANTILE FUNCTION REPRESENTATIONS

We now briefly cover several advanced quantile probability distribution systems. By "advanced", we allude to two specific attributes of the system:

- Its quantile function representation is built upon the quantile functions for one or more of the elemental distributions listed in Table 2.1.
- It has *at least two* separate (and independent) shape parameters. That is, these two parameters must affect more than simple location and scale changes upon the distribution. For example, the beta distributions have two shape parameters.

The Exponentiated Weibull (EW) Distribution

We now revisit the quantile function for the Weibull distribution listed in Table 2.1:

$$Q(p) = \left(-\log(1-p)\right)^a, \; a > 0. \tag{2.5}$$

The Weibull distribution is formed by applying the Q-transformation, $T(x) = x^a$ ($a > 0$), to the quantile function for the exponential distribution. The Weibull distribution has its roots in system reliability theory, and is often used to model the time between system failures. While it is arguably flexible, the Weibull distribution has only one shape parameter (represented by a), like the gamma and lognormal distributions. This shape parameter can capture an increased frequency of failures in a system over longer periods of time due to system aging and "wear-and-tear", but is not capable of capturing increased failures associated with infant mortality in the early life of a system.

To remedy this shortcoming, Mudholkar and Srivastava (1993) developed the *Exponentiated Weibull* (EW) distribution by introducing a second shape parameter into the standard Weibull quantile function as follows:

$$Q(p) = \left(-\log(1-p^k)\right)^a, \; a > 0, \; k > 0. \tag{2.6}$$

Thus, the EW quantile function is formed by additionally applying a p-transformation to the Weibull quantile function, resulting in the second shape parameter, k. The EW system of distributions has support on [0, ∞), and is quite flexible. We revisit the EW system further in Chapter 5, where we compare it to our new J-QPD system.

The Burr and Dagum Distributions

Burr (1973) introduced a system defined on (0, ∞), also known as the Singh-Maddala (1976) distribution, which is used to model household income in the United States. The Burr distribution quantile function is given by:

$$Q(p) = \left((1-p)^{-k} - 1\right)^a, \; a > 0, \; k > 0. \tag{2.7}$$

The Burr system is a generalization of the log-logistic distribution[3], and includes the Pareto Type II distribution as a special case. The Burr distributions are smooth and unimodal in shape, mostly having heavy tails. Another distribution system used to model income, which stems from the Burr distribution, is the Dagum (1977) distribution, characterized by the quantile function:

$$Q(p) = \left(p^{-k} - 1 \right)^{-a}, \; a > 0, \; k > 0. \tag{2.8}$$

The Dagum distribution results from applying the **Reciprocal Rule** to the Burr quantile function. That is, if X is an uncertainty having a Burr distribution with parameters $\{k, a\}$, then $1/X$ has a Dagum distribution with parameters $\{k, a\}$.

The Simple Q-Normal (SQN) Distribution

Keelin and Powley (2011) developed a system of quantile-parameterized distributions (QPDs), known as the *Simple Q-Normal* (SQN) system, specified by its quantile function:

$$Q_{SQN}(p) = a + b \cdot p + c \cdot \Phi^{-1}(p) + d \cdot p \cdot \Phi^{-1}(p), \tag{2.9}$$

where $\Phi^{-1}(p)$ is the quantile function for the standard normal distribution. SQN distributions have support on $(-\infty, \infty)$. The joint requirements on the allowable values for the parameters, $\{a, b, c, d\}$, are quite complicated, since not all combinations of values for $\{a, b, c, d\}$ result in $Q_{SQN}(p)$ being a quantile function, as required. We discuss the SQN system in more detail in Chapter 3.

The Johnson Distribution System

Perhaps one of the most well-known of the advanced quantile distribution systems is the Johnson (1949) system, which consists of three subfamilies of distributions:

- The **SU** family, with support on $(-\infty, \infty)$.
- The **SB** family, with bounded support.

[3] For more on the log-logistic distributions, see Tadikamalla and Johnson (1982), and Tadikamalla (1980).

- The **SL** family, or lognormal distributions, having positive support.

The Johnson system is attractive since it is highly flexible, has well-defined moments, and has simple mathematical expressions for its: quantile functions; CDFs; PDFs. The Johnson quantile functions arise from Q-transformations applied to $\Phi^{-1}(p)$, the quantile function for the standard normal distribution. Table 2.4 provides the quantile function for each subfamily, including support, and associated Q-transformations applied to $\Phi^{-1}(p)$ in each case. For SU and SB distributions, ξ and λ are location and scale parameters, respectively, and $\{\gamma, \delta\}$ are shape parameters. We revisit the Johnson system in Chapter 4, where we develop our new J-QPD distribution system.

Subfamily	Quantile function	Support	Requirements	Q-Transformation
SU	$\xi + \lambda \sinh\left(\delta\left(\Phi^{-1}(p) + \gamma\right)\right)$	$(-\infty, \infty)$	$\lambda, \delta > 0$	Hyperbolic sine
SB	$\xi + \frac{\lambda \exp\left(\delta\left(\Phi^{-1}(p) + \gamma\right)\right)}{1 + \exp\left(\delta\left(\Phi^{-1}(p) + \gamma\right)\right)}$	$(\xi, \xi + \lambda)$	$\lambda, \delta > 0$	Logit
SL	$\exp\left(\mu + \sigma \cdot \Phi^{-1}(p)\right)$	$(0, \infty)$	$\sigma > 0$	"Exp"

Table 2.4. Quantile Functions for the Johnson SU, SB, and SL Subfamilies.

THE ADVANTAGES OF QUANTILE FUNCTIONS OVER CDFS AND PDFS

We close this chapter by noting several key advantages to having simple (e.g., closed-form) quantile functions for a probability distribution:

- We can easily calculate any percentile of the distribution.
- We can directly use the quantile function to perform Monte Carlo simulation via inverse-transform sampling.
- We can easily build other distribution forms by direct application of transformations; e.g., Q-transformations.
- When computing moments via analytical or numerical integration, we need not specify the support, since quantile functions range from 0 to 1.

Chapter 3 : Quantile-Parameterized Distributions (QPDs)[1]

In decision analysis practice, it is very helpful to have a tool that enables an analyst to go directly from assessed points to a distribution, without the need for a fit procedure. Recall our goal of developing a distribution system that is parameterized by, and thus precisely honors, a set of assessed QP pairs, such as the $\{10^{th}, 50^{th}, 90^{th}\}$ percentiles. That is, no fitting approximation, such as least-squares, is needed. Toward achieving this goal, Keelin and Powley (2011) pioneered the notion of *quantile-parameterized distributions* (QPDs), which amount to probability distributions that are parameterized by the assessed points, $\{x_1, x_2, x_3, \cdots\}$, along with their corresponding cumulative probabilities, $\{p_1, p_2, p_3, \cdots\}$. In this chapter, we discuss QPDs in more detail, since they most closely relate to our new J-QPD system, which we develop in Chapter 4.

QUANTILE-PARAMETERIZED DISTRIBUTIONS

QPDs characterize probability distributions in quantile function form, expressed as a linear combination of strategically-selected basis functions. As formalized by Powley (2013), QPDs are probability distributions whose quantile function can be written:

$$Q(p) = \sum_{i=1}^{n} \beta_i g_i(p), \; 0 < p < 1, \tag{3.1}$$

Where $\beta \in \mathbb{R}^n$, and $\{g_i(p) \mid i \in 1{:}n, \; p \in (0,1)\}$ is a regular set of basis functions. Based on this definition, the uniform, normal, exponential, logistic, and skewed-logistic distributions are all QPDs. For example, a normal distribution having mean (standard deviation), μ (σ), is a QPD with basis functions, $\{g_1(p), g_2(p)\} = \{1, \Phi^{-1}(p)\}$, and parameters given by: $\{\beta_1, \beta_2\} = \{\mu, \sigma\}$. Also, this definition of a QPD implies that a basis

[1] This is a background chapter, and borrows heavily from Keelin and Powley (2011), Powley (2013), and from Keelin (2016).

function, $g_i(p)$, need not be non-decreasing, as long as $Q(p)$ is strictly increasing – as imposed by Powley (2013).

Linearity of QPD Parameters and Assessed Quantiles

Since a QPD's quantile function is a linear combination of a given set of basis functions, the vector of parameters, β, can be solved for via solution to a linear system of equations, given a set of distinct QP pairs, whose number of pairs is equal to the cardinality of β. Powley (2013) formalizes this concept with the Quantile Parameters Theorem:

The Quantile Parameters Theorem

A set of n distinct QP pairs, $\{(x_i, p_i) \mid i \in 1:n\}$*, uniquely determines* $\beta \in \mathbb{R}^n$ *of a QPD by the matrix equation,* $\beta = Y^{-1}x$*, where the set of basis functions,* $\{g_i(p) \mid i \in 1:n,\ p \in (0,1)\}$*, is regular, and*

$$Y = \begin{pmatrix} g_1(p_1) & \cdots & g_n(p_1) \\ \vdots & \ddots & \vdots \\ g_1(p_n) & \cdots & g_n(p_n) \end{pmatrix}$$

if and only if:

i. *the matrix, Y, is non-singular (invertible)*

ii. $\sum_{i=1}^{n} \beta_i \frac{dg_i(p)}{dp} \geq 0,$ *for all* $p \in (0,1).$

Note that (ii) implies that $Q(p)$ must be a valid (non-decreasing) quantile function.

AN EXAMPLE QPD: THE SIMPLE Q-NORMAL (SQN) DISTRIBUTION

One of the first such QPDs developed by Keelin and Powley (2011) is the Simple Q-Normal (SQN) distribution, having the following quantile function representation:

$$Q_{SQN}(p) = a + b \cdot p + c \cdot Q_N(p) + d \cdot p \cdot Q_N(p), \tag{3.2}$$

where $Q_N \equiv \Phi^{-1}$ is the standard normal quantile function. In this case, the basis functions are: $\{1, p, Q_N(p), pQ_N(p)\}$. The parameters, $\{a, b, c, d\}$, uniquely determine a distribution

within the SQN system, by solution to a linear system. For example, if the $\{x_{0.25}, x_{0.50}, x_{0.75}, x_{0.90}\}$ quantiles (i.e., 25th, 50th, 75th, and 90th percentiles) are given, then we can easily obtain $\{a, b, c, d\}$ by solving:

$$\begin{pmatrix} x_{0.25} \\ x_{0.50} \\ x_{0.75} \\ x_{0.90} \end{pmatrix} = \begin{pmatrix} 1 & 0.25 & \Phi^{-1}(0.25) & 0.25\Phi^{-1}(0.25) \\ 1 & 0.50 & \Phi^{-1}(0.50) & 0.50\Phi^{-1}(0.50) \\ 1 & 0.75 & \Phi^{-1}(0.75) & 0.75\Phi^{-1}(0.75) \\ 1 & 0.90 & \Phi^{-1}(0.90) & 0.90\Phi^{-1}(0.90) \end{pmatrix} \begin{pmatrix} a \\ b \\ c \\ d \end{pmatrix}.$$

Figure 3.1 shows an example SQN for $\{x_{0.10}, x_{0.50}, x_{0.90}, x_{0.99}\} = \{10, 14, 25, 35\}$, including quantile function and sample histogram. Notice, by design, that the distribution precisely honors the specified points, making QPDs particularly powerful for analysts.

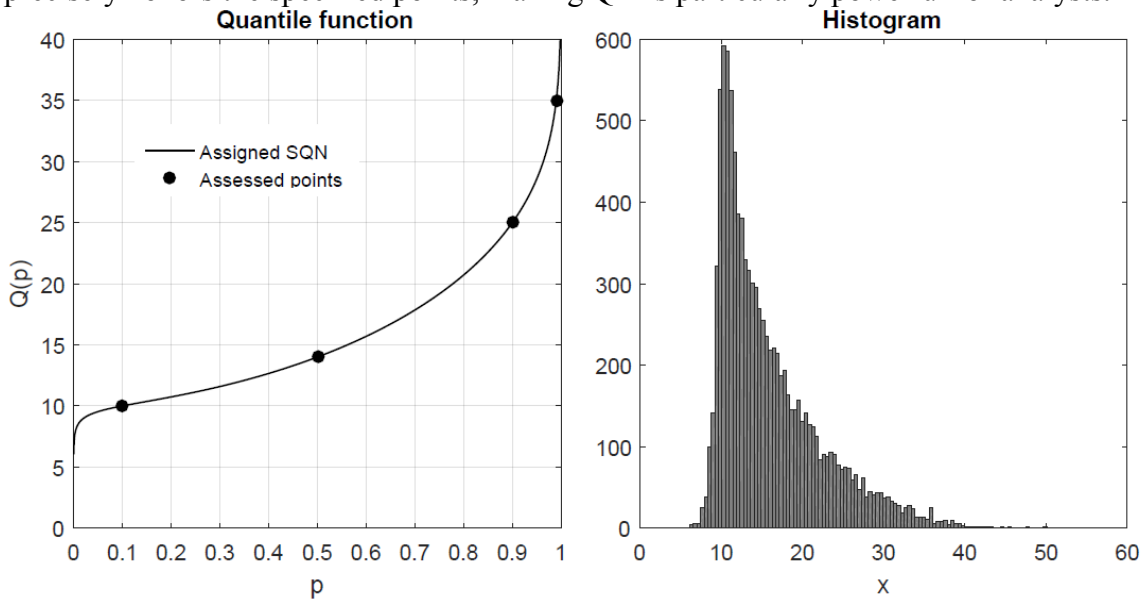

Figure 3.1. QF and Histogram for the SQN with $\{x_{0.10}, x_{0.50}, x_{0.90}, x_{0.99}\}=\{10, 14, 25, 35\}$.

FEASIBILITY OF QPDS

Recall that $Q(p)$ must be non-decreasing, as formally expressed by:

$$Q(p) = \sum_{i=1}^{n} \beta_i \frac{dg_i(p)}{dp} \geq 0, \text{ for all } p \in (0,1). \tag{3.3}$$

Given a set of basis functions, $\{g_i(p) \mid i \in 1:n,\ p \in (0,1)\}$, this implies that not all vectors, $\beta \in \mathbb{R}^n$, are *feasible* – i.e., result in (3.3) being satisfied for the given set of basis

functions. Furthermore, this implies that some sets of distinct QP pairs, $\{(x_i, p_i) \mid i \in 1:n\}$, are *infeasible* for the given set of basis functions, meaning that the function, $Q(p)$, generated is not a quantile function.

Figure 3.2 provides an example of infeasibility for the SQN, where the QP pairs are: $\{x_{0.10}, x_{0.50}, x_{0.90}, x_{0.99}\} = \{10, 20, 30, 70\}$. Since part of $Q(p)$ is decreasing, and thus $Q(p)$ is not a quantile function in this case.

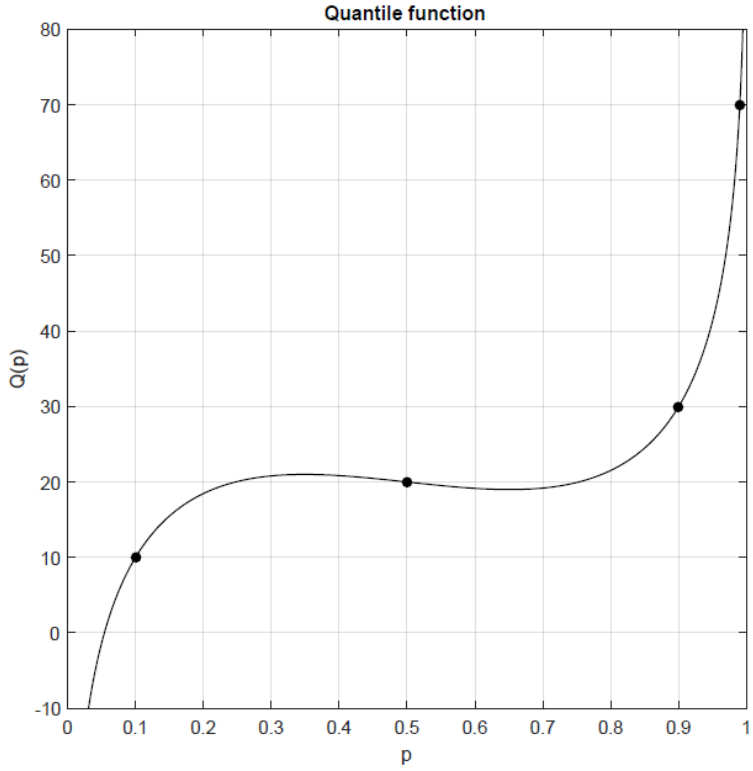

Figure 3.2. An SQN that Yields Infeasibility: $\{x_{0.1}, x_{0.5}, x_{0.9}, x_{0.99}\} = \{10, 20, 30, 70\}$.

THE METALOG DISTRIBUTIONS

Keelin (2016) extended the work of Keelin and Powley (2011) and Powley (2013) by developing a much broader set of QPDs known as the Metalog (ML) system. ML is arguably the most flexible distribution system to-date, since it can be parameterized by an

arbitrarily large number of QP pairs, by systematically appending the required number of basis functions. When constructing these QPDs, however, nontrivial issues faced are:

- **Choice of basis functions** – For example, the choice of basis functions can affect both support and tail behavior.
- **Feasibility** – Some sets of QP pairs, while coherent[2], may yield a function that is not a quantile function.
- **Engineering distribution support** – monotonic Q-transformations can be applied to a QPD to obtain the desired support. For example, if X is a random variable having a QPD with doubly-unbounded support (such as SQN), but non-negative support is desired, then taking $Y = e^X$ may suffice. However, different transformations have different effects on tail behavior, and some transformations may yield undefined moments. Thus, the appropriate choice of transformation is not always clear.

While motivated by the major advances of Keelin and Powley (2011), Powley (2013), and Keelin (2016), we take an alternative approach to QPDs in this dissertation, when we develop our new J-QPD system in Chapter 4. Ultimately, we compare the pros and cons of both QPDs and the new J-QPD system.

[2] By *coherent*, we mean that the QP pairs satisfy the axioms of probability. For example, a 50^{th} percentile cannot be less than a 25^{th} percentile.

Chapter 4 : The New J-QPD Distribution Systems[1]

In this chapter, we develop a new family of smooth probability distributions that are parameterized by their quantiles, based on two support regimes: bounded; semi-bounded. Our focus on the bounded and semi-bounded cases is based on the presumption that many physical quantities have a finite and known lower (but not necessarily upper) limit of support (e.g., oil reserves cannot be negative). However, we also generate several unbounded distributions as parametric limiting cases to our new distribution system in Chapter 7.

Our system is an extension of the Johnson distribution system (JDS), and can honor any *symmetric percentile triplet* (SPT), which we formally define shortly. We refer to our new family of probability distributions as the "Johnson Quantile-Parameterized Distribution" (or "J-QPD") system, which serves as the central contribution in this dissertation. We also show that our J-QPD system can closely approximate a vast array of commonly-named distributions (e.g., beta, gamma, lognormal, Weibull, etc.) using a single system. While our system is new, we stress that it is not unique, since there are an infinite number of distributions that can honor any finite set of QP pairs. As we explain more fully below, our objective is to develop a family of smooth distributions that honor assessed quantiles, are straight-forward to implement in practice, and closely approximate a wide array of commonly-named distributions.

INTRODUCTION AND MOTIVATION

Suppose X is a continuous random variable with cumulative distribution function (CDF)

$$p = F_X(x) \equiv P(X \le x), \tag{4.1}$$

[1] Summaries of the results of this chapter are published with my advisor, Eric Bickel, in the following: Hadlock, Christopher and J. Eric Bickel. 2017. Johnson Quantile-Parameterized Distributions. *Decision Analysis* **14**(1) 35-64.

and quantile function

$$x_p = Q_X(p) \equiv \inf\{x \in \mathbb{R} : p \le F(x)\}. \tag{4.2}$$

If F_x is continuous and increasing over the support of X, which we assume here, then Q_X is the inverse-CDF of X. We refer to x_p as the p-level quantile of X or the $(p \cdot 100)^{th}$ percentile of X. For example, $x_{0.5} = Q_X(0.5)$ denotes the 0.5-level quantile, or 50^{th} percentile (P50) of X.

In many decision analysis applications, analysts assess uncertainty by eliciting a limited number (three is common) of (p, x_p) pairs from an expert. For example, it is common to assess the 0.10-, 0.50-, and 0.90-level quantiles or, equivalently, the 10^{th}, 50^{th}, and 90^{th} percentiles[2]. As noted in Chapter 1, we assume that the (p, x_p) pairs are coherent – they satisfy the axioms of probability. Recall that analysts cannot assess the infinite number of QP pairs on an expert's CDF for a continuous uncertainty. Instead, given a finite set of assessments in the form of QP pairs, analysts may then fit a continuous CDF to these points. As noted in Chapter 1, such fitting often requires solving a non-linear optimization problem for the distribution parameters, a process which some analysts may find inefficient or difficult to implement. More importantly, however, recall that the best-fit CDF often never honors the assessed QP pairs. For example, if the best-fit distribution is specified by two parameters, such as the mean and variance, then it is likely that the selected distribution will not pass through any points provided by the expert – Recall the normal distribution fit in Figure 1.7. This can cause confusion and decrease trust in the analysis.

[2] For examples, see McNamee and Celona (1990), Hammond and Bickel (2013a, b), and Hurst et al. (2000).

The QPD work initiated by Keelin and Powley (2011), and the extensions by Powley (2013) and Keelin (2016) are arguably the most notable contributions to the decision analysis literature, in terms of providing smooth distributions that are parameterized by (and precisely honor) a set of QP pairs. Also, as we saw in Chapter 3, Keelin and Powley's notion of QPDs can handle any arbitrary positive integer number (say "*n*") of assessed QP pairs, by constructing a QPD with *n* basis functions. However, recall that several issues must be addressed by the analyst when employing these QPDs:

(1) **Feasibility** – As we saw in Chapter 3, not all sets of coherent QP pairs yield a valid quantile function (distribution) – Recall the example of Figure 3.2. We further address this point in more detail shortly.

(2) **Choosing Basis Functions** – While the SQN and certain Metalog distributions contain a prescribed set of basis functions, the choice of basis functions is generally unclear when an arbitrary set of *n* QP pairs of assessments are collected.

(3) **Engineering Support** – Recall that in standard form, QPDs (such as SQN and Metalog) have unbounded support on $(-\infty, \infty)$. For uncertainties such as market share forecasts, the standard-form SQN or Metalog distributions violate the bounds of 0% to 100% (0 to 1) – i.e., they allow for negative market shares or shares that exceed the size of the market. This is problematic for practical applications. As noted in Powley (2013) and Keelin (2016), a monotonic Q-transformation must be applied to the standard-form QPD that yields the appropriate support for the given uncertainty. A logit or probit Q-transformation can be applied to yield a bounded quantile function, whereas the log ("exp") Q-transformation can be applied to yield a semi-bounded quantile function.

In this chapter, we take a slightly different approach in developing a new quantile-parameterized distribution system, which directly resolves issue (1) within a specific (but

important) context, while circumventing issues (2) and (3). Ultimately, we offer our system as an advantageous tool within the popular context of assessing *symmetric percentile triplets* (SPTs), which we define below.

In this chapter, we first specify five desiderata that guide the development of our new distribution family. Next, we extend the JDS to design our new J-QPD distribution system, which serves as the central contribution of this chapter. In the chapters immediately following the development of our new system, we examine the feasibility of the J-QPD system, and we also rigorously quantify the ability of J-QPD to closely approximate a vast array of commonly-named distributions. We then examine the flexibility of the J-QPD system, and identify several limiting distributions.

DESIDERATA

Given the wide array of potential continuous distribution families from which one may choose, it is helpful to have some criteria or desiderata that the distribution family should meet, if possible. Keelin (2016) notes three criteria for measuring the desirability of a probability distribution in the modern environment of decision analysis practice, building upon earlier criteria suggested by Johnson (1949), Mead (1965), and Johnson et al. (1994): flexibility; simplicity; ease/speed of use. In this section, we more precisely outline a set of desiderata that seem, to us, desirable from the perspective of decision analysis practice. We begin with some definitions that make our development more efficient.

Definitions

When assessing an uncertainty from an expert, a common practice is to elicit a triplet of low-base-high quantile values of the form: $\mathbf{x}_\alpha = (x_\alpha, x_{0.50}, x_{1-\alpha})$. For example, $\mathbf{x}_{0.1} = (x_{0.10},$

$x_{0.50}$, $x_{0.90}$) denotes the vector of 10th, 50th, and 90th percentiles. To streamline the discussion, we begin with several definitions:

Definition 1. Consider any $\alpha \in (0, 0.50)$, and define an ***α*-level symmetric percentile triplet (*α*-SPT)** as a vector, $\mathbf{x}_\alpha = (x_\alpha, x_{0.50}, x_{1-\alpha})$, where x_α denotes the α-level quantile for the random variable, X.

Definition 2. Presume that the lower, l, and upper, u, support bounds ($l < u$) of X are specified and that an expert provides $\mathbf{x}_\alpha = (x_\alpha, x_{0.50}, x_{1-\alpha})$, for some $\alpha \in (0, 0.50)$. Collectively, define: $\boldsymbol{\theta}_\alpha = (l, \mathbf{x}_\alpha, u) = (l, x_\alpha, x_{0.50}, x_{1-\alpha}, u)$.

Definition 3. The vector $\boldsymbol{\theta}_\alpha = (l, \mathbf{x}_\alpha, u)$ is **compatible** if and only if $\alpha \in (0, 0.50)$ and $l < x_\alpha < x_{0.50} < x_{1-\alpha} < u$.

Definition 4. Define $Q(p;\boldsymbol{\theta}_\alpha)$ as a quantile function on $p \in [0, 1]$ for some probability distribution, and having distribution parameters given by: $\boldsymbol{\theta}_\alpha = (l, \mathbf{x}_\alpha, u)$.

While the QPDs developed by Keelin and Powley can take on sets of QP pairs that are of non-SPT structure, we focus upon the SPT context in developing our new system, not simply for mathematical tractability, but because of the prevalence of the SPT structure in practice. For examples, see McNamee and Celona (1990), Hammond and Bickel (2013a), and Hurst et al. (2000).

Desiderata

We seek a smooth probability distribution system, denoted $Q(p;\boldsymbol{\theta}_\alpha)$, satisfying five desiderata:

(1) Quantile-Parameterized: The distribution is characterized in closed-form[3] by $Q(p;\boldsymbol{\theta}_\alpha)$, which is directly parameterized by $\boldsymbol{\theta}_\alpha$, the assessed quantiles and specified support bounds. This has several benefits:

   a. No fit procedure (e.g., solving an optimization problem) is needed.
   b. $Q(p;\boldsymbol{\theta}_\alpha)$ honors $\boldsymbol{\theta}_\alpha$, the assessed quantiles and support bounds.
   c. Having $Q(p;\boldsymbol{\theta}_\alpha)$ in closed-form allows the analyst to efficiently implement Monte Carlo simulation via inverse transform sampling.
   d. Having $Q(p;\boldsymbol{\theta}_\alpha)$ in closed-form allows for efficient computation of additional quantiles, allowing the analyst to verify the assessment with an expert by checking additional points.
   e. Having $Q(p;\boldsymbol{\theta}_\alpha)$ in closed-form facilitates efficient construction of discrete distributions via a process of discretization; see Bickel et al. (2011) and Hammond and Bickel (2013a, 2013b), for a review of discretization methods, along with recent extensions.

(2) Availability of CDF: $Q(p;\boldsymbol{\theta}_\alpha)$ is invertible, so that the CDF, denoted $F(p;\boldsymbol{\theta}_\alpha)$, is readily available in closed-form. This allows the analyst to efficiently verify assessments with an expert by checking additional points, similar to $Q(p;\boldsymbol{\theta}_\alpha)$. Also, density functions (pdfs) can readily be obtained from $F(p;\boldsymbol{\theta}_\alpha)$ via differentiation.

(3) Maximally-Feasible: For any compatible $\boldsymbol{\theta}_\alpha$, the quantile function given by $Q(p;\boldsymbol{\theta}_\alpha)$ satisfies: $Q(0;\boldsymbol{\theta}_\alpha) = l$, $Q(\alpha;\boldsymbol{\theta}_\alpha) = x_\alpha$, $Q(0.5;\boldsymbol{\theta}_\alpha) = x_{0.5}$, $Q(1-\alpha;\boldsymbol{\theta}_\alpha) = x_{1-\alpha}$, and $Q(1;\boldsymbol{\theta}_\alpha) = u$. That is, the distribution characterized by $Q(p;\boldsymbol{\theta}_\alpha)$ honors both the specified support bounds, and the assessed quantiles given by $\mathbf{x}_\alpha$, for any

[3] Due to its pervasiveness, we include cumulative probability and quantile function computations for the standard normal (Gaussian) distribution in our definition for "closed-form". Under this setup, the Johnson SB, SU, and SL (lognormal) distributions, for example, all have closed-form CDFs and quantile functions.

compatible $\boldsymbol{\theta}_\alpha$. We refer to this as the **maximally-feasible (MF) property**, within the context of our SPT structure. In this context, it is important to note that maximally-feasible (MF) does not necessarily guarantee that there exists a J-QPD distribution that satisfies a set of five consistent (p, x_p) pairs that are *not* of the SPT structure defined in Definitions 1 and 2; for example, the $\{0^{th}$, 25^{th}, 50^{th}, 95^{th}, $100^{th}\}$ percentiles, which [collectively] are not of SPT form for some $\alpha \in (0, 0.50)$.

(4) Closeness to Commonly-Named Distributions: $Q(p;\boldsymbol{\theta}_\alpha)$ closely approximates the quantile function of numerous commonly-named distributions that share the same $\boldsymbol{\theta}_\alpha$; i.e., the same α-SPT and support. In the case of bounded support, we would like the distribution family to closely approximate the ∩- (bell-), J-, and U-shaped distributions contained in the beta family. For semi-bounded support, we would like the distribution family to closely approximate the shapes of the lognormal, gamma, inverse-gamma, and beta-prime distributions. We introduce measures of *closeness* in Chapter 6.

(5) Highly Flexible: By *flexibility*, we specifically refer to the span of a system within the skewness-kurtosis space developed by Pearson (1895, 1901, 1916), which we discuss in more detail in Chapter 6.

There are several recently-proposed distributions that nearly meet these five desiderata. Maximum-entropy methods presented in Abbas (2003a and 2003b) seek to add no additional information to an uncertainty other than the assessed quantile-probability pairs, by assigning uniform conditional distributions between adjacent percentile assessments – recall the example in Figure 1.8. These methods (and their variants) are maximally-feasible within our construct, and have closed-form PDFs, CDFs, and quantile functions. The same applies to the General Segmented Distributions (GSD)

proposed by Vander Wielen and Vander Wielen (2015), among others[4], and to discrete approximations. However, if knowledge of smoothness is present, then the unwarranted "kinks" (discontinuous derivatives) inherent in these distributions may less-accurately represent an expert's knowledge, as suggested in Keelin (2016) and Garthwaite et al. (2005).

Also, due to their lumpy nature, these distributions generally fail to satisfy Desiderata 4, which is motivated in part by the desire for our distributions to be able to capture phenomena whose distribution is derived from a well-known underlying physical process – what Keelin (2016) refers to as Type I distributions. Examples include: the normal (lognormal) distributions, which approximately occur as the summation (product) of independent or weakly-dependent random variables due to Central Limit Theorem (CLT) effects; exponential distributions for inter-arrival times within a Poisson Process; Weibull distributions, and related extensions[5], in reliability theory for modeling the time between adjacent component failures in complex systems. Unlike straight-line, maximum entropy, GSD, etc., our inherently smooth J-QPD distributions presented in this chapter precisely subsume the pervasive normal and lognormal distributions as special cases, but can also approximate Weibull, gamma, beta, and numerous other commonly-named distributions with potent accuracy, using a single system. Moreover, we show that J-QPD, while smooth, can approximate triangular distributions with reasonable accuracy.

Illustrative Examples

In this chapter, we rely on two illustrative examples (bounded and semi-bounded support) to demonstrate our new distribution system. In the case of bounded support, suppose an expert has been asked to assess peak market share for a new product and provides {10^{th},

[4] See, for example: Kotz and Van Dorp (2002a, 2002b, 2006), and Herrerias-Velasco et al. (2009).
[5] For example, see Mudholkar and Srivastava (1993).

50^{th}, 90^{th}} percentiles of {60, 70, 90} %, respectively, so that in this case, $\boldsymbol{\theta}_{0.10}$ = (0, 0.6, 0.7, 0.9, 1) in decimal form. Figure 4.1 presents the CDF for the best fit beta distribution for this SPT of assessments, subject to honoring the bounds[6]. There is no beta distribution satisfying all five points in $\boldsymbol{\theta}_{0.10}$, since generalized beta distributions are specified by four points, and thus the best we can do is fit a distribution through these five given points.

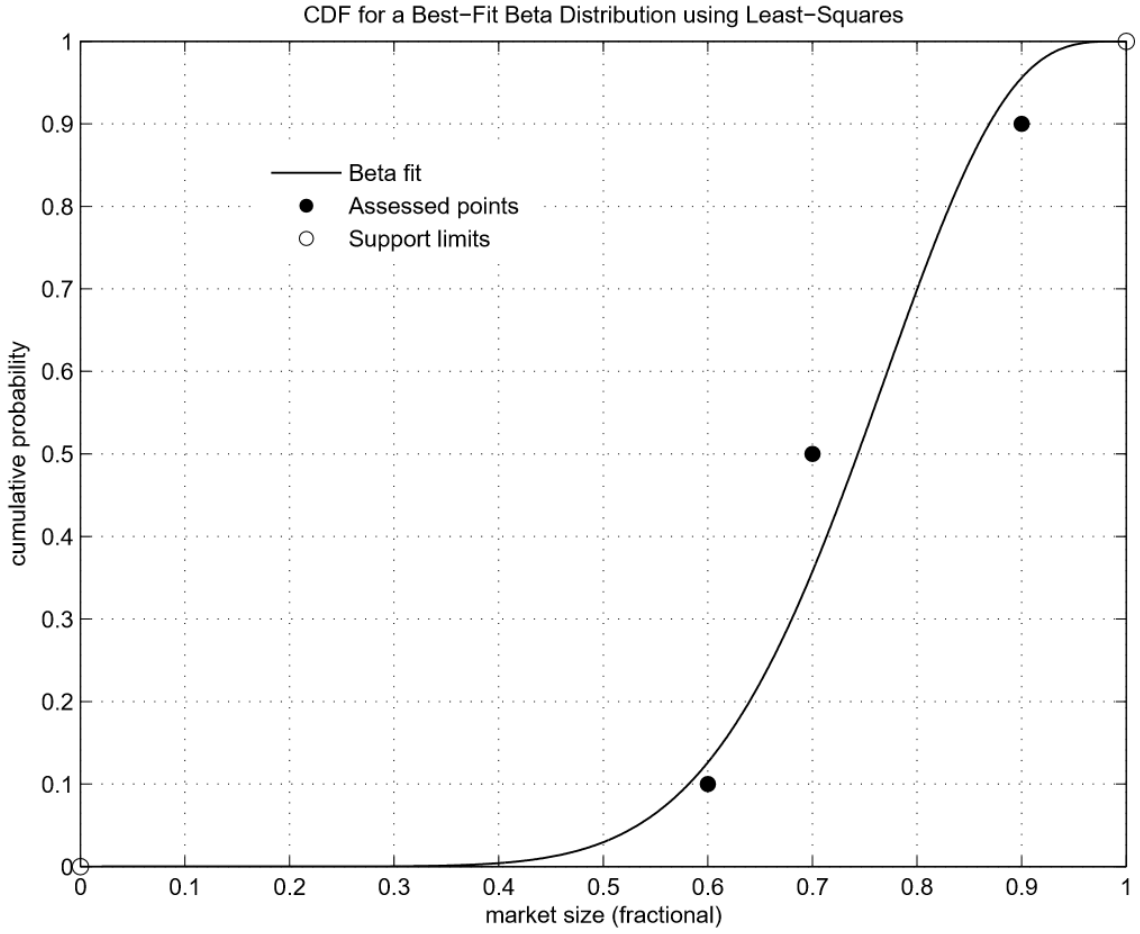

Figure 4.1. Beta Least-Squares Fit for $\boldsymbol{\theta}_{0.10}$ = (0, 0.32, 0.40, 0.60, 1).

Alternatively, Figure 4.2 presents an example with semi-bounded support. In this case, an expert is assessing the uncertainty surrounding the capital expenditures

[6] We want to eliminate the possibility of negative market shares, or shares that exceed market size.

(CAPEX) of a drilling venture and provides $\boldsymbol{\theta}_{0.10} = (0, 30, 40, 60, \infty)$ \$MM[7]. Figure 4.2 shows least-squares fits for $\boldsymbol{\theta}_{0.10} = (0, 30, 40, 60, \infty)$ using lognormal and Weibull distributions. In this case, there is no distribution within the Weibull or lognormal families that honors $\boldsymbol{\theta}_{0.10}$. Also, while not shown, no gamma or beta-prime distribution honors $\boldsymbol{\theta}_{0.10}$ either.

In the market share (CAPEX) example, the least-squares fit entails solving a non-linear optimization problem over the shape parameters for the beta (lognormal, Weibull) distribution(s), to minimize mean-squared error. More importantly, however, the commonly-named distributions selected for the fit in each case do not honor $\boldsymbol{\theta}_{0.10}$. Thus, the beta, Weibull, lognormal, and gamma distributions fail to satisfy Desideratum 1 (quantile-parameterized) and 3 (maximally-feasible). More generally, distributions within the flexible family developed by Pearson (1895, 1901, and 1916) also fail to satisfy Desiderata 1 and 3, including: beta, beta-prime, gamma, inverse-gamma, and Type IV.

[7] Of course, CAPEX cannot be infinite. Assuming it is unbounded above is a modeling decision representing the fact that the upper bound is unknown and possibly several orders of magnitude larger than the 90th percentile.

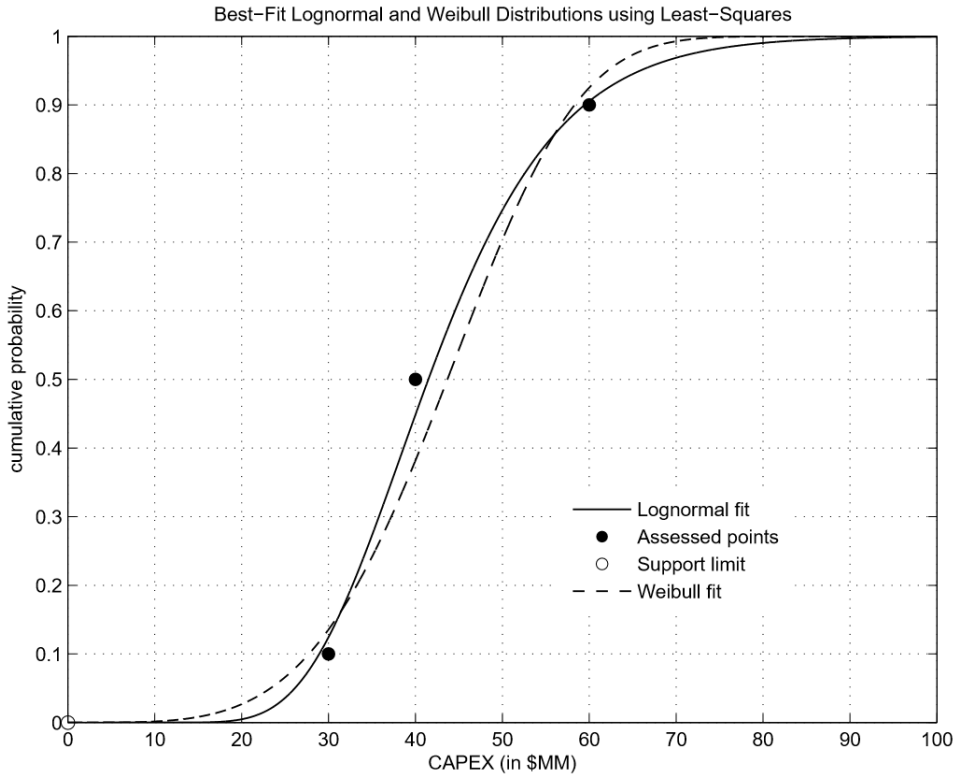

Figure 4.2. Least-Squares Fits for $\boldsymbol{\theta}_{0.10} = (0, 30, 40, 60, \infty)$.

We could, however, find distributions for the market share and CAPEX examples by using the Metalog distributions. To compare apples to apples, we use the bounded three-term Metalog distribution for the market share example, and the semi-bounded three-term Metalog distribution for the CAPEX example. Figure 4.3 displays the CDFs for the corresponding Metalog assignments for both the market share and CAPEX examples, including their corresponding quantile function expressions[8].

[8] See Keelin (2016), pages 269–271, for more information on how to obtain these distribution assignments.

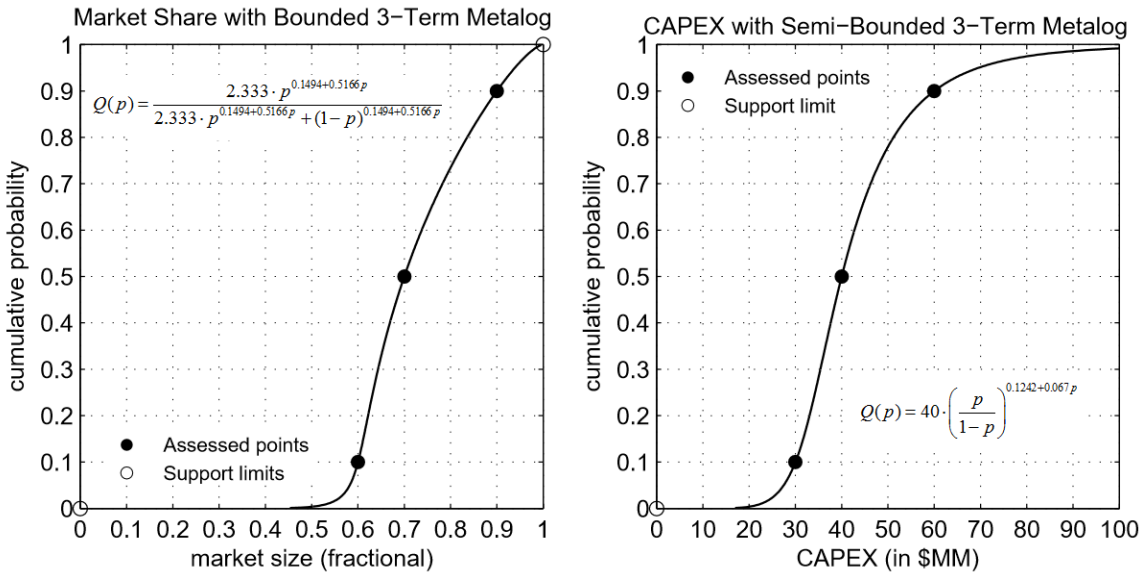

Figure 4.3. Metalog Assignments (CDFs) for Market Share and CAPEX Examples.

Thus, unlike the beta distribution, the Metalog satisfies Desideratum 1 (quantile parameterized), by design. However, the quantile function expressions shown in Figure 4.3 are not invertible, and thus Metalog does not satisfy Desideratum 2 (availability of the CDF). More importantly, however, Metalog does not satisfy Desideratum 3 (maximally-feasible). To illustrate, consider a more skewed version of the market share example where the expert instead provides $\mathbf{\theta}_{0.10}$ = (0, 0.7, 0.75, 0.95, 1). Figure 4.4 shows the corresponding bounded three-term Metalog assignment for $\mathbf{\theta}_{0.10}$ in this case. Although this Metalog assignment satisfies $\mathbf{\theta}_{0.1}$, it is not a valid CDF because it is not a function and violates the monotonicity of percentiles; for example, the 20th percentile shown is less than the 10th percentile shown. Thus, we say that $\mathbf{\theta}_{0.10}$ = (0, 0.7, 0.75, 0.95, 1) is infeasible for the three-term Metalog system, thus illustrating that the Metalog system does not satisfy Desideratum 3 (maximally-feasible) as defined in terms of our α-SPT context. Alternatively, as we show in the next section, our new J-QPD system meets our desiderata outlined above. The J-QPD system consists of two major subfamilies:

(1) J-QPD-B (bounded): Has finite lower and upper support bounds, [l, u], and is parameterized by any compatible $\boldsymbol{\theta}_\alpha = (l, \mathbf{x}_\alpha, u)$.

(2) J-QPD-S (semi-bounded): Has support on [l, ∞) and is parameterized by any compatible $\boldsymbol{\theta}_\alpha = (l, \mathbf{x}_\alpha, u)$.

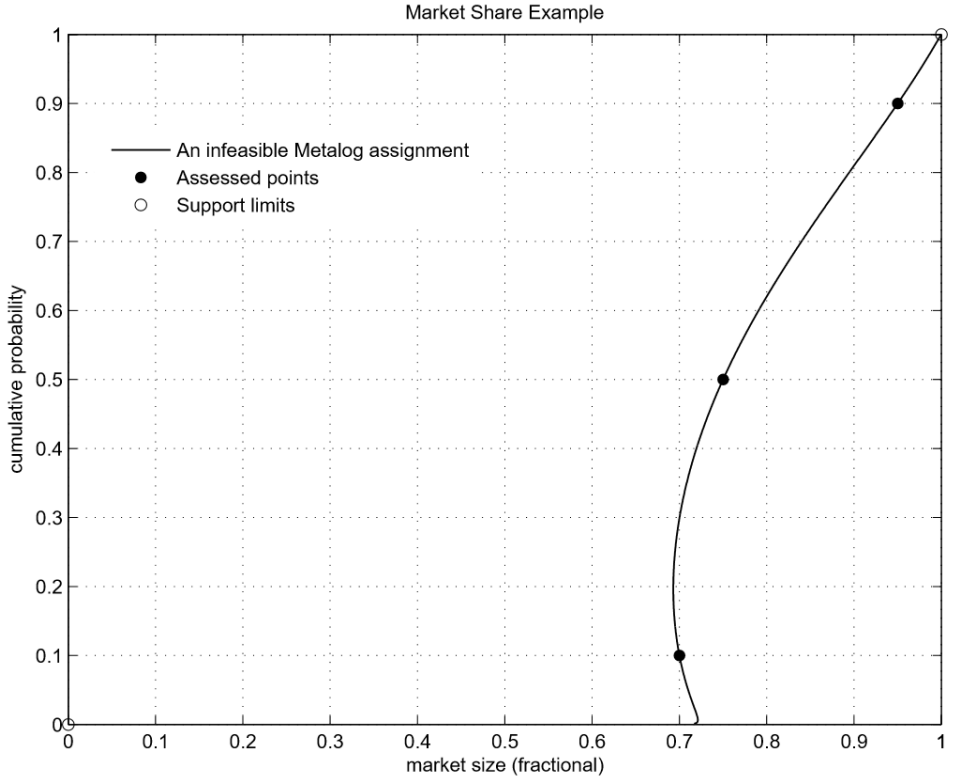

Figure 4.4. Bounded 3-Term Metalog Assignment for $\boldsymbol{\theta}_{0.1} = (0, 0.7, 0.75, 0.95, 1)$.

DESIGNING THE NEW J-QPD DISTRIBUTION SYSTEM

In this section, we design our new J-QPD system, using the Johnson SU system as a basis for construction, and the five desiderata as a basis of design.

Engineering the Support of the JDS

One of the most powerful methods for engineering the support of a distribution is by the use of a Q-transformation. Recall the Q-Transformation Rule (QTR), adopted from Gilchrist (2000), is as follows:

The Q-Transformation Rule (QTR) – If $T(x)$ is a non-decreasing function of x, and $Q(p)$ is a quantile function, then $T(Q(p))$ is a quantile function.

A corollary of the QTR is that if X is a random variable with quantile function given by $Q(p)$, then the quantile function of the transformed variable, $Y=T(X)$, is $T(Q(p))$ (Gilchrist 2000). One well-known Q-transformation used to transform a distribution with support on $(-\infty, \infty)$ into a distribution with support on [0,1], is by applying the *inverse-probit Q-transformation* (IP-QT) to its quantile function. The IP-QT is simply the CDF of the standard normal distribution: $T(x) = \Phi(x)$.

The J-QPD-B Distributions

Recall that SU distributions have support on $(-\infty, \infty)$. To obtain a distribution having arbitrary, finite support bounds, $\{l, u\}$, a natural idea is to apply the well-known IP-QT to the SU quantile function, followed by shifting and scaling to satisfy $\{l, u\}$:

$$Q_1(p) = l + (u-l)\Phi\left(Q_{SU}(p)\right) = l + (u-l)\Phi\left(\xi + \lambda \sinh\left(\delta\left(\Phi^{-1}(p) + \gamma\right)\right)\right). \qquad (4.3)$$

The QTR guarantees that $Q_1(p)$ is a quantile function, corresponding to a distribution with support on $[l, u]$, as long as we maintain the SU parameter requirements: $\lambda > 0$, $\delta > 0$. Now, we desire for $Q_1(p)$ to be fully parameterized by any compatible $\boldsymbol{\theta}_\alpha$. By inspection, l and u correspond to the 0^{th} and 100^{th} percentiles, respectively, as desired.

With $\{l, u\}$ specified, we have four unknowns: $\{\lambda, \delta, \gamma, \xi\}$. However, we can only produce three non-degenerate equations with the low-base-high assessments given in the SPT[9]: $\mathbf{x}_\alpha$. A natural idea is to fix one of the parameters, but it is not immediately obvious what constitutes good choices for the fixed parameter and corresponding value(s). Since $Q_1(p)$ is invertible (Desideratum 2), we focus on Desideratum 1 (quantile-parameterized)

[9] Recall that the SU distributions have two shape parameters in $\{\delta, \gamma\}$. Applying the inverse-probit Q-transformation transforms the location and scale parameters, $\{\xi, \lambda\}$, into shape parameters as well, yielding a total of four shape parameters in the transformed distribution. However, since an SPT on (0, 1) amounts to three shape parameters, we seek to remove one of the four shape parameters from $Q_1(p)$.

and 3 (maximally-feasible) in making a strategic selection for the choice of the fixed parameter. In particular, the choice of the fixed parameter and value should yield a quantile function that:

i. Can accommodate any compatible $\boldsymbol{\theta}_\alpha$ (Desideratum 3).

ii. Is easy to re-parameterize in terms of $\boldsymbol{\theta}_\alpha = (l, \mathbf{x}_\alpha, u)$ (Desideratum 1).

Consider any given real number, $c > 0$. As we soon show, allowing γ to assume one of three possible values, $\{-c, 0, c\}$, yields a quantile function that satisfies (i) for any $c > 0$. It turns out that this property does not hold when fixing values for $\{\lambda, \delta, \xi\}$. In choosing a specific value for c, we now bear (ii) in mind. Letting $c = \Phi^{-1}(1-\alpha)$ results in a simple, explicit solution to the distribution parameters in terms of $\boldsymbol{\theta}_\alpha = (l, \mathbf{x}_\alpha, u)$. For assessments and bounds jointly given in $\boldsymbol{\theta}_\alpha = (l, \mathbf{x}_\alpha, u)$, the resulting quantile function for the J-QPD-B distributions, is:

$$Q_B(p) = l + (u-l)\Phi\left(\xi + \lambda \sinh\left(\delta\left(\Phi^{-1}(p) + nc\right)\right)\right). \tag{4.4}$$

where,

$$c = \Phi^{-1}(1-\alpha),$$

$$L = \Phi^{-1}\left(\frac{x_\alpha - l}{u-l}\right),\ B = \Phi^{-1}\left(\frac{x_{0.50} - l}{u-l}\right),\ H = \Phi^{-1}\left(\frac{x_{1-\alpha} - l}{u-l}\right),$$

$$n = \operatorname{sgn}(L + H - 2B),$$

$$\xi = \begin{cases} L, & n = 1 \\ B, & n = 0 \\ H, & n = -1 \end{cases}$$

$$\delta = \left(\frac{1}{c}\right)\cosh^{-1}\left(\frac{H-L}{2\min(B-L, H-B)}\right),$$

$$\lambda = \frac{H-L}{\sinh(2\delta c)}.$$

Note the following observations regarding equation (4.4):

(1) $\{\lambda, \delta, \xi\}$ are all specified directly in terms of $\boldsymbol{\theta}_\alpha$, along with constant c and parameter n (which assumes {-1, 0, 1}, depending on the values of $(l, \mathbf{x}_\alpha, u)$.

(2) One can easily verify that:

- $Q_B(0) = l$
- $Q_B(\alpha) = x_\alpha$
- $Q_B(0.5) = x_{0.50}$
- $Q_B(1-\alpha) = x_{1-\alpha}$
- $Q_B(1) = u$

(3) Given the simple invertible form of the J-QPD-B quantile function, we can also produce the CDF (Desideratum 2):

$$F_B(x) = \Phi\left(\left(\frac{1}{\delta}\right)\sinh^{-1}\left(\left(\frac{1}{\lambda}\right)\left(\Phi^{-1}\left(\frac{x-l}{u-l}\right)-\xi\right)\right)-nc\right). \tag{4.5}$$

(4) Recall that sgn(0) = 0. Examining the expression for n in (4.4) above, this occurs ($n = 0$) when: $L + H - 2B = 0$.

$L + H - 2B = 0 \rightarrow \delta = 0, \lambda = \infty$.

Thus, this case violates the parameter requirements ($\delta > 0$) as is. However, we note the following:

$$\lim_{y\to 0}\frac{\sinh(y)}{y} = 1 \rightarrow \lim_{\delta\to 0}\frac{\lambda\sinh\left(\delta\left(\Phi^{-1}(p)+nc\right)\right)}{\lambda\delta\left(\Phi^{-1}(p)+nc\right)} = 1.$$

However,

$$\lim_{\delta\to 0}\lambda\delta = \lim_{\delta\to 0}\frac{\delta(H-L)}{\sinh(2\delta c)} = \frac{H-L}{2c}.$$

Therefore, for the special case in which $n = 0$, we define the quantile function in (4.4) as follows:

$$Q_B(p) = l + (u-l)\Phi\left(B + \left(\frac{H-L}{2c}\right)\Phi^{-1}(p)\right). \tag{4.6}$$

Illustrative Example

To illustrate, we now revisit the market share example. Given $\boldsymbol{\theta}_{0.10} = (0, 0.6, 0.7, 0.9, 1)$, and using the expressions given in (4.4), we compute the parameters and construct the corresponding J-QPD-B quantile function assignment as follows:

$$c = \Phi^{-1}(1-\alpha) = \Phi^{-1}(0.90) = 1.2816,$$

$$L = \Phi^{-1}\left(\frac{x_{\alpha} - l}{u - l}\right) = \Phi^{-1}\left(0.6\right) = 0.2533,$$

$$B = \Phi^{-1}\left(\frac{x_{0.50} - l}{u - l}\right) = \Phi^{-1}\left(0.7\right) = 0.5244,$$

$$H = \Phi^{-1}\left(\frac{x_{1-\alpha} - l}{u - l}\right) = \Phi^{-1}\left(0.9\right) = 1.2816,$$

$$n = \text{sgn}(L + H - 2B) = \text{sgn}(0.2533 + 1.2816 - 2(0.5244)) = 1,$$

$$\xi = \begin{cases} L, & n = 1 \\ B, & n = 0 \\ H, & n = -1 \end{cases} = L = -0.2533,$$

$$\delta = \left(\frac{1}{c}\right)\cosh^{-1}\left(\frac{H - L}{2\min(B - L, H - B)}\right) = 0.9794,$$

$$\lambda = \frac{H - L}{\sinh(2\delta c)} = 0.1682,$$

$$Q_B(p) = l + (u - l)\Phi(\xi + \lambda \sinh(\delta(\Phi^{-1}(p) + nc))) \,.$$

Thus,

$$Q_B(p) = \Phi\left(-0.2533 + 0.1682 \cdot \sinh\left(0.9794\left(\Phi^{-1}(p) + 1.2816\right)\right)\right).$$

Figure 4.5 provides a plot of this J-QPD-B assignment. Using this newly-constructed quantile function, one can easily confirm that:

$$Q_B(0) = 0,\ Q_B(0.10) = 0.6,\ Q_B(0.50) = 0.7,\ Q_B(0.90) = 0.9,\ Q_B(1) = 1.$$

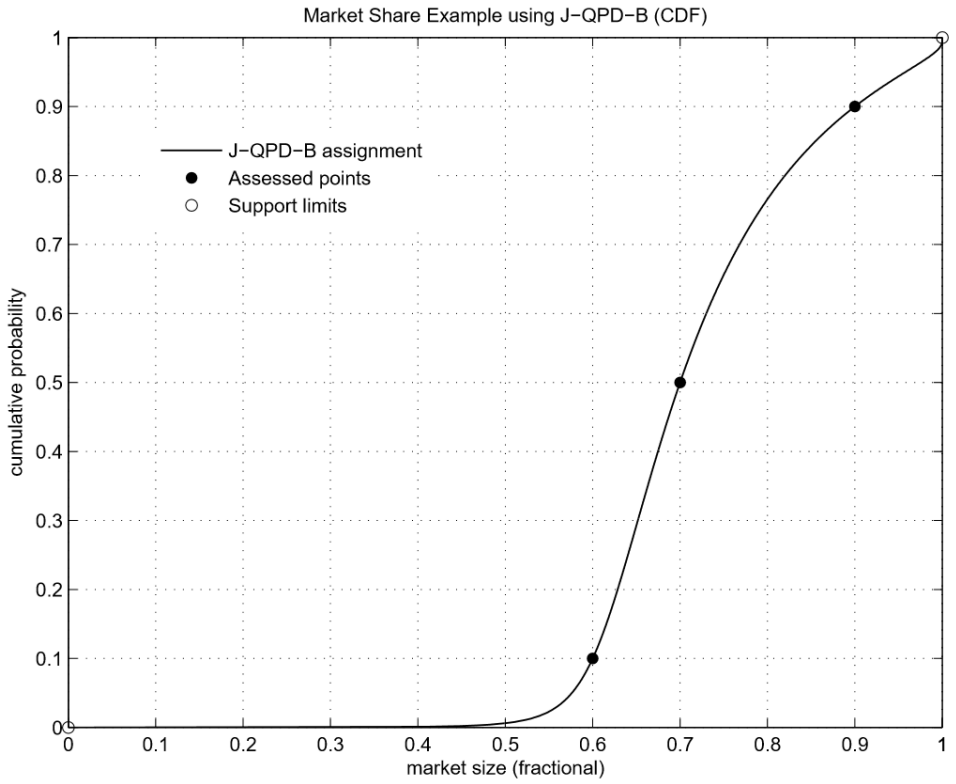

Figure 4.5. J-QPD-B Assignment for $\boldsymbol{\theta}_{0.10} = (0, 0.6, 0.7, 0.9, 1)$.

The J-QPD-S Distributions

While a finite lower limit of support is sensible for many physical quantities (e.g., non-negativity), experts and/or analysts may not always deem it appropriate to impose a finite value for an upper bound, u. Thus, we now develop the J-QPD-S distributions, designed to have support on $[l, \infty)$, by once again starting with the SU distributions.

Since SU distributions have support on $(-\infty, \infty)$, to obtain a distribution having support on $[l, \infty)$ (for some specified l), a natural idea is to apply the well-known exponential Q-transformation (Exp) to the SU quantile function, along with shifting to satisfy l:

$$Q_1(p) = l + \exp\left(\xi + \lambda \sinh(\delta(\Phi^{-1}(p) + \gamma))\right)$$
$$= l + \theta \exp\left(\lambda \sinh(\delta(\Phi^{-1}(p) + \gamma))\right),\ \delta > 0,\ \lambda > 0,\ \theta = \exp(\xi).$$

$Q_1(p)$, as given, has infinite positive moments (see Appendix B for discussion). We thus embed one more strategically-chosen transformation within this quantile function, along with a re-parameterization analogous to the one we used for J-QPD-B[10]. Given $\boldsymbol{\theta}_\alpha = (l, \mathbf{x}_\alpha, \infty)$, where l is presumed specified and finite, the resulting quantile function for the J-QPD-S distributions, is:

$$Q_S(p) = l + \theta \exp\left(\lambda \sinh\left(\sinh^{-1}\left(\delta \Phi^{-1}(p)\right) + \sinh^{-1}(nc\delta)\right)\right), \tag{4.7}$$

where,

$$c = \Phi^{-1}(1-\alpha),$$

$$L = \log(x_\alpha - l),\ B = \log(x_{0.5} - l),\ H = \log(x_{1-\alpha} - l),$$

$$n = \text{sgn}(L + H - 2B)$$

$$\theta = \begin{cases} x_\alpha - l, & n = 1 \\ x_{0.50} - l, & n = 0 \\ x_{1-\alpha} - l, & n = -1 \end{cases}$$

$$\delta = \left(\frac{1}{c}\right)\sinh\left(\cosh^{-1}\left(\frac{H-L}{2\min(B-L, H-B)}\right)\right),$$

$$\lambda = \left(\frac{1}{\delta c}\right)\min(H-B, B-L).$$

(5) The application of the $\sinh^{-1}$ operator[11] in (4.7) results in all moments being finite (see Appendix C for a proof). Also, if $L + H - 2B = 0$, then $n = \text{sgn}(L + H - 2B) = \text{sgn}(0) = 0$, in which case we have:

$$Q_S(p) = l + \theta \exp\left(\lambda \sinh\left(\sinh^{-1}\left(\delta \Phi^{-1}(p)\right)\right)\right) = l + \theta \exp\left(\lambda \delta \Phi^{-1}(p)\right). \tag{4.8}$$

---

[10] Recall that the SU distributions have two shape parameters in $\{\delta, \gamma\}$. In this case, applying the "Exp" Q-transformation transforms only the scale parameter, λ, into a shape parameter, yielding a total of three shape parameters in the transformed distribution. However, since an SPT on $(0, \infty)$ amounts to two shape parameters, we seek to remove one of the three shape parameters from $Q_1(p)$.

[11] This work does not represent the first characterization of a distribution quantile function using a combination of the sinh and arcsinh operators. See Jones and Pewsey (2009) for the development and application of a "sinh-arcsinh" type transformation upon random variables to generate new probability distributions. To the best of our knowledge, however, our particular combination of sinh and arcsinh applications, along with our strategic re-parameterization amounts to a novel probability distribution system parameterized by quantiles.

That is, we precisely recover a lognormal distribution with $\mu = \log(\theta) = \log(x_{0.5} - l)$ and $\sigma = \lambda\delta = (H–B)/c$, and shifted to have support on $[l, \infty)$. Thus, J-QPD-S is a generalization of lognormal distributions, but parameterized by any compatible SPT and specified lower bound (Desideratum 1), and effectively having two shape parameters, (λ, δ), whereas lognormal distributions only have the single shape parameter, σ. Recall that the Burr, Dagum, and Exponentiated Weibull distributions all have semi-bounded support and two shape parameters, like J-QPD-S. However, we illustrate in Chapter 5 that unlike J-QPD-S, these systems are not maximally-feasible.

As with J-QPD-B, we can obtain the CDF (Desideratum 2) of J-QPD-S by inverting its quantile function given in (4.7). This yields:

$$F_S(x) = \Phi\left(\left(\frac{1}{\delta}\right)\sinh\left(\sinh^{-1}\left(\left(\frac{1}{\lambda}\right)\log\left(\frac{x-l}{\theta}\right)\right) - \sinh^{-1}(nc\delta)\right)\right) \tag{4.9}$$

Illustrative Example

We now apply J-QPD-S to the CAPEX example introduced previously, in which $\boldsymbol{\theta}_{0.10}$ = (0, 30, 40, 60, ∞) \$MM. Using the expressions given in (4.7), we obtain the following quantile function assignment:

$$Q_S(p) = 30 \cdot \exp\left(0.4282 \cdot \sinh\left(0.6294 + \sinh^{-1}\left(0.5242 \cdot \Phi^{-1}(p)\right)\right)\right).$$

Figure 4.6 shows the CDF and PDF for the CAPEX example. Like J-QPD-B in the market share example, notice in Figure 4.6 that the J-QPD-S assignment precisely honors the low-base-high assessments – in this case, the {10th, 50th, 90th} percentile assessment values of {30, 40, 60} \$MM – and the specified lower limit of support (zero, in this case). Thus far, we have demonstrated that J-QPD-S satisfies Desiderata 1 and 2. In the next chapter, we demonstrate its conformity to Desideratum 3, the *maximally-feasible* (MF) property.

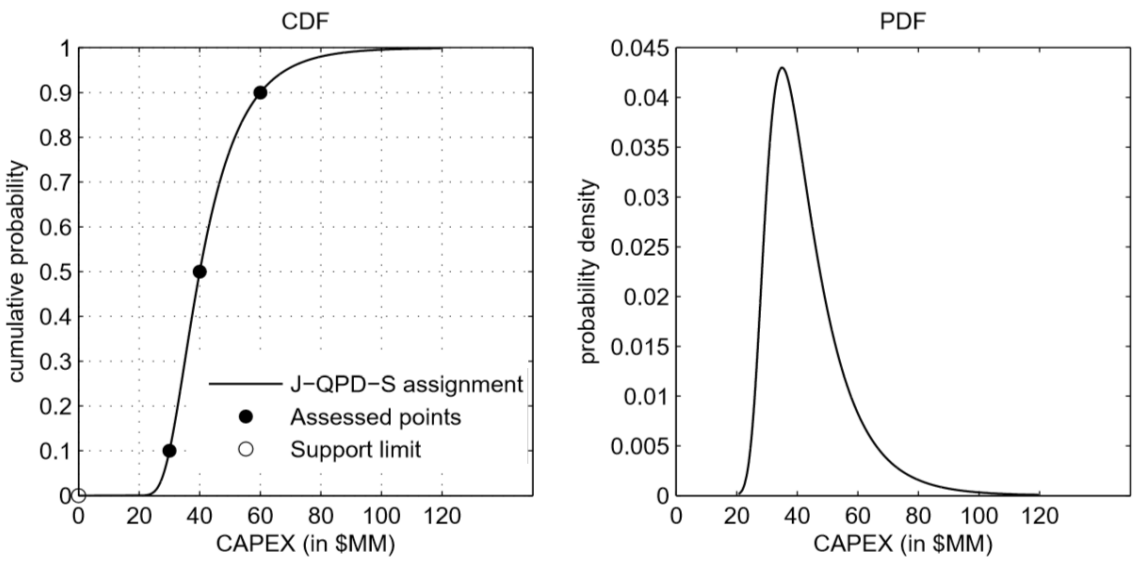

Figure 4.6. J-QPD-S Assignment for the CAPEX Example.

Chapter 5 : The Maximally-Feasible Property of the J-QPD System[1]

We now establish the *maximally-feasible* (MF) property for the J-QPD-B (bounded) and J-QPD-S (semi-bounded) distribution systems, and then compare the extent of their feasibility to that of several commonly-named distributions. We begin with J-QPD-S, since it has one less degree of freedom (four parameters instead of the five needed for J-QPD-B, not counting α, which is also a shape parameter), and can thus be more intuitively described in terms of feasibility than J-QPD-B.

THE MF PROPERTY FOR THE J-QPD-S DISTRIBUTIONS

We present the MF property for J-QPD-S (Desideratum 3), and then lend intuition to the property by providing a visual comparison of the feasibility of J-QPD-S distributions with respect to several named distributions.

Proposition 1 (MF Property). Consider any compatible $\boldsymbol{\theta}_\alpha = (l, \mathbf{x}_\alpha, \infty)$. There exists a unique quantile function, Q, characterized by (4.7), that satisfies:

- $Q_S(0) = l$,
- $Q_S(\alpha) = x_\alpha$,
- $Q_S(0.5) = x_{0.5}$,
- $Q_S(1-\alpha) = x_{1-\alpha}$,
- $Q_S(1) = \infty$.

Proof. See Appendix D.

Proposition 1 implies that J-QPD-S provides a unique (and feasible) probability distribution assignment for each compatible $\boldsymbol{\theta}_\alpha = (l, \mathbf{x}_\alpha, \infty)$ vector. Since J-QPD-S has semi-bounded support and *two* shape parameters (for each given α), we can compare the

[1] Summaries of the results of this chapter are published with my advisor, Eric Bickel, in the following: Hadlock, Christopher and J. Eric Bickel. 2017. Johnson Quantile-Parameterized Distributions. *Decision Analysis* **14**(1) 35-64.

extent of their feasibility to several existing distribution systems also having semi-bounded support and two shape parameters, using a *two*-dimensional region. Without loss of generality, we normalize J-QPD-S by removing location and scale. Fix any $\alpha \in (0, 0.50)$, and consider the following normalizing measures:

$$s_\alpha = \frac{x_{0.50} - l}{x_{1-\alpha} - l}, \tag{5.1}$$

$$t_\alpha = \frac{x_\alpha - l}{x_{0.50} - l}. \tag{5.2}$$

Note that s_α and t_α are normalized quantities used to depict the span of a distribution's feasibility – the span of compatible $\boldsymbol{\theta}_\alpha$ vectors that a system can satisfy, within the context of our SPT setup - rather than direct measures of "shape" (e.g., skewness, or tail-width). Reference Chapter 2 and the footnotes in Chapter 7 for measures of shape. Note the following important observations:

- s_α and t_α are invariant to changes of location or scale.
- Since $l = Q(0)$, by the monotonicity of percentiles, s_α and t_α are bounded between zero and one.
- For each $\alpha \in (0, 0.50)$, all non-degenerate univariate probability distributions live in the unit square defined by: $s_\alpha \in [0,1],\ t_\alpha \in [0,1]$.

Figure 5.1 shows the span of the Burr, Dagum, EW, and J-QPD-S systems in the $\{s_\alpha, t_\alpha\}$ space[2] for $\alpha = 0.1$. The normal and exponential distributions occur as *points* in the $\{s_\alpha, t_\alpha\}$ space, since they lack shape parameters. Recall that exponential distributions are a special case of Weibull distributions, which are a special case of the EW system. The normal distribution occurs as a limiting case for the Burr, Dagum, and J-QPD-S distributions. Since the Weibull (lognormal) distributions have one shape parameter, they

[2] We also present the span of the beta-prime distributions in Chapter 6, where we compare the closeness of J-QPD to commonly-named distributions.

occur as *curves* in the $\{s_\alpha, t_\alpha\}$ space shown in panel c (d) of Figure 5.1. The lognormal distributions occur as the line segment, $s_\alpha = t_\alpha$, in the $\{s_\alpha, t_\alpha\}$ space, for each $\alpha \in (0, 0.50)$.

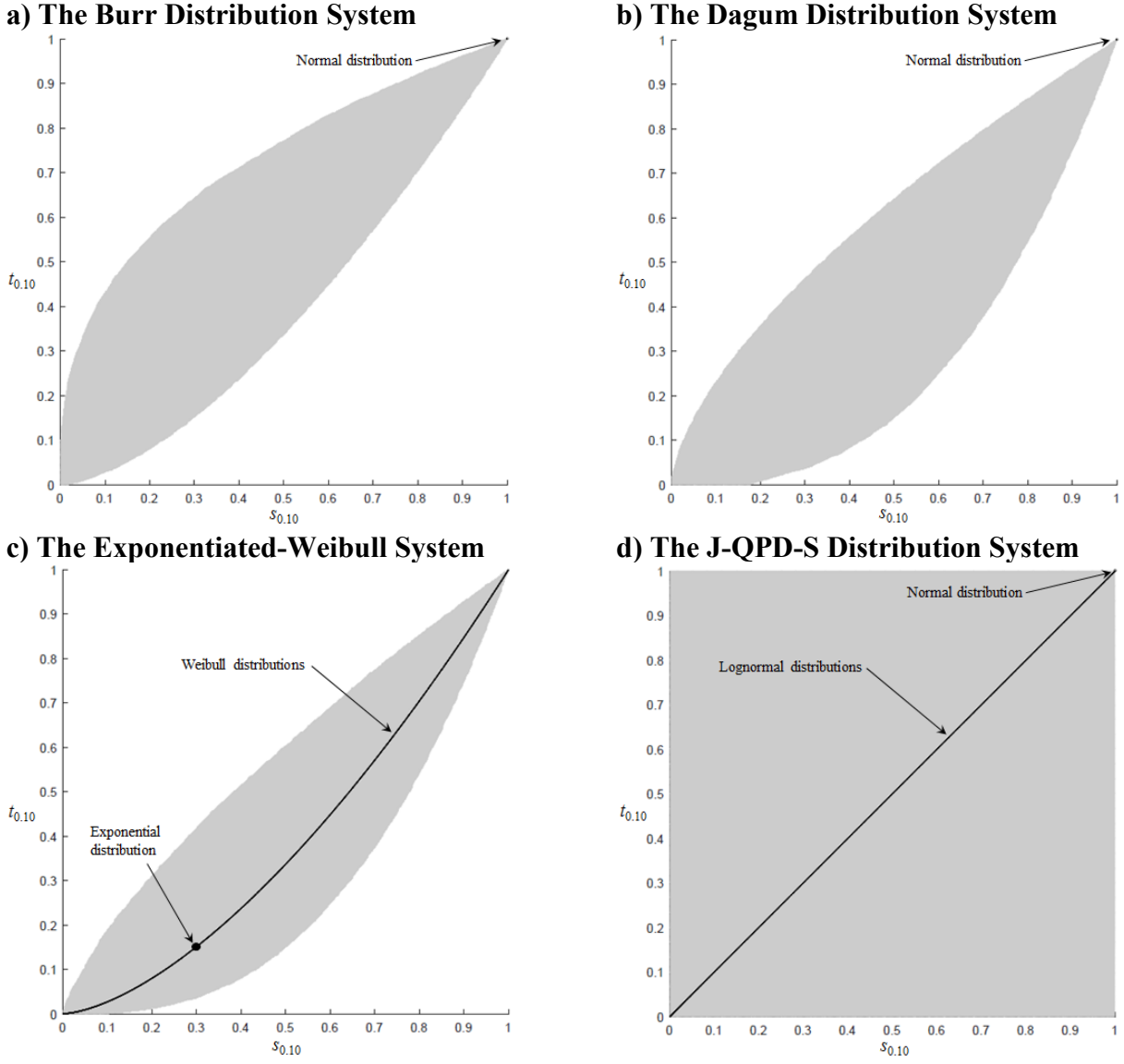

Figure 5.1. Span of the Burr, Dagum, EW, and J-QPD-S systems in the $\{s_{0.1}, t_{0.1}\}$ Space.

Due to the presence of two shape parameters, the entirety of the Burr, Dagum, and EW systems occupy a two-dimensional (shaded) *area* within the $\{s_\alpha, t_\alpha\}$ space, as shown in panels a, b, and c of Figure 5.1 (respectively). Since Dagum distributions correspond to

the reciprocal of Burr-distributed random variables, their span within the $\{s_\alpha, t_\alpha\}$ space occurs as the mirror image of the span of the Burr system about the line: $s_\alpha = t_\alpha$. Since the Burr, Dagum, and EW systems do no occupy the entire interior of the unit square defined by: $s_\alpha \in (0,1)$, $t_\alpha \in (0,1)$, this implies that they are not maximally-feasible. By contrast, the MF property of the J-QPD-S system implies that these distributions span the entire interior of the $\{s_\alpha, t_\alpha\}$ space, as shown in Figure 5.1 (panel d). We revisit the $\{s_\alpha, t_\alpha\}$ space in Chapter 6, where we compare the closeness (Desideratum 4) of J-QPD distributions to a vast array of commonly-named distributions.

Figure 5.2 provides several examples of J-QPD-S PDFs, parameterized by various $\{s_{0.10}, t_{0.10}\}$ pairs, for the case in which $l = 0$ (i.e., support on $(0, \infty)$) and $x_{0.50} = 1$. The yellow and purple curves are precisely lognormal distributions, since they both correspond to the special case in which $s_\alpha = t_\alpha$. However, since J-QPD-S distributions possess an additional shape parameter over lognormal distributions (two additional shape parameters if we count α), we can produce additional shapes. The green curve represents a "near-lognormal" shape, the blue curve a bimodal shape, and the orange curve corresponds to transitional shapes between unimodal and bimodal forms.

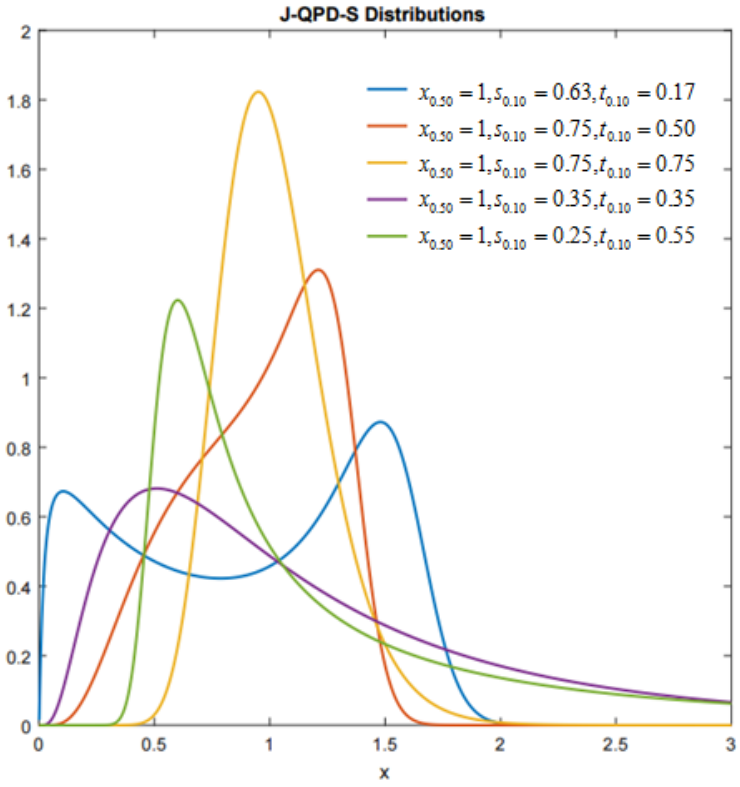

Figure 5.2. Examples of Additional Shapes Produced by J-QPD-S Distributions.

THE MF PROPERTY FOR THE J-QPD-B DISTRIBUTIONS

Recall that the J-QPD-B distributions have a total of five degrees of freedom – location, scale, and three shape parameters, not counting α. Thus, the MF property for the J-QPD-B distributions essentially has the same conceptual definition as that for the J-QPD-S distributions, but instead applies to the five-dimensional vector given in: $\boldsymbol{\theta}_\alpha = (l, \mathbf{x}_\alpha, u) = (l, x_\alpha, x_{0.50}, x_{1-\alpha}, u)$.

Proposition 2 (MF Property). Consider any compatible $\boldsymbol{\theta}_\alpha = (l, \mathbf{x}_\alpha, u) = (l, x_\alpha, x_{0.50}, x_{1-\alpha}, u)$. There exists a unique quantile function, Q, characterized by (4.4), that satisfies:

- $Q_B(0) = l$,
- $Q_B(\alpha) = x_\alpha$,

- $Q_B(0.5) = x_{0.5}$,
- $Q_B(1-\alpha) = x_{1-\alpha}$,
- $Q_B(1) = u$.

Proof. See Appendix A.

Since J-QPD-B distributions possess three shape parameters (again, for each given α), we need a three-dimensional space to visually depict the MF property in this case. Without loss of generality, we can remove location and scale by only considering vectors, $\boldsymbol{\theta}_\alpha = (l, \mathbf{x}_\alpha, u) = (l, x_\alpha, x_{0.50}, x_{1-\alpha}, u)$, having $\{l, u\} = \{0, 1\}$. For any given $\alpha \in (0, 0.50)$, Figure 5.3 shows the polyhedron corresponding to every such compatible $\boldsymbol{\theta}_\alpha$; i.e., every possible triplet, $\{x_\alpha, x_{0.50}, x_{1-\alpha}\}$, such that $0 < x_\alpha, < x_{0.50}, < x_{1-\alpha} < 1$, which corresponds to the span of the J-QPD-B system (by the MF property).

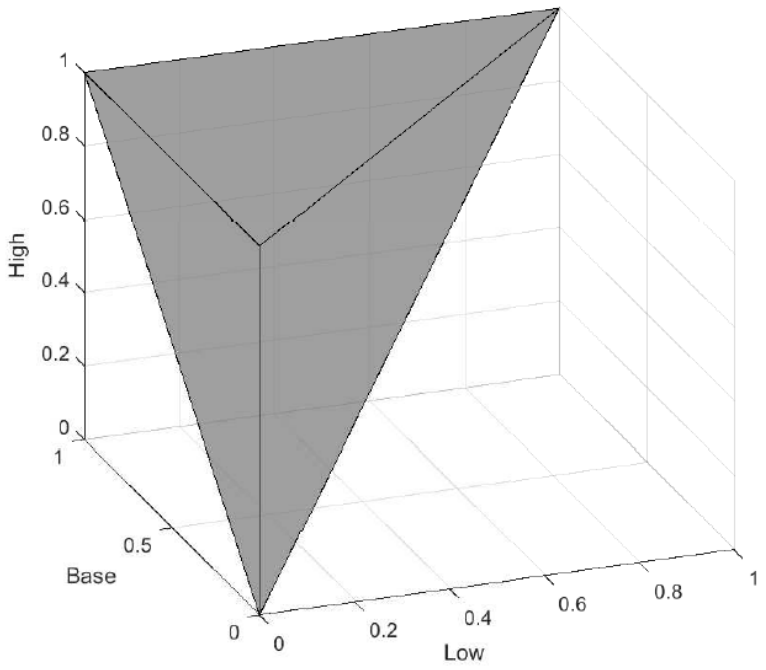

Figure 5.3. Span of the J-QPD-B system for $\{l, u\} = \{0, 1\}$ and any $\alpha \in (0, 0.5)$.

There are no commonly-named distributions having bounded support and three shape parameters. Alternatively, most named distributions having bounded support have two shape parameters. These include, to name a few:

- The beta distributions.
- The Johnson (1949) SB distributions.
- The logit-normal distributions[3].
- The Kumaraswamy (1980) distributions.

Illustrative Examples

Recall the revised market share example from Figure 4.4, where $\mathbf{\theta}_{0.1} = (0, 0.7, 0.75, 0.95, 1)$, and where the three-term bounded Metalog results in infeasibility. If we apply the J-QPD-B distribution to these five points, we obtain the following quantile function:

[3] See Aitchison and Shen (1980), or Mead (1965).

$$Q_B(p) = \Phi\left(0.5244 + 0.0417 \cdot \sinh\left(1.5542 \cdot \left(\Phi^{-1}(p) + 1.2816\right)\right)\right).$$

Figure 5.4 provides a plot of this J-QPD-B assignment. The odd shape is due to the unusual percentile spacing in this example. However, the point is to illustrate the MF property, by showing that the J-QPD-B distribution produces a valid quantile function exactly honoring $\boldsymbol{\theta}_{\alpha}$, where the Metalog fails, as we saw in Figure 4.4.

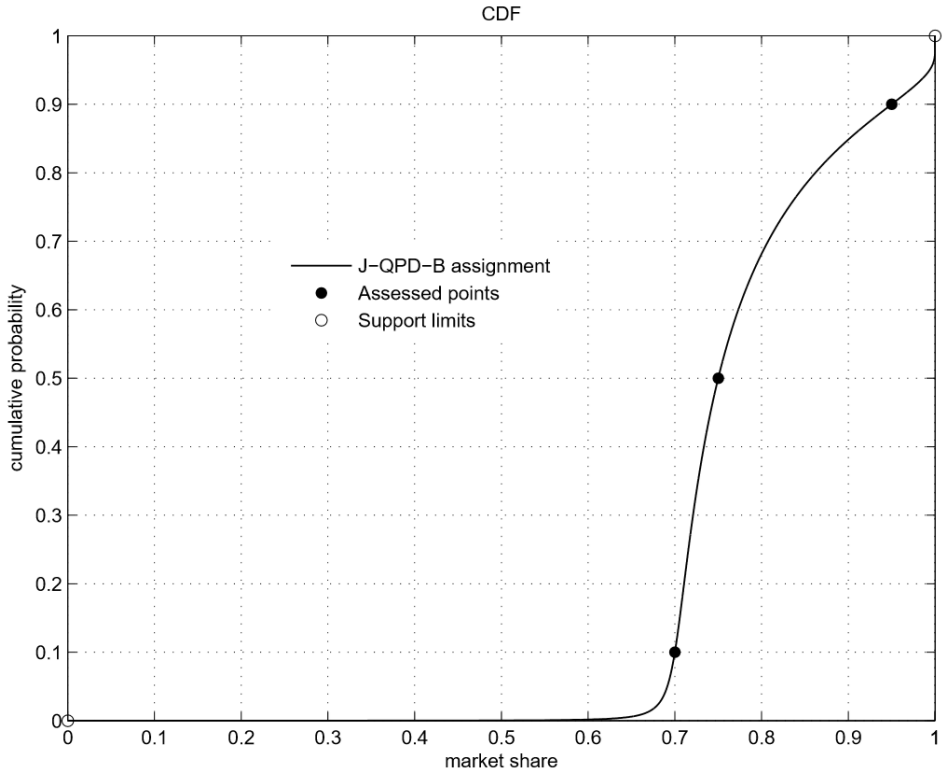

Figure 5.4. J-QPD-B CDF for $\boldsymbol{\theta}_{0.1}$ = (0,0.7,0.75,0.95,1).

J-QPD-B distributions are sort of like a three-shape-parameter version of beta distributions (four shape parameters when we include α), except that in addition to having more shape parameters than beta distributions, J-QPD-B distributions are quantile-parameterized (by SPT and bounds) and maximally-feasible. Figure 5.5 provides additional examples of J-QPD-B PDFs (right), parameterized by $\boldsymbol{\theta}_{0.10}$ (in this case, the {10th, 50th, 90th} percentiles, and the support bounds of [0, 1]) for the corresponding beta

distributions shown in the left panel[4]. Note that J-QPD-B captures the J-, U-, and symmetric/skewed bell-shapes inherent in beta distributions, and that differences in shape in Figure 5.5 are nearly indiscernible. We more rigorously compare the closeness of beta distributions to their corresponding J-QPD-B assignments (approximations) in Chapter 6.

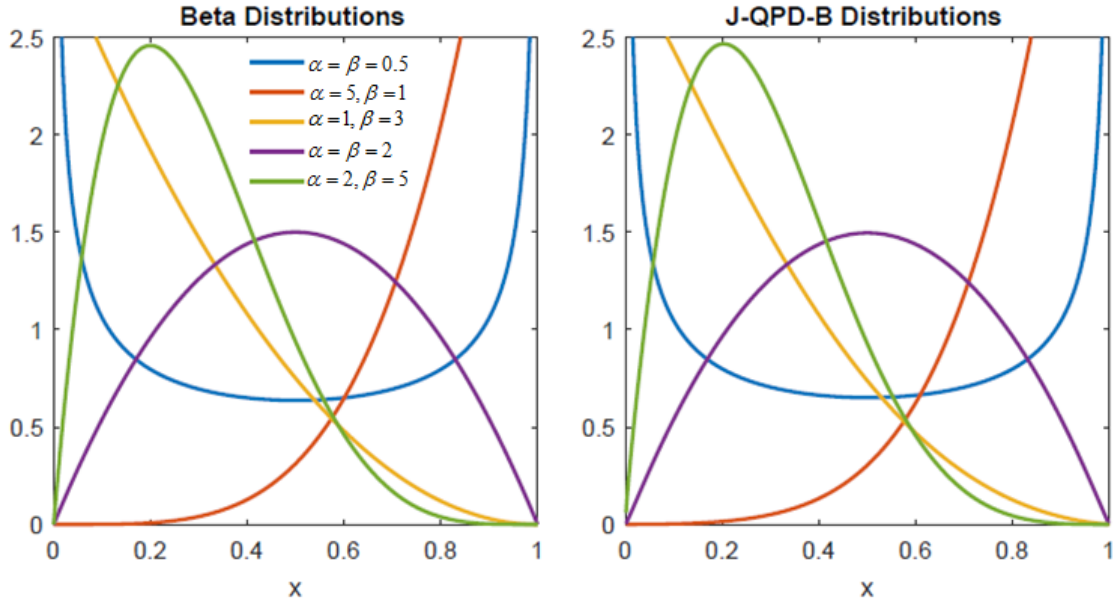

Figure 5.5. Examples of J-QPD-B Parameterized by $\boldsymbol{\theta}_{0.10}$ for Several Beta Distributions.

However, due to the added shape parameters, J-QPD-B distributions can generate more shapes than the beta-type shapes shown in Figure 5.5, as illustrated in Figure 5.6. We refer to the green, purple, and red densities in Figure 5.6 as having "double-hooked bell-shaped" distributions of varying skewness, due to their sharp adhesion to either end of support. The blue density is a left-skewed bell-shaped distribution that more closely resembles a beta distribution than does the other curves, except that it is more triangular. Finally, the yellow density in Figure 5.6 has a right-skewed "boot" shape.

[4] These are the examples shown on the Wikipedia page for beta distributions: https://en.wikipedia.org/wiki/Beta_distribution.

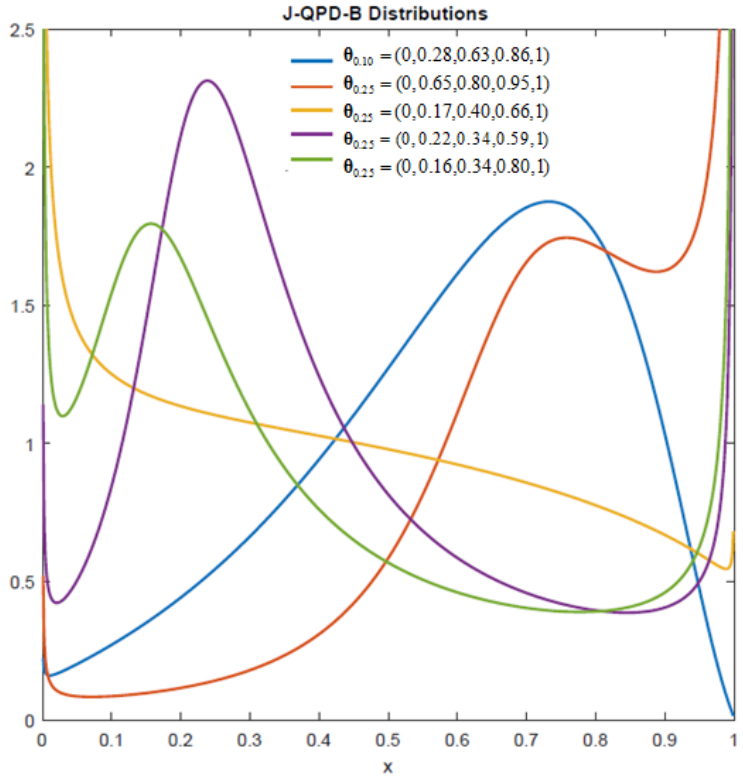

Figure 5.6. Examples of Additional Shapes Produced by J-QPD-B.

ADDITIONAL COMPARISONS TO J-QPD

Still, it is useful to consider two-shape parameter bounded distributions within the $\{s_\alpha, t_\alpha\}$ space. Recall that both J-QPD-B and J-QPD-S distributions presume a specified and finite lower bound, l. Although our default suggestion is to employ J-QPD-S when an expert cannot comfortably provide a hard (finite) upper bound, an approach sometimes used in practice is to assign a bounded distribution (such as beta) with a specified lower bound (such as zero), but with an unspecified upper bound that is determined ex post.

Using this latter case as context, Figure 5.7 shows the span of the beta and Johnson SB distributions[5] within the $\{s_\alpha, t_\alpha\}$ space for $\alpha = 0.10$. The uniform and

[5] Like the J-QPD-S system, it is possible to parameterize a Johnson SB distribution using four QP pairs. For examples, see Johnson (1949), and see Mage (1980), following earlier work by Bukac (1972).

exponential distributions correspond to a single *point* within this space, since they lack shape parameters. Alternatively, the lognormal and gamma distribution systems each have a single shape parameter, and thus correspond to a *curve* within the $\{s_\alpha, t_\alpha\}$ space. The family of lognormal distributions lies along the line segment, $s_\alpha = t_\alpha$, within the $\{s_\alpha, t_\alpha\}$ space, for any value of $\alpha \in (0, 0.50)$. Since the family of beta distributions (with unspecified upper bound) has two separate shape parameters, it is contained in the two-dimensional (shaded) *area* within the $\{s_\alpha, t_\alpha\}$ space, for each value of α. Finally, the SB distributions occupy the lower half of the unit square in Figure 5.7, defined by $s_\alpha > t_\alpha$. By contrast, the MF property of the J-QPD system implies that these distributions span the *entire* interior of the unit square defined by: $s_\alpha \in (0,1)$, $t_\alpha \in (0,1)$.

a) The Beta (and Limiting) Distributions **b) The SB (and Limiting) Distributions**

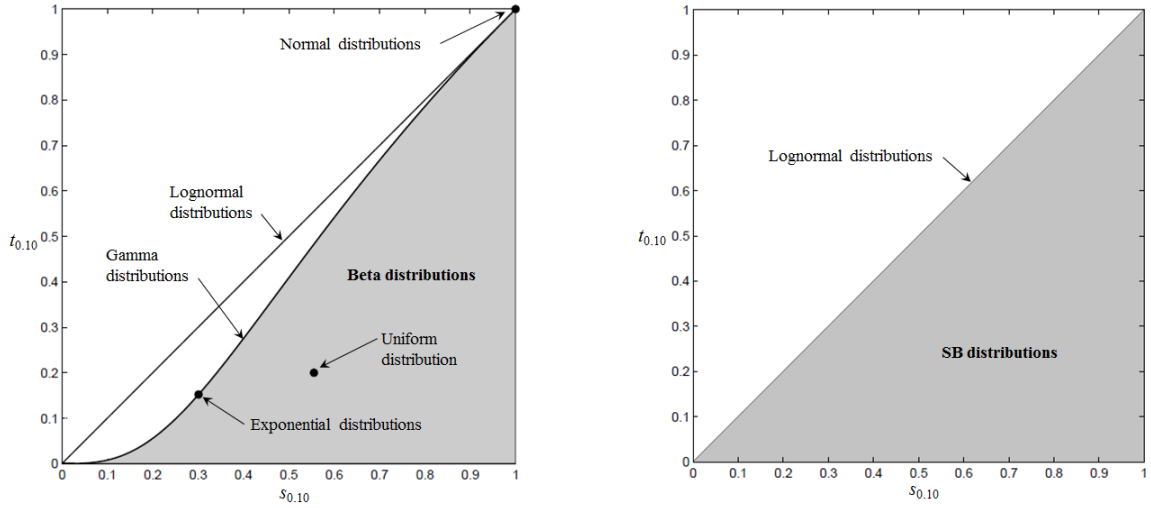

Figure 5.7. Span of the Beta and SB Systems in the $\{s_\alpha, t_\alpha\}$ Space for $\alpha = 0.10$.

We have established conformity of J-QPD distributions to Desiderata 1-3. We revisit the $\{s_\alpha, t_\alpha\}$ space in Chapter 6, where we compare the closeness of J-QPD distributions to a vast array of commonly-named distributions – Desideratum 4.

Chapter 6 : The Closeness of J-QPD to Named Distributions[1]

We have seen that J-QPD satisfies Desiderata 1 through 3, of those presented in Chapter 4. However, a natural question is how close the J-QPD distributions are to commonly-named distributions (Desideratum 4). In this chapter, we compare:

(1) J-QPD-B to beta distributions, including gamma as a limiting case, assuming (without loss of generality) support on [0, 1].

(2) J-QPD-S to beta-prime distributions, including gamma and inverse-gamma distributions as limiting cases, assuming support on $[0, \infty)$[2].

In both cases, we perform the comparison with respect to two common SPTs – the $\{10^{th}, 50^{th}, 90^{th}\}$ and the $\{5^{th}, 50^{th}, 95^{th}\}$ percentiles. To give context, suppose an expert provides $\{10^{th}, 50^{th}, 90^{th}\}$ or $\{5^{th}, 50^{th}, 95^{th}\}$ percentile assessments consistent with each commonly-named distribution, presumed to represent the "true" distribution. We then compare each commonly-named distribution to the corresponding J-QPD-B (J-QPD-S) assignment, sharing the same SPT, and support on [0, 1] ($[0, \infty)$).

MEASURES OF CLOSENESS

To compare each commonly-named distribution, assumed to be the "true" distribution, to the corresponding J-QPD assignment, we introduce several measures of closeness:

(1) **APDM** – Absolute percent difference in means by inter-decile range: (P90-P10).

(2) **APDV** – Absolute percent difference in variance with respect to the true variance.

(3) **KS** – The Kolmogorov-Smirnov (KS) distance.

---

[1] Summaries of the results of this chapter are published with my advisor, Eric Bickel, in the following: Hadlock, Christopher and J. Eric Bickel. 2017. Johnson Quantile-Parameterized Distributions. *Decision Analysis* **14**(1) 35-64.

[2] We do not compare J-QPD-S to the lognormal distributions, since we showed in Chapter 4 that J-QPD-S subsumes the lognormal family as a special case.

(4) **KL** – The Kullback-Leibler (KL) divergence.

APDM

When comparing mean values for two distributions, the error measure should be invariant to changes of location and scale. Let μ denote the mean of the true (commonly-named) distribution, and μ' denote the mean of the corresponding J-QPD assignment. The '*absolute percent difference by mean*', or APDM error measure is:

$$APDM = 100 \cdot \left| \frac{\mu' - \mu}{x_{90} - x_{10}} \right|. \tag{6.1}$$

APDM, as defined, is invariant to location and scale, as desired. It is more common to divide by the standard deviation, σ, of the true distribution. However, we use $x_{90} - x_{10}$ as the normalizing measure of spread since σ is typically unknown in practice, and since the standard deviations of the true and assigned (J-QPD) distributions will be different – recall that we are matching percentiles, and not standard deviations.

APDV

Alternatively, when comparing the variance of two distributions, we remove location and scale by comparing with respect to the variance of the true distribution. Thus, using v and v' to denote the two variances in analogous fashion, the '*absolute percent difference by variance*', or APDV error measure is:

$$APDV = 100 \cdot \left| \frac{v' - v}{v} \right|. \tag{6.2}$$

KS Distance

While APDM and APDV measure the closeness of two distributions based on moments, they do not necessarily tell us how close the *shape* of the J-QPD assignment is to the true distribution. Figure 6.1 provides an illustration of two distributions sharing the same first

six moments (including mean, variance, skewness, and kurtosis). However, we can see from their CDFs that these two distributions have drastically different shapes[3].

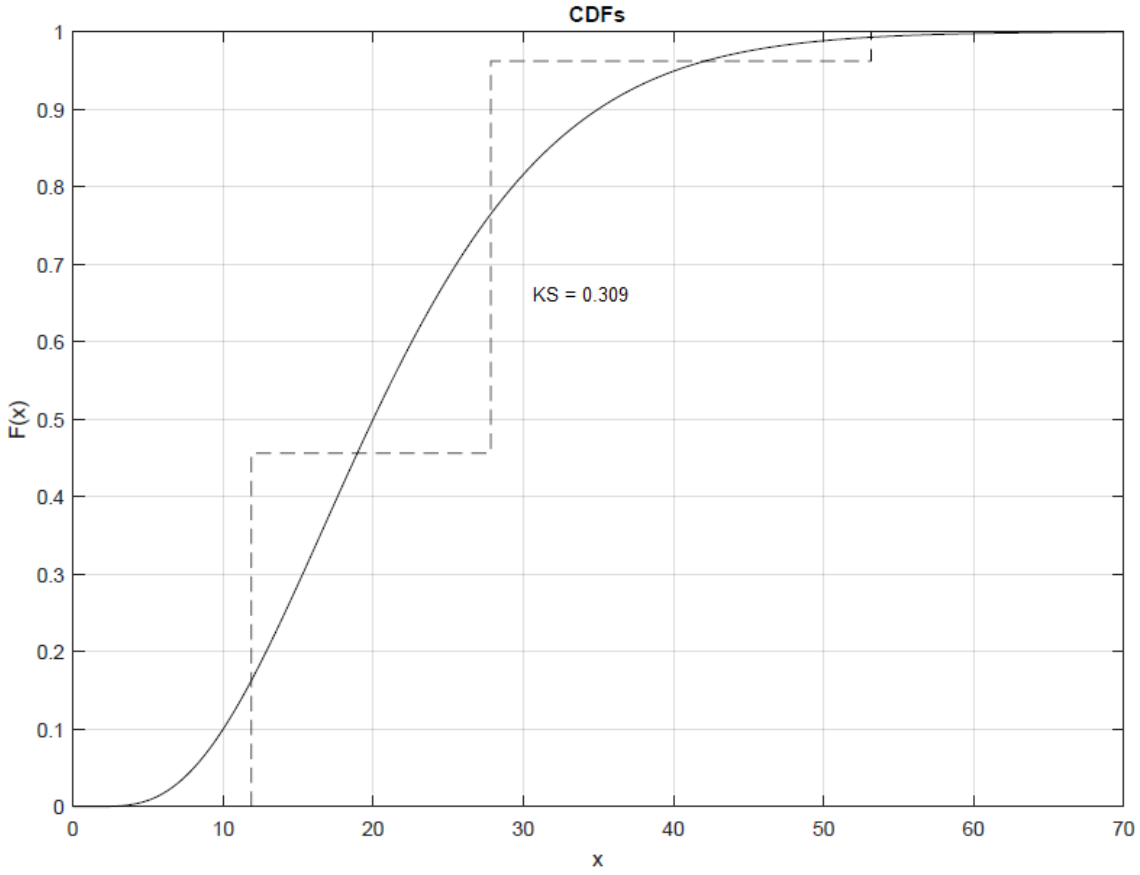

Figure 6.1. Distributions with Similar Moments but very Different Shapes.

One conventional approach used to measure the degree to which two distributions differ in shape is via the Kolmogorov-Smirnov (or KS) distance[4]. For two separate CDFs, denoted $F(x)$ and $G(x)$, the KS distance between them is:

$$D_{KS}(F,G) = \sup_x |F(x) - G(x)|. \tag{6.3}$$

[3] The example distinction here is intentionally extreme. The smooth distribution shown is a J-QPD-S having $\boldsymbol{\theta}_{0.1} = (0, 10, 20, 35, \infty)$, while the dashed distribution is its three-point Gaussian quadrature (moment matching) discretization using the algorithm proposed by Miller and Rice (1983)

[4] For more detailed discussion, see Darling (1957).

The KS distance is the largest absolute vertical deviation between $F(x)$ and $G(x)$, as depicted in Figure 6.2. There is also a "quantile way" of computing the KS distance between F and G. Letting $p = F(x)$, if F is invertible, then we can also express the KS distance between F and G as:

$$D_{KS}(F,G) = \sup_{p\in(0,1)} \left| p - G\left(F^{-1}(p)\right) \right|. \tag{6.4}$$

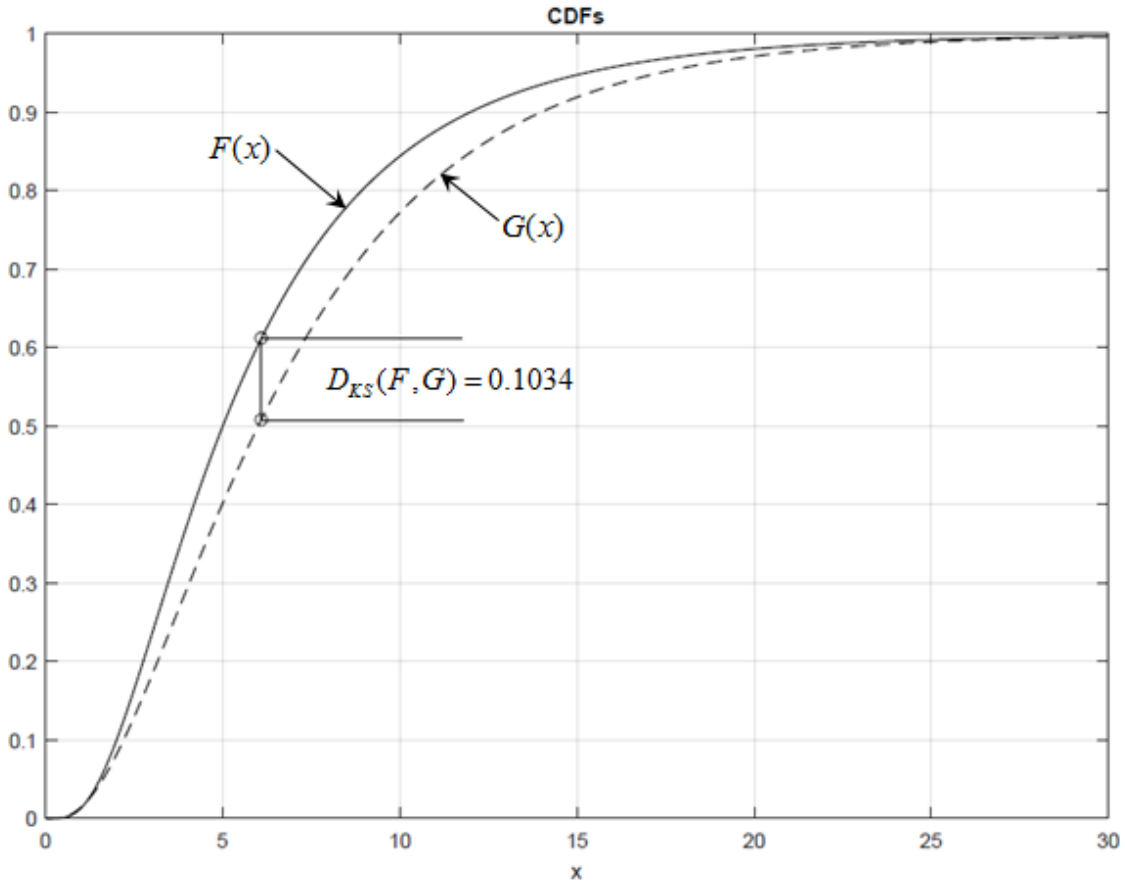

Figure 6.2. Illustration of the KS Distance between CDFs F and G.

We consider both the KS distance, and moment-based differences, since these measures are not always closely correlated. Figure 6.1 provides an example where two distributions are close based on moments, but differ greatly in shape, based on the KS

metric. Figure 6.3 provides an example of the opposite extreme, where two distributions are quite close in shape (based on the KS metric), but differ drastically in terms of moments. This is because one is a heavy-tailed, Student's t distribution with 3 degrees of freedom, and the other is a normal distribution, intentionally scaled so that both distributions have the same $\{10^{th}, 50^{th}, 90^{th}\}$ percentiles. Although the KS distance between the two distributions is 0.025, the percent difference in the variance (kurtosis) with respect to the normal distribution is 84% (∞ %). The latter is because the kurtosis of a Student's t distribution with three degrees of freedom is infinite. The examples of Figure 6.1 and Figure 6.3 jointly suggest that the KS and moment-based metrics provide very alternative measures of closeness between two distributions, and that one metric should not supplant the other as an "end-all" measure of closeness.

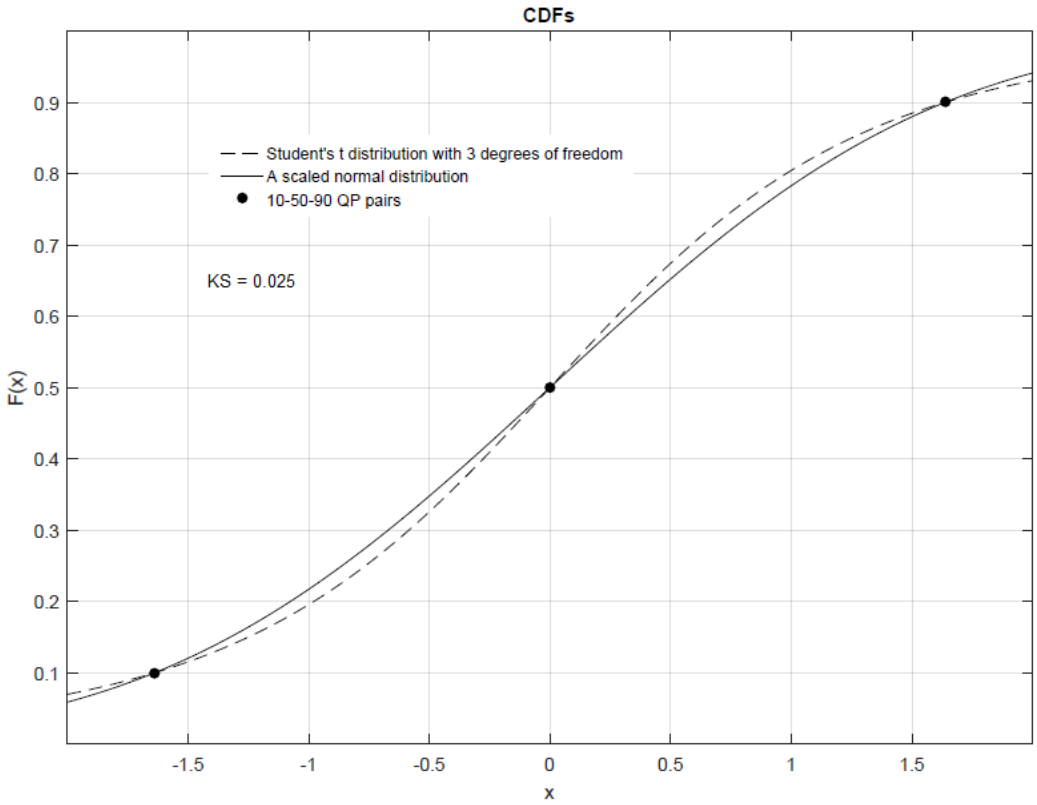

Figure 6.3. Distributions with Similar Shapes but very Different Moments.

KL Divergence

Finally, another important closeness measure used in probability theory is the Kullback-Leibler (KL) divergence, or cross-entropy between two probability distributions. KL divergence measures the information lost when approximating a reference distribution, F, with another distribution, G. Letting f and g denote the PDFs for F and G, respectively, the KL divergence is given by:

$$D_{KL}(F,G) = \int_x \log\left(\frac{f(x)}{g(x)}\right) f(x)dx. \tag{6.5}$$

Unlike KS distance, KL divergence is reference-dependent. That is, $D_{KL}(F, G) \neq D_{KL}(G, F)$, whereas $D_{KS}(F, G) = D_{KS}(G, F)$. However, like KS distance, there is a "quantile way" of computing $D_{KL}(F, G)$, as noted by Powley (2013):

$$D_{KL}(F,G) = \int_{p=0}^{1} \log\left(Q'_G\left(G\left(Q_F(p)\right)\right)\right)dp - \int_{p=0}^{1} \log\left(Q'_F(p)\right)dp, \tag{6.6}$$

Where Q_F and Q_G denote the quantile functions for F and G, respectively, and where Q' denotes the derivative of Q with respect to p. For more background information on KL divergence, see Kullback and Leibler (1951), and Kullback (1959).

METHODOLOGY FOR COMPARING J-QPD TO COMMONLY-NAMED DISTRIBUTIONS

Figure 6.4 displays the span of the beta distributions in the $\{s_{0.1}, t_{0.1}\}$ space. Each point in the shaded region corresponds to a specific beta distribution; i.e., a specific pair of $\{a, b\}$ parameters. The beta distributions are partitioned into several key subfamilies: ∩-shaped (region I-∩, where $a \geq 1$, $b \geq 1$), U-shaped (region I-U, where $a < 1$, $b < 1$), right-skewed J-shaped (region I-J, with $a < 1$, $b \geq 1$), and left-skewed J-shaped (region I-J, with $a \geq 1$, $b < 1$). The uniform distribution ($a = 1$, $b = 1$) occurs as the intersection of the four subfamilies, while the exponential distribution is a special case of the gamma distributions, and occurs as a limiting case of right-skewed J-shaped distributions.

We construct a grid of approximately 104,000 points covering the feasible region shown in Figure 6.4, spaced 0.002 in each dimension. For each point, we identify the corresponding beta distribution by solving for the corresponding $\{a, b\}$ parameter pair. Next, we compute $\boldsymbol{\theta}_\alpha = (0, x_\alpha, x_{0.50}, x_{1-\alpha}, 1)$ for this beta distribution, and construct the corresponding J-QPD-B distribution, parameterized by $\boldsymbol{\theta}_\alpha$. Then, we compute the mean and variance for both the beta distribution, and its corresponding J-QPD-B assignment, and then compute the APDM and APDV errors. Finally, we compute the KS (KL) distance (divergence) between the beta distribution, and its corresponding J-QPD-B assignment.

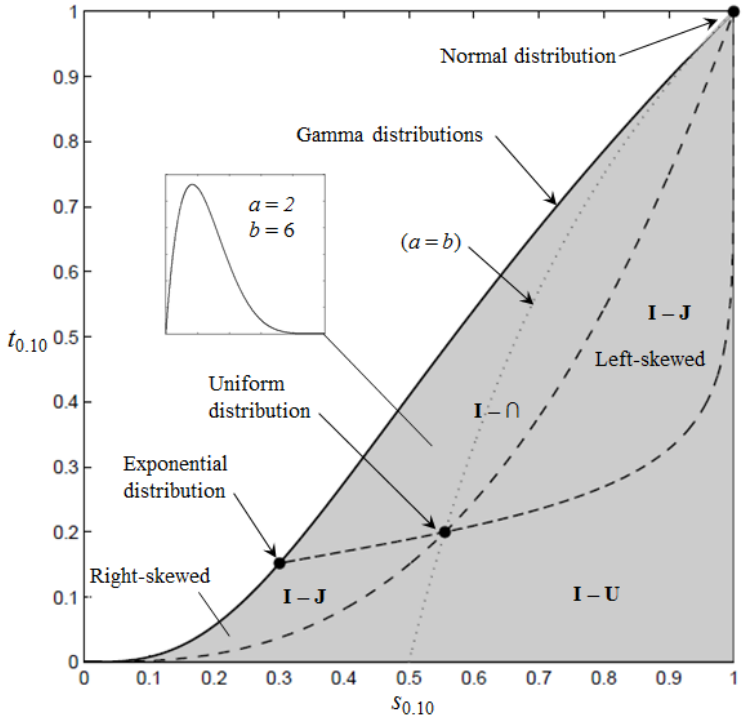

Figure 6.4. Feasible Region for Beta Distributions in the $\{s_{0.1}, t_{0.1}\}$ Space.

THE CLOSENESS OF J-QPD-B TO COMMONLY-NAMED DISTRIBUTIONS

Before rigorously comparing J-QPD-B to beta distributions, we provide several examples to build context and intuition. Figure 6.5 (Figure 6.6) provides PDFs (CDFs) for nine J-QPD-B distributions, each parameterized by $\boldsymbol{\theta}_{0.10} = (0, x_{0.10}, x_{0.50}, x_{0.90}, 1)$ for some commonly-named distributions. Figure 6.6 also displays closeness measures in each case.

Except for the two triangular distributions, PDFs for J-QPD-B (dashed) are barely discernible from the named distributions. CDFs are nearly indiscernible in all nine cases. Except for the two J-shaped beta distributions, beta(10, 1) and beta(0.7, 5), APDM (APDV) errors are less than 0.03% (1%). Except for the two triangular distributions, KS (KL) distances (divergences) are no greater than 0.0035 (0.0021). Excluding the J-shaped beta distributions, KS (KL) distances (divergences) are no greater than 0.0017 (0.0003) for all other beta distribution examples.

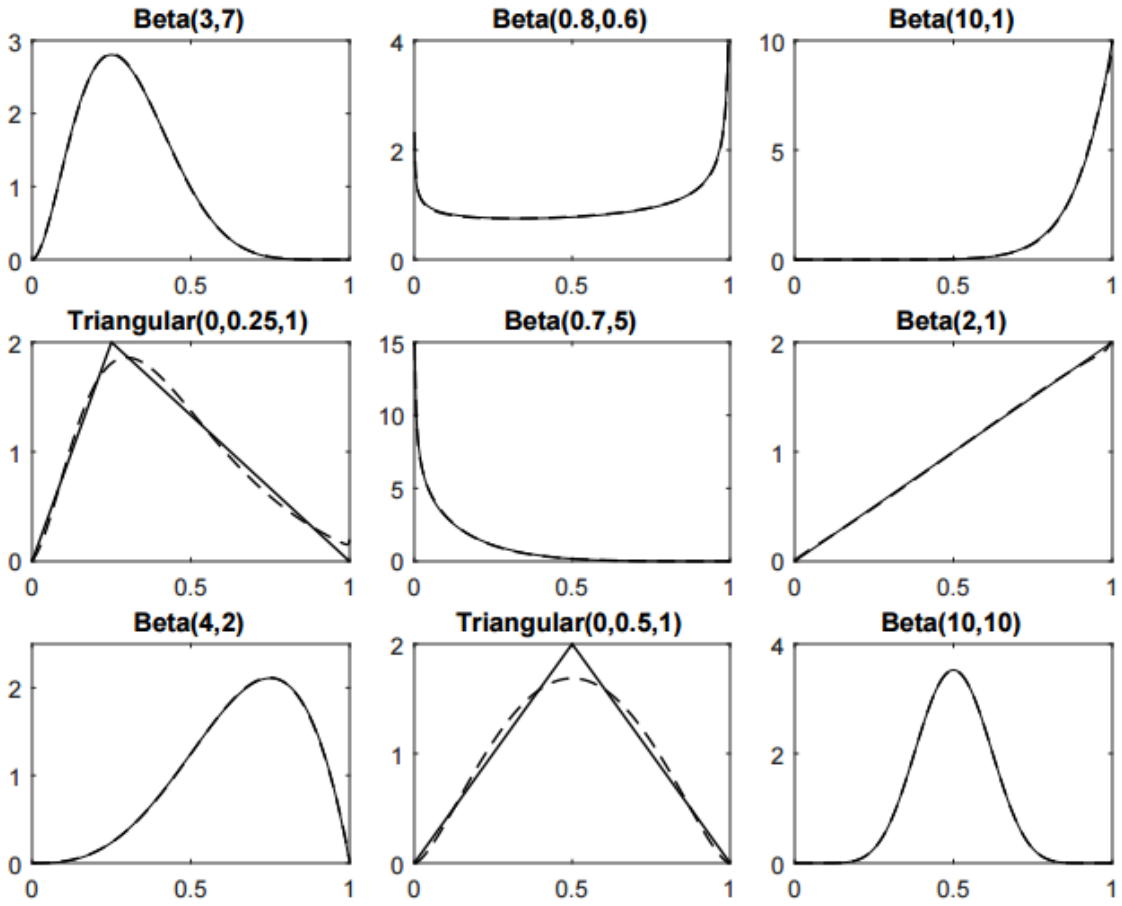

Figure 6.5. J-QPD-B PDFs Parameterized by $\boldsymbol{\theta}_{0.1}$ for Some Named Distributions (solid).

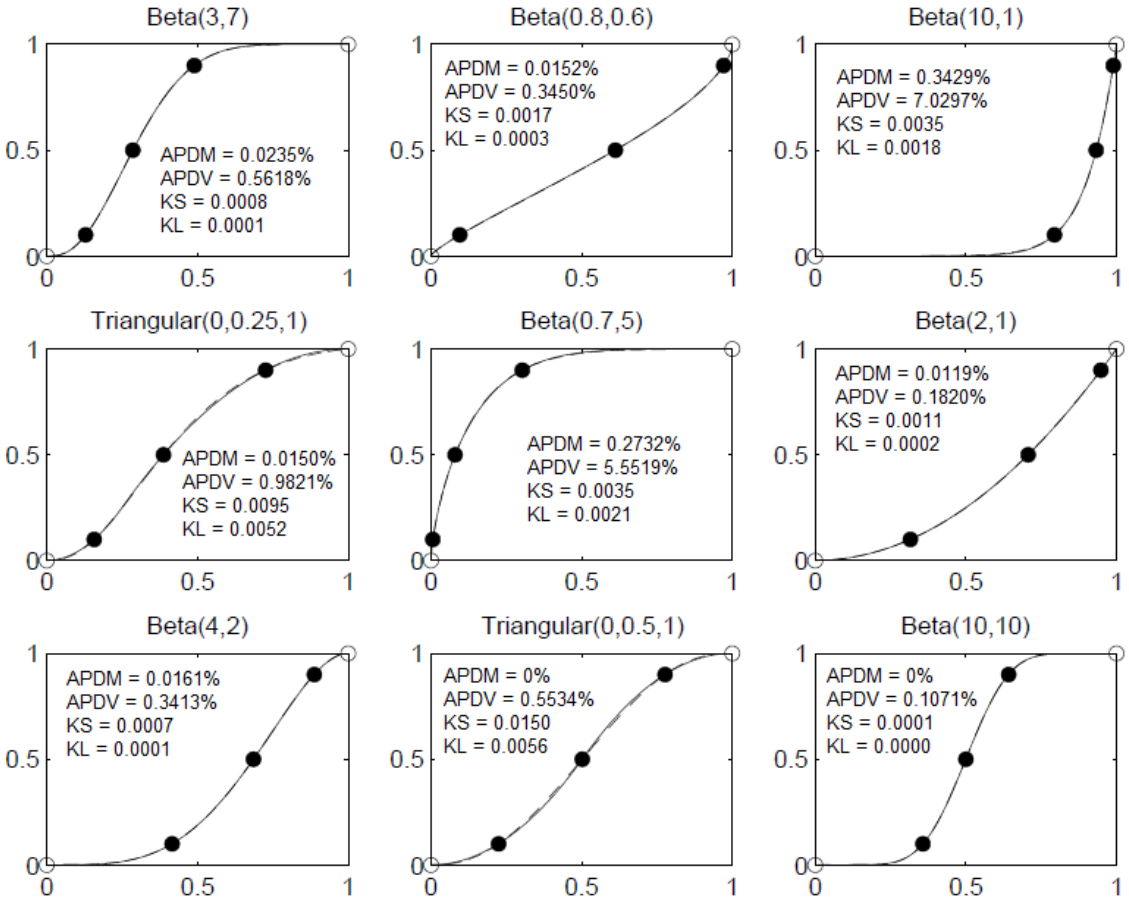

Figure 6.6. J-QPD-B CDFs Parameterized by $\boldsymbol{\theta}_{0.1}$ for Some Named Distributions (Solid).

We now compare J-QPD-B to the uniformly-spaced grid of roughly 104,000 beta distributions, covering the region depicted in Figure 6.4. Figure 6.7 depicts the span of the beta distributions in the $\{s_{0.05}, t_{0.05}\}$ and $\{s_{0.10}, t_{0.10}\}$ spaces, along with shaded error contours for APDM, APDV, and KS (KL) distances (divergences) of the J-QPD-B distributions with respect to the corresponding beta distribution sharing the same SPT. Recall from Figure 5.7 that due to the presence of two separate shape parameters, the beta distributions occupy a region for each α within the $\{s_\alpha, t_\alpha\}$ space, while the gamma distributions occupy a curve at the boundary.

a) APDM using $\boldsymbol{\theta}_{0.05} = (0, x_{0.05}, x_{0.50}, x_{0.95}, 1)$

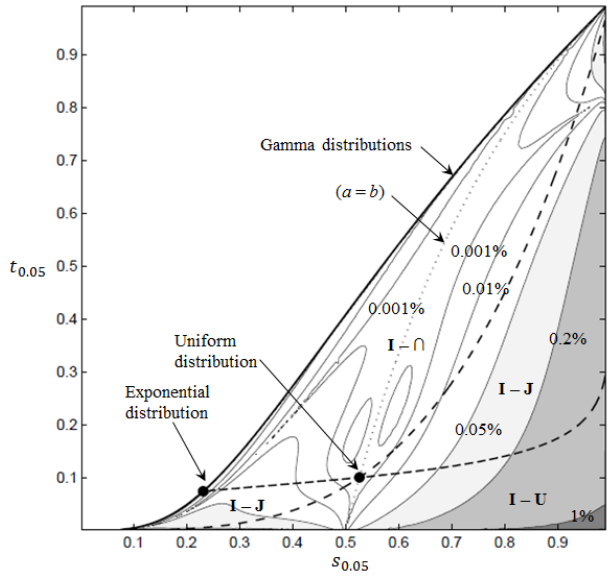

b) APDM using $\boldsymbol{\theta}_{0.10} = (0, x_{0.10}, x_{0.50}, x_{0.90}, 1)$

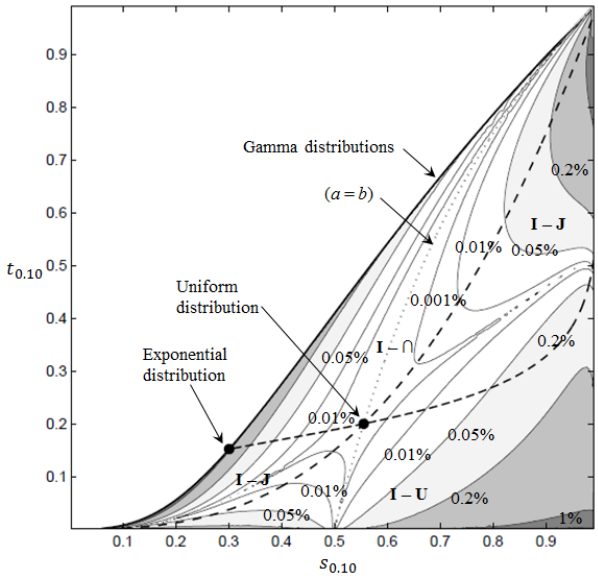

c) APDV using $\boldsymbol{\theta}_{0.05} = (0, x_{0.05}, x_{0.50}, x_{0.95}, 1)$

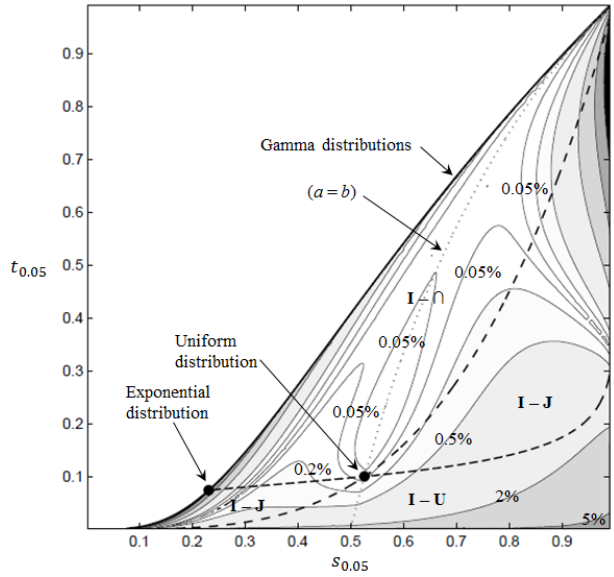

d) APDV using $\boldsymbol{\theta}_{0.10} = (0, x_{0.10}, x_{0.50}, x_{0.90}, 1)$

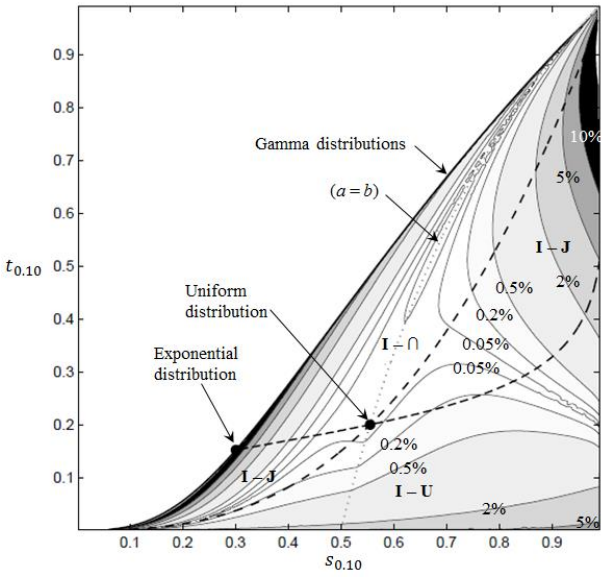

e) KS distance using $\boldsymbol{\theta}_{0.05}$=(0, $x_{0.05}$, $x_{0.5}$, $x_{0.95}$, 1)

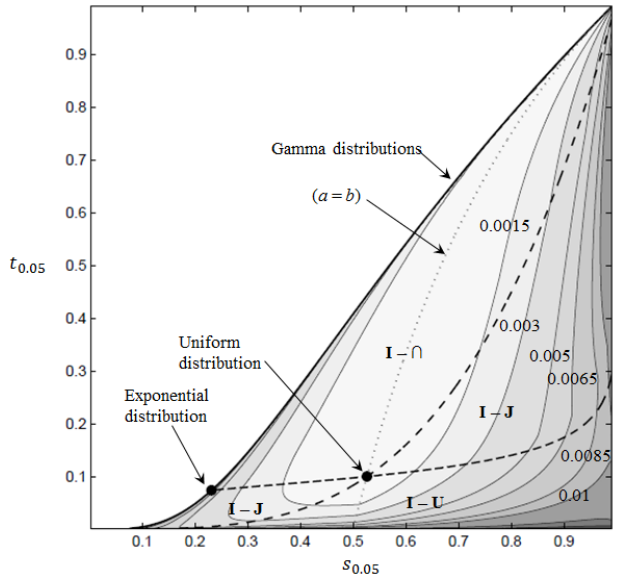

f) KS distance using $\boldsymbol{\theta}_{0.1}$ = (0, $x_{0.10}$, $x_{0.50}$, $x_{0.90}$, 1)

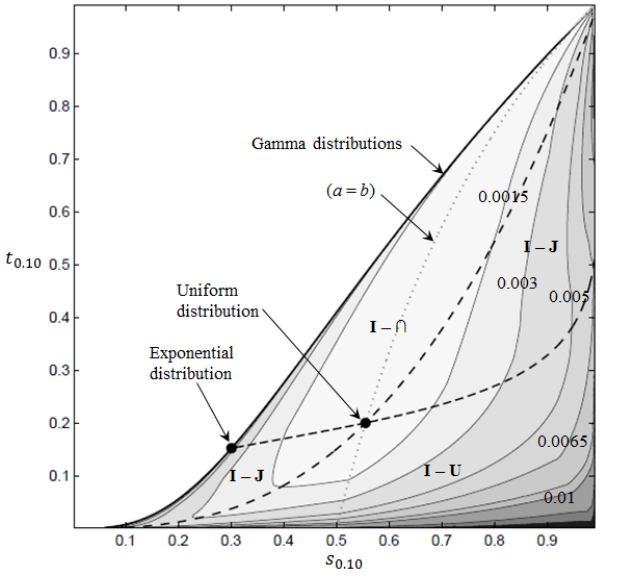

g) KL divergence for $\boldsymbol{\theta}_{0.05}$=(0, $x_{0.05}$, $x_{0.5}$, $x_{0.95}$, 1)

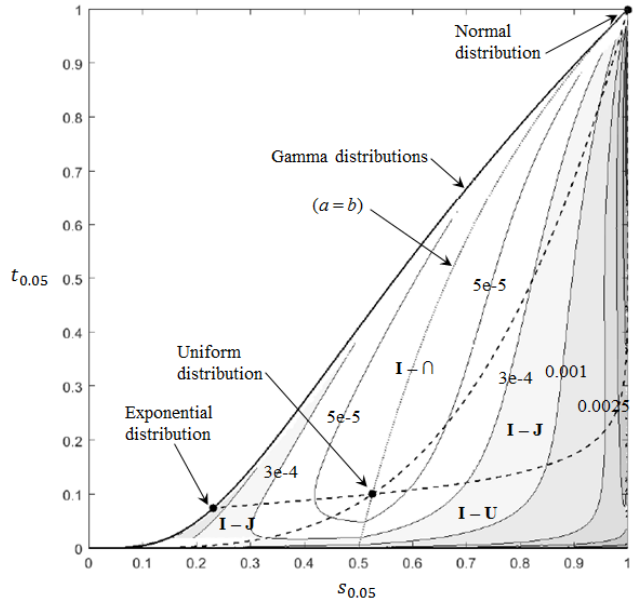

h) KL divergence for $\boldsymbol{\theta}_{0.1}$ = (0, $x_{0.1}$, $x_{0.5}$, $x_{0.9}$, 1)

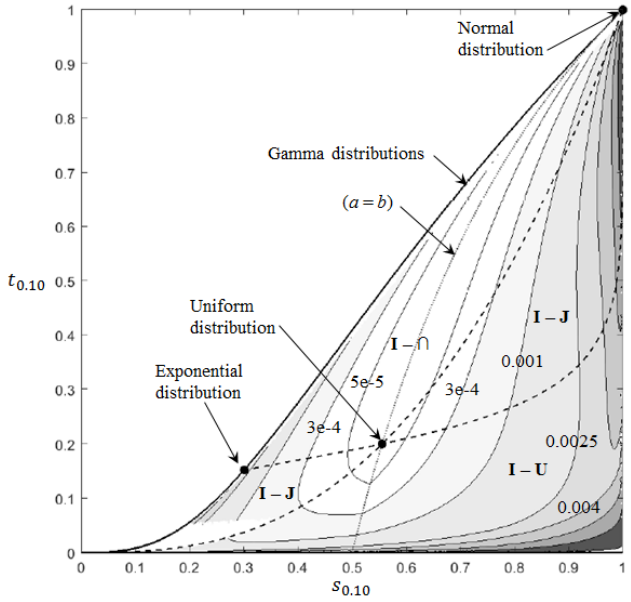

Figure 6.7. Error Measures of J-QPD-B w.r.t. Beta: $\boldsymbol{\theta}_{0.05}$ (left) and $\boldsymbol{\theta}_{0.10}$ (right).

Table 6.1 provides summary statistics for each error measure across the grid of 104,000 points in Figure 6.7. For the I-∩ region, APDM (APDV) values are generally less than 0.2% (5%), which are comparable to the "Beta (3,7)" panel in Figure 6.6, and

errors grow largest as we approach the exponential distribution at the boundary in Figure 6.7. KS (KL) distances (divergences) for the I-∩ region are generally less than 0.003 (0.001), a value comparable to the "Beta (10,1)" panel of Figure 6.6.

Metric (by region)	Min.	Median	Max.	Mean
I-∩ (Beta)				
APDM ($\boldsymbol{\theta}_{0.05}$)	0.0%	0.0%	0.6%	0.0%
APDM ($\boldsymbol{\theta}_{0.10}$)	0.0%	0.0%	1.6%	0.1%
APDV ($\boldsymbol{\theta}_{0.05}$)	0.0%	0.1%	51.7%	0.3%
APDV ($\boldsymbol{\theta}_{0.10}$)	0.0%	0.3%	46.6%	1.1%
KS distance ($\boldsymbol{\theta}_{0.05}$)	0.000	0.001	0.014	0.001
KS distance ($\boldsymbol{\theta}_{0.10}$)	0.000	0.001	0.007	0.001
KL divergence ($\boldsymbol{\theta}_{0.05}$)	0.000	3.4e-5	0.0017	1.1e-4
KL divergence ($\boldsymbol{\theta}_{0.10}$)	0.000	8.0e-5	0.0033	2.4e-4
$\mathrm{I}-\mathrm{J}$(Beta)				
APDM ($\boldsymbol{\theta}_{0.05}$)	0.0%	0.1%	2.5%	0.2%
APDM ($\boldsymbol{\theta}_{0.10}$)	0.0%	0.0%	9.7%	0.2%
APDV ($\boldsymbol{\theta}_{0.05}$)	0.0%	0.6%	445.0%	2.3%
APDV ($\boldsymbol{\theta}_{0.10}$)	0.0%	1.0%	809.0%	4.1%
KS distance ($\boldsymbol{\theta}_{0.05}$)	0.000	0.005	0.032	0.006
KS distance ($\boldsymbol{\theta}_{0.10}$)	0.000	0.003	0.014	0.003
KL divergence ($\boldsymbol{\theta}_{0.05}$)	0.000	8.3e-4	0.0122	0.0014
KL divergence ($\boldsymbol{\theta}_{0.10}$)	0.000	0.0013	0.0175	0.0021
$\mathrm{I}-\mathrm{U}$(Beta)				
APDM ($\boldsymbol{\theta}_{0.05}$)	0.0%	0.3%	2.0%	0.4%
APDM ($\boldsymbol{\theta}_{0.10}$)	0.0%	0.1%	2.2%	0.2%
APDV ($\boldsymbol{\theta}_{0.05}$)	0.0%	1.7%	9.8%	2.0%
APDV ($\boldsymbol{\theta}_{0.10}$)	0.0%	0.7%	9.3%	1.1%
KS distance ($\boldsymbol{\theta}_{0.05}$)	0.000	0.007	0.042	0.007
KS distance ($\boldsymbol{\theta}_{0.10}$)	0.000	0.005	0.042	0.006
KL divergence ($\boldsymbol{\theta}_{0.05}$)	0.000	0.0011	0.0125	0.0015
KL divergence ($\boldsymbol{\theta}_{0.10}$)	0.000	0.0017	0.0434	0.0026

Table 6.1. Error Measures for J-QPD-B w.r.t. Beta Distributions.

Errors are generally larger for the I-J and I-U regions, compared to the I-∩ region. For example, based on APDM and APDV in Table 6.1, error values grow rapidly for distributions at the boundaries of the I-J and I-U regions, while overall errors across these

regions are small based on median values. For example, for the I-J region, errors only increase rapidly as $a \to 0$ and $b \to \infty$, or vice versa. Such distributions exist at the lower left and upper right corners of the region depicted in Figure 6.4.

THE CLOSENESS OF J-QPD-S TO COMMONLY-NAMED DISTRIBUTIONS

This section parallels the previous section, except that we now compare J-QPD-S to the beta-prime distributions. We first build context with several examples. Figure 6.8 (Figure 6.9) provides PDFs (CDFs) for six J-QPD-S distributions, each parameterized by $\boldsymbol{\theta}_{0.10} = (0, x_{0.10}, x_{0.50}, x_{0.90}, \infty)$ for the PDFs (CDFs) of the six commonly-named distributions shown, all having semi-bounded support. Figure 6.9 also provides the APDM, APDV, and KS (KL) distances (divergences) in each case.

Like the J-QPD-B comparisons, each J-QPD-S distribution is barely discernible from the corresponding named distribution, particularly with respect to CDFs. Note that errors are zero for the lognormal case shown in Figure 6.9, since J-QPD-S subsumes lognormal distributions as a special case. Among the six examples shown, APDM values are relatively the largest for the Weibull distribution examples. APDV values are relatively largest when the base distribution is Weibull, but also for highly-skewed, J-shaped distributions, as in the examples for Weibull (10, 0.5) and Gamma (0.5, 1). Interestingly, KS distances and KL divergences are equal to four decimal places for the top three examples (panels) in Figure 6.9. Overall, the disparity in values for all four error measures across these six examples further suggests that no one of the four measures alone provides a complete notion of "closeness" between probability distributions.

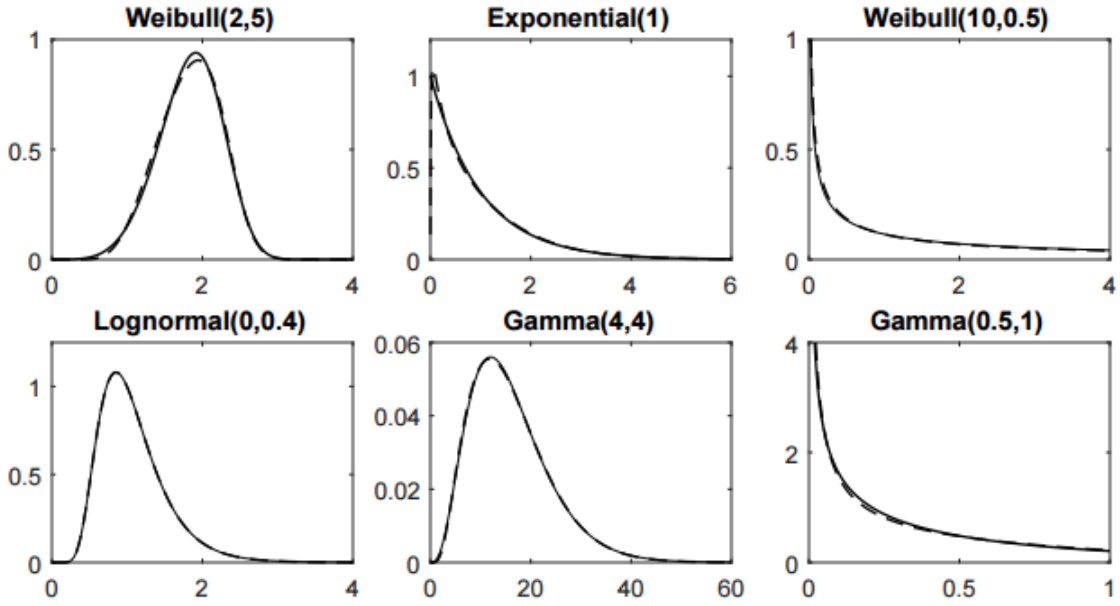

Figure 6.8. J-QPD-S PDFs Parameterized by $\boldsymbol{\theta}_{0.10}$ for Some Named Distributions (Solid).

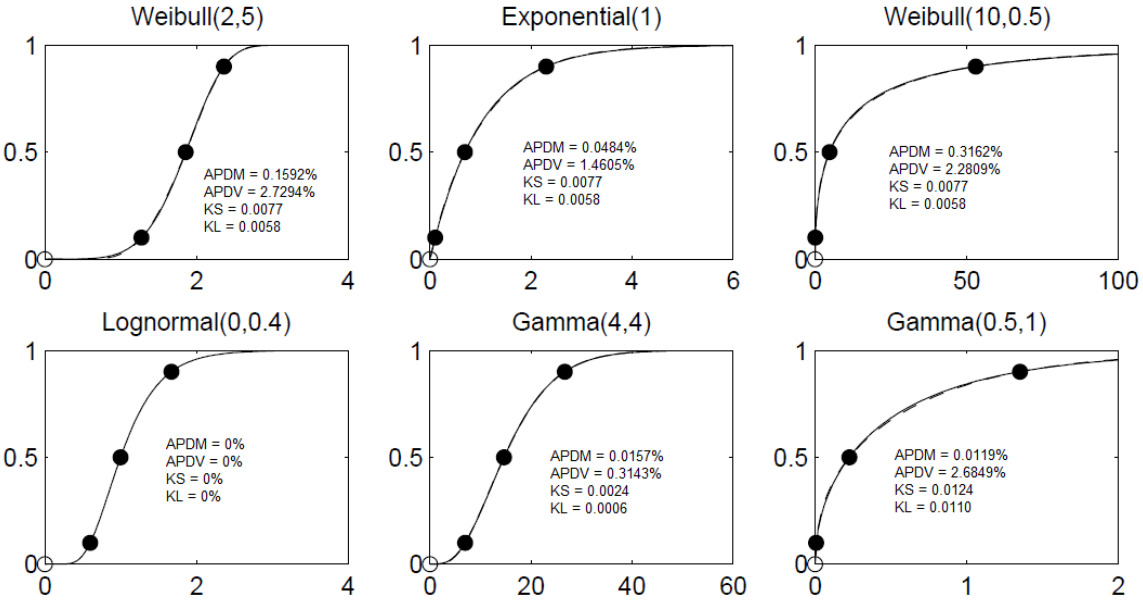

Figure 6.9. J-QPD-S CDFs Parameterized by $\boldsymbol{\theta}_{0.10}$ for Some Named Distributions (Solid).

We now compare J-QPD-S to beta-prime distributions, following a procedure analogous to the comparison between J-QPD-B and beta distributions. We construct a

grid of approximately 35,000 points across the feasible region for the beta-prime distributions, spaced 0.002 in each dimension. Figure 6.10 depicts the feasible region for the beta-prime distributions in the $\{s_{0.05}, t_{0.05}\}$ and $\{s_{0.1}, t_{0.1}\}$ spaces, along with shaded error contours for APDM, APDV, and KS (KL) distances (divergences) of the J-QPD-S distributions with respect to the corresponding beta-prime distribution sharing the same SPT and lower bound of zero. Like beta distributions, beta-prime distributions have two shape parameters, and thus occupy a region for each α in the $\{s_\alpha, t_\alpha\}$ space, whereas the gamma and inverse-gamma distributions each occupy a curve at the boundary.

a) APDM using $\boldsymbol{\theta}_{0.05} = (0, x_{0.05}, x_{0.50}, x_{0.95}, \infty)$

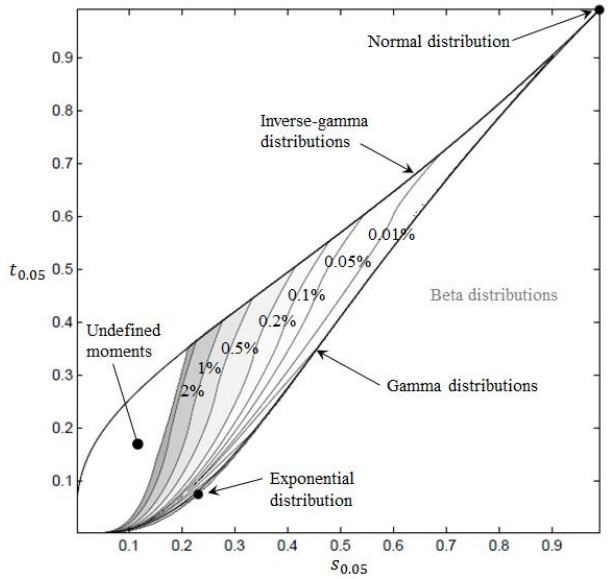

b) APDM using $\boldsymbol{\theta}_{0.10} = (0, x_{0.10}, x_{0.50}, x_{0.90}, \infty)$

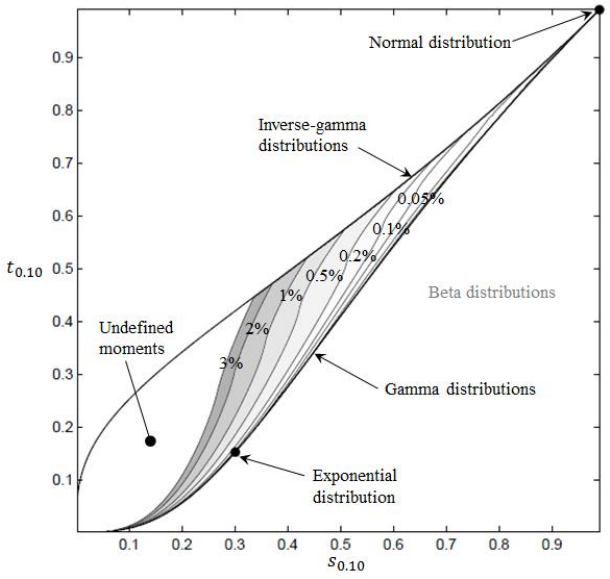

c) APDV using $\boldsymbol{\theta}_{0.05} = (0, x_{0.05}, x_{0.50}, x_{0.95}, \infty)$

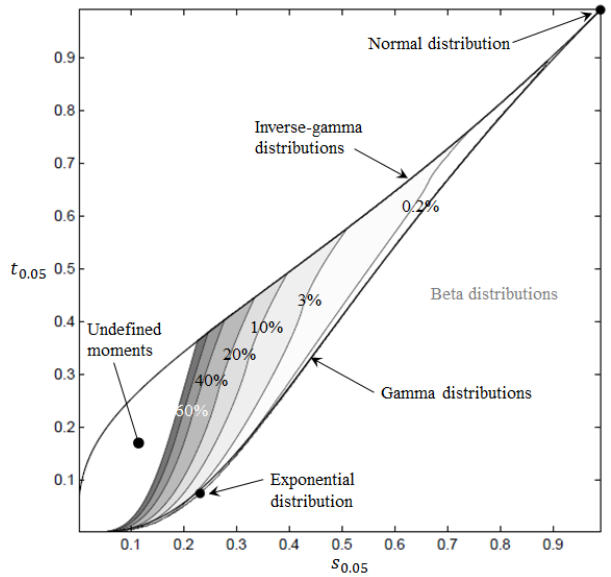

d) APDV using $\boldsymbol{\theta}_{0.10} = (0, x_{0.10}, x_{0.50}, x_{0.90}, \infty)$

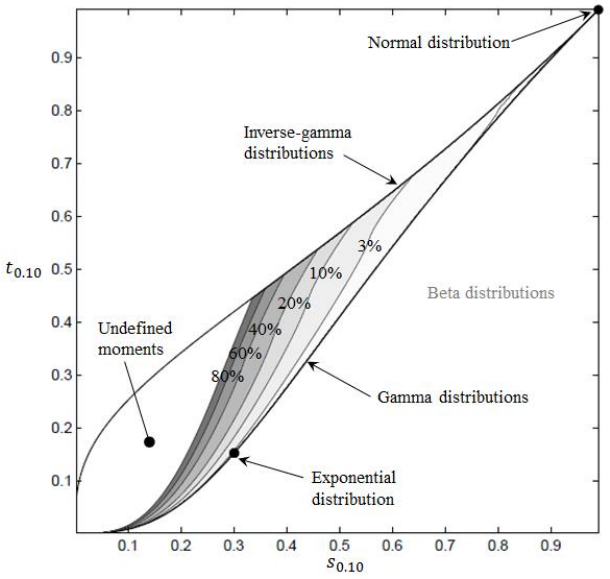

e) KS distance with $\boldsymbol{\theta}_{0.05}$=(0, $x_{0.05}$, $x_{0.5}$, $x_{0.95}$, ∞)

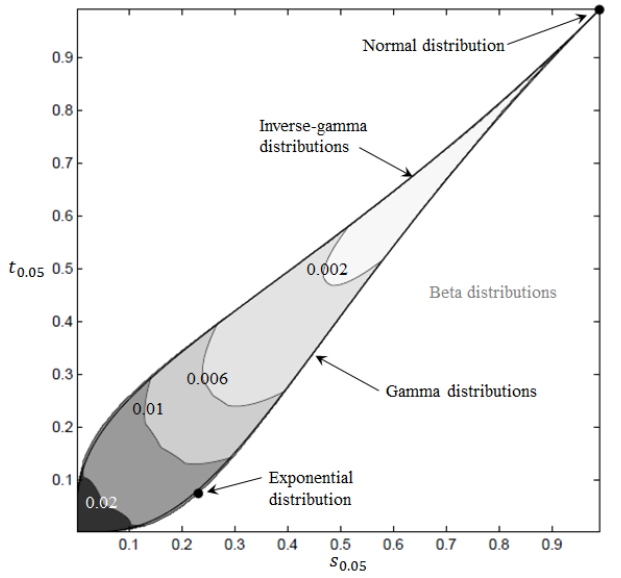

f) KS distance with $\boldsymbol{\theta}_{0.1}$ = (0, $x_{0.10}$, $x_{0.50}$, $x_{0.90}$, ∞)

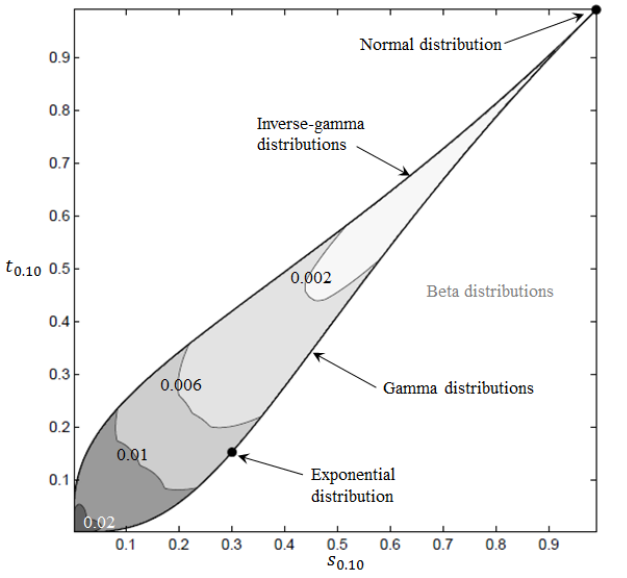

g) KL divergence for $\boldsymbol{\theta}_{0.05}$=(0, $x_{0.05}$, $x_{0.5}$, $x_{0.95}$,∞)

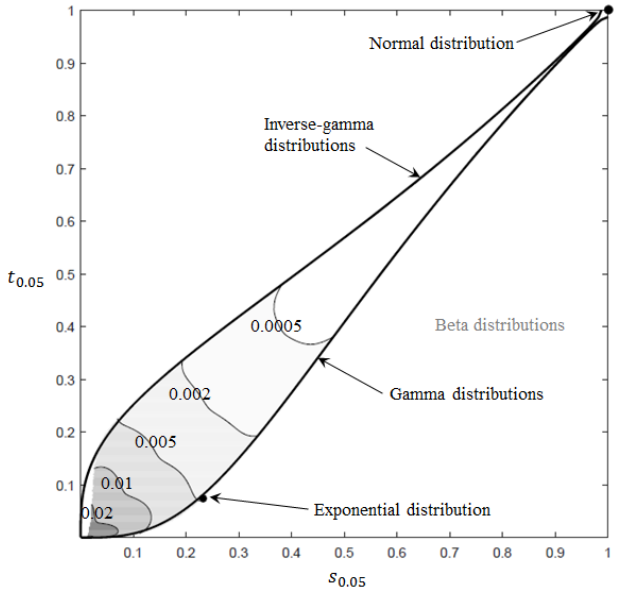

h) KL divergence for $\boldsymbol{\theta}_{0.1}$ = (0, $x_{0.1}$, $x_{0.5}$, $x_{0.9}$, ∞)

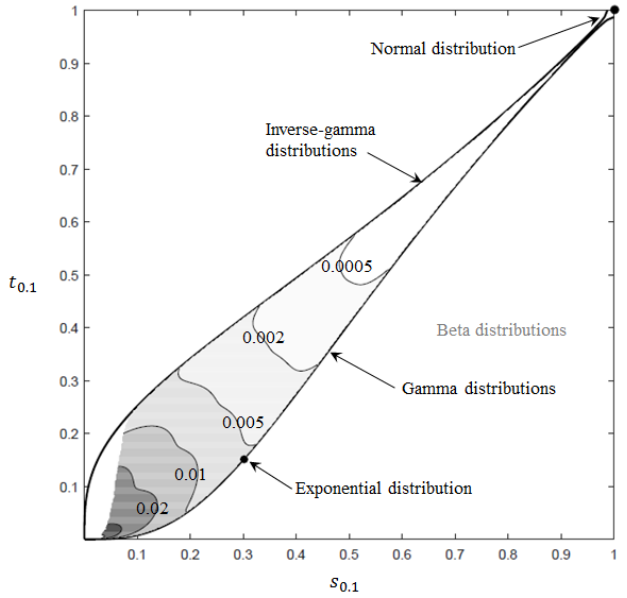

Figure 6.10. Error Measures of J-QPD-S w.r.t. Beta-Prime: $\boldsymbol{\theta}_{0.05}$ (left) and $\boldsymbol{\theta}_{0.10}$ (right).

In panels "a" through "d" of Figure 6.10, there exists a white region within the span of the beta-prime system shown, labeled "undefined moments". The mean and variance of the beta-prime distributions in these white regions are undefined, as are the

higher-order moments. Thus, we exclude them from our comparison to J-QPD-S based on APDM and APDV[5]. However, we include these distributions when comparing with respect to KS distance, since the KS distance between any two distributions is necessarily bounded between zero and one, regardless of whether the moments associated with the reference beta-prime distribution are defined.

Table 6.2 provides summary statistics for each error measure across our grid of roughly 35,000 points in Figure 6.10. For all four measures, errors increase as both s_α and t_α decrease. For APDM and APDV, errors increase rapidly as we approach the "undefined moments" region shown, thus yielding the large maximum values shown for these measures in Table 6.2. This is because while J-QPD-S has finite moments, the moments of the beta-prime distribution diverge upwards near the "undefined moments" boundary. However, for most of the region shown in panels "a" and "b" of Figure 6.10, APDM errors are generally less than 2%. For the ∩-shaped gamma distributions, shown along the "gamma distributions" curve between the "exponential distribution" and "normal distribution" points, the worst-case APDM error is only 0.196% for $\alpha = 0.05$, and only 0.048% for $\alpha = 0.1$ – both corresponding to the exponential distribution.

[5] For the KL comparisons in panels "g" and "h" of Figure 6.10, there is a white region like those in panels "a" through "d", except smaller in area. In this case, these white regions correspond to those beta prime distributions for which the KL divergence integral does not converge.

Metric	Min.	Median	Max.	Mean
APDM ($\boldsymbol{\theta}_{0.05}$)	0.0%	0.1%	6.9%	0.5%
APDM ($\boldsymbol{\theta}_{0.10}$)	0.0%	0.5%	70.5%	1.2%
APDV ($\boldsymbol{\theta}_{0.05}$)	0.0%	5.2%	180.4%	17.3%
APDV ($\boldsymbol{\theta}_{0.10}$)	0.0%	11.2%	1.6e+03%	24.6%
KS distance ($\boldsymbol{\theta}_{0.05}$)	0.000	0.006	0.040	0.008
KS distance ($\boldsymbol{\theta}_{0.10}$)	0.000	0.005	0.031	0.006
KL divergence ($\boldsymbol{\theta}_{0.05}$)	0.0000	0.0014	0.0429	0.0031
KL divergence ($\boldsymbol{\theta}_{0.10}$)	0.0000	0.0032	0.0749	0.006

Table 6.2. Error Measures for J-QPD-S w.r.t. Beta-Prime Distributions.

For APDV, we evaluate the worst-case error for the bell-shaped gamma distributions to be only 0.742% for α = 0.05, and 1.461% for α = 0.1. Like APDM, APDV values grow large near the "undefined moments" boundary line. In panels "e" and "f" of Figure 6.10, KS distances are generally less than 0.02 for the entire region. To lend context, the mean value of 0.008 (0.006) shown in Table 6.2 and corresponding to panel "e" ("f") is similar in magnitude to the "Weibull (2,5)", "Exponential(1)", and "Weibull (10,0.5)" examples provided in Figure 6.9. Finally, in panels "g" and "h" of Figure 6.10, KL divergences are generally less than 0.02 for the entire region. The mean value of 0.006 shown in Table 6.2, corresponding to panel "h" is similar in magnitude to the "Weibull (2,5)", "Exponential (1)", and "Weibull (10,0.5)" examples in Figure 6.9.

The main takeaway of this chapter is the notable conformity of J-QPD to Desideratum 4 based on the APDM, APDV, KS, and KL measures of closeness. We now examine the flexibility of the J-QPD-B (-S) systems – Desideratum 5.

Chapter 7 : The Flexibility of the J-QPD Distributions[1]

We now examine J-QPD with respect to Desideratum 5 – *flexibility*. One of the earliest approaches for achieving this task originates with Pearson (1895, 1901, and 1916), in which he expresses the flexibility of the Pearson system[2] by plotting its span within a two-dimensional space characterized by kurtosis (β_2) versus squared-skewness (β_1). Johnson subsequently plotted his own system within the same space. Figure 7.1 shows the span of both systems in the $\{\beta_1, \beta_2\}$ space.

Although the literature presents alternative ways for measuring distribution flexibility, we use Pearson's moment-ratio space here due to its conventional use[3]. We first point out the distinction in the role of our $\{s, t\}$ space introduced in Chapter 5, compared to Pearson's $\{\beta_1, \beta_2\}$ (i.e., squared-skewness, kurtosis) space. The latter refers to conventional measures of shape, whereas s and t are normalized quantities used to depict the span of a distribution's *feasibility* – the span of compatible $\boldsymbol{\theta}_\alpha$ vectors that a

[1] Summaries of the results of this chapter are published with my advisor, Eric Bickel, in the following: Hadlock, Christopher and J. Eric Bickel. 2017. Johnson Quantile-Parameterized Distributions. *Decision Analysis* **14**(1) 35-64.

[2] The Pearson system contains most well-known distributions, including (but not limited to): normal, gamma (which includes the exponential distribution), beta (which includes the uniform distribution), inverse-gamma, and beta-prime distributions. We do not go into more mathematical detail of the Pearson system here since many of its distributions have complex mathematical forms, particularly for quantile functions (e.g., for beta, beta-prime, and Type IV distributions). Rather, we introduce the Pearson system since it serves as a basis for comparison against our new J-QPD distributions in later chapters.

[3] For examples in the statistics literature, see: Ord (1972); Johnson (1949); Johnson, Kotz, and Balakrishnan (1994); and Tadikamalla and Johnson (1982). In the decision analysis literature, see (for example), Hammond and Bickel (2013a and 2013b), and Keelin (2016). For alternative, percentile-based measures of flexibility, see (for example) Moors (1988) and Moors et al. (1996) in the statistics literature, and Powley (2013) in the decision analysis literature.

system can satisfy, within the context of our SPT setup[4] – rather than direct measures of "shape".

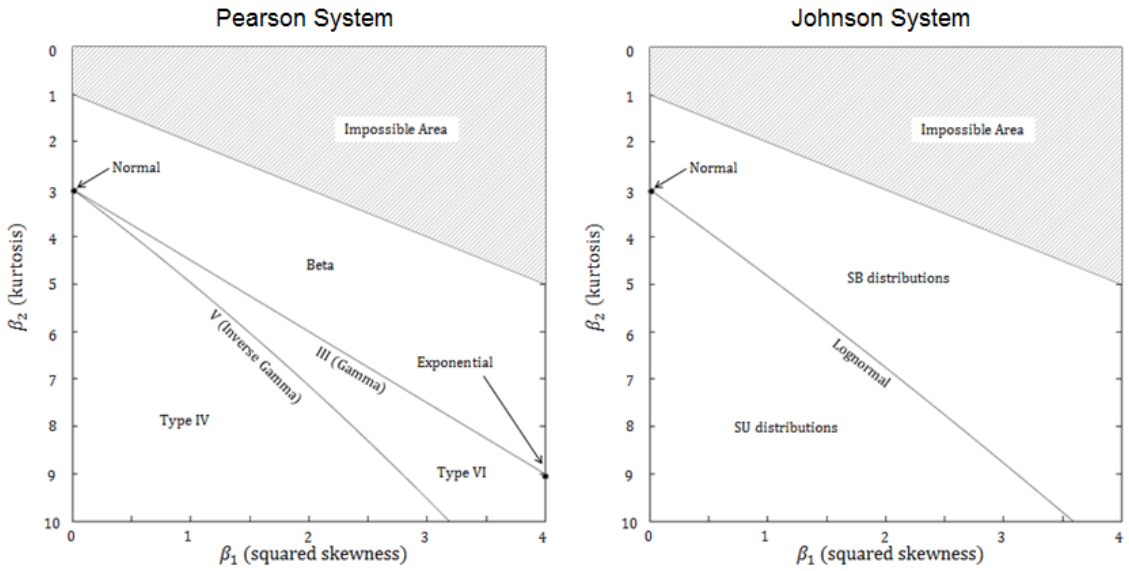

Figure 7.1. Pearson and Johnson Systems in the $\{\beta_1, \beta_2\}$ Space.

Figure 7.2 (Figure 7.3) (left) shows the span of J-QPD-B (J-QPD-S) in light grey within the $\{\beta_1, \beta_2\}$ space, over the region considered by Hammond and Bickel (2013a and 2013b). In both cases, we overlay Pearson's [Type] distributions, and the curve of lognormal distributions. Since the $\{\beta_1, \beta_2\}$ space extends toward infinity in both β_1 and β_2, we compactly visualize the entire space by implementing the following monotonic transformations:

$$H_1 = \frac{1}{1+\beta_1}, \tag{7.1}$$

$$H_2 = \frac{1}{\beta_2}. \tag{7.2}$$

[4] Thanks go to Tom Keelin and Brad Powley for holding a thoughtful discussion on the distinction between feasibility and flexibility.

The $\{H_1, H_2\}$ space for J-QPD-B (J-QPD-S) is shown in the right panel of Figure 7.2 (Figure 7.3). The triangle characterized by $H_2 \leq H_1 \cap H_1 \in (0,1) \cap H_2 \in (0,1)$ is the feasible region for all univariate distributions. Since J-QPD-B has three shape parameters for each $\alpha \in (0, 0.5)$, each point in the $\{H_1, H_2\}$ or $\{\beta_1, \beta_2\}$ space may correspond to more than one location-scale J-QPD-B subfamily.

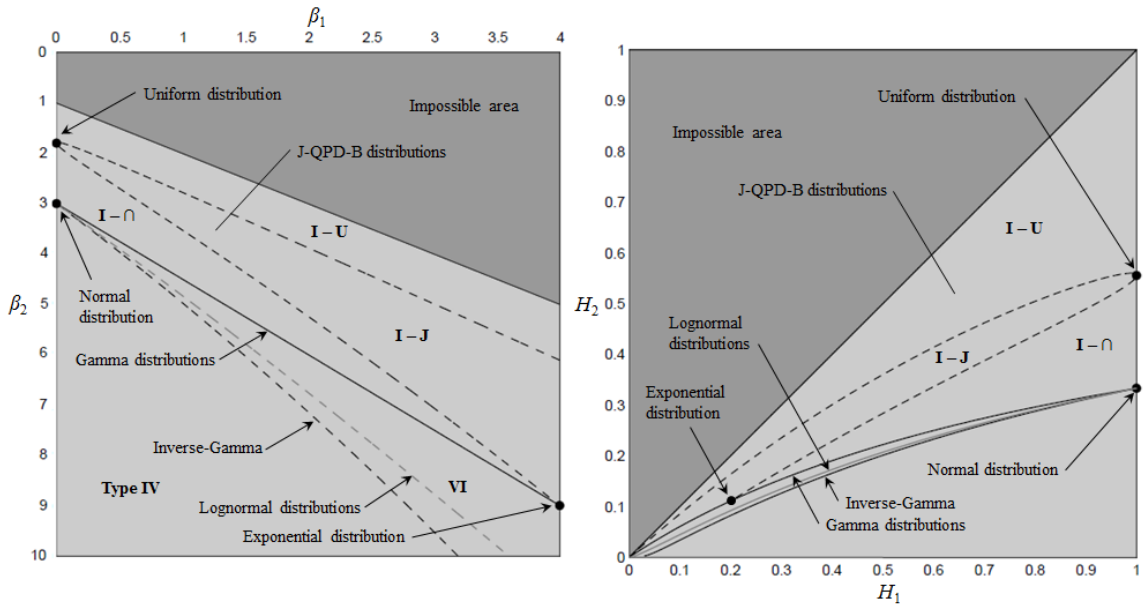

Figure 7.2. Span of J-QPD-B in the $\{\beta_1, \beta_2\}$ (left) and $\{H_1, H_2\}$ Spaces.

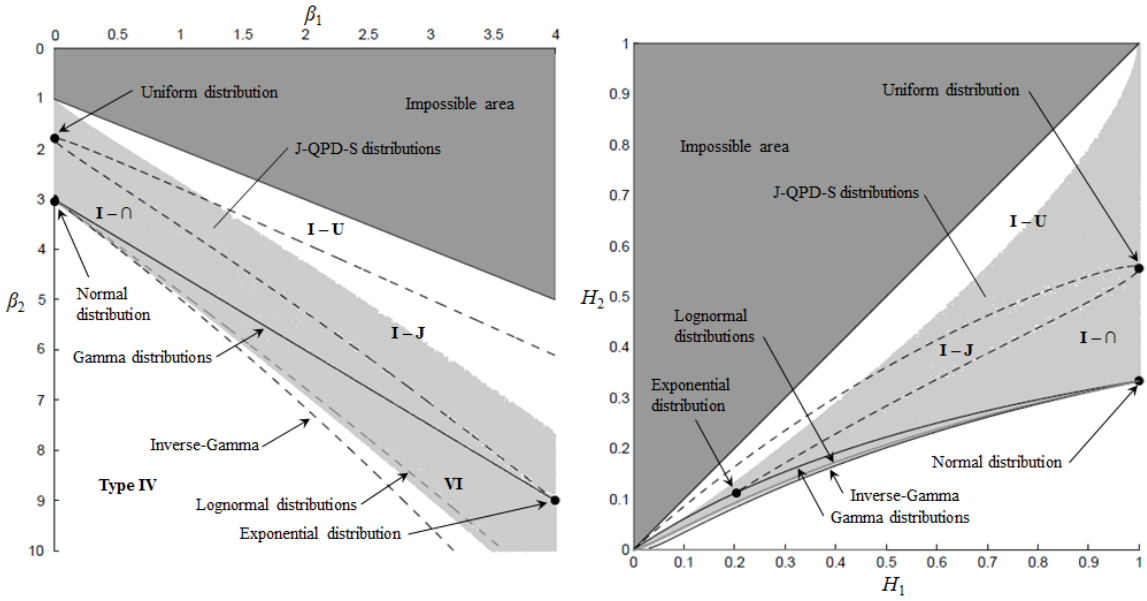

Figure 7.3. Span of J-QPD-S in the $\{\beta_1, \beta_2\}$ (left) and $\{H_1, H_2\}$ Spaces.

LIMITING DISTRIBUTIONS

Table 7.1 lists several distributions that occur as parametric limiting cases for J-QPD-B, characterized in standard (no location or scale parameters) quantile function form. Perhaps the most notable of these is S-II, since it is the only subfamily that can be expressed in our SPT-QPD form and is maximally-feasible. Given $\boldsymbol{\theta}_\alpha = (l, \mathbf{x}_\alpha, \infty)$, where l is a specified and finite lower bound of support, the quantile function for the S-II distributions is:

$$Q_{S-\mathrm{II}}(p) = l + \theta \cdot \exp\left(\lambda \cdot \sinh\left(\delta \cdot \left(nc + \Phi^{-1}(p)\right)\right)\right), \tag{7.3}$$

where,

$$c = \Phi^{-1}(1-\alpha),$$

$$L = \log(x_\alpha - l),\ B = \log(x_{0.5} - l),\ H = \log(x_{1-\alpha} - l),$$

$$n = \mathrm{sgn}(L + H - 2B)$$

$$\theta = \begin{cases} x_\alpha - l, & n = 1 \\ x_{0.50} - l, & n = 0 \\ x_{1-\alpha} - l, & n = -1 \end{cases}$$

$$\delta = \left(\frac{1}{c}\right)\left(\cosh^{-1}\left(\frac{H - L}{2\min(B - L, H - B)}\right)\right),$$

$$\lambda = \left(\frac{1}{\sinh(\delta c)}\right)\min(H - B, B - L).$$

S-II has unbounded moments, except in the special case where it corresponds to lognormal distributions, and corresponds to the special case of J-QPD-B in which (l, $\mathbf{x}_\alpha$) are fixed finite values, and where the upper bound (u) approaches infinity. S-II satisfies Desiderata 1 through 4, but is not applicable to the $\{\beta_1, \beta_2\}$ space, due to its unbounded moments. Like J-QPD-S, S-II has semi-bounded support, two shape parameters, and is maximally-feasible in the $\{s_\alpha, t_\alpha\}$ space. Figure 7.4 (Figure 7.5) provides CDFs (PDFs) for several S-II distributions, compared to the corresponding J-QPD-S distribution sharing the same $\boldsymbol{\theta}_\alpha$ vector in each case. Notice that S-II distributions are generally a

"more heavy-tailed version" of J-QPD-S, but can sometimes produce different shapes than J-QPD-S, as shown in Figure 7.5 for the case in which $\boldsymbol{\theta}_{0.10} = (0, 10, 20, 25, \infty)$.

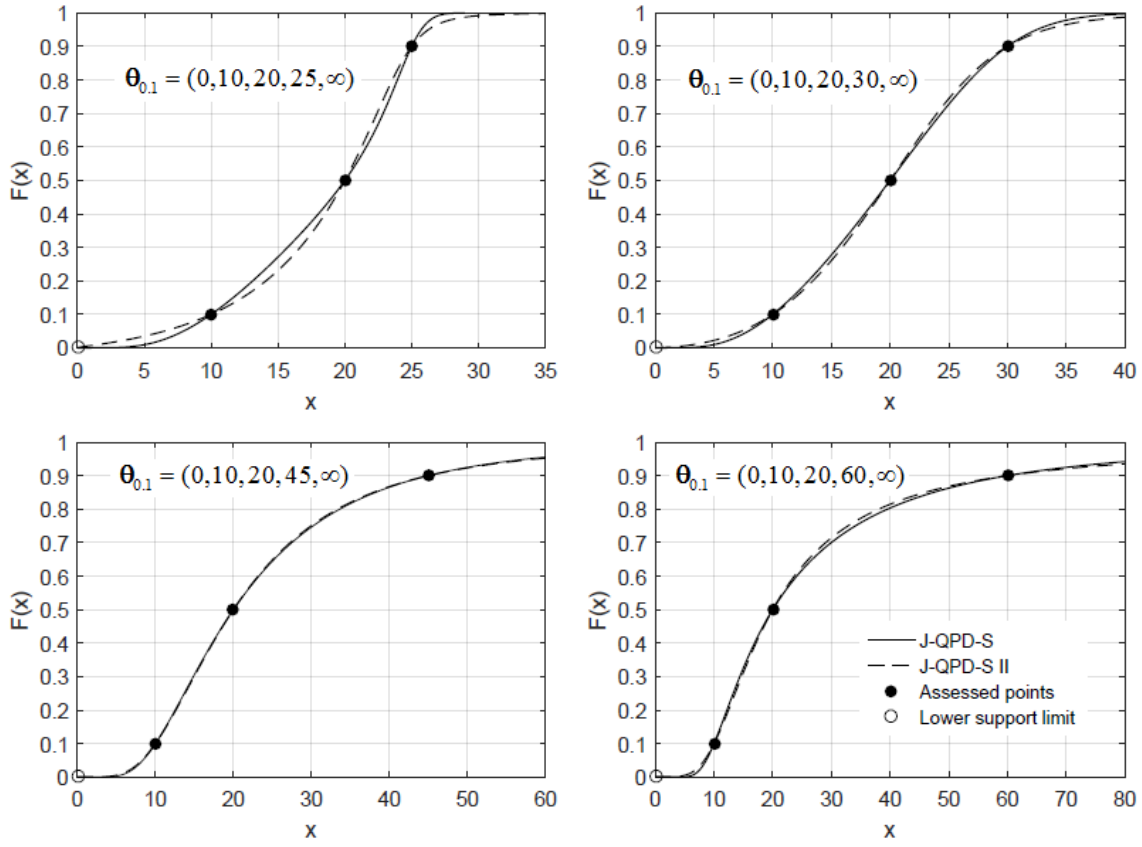

Figure 7.4. Comparison of Several S-II and J-QPD-S CDFs with the same $\boldsymbol{\theta}_{\alpha}$.

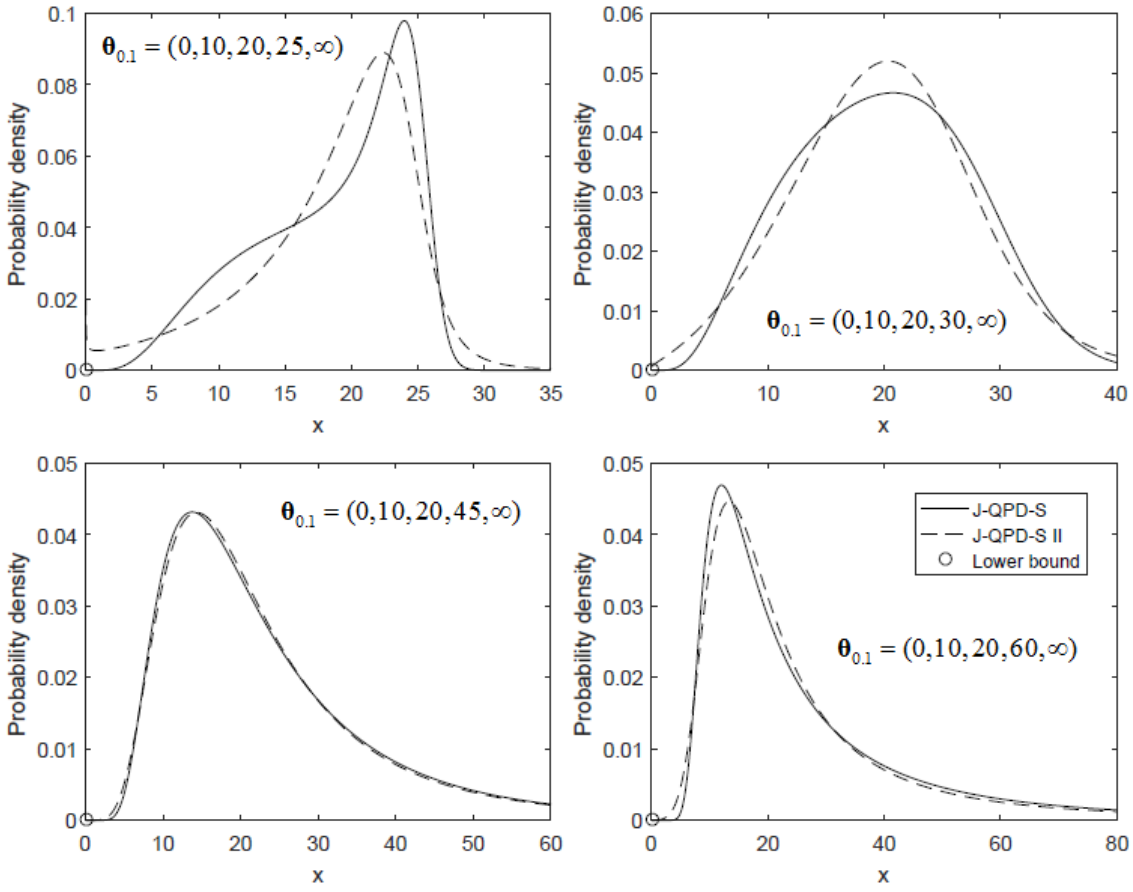

Figure 7.5. Comparison of Several S-II and J-QPD-S PDFs with the same $\boldsymbol{\theta}_{\alpha}$.

The S-II distributions might be well-suited for modeling uncertainties with heavy, Pareto-type tails. The B-III distributions have unbounded support, a single shape parameter, and correspond to a special case of the Johnson-SU distributions. Finally, B-IV distributions have bounded support and two shape parameters, and are similar in shape to the beta distributions.

Name	Quantile function	Parameters	Also contains	Comments
S-II	$\exp\left(\lambda \cdot \sinh\left(\delta\left(\pm c + \Phi^{-1}(p)\right)\right)\right)$	$\lambda > 0$, $\delta > 0$	Lognormal, normal distributions	Moments are unbounded except in lognormal/normal cases
B-III	$\sinh\left(\delta\left(\pm c + \Phi^{-1}(p)\right)\right)$	$\delta > 0$	Normal distributions	Special case of Johnson distributions
B-IV	$\Phi\left(\xi + \lambda \cdot \Phi^{-1}(p)\right)$	$\lambda > 0$	Lognormal, normal, uniform distributions	

Table 7.1. Limiting Distributions in the J-QPD-B System.

Name	Quantile function	Parameters	Also contains	Comments
S-III	$\exp\left(\lambda \cdot \left(\Phi^{-1}(p) \pm \left\lvert\Phi^{-1}(p)\right\rvert\right)\right)$	$\lambda > 0$	None	None
S-IV	$\exp\left(\sigma \cdot \Phi^{-1}(p)\right)$	$\sigma > 0$	Normal distributions	Lognormal distributions
S-V	$\sinh\left(\sinh^{-1}\left(\delta\,\Phi^{-1}(p)\right) \pm \sinh^{-1}(c\delta)\right)$	$\delta > 0$	Normal distributions	None

Table 7.2. Limiting Distributions in the J-QPD-S System.

Alternatively, Figure 7.3 illustrates that the J-QPD-S partially spans the $\{H_1, H_2\}$ and $\{\beta_1, \beta_2\}$ spaces, partly due to the arc-sinh operator, which results in finite moments. Also, J-QPD-S has two shape parameters, as opposed to three in the case of J-QPD-B. It is important to note that while J-QPD-S is maximally-feasible, meaning that it can accommodate any $\boldsymbol{\theta}_\alpha$ vector, the fatness of its tails (in terms of kurtosis) is approximately limited by lognormal distributions. However, note that J-QPD-S covers the entire region corresponding to the bell-shaped beta distributions in the $\{\beta_1, \beta_2\}$ space, most of the J-shaped region shown, including the exponential distribution, and subsumes the normal and lognormal distributions as limiting cases. Recall that J-QPD-S also includes several bimodal forms. Table 7.2 lists several limiting distributions for J-QPD-S. The S-IV

distributions are the lognormal distributions. S-III represents hybrid distributions having a point mass at one end of support, and continuity elsewhere. S-III distributions are bounded (semi-bounded) when “+/-“ is replaced with “-“ (“+”). Finally, S-V are bell-shaped distributions with one shape parameter (affecting both skewness and kurtosis) and unbounded support.

Chapter 8 : A Logistic Alternative to the J-QPD Distributions

Recall that our desiderata outlined in Chapter 4 require that our J-QPD systems have closed-form PDFs, CDFs, and quantile functions. Generally, there is some contention as to whether computations of cumulative probabilities and quantiles for a standard normal distribution (which is rooted within our J-QPD distributions) are admissible (for all practical purposes) as closed-form. In this chapter, we introduce a "logistic version" of J-QPD, denoted "L-QPD[1]", where Φ (Φ^{-1}) instead refers to the CDF (quantile function) of the standard logistic distribution (rather than the standard normal distribution), given by:

$$\Phi(x) = \frac{\exp(x)}{1+\exp(x)}, \tag{8.1}$$

$$\Phi^{-1}(p) = \log\left(\frac{p}{1-p}\right). \tag{8.2}$$

In this case, quantile function and parameter expressions for L-QPD-B (bounded) and L-QPD-S (semi-bounded) are the same as given in (4.4) and (4.7), respectively, and all five desiderata remain preserved. Figure 8.1 provides several illustrative examples, based on beta distributions, comparing PDFs of L-QPD-B to J-QPD-B distributions sharing the same SPT and bounds. For example, "SPT based on beta (α = 10, β = 1)" means that we provide L-QPD-B and J-QPD-B distribution assignments sharing the same {10^{th}, 50^{th}, 90^{th}} percentiles as a beta(10, 1) distribution, and having support on [0, 1].

[1] This follows the main idea of Tadikamalla and Johnson (1982), where Johnson distributions are transformed to have the standard logistic distribution as the root distribution in place of the standard normal distribution. More details for the L-QPD distributions are available from the authors upon request.

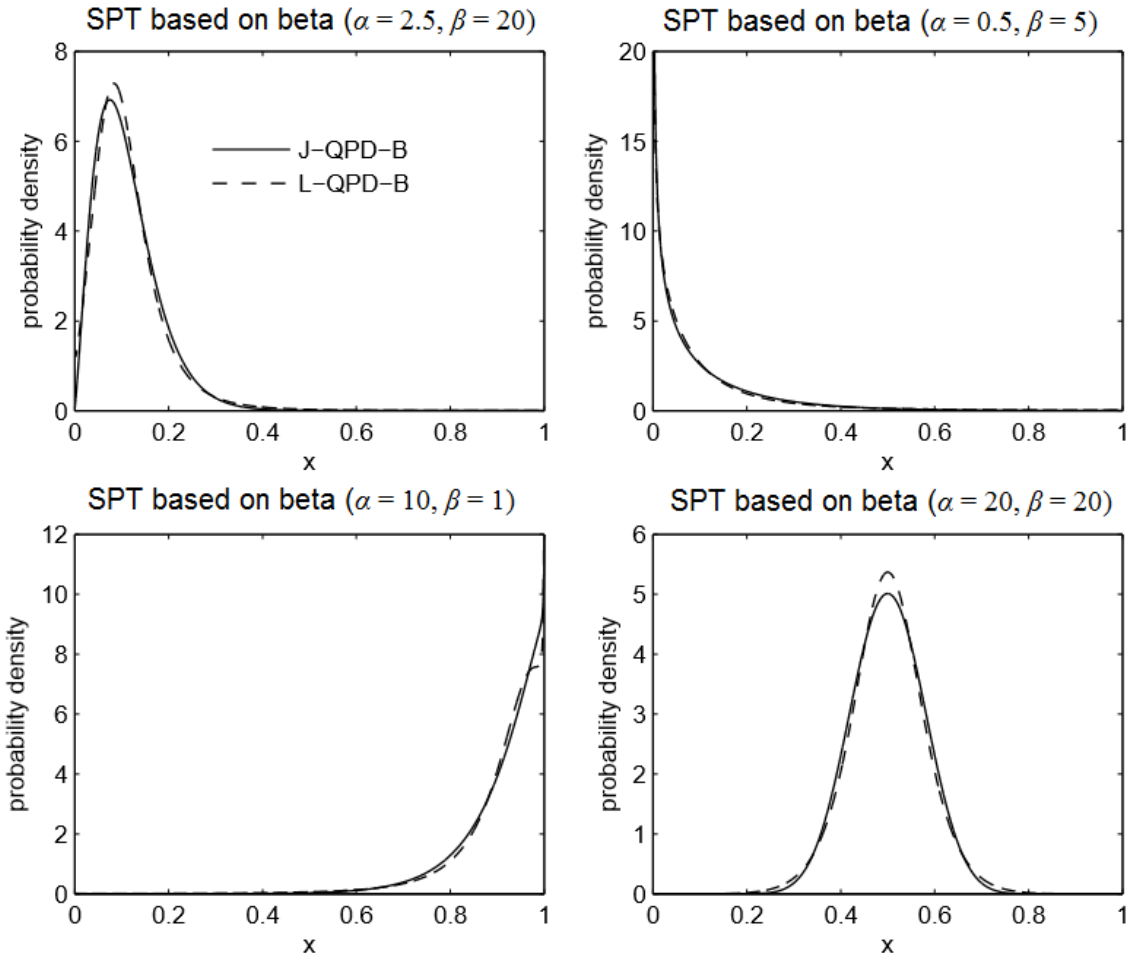

Figure 8.1. Examples Comparing L-QPD-B to J-QPD-B.

Special Case for L-QPD-B (bounded)

For J-QPD-B, recall that for the special case in which $n = 0$, the quantile function is:

$$Q_B(p) = l + (u - l)\Phi\left(B + \left(\frac{H - L}{2c}\right)\Phi^{-1}(p)\right). \tag{8.3}$$

For L-QPD-B, (where Φ corresponds to the logistic distribution), (8.3) corresponds to the bounded "LB" distributions proposed by Tadikamalla and Johnson (1982), which are like beta distributions in terms of shapes and flexibility.

Special Case for L-QPD-S (semi-bounded)

For J-QPD-S, recall that for the special case in which $L+H-2B = 0$, we have $n = \text{sgn}(L+H-2B) = \text{sgn}(0) = 0$, in which case:

$$Q_S(p) = l + \theta \exp\left(\lambda \sinh\left(\sinh^{-1}\left(\delta \Phi^{-1}(p)\right)\right)\right) = l + \theta \exp\left(\lambda \delta \Phi^{-1}(p)\right). \quad (8.4)$$

Recall that for J-QPD-S, (8.4) corresponds to the lognormal distributions, shifted to have support on (l, ∞). For L-QPD-S, where Φ is the logistic distribution, (8.4) corresponds to the log-logistic distributions with scale (shape) parameter given by θ ($\beta = 1/\lambda\delta$), shifted to have support on $[l, \infty)$. Thus, L-QPD-S is a generalization of log-logistic distributions, parameterized by any compatible SPT and finite lower bound, having two shape parameters, $\{\lambda, \delta\}$, whereas log-logistic distributions only have one shape parameter.

PROPERTIES AND TRADEOFFS BETWEEN L-QPD AND J-QPD

There are several important tradeoffs to note between J-QPD and L-QPD.

Computational Efficiency

Since error functions (or their inverses) are replaced with log (or exp) computations, PDF, CDF, and quantile function calculations for L-QPD are computationally more efficient than those for J-QPD. Specifically, the computational efficiency of computing cumulative probabilities and quantiles for the logistic distribution is about an order-of-magnitude better than when using the normal distribution. For example, computing normal quantiles with MATLAB using the method proposed by Cody (1969) takes over ten times longer than computing quantiles for the logistic distribution.

Moments

Although J-QPD-S has finite moments (like lognormal distributions), L-QPD-S can have finite, infinite, or undefined moments, like log-logistic distributions[2]. The k^{th} raw moment for L-QPD-S exists if and only if:

$$k\lambda\delta\left(nc\delta+\sqrt{1+(cd)^2}\right)<1. \tag{8.5}$$

For a proof, see Appendix E.

Figure 8.2 shows boundary lines for L-QPD-S in the $\{s_{0.10}, t_{0.10}\}$ space, beyond which mean and variance are undefined. For example, L-QPD-S distributions with $\{s_{0.10}, t_{0.10}\} = \{0.25, 0.7\}$ have finite mean, but undefined variance. Note that the region for finite variance is smaller than that for finite mean. Higher-order moments have a smaller span in the $\{s_{0.10}, t_{0.10}\}$ space for which they are finite.

[2] For more on the log-logistic distributions, see Tadikamalla and Johnson (1982), and Tadikamalla (1980).

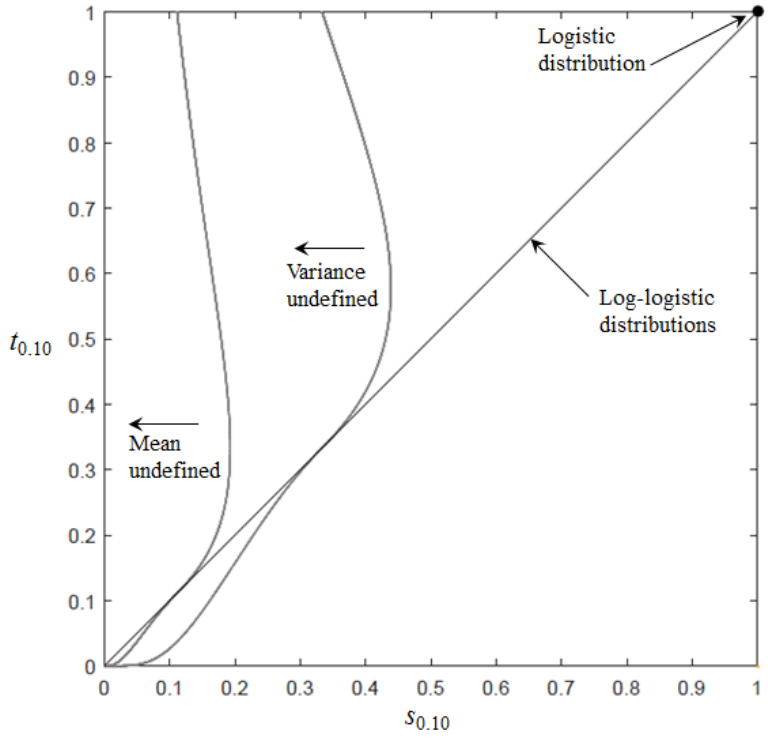

Figure 8.2. Mean and Variance Boundary Lines for L-QPD-S in the $\{s_{0.10}, t_{0.10}\}$ Space.

Flexibility in the Moment-Ratio Space

Figure 8.3 (Figure 8.4) compares J-QPD-S to L-QPD-S in the $\{\beta_1, \beta_2\}$ space for $\alpha = 0.1$ (for $\alpha \in (0, 0.5)$). Note that while both J-QPD-S and L-QPD-S are maximally-feasible for each $\alpha \in (0, 0.5)$, L-QPD-S spans a larger portion of the $\{\beta_1, \beta_2\}$ space than J-QPD-S[3].

[3] We do not include plots for L-QPD-B, since it spans the entire $\{\beta_1, \beta_2\}$ space shown, like J-QPD-B.

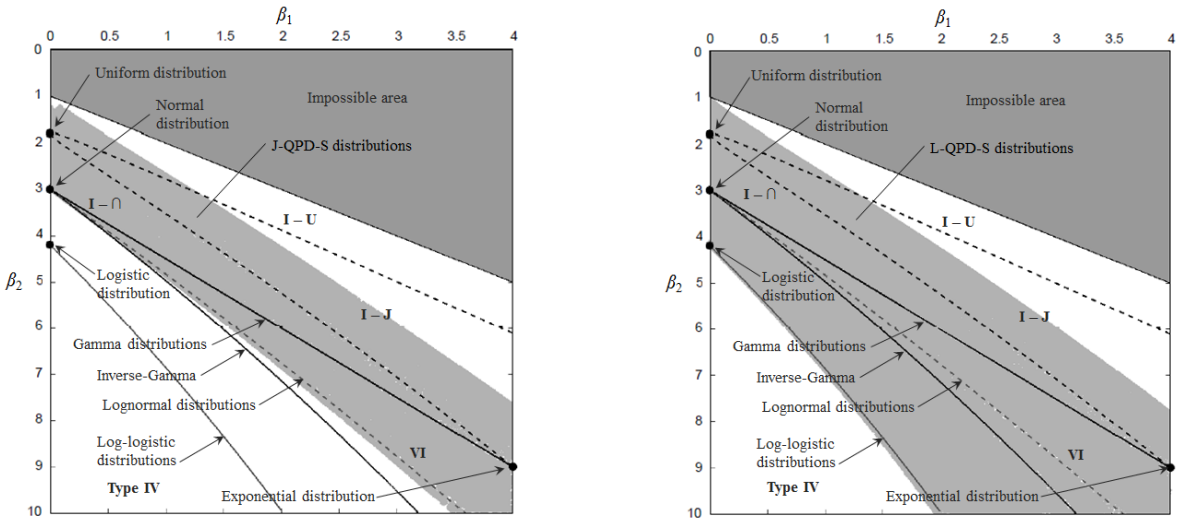

Figure 8.3. Span of J-QPD-S (left) and L-QPD-S (right) in the $\{\beta_1, \beta_2\}$ Space for $\alpha = 0.1$.

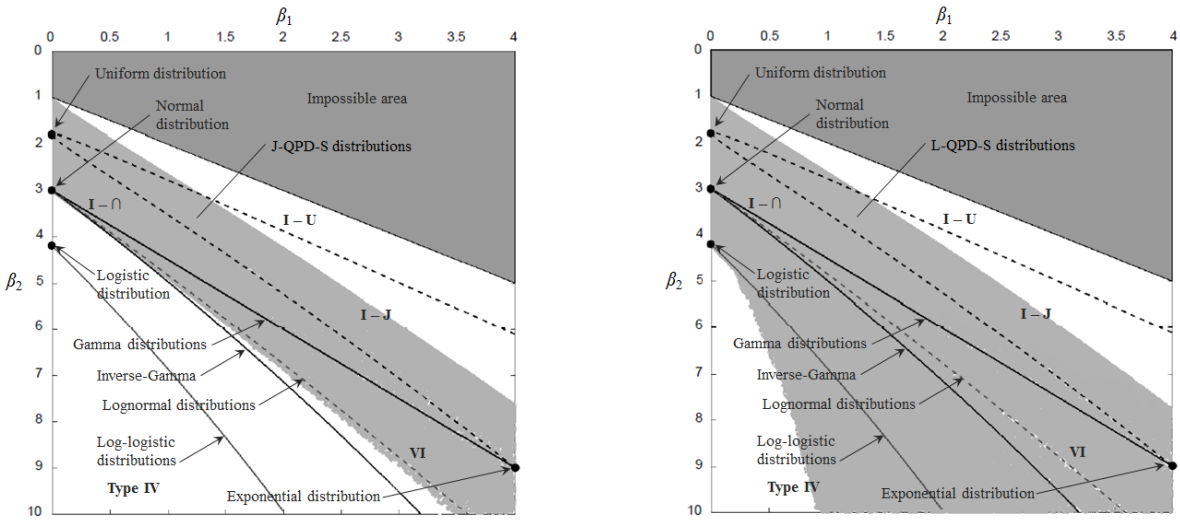

Figure 8.4. Span of J-QPD-S (left) and L-QPD-S (right) in the $\{\beta_1, \beta_2\}$ Space for $\alpha \in (0, 0.5)$.

Limiting Distributions

Table 8.1 (Table 8.2) lists parametric limiting distributions for L-QPD-B (L-QPD-S), expressed in standard form – location and scale parameters omitted. Like the S-II system, LS-II is the only special case that can be quantile-parameterized by an SPT, and satisfies

our SPT-based notion of maximally-feasible. The quantile function is the same as that for S-II given in (7.3), except using our new definition for Φ^{-1}.

LS-II is the special case of L-QPD-B where $\{l, x_\alpha, x_{0.5}, x_{1-\alpha}\}$ are fixed finite values, and where the upper bound approaches infinity. Like S-II, LS-II meets Desiderata 1 through 4, but cannot be expressed in the $\{\beta_1, \beta_2\}$ space, since it has unbounded moments. LS-II distributions have semi-bounded support, two shape parameters, and shapes similar to L-QPD-S, but with fatter tails. Figure 8.5 (Figure 8.6) compares CDFs (PDFs) for several LS-II and L-QPD-S distributions sharing the same $\boldsymbol{\theta}_\alpha$ vector.

Name	Quantile function	Parameters	Also contains	Comments
LS-II	$\exp\left(\lambda \cdot \sinh\left(\delta\left(\pm c + \Phi^{-1}(p)\right)\right)\right)$	$\lambda > 0$, $\delta > 0$	Log-logistic, logistic distributions	Moments are unbounded except in some cases of the log-logistic.
LU-I	$\sinh\left(\delta\left(\pm c + \Phi^{-1}(p)\right)\right)$	$\delta > 0$	Logistic distributions	Special case of "LU" distributions
LB-II	$\Phi\left(\xi + \lambda \cdot \Phi^{-1}(p)\right)$	$\lambda > 0$	Log-logistic, logistic, uniform distributions	The "LB" distributions

Table 8.1. Limiting Distributions in the L-QPD-B System.

Name	Quantile function	Parameters	Also contains	Comments
LH-II	$\exp\left(\lambda \cdot \left(\Phi^{-1}(p) \pm \left\|\Phi^{-1}(p)\right\|\right)\right)$	$\lambda > 0$	None	None
LS-III	$\exp\left(\sigma \cdot \Phi^{-1}(p)\right)$	$\sigma > 0$	Logistic distributions	Log-logistic distributions
LU-II	$\sinh\left(\sinh^{-1}\left(\delta\,\Phi^{-1}(p)\right) \pm \sinh^{-1}(c\delta)\right)$	$\delta > 0$	Logistic distributions	None

Table 8.2. Limiting Distributions in the L-QPD-S System.

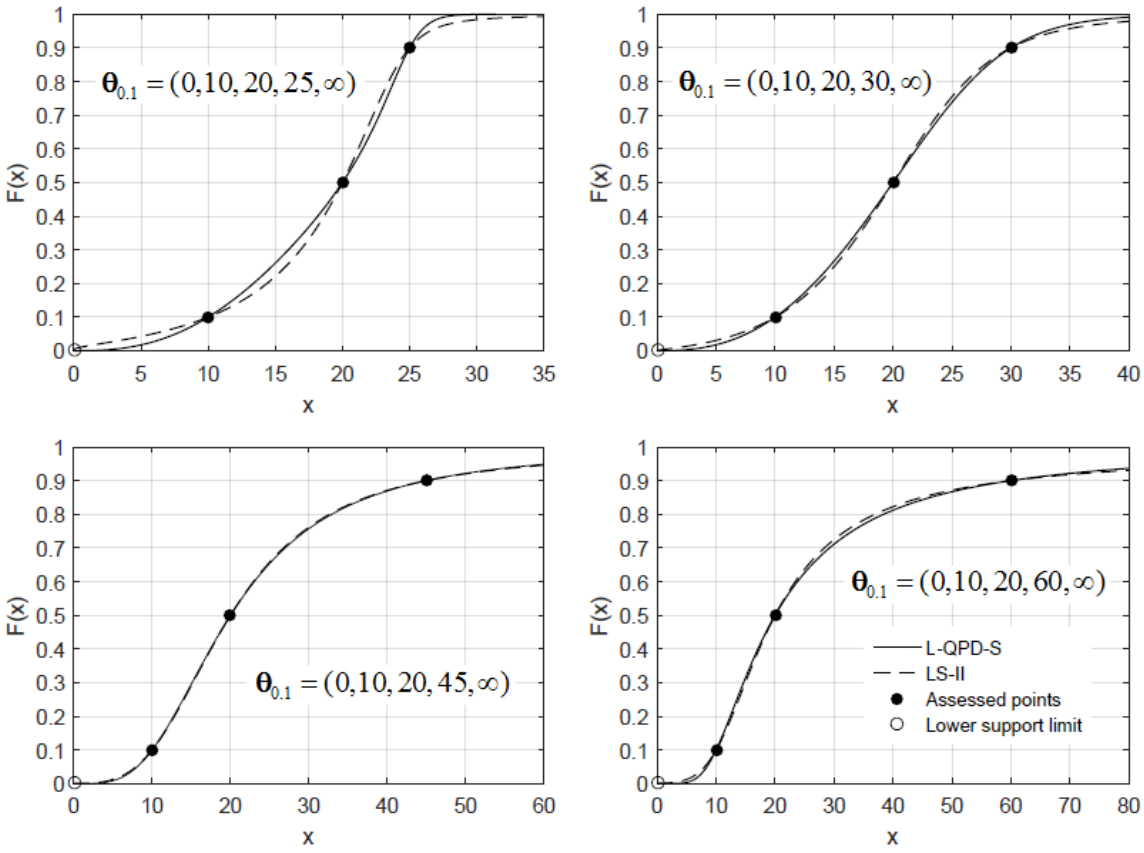

Figure 8.5. Comparison of Several LS-II and L-QPD-S CDFs with the same $\boldsymbol{\theta}_{\alpha}$.

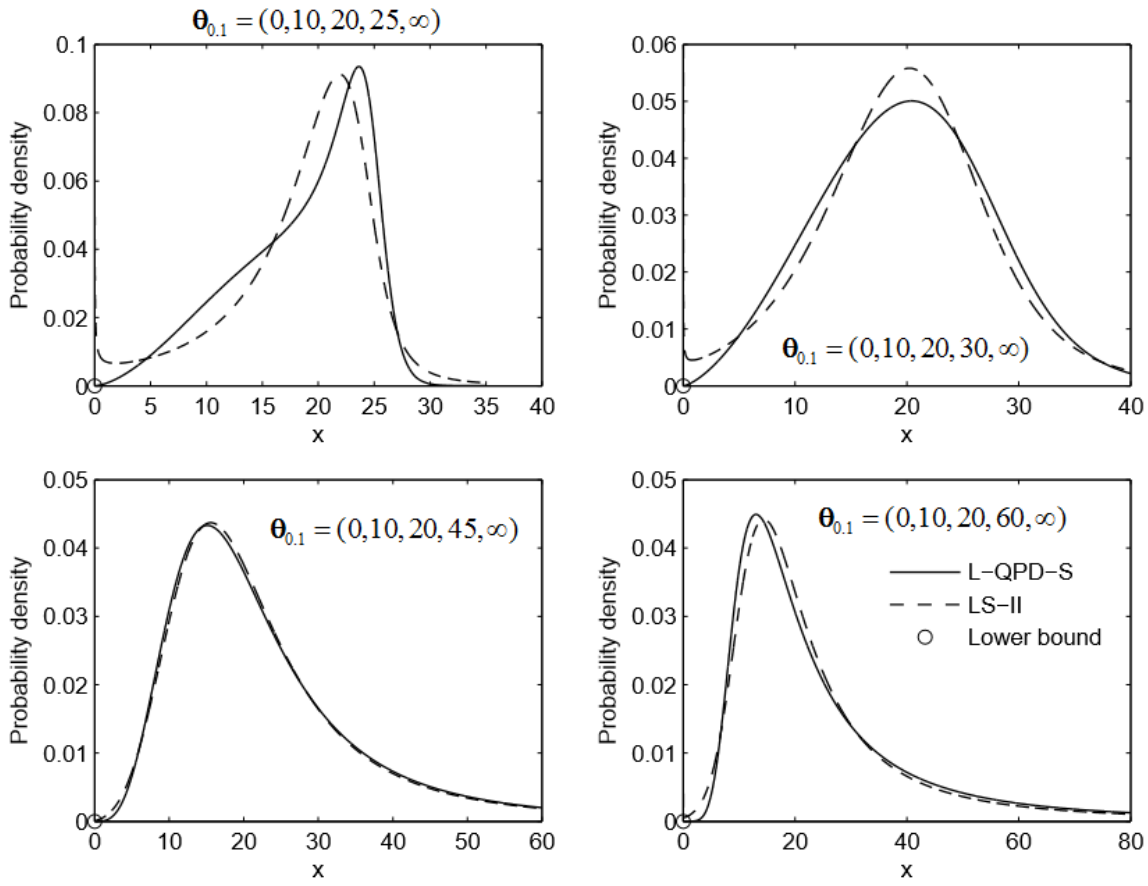

Figure 8.6. Comparison of Several LS-II and L-QPD-S PDFs with the same $\boldsymbol{\theta}_{\alpha}$.

The remaining subfamilies in Table 8.1 and Table 8.2 are not amenable to our QPD setup, but are worth mentioning briefly. LU-I distributions have unbounded support, a single shape parameter, and are a special case of the "LU" distributions – see Tadikamalla and Johnson (1982). LB-II distributions correspond to the "LB" distributions, which have bounded support and two shape parameters (like beta distributions), and are well-studied – see Tadikamalla and Johnson (1982) for more on the "LB" distributions. LS-III distributions are the log-logistic distributions. LH-II is a system of hybrid distributions having a point mass at one end of support, and continuity elsewhere. LH-II distributions are bounded (semi-bounded) when "+/-" is replaced with

"-" ("+"). Finally, LU-II distributions are bell-shaped, have one shape parameter (affecting both skewness and kurtosis), and unbounded support.

Closeness to Commonly-Named Distributions

Like J-QPD, L-QPD distributions are generally accurate at preserving the shapes of a wide array of commonly-named distributions (Desideratum 4). We compare both J-QPD-B and L-QPD-B (J-QPD-S and L-QPD-S) to the beta (beta-prime) distributions, as depicted by their respective spans in the $\{s_{0.10}, t_{0.10}\}$ space, using the four closeness measures from Chapter 6 – APDM, APDV, KS distance, and KL divergence.

Comparison of L-QPD-B and J-QPD-B to Beta Distributions

Figure 8.7 displays the span of the beta distributions in the $\{s_{0.10}, t_{0.10}\}$ space, including shaded error contours for APDM, APDV, KS distance, and KL divergence for J-QPD-B and L-QPD-B with respect to the corresponding beta distribution sharing the same $\{10^{th}, 50^{th}, 90^{th}\}$ percentiles and bounds. Table 8.3 provides summary statistics for each error measure across the grid of 104,000 points (distributions) on which the contours in Figure 8.7 are generated. Highlighted cells in Table 8.3 indicate which distribution (J-QPD-B or L-QPD-B) better-approximates beta distributions overall for the given summary statistic. Based on median values for ∩- and J-shaped distribution regions, J-QPD-B more-closely approximates beta distributions than L-QPD-B by one or more orders of magnitude for all three error metrics. However, L-QPD-B and J-QPD-B perform almost equally well in proximity to the uniform distribution, since both systems contain the uniform distribution. Also, J-QPD-B and L-QPD-B approximate U-shaped distributions to nearly the same degree of closeness. Generally, the performance of L-QPD-B, relative to J-QPD-B, degrades most notably near the gamma distributions at the boundary.

J-QPD-B more-closely approximates beta distributions for roughly 85% (80%) of the $\{s_{0.10}, t_{0.10}\}$ space for APDM (APDV), and for about 95% of the $\{s_{0.10}, t_{0.10}\}$ space for KS distance (KL divergence). Also, J-QPD-B better-approximates nearly all bell-shaped beta distributions than L-QPD-B, while L-QPD-B is generally a better approximation for highly skewed J- or U-shaped beta distributions than J-QPD-B.

a) APDM (J-QPD-B)

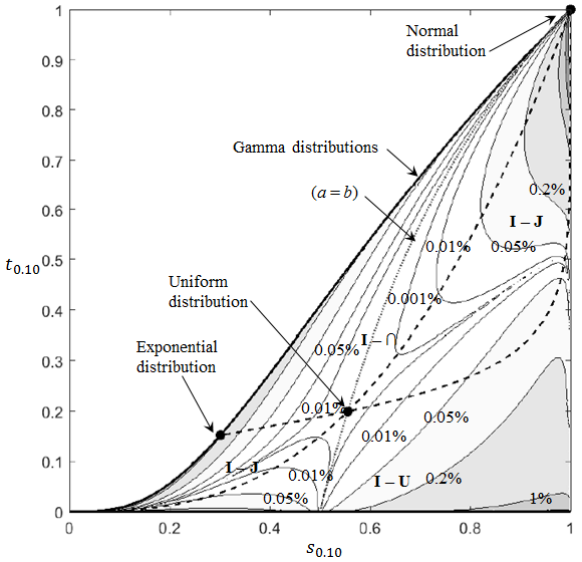

b) APDM (L-QPD-B)

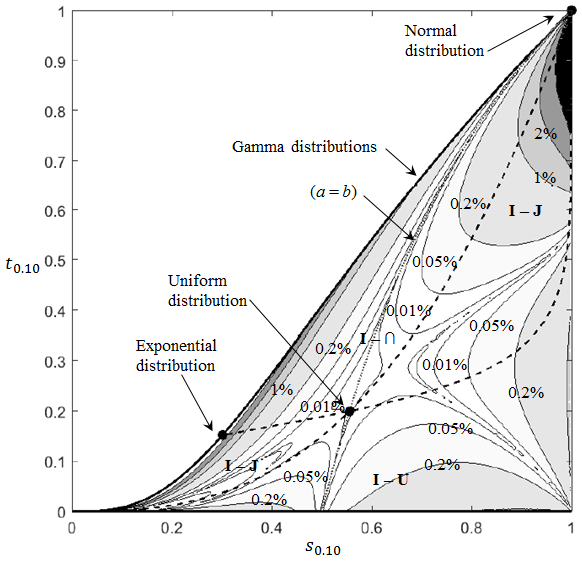

c) APDV (J-QPD-B)

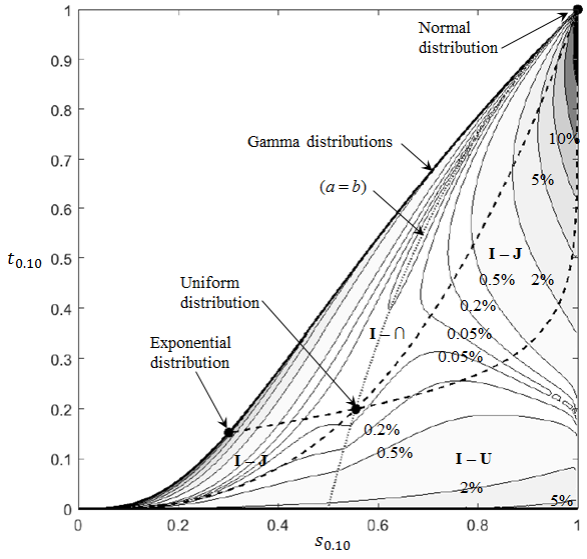

d) APDV (L-QPD-B)

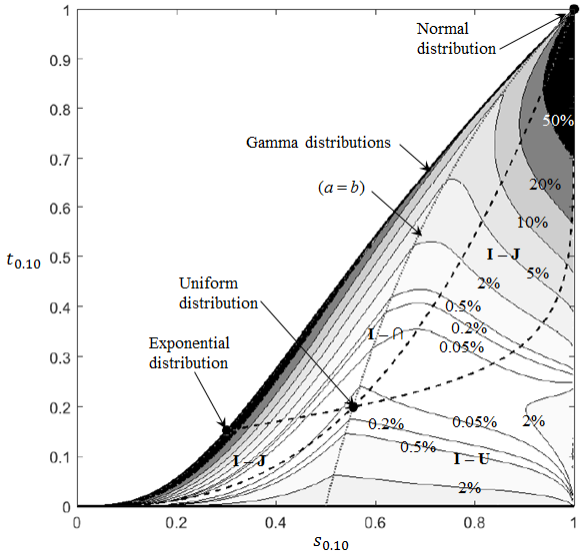

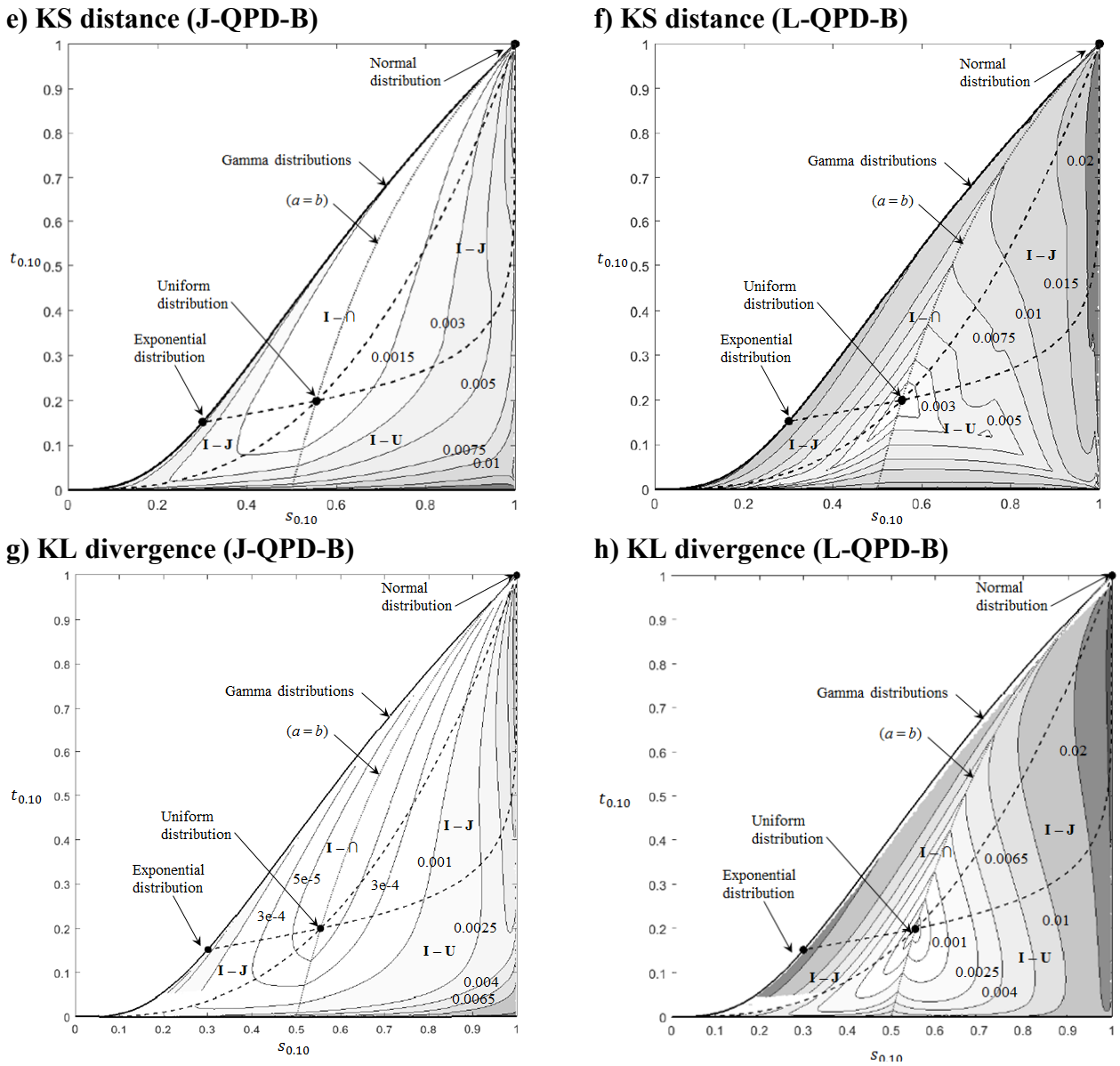

Figure 8.7. Error Contours for J- and L-QPD-B w.r.t. Beta Distributions.

Metric (by region)	Minimum	Median	Maximum	Mean
I-∩ (Beta)				
APDM (L-QPD-B)	0.0%	0.2%	45.7%	0.5%
APDM (J-QPD-B)	0.0%	0.0%	1.6%	0.1%
APDV (L-QPD-B)	0.0%	5.3%	1.2e6%	173.9%
APDV (J-QPD-B)	0.0%	0.3%	46.6%	1.1%
KS distance (L-QPD-B)	0.000	0.011	0.019	0.010
KS distance (J-QPD-B)	0.000	0.001	0.007	0.001
KL divergence (L-QPD-B)	0.0000	0.0089	0.0262	0.0092
KL divergence (J-QPD-B)	0.0000	8e-5	0.0033	2.4e-4
$I - J(\text{Beta})$				
APDM (L-QPD-B)	0.0%	0.1%	334.1%	0.8%
APDM (J-QPD-B)	0.0%	0.0%	9.7%	0.2%
APDV (L-QPD-B)	0.0%	3.6%	1.9e6%	252.3%
APDV (J-QPD-B)	0.0%	1.0%	809.0%	4.1%
KS distance (L-QPD-B)	0.000	0.012	0.033	0.012
KS distance (J-QPD-B)	0.000	0.003	0.014	0.003
KL divergence (L-QPD-B)	0.0000	0.0133	0.0608	0.0152
KL divergence (J-QPD-B)	0.0000	0.0013	0.0175	0.0021
$I - U(\text{Beta})$				
APDM (L-QPD-B)	0.0%	0.1%	1.4%	0.2%
APDM (J-QPD-B)	0.0%	0.1%	2.2%	0.2%
APDV (L-QPD-B)	0.0%	0.6%	27.3%	1.2%
APDV (J-QPD-B)	0.0%	0.7%	9.3%	1.1%
KS distance (L-QPD-B)	0.000	0.008	0.037	0.009
KS distance (J-QPD-B)	0.000	0.005	0.042	0.006
KL divergence (L-QPD-B)	0.0000	0.0055	0.0512	0.0083
KL divergence (J-QPD-B)	0.0000	0.0017	0.0434	0.0026

Table 8.3. Error Measures for J- and L-QPD-B w.r.t. Beta Distributions.

Comparison of L-QPD-S and J-QPD-S to Beta-Prime Distributions

Since L-QPD-S and beta-prime have finite moments over small, non-coincident regions of the $\{s_{0.10}, t_{0.10}\}$ space, Figure 8.8 compares J-QPD-S and L-QPD-S to beta-prime only on KS distance and KL divergence. Since J-QPD-S and beta-prime share the normal distribution, the KS distance is zero here for J-QPD-S. L-QPD-S exhibits larger errors near the upper right corner of Figure 8.8, since here it substitutes the logistic- for the normal distribution. However, L-QPD-S more accurately approximates beta-prime as $s_{0.1}$ and $t_{0.1}$ decrease, corresponding to distributions of greater skew.

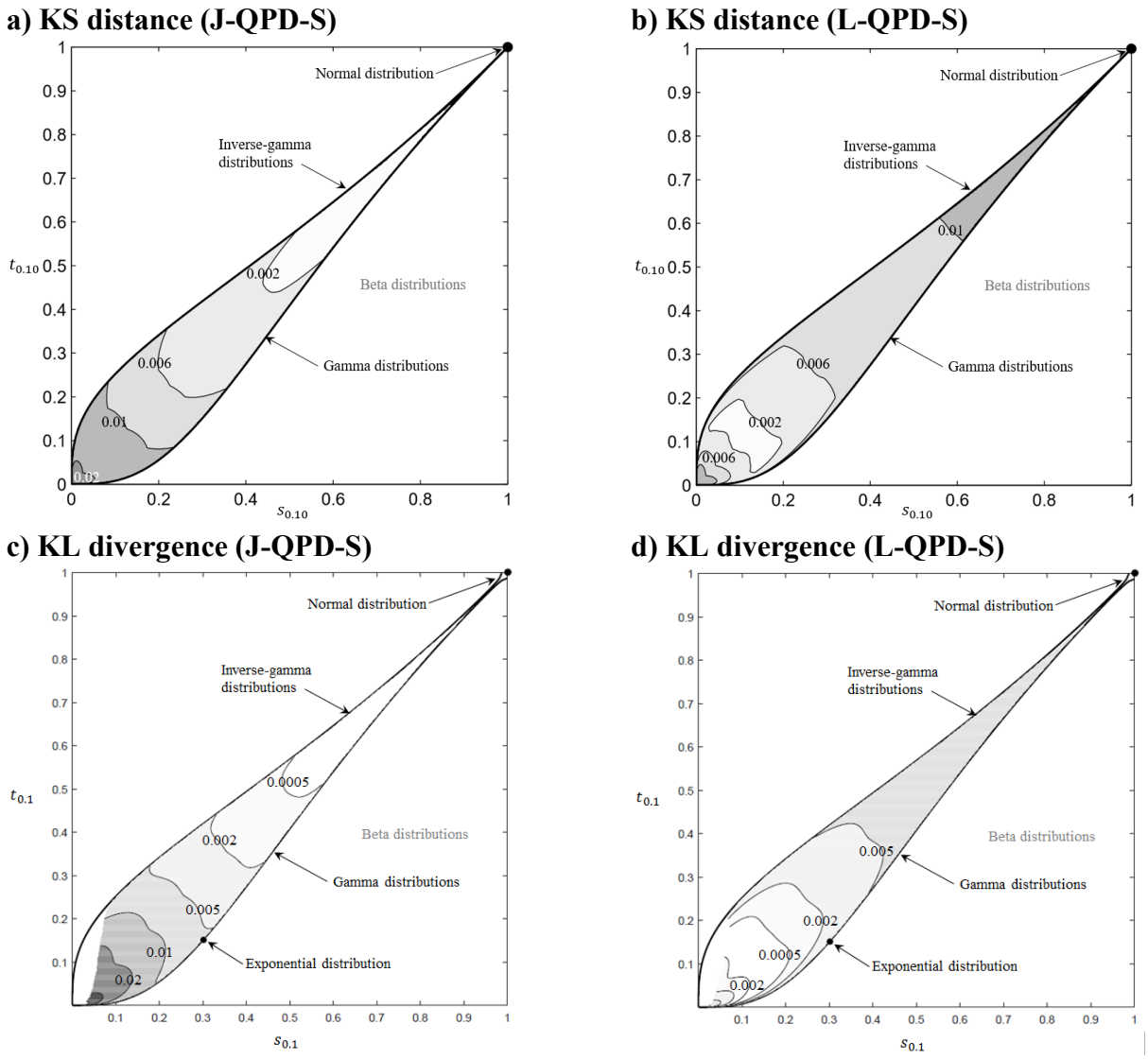

Figure 8.8. Error Contours for J- and L-QPD-S w.r.t. Beta-Prime Distributions.

Table 8.4 gives summary statistics for KS distances and KL divergences computed across the grid of 35,000 points (distributions) on which contours in Figure 8.8 are generated. Highlighted cells in Table 8.4 indicate which distribution (J-QPD-S or L-QPD-S) better-approximates beta-prime overall – the smaller the closeness measure, the better the approximation. Note that while J-QPD-S generally better-approximates beta-prime based on median values for KS distance and KL divergence, orders of magnitude

are similar. We note that L-QPD-B more closely approximates beta-prime for about 40% of the $\{s_{0.10}, t_{0.10}\}$ space, mostly where $s_{0.1}$ and $t_{0.1}$ are small, corresponding to distributions with heavier tails and greater skew.

Metric	Min.	Median	Max.	Mean
KS distance (J-QPD-S)	0.000	0.005	0.031	0.006
KS distance (L-QPD-S)	0.000	0.007	0.020	0.007
KL divergence (J-QPD-S)	0.0000	0.0032	0.0749	0.006
KL divergence (L-QPD-S)	0.0000	0.0036	0.0125	0.0039

Table 8.4. Error Measures for J- and L-QPD-S w.r.t. Beta-Prime Distributions.

SUMMARY AND RECOMMENDATIONS FOR PRACTICE

In this chapter, we presented the L-QPD-B (bounded) and L-QPD-S (semi-bounded) distribution systems by replacing cumulative probability and quantile function operations for the normal distribution with those for the logistic distribution (respectively), within the expressions for J-QPD-B and J-QPD-S developed in Chapter 4. Like J-QPD, L-QPD distributions are smooth, and satisfy all five desiderata presented in Chapter 4. In particular, L-QPD distributions are conveniently parameterized by an SPT of low-base-high assessments (e.g., 10^{th}, 50^{th}, 90^{th} percentiles), support bounds, and are maximally-feasible – they can honor any SPT and bounds that satisfy the axioms of probability. Also, L-QPD is highly flexible in Pearson's moment-ratio space, and closely-approximates numerous commonly-named distributions, including: beta; beta prime; lognormal; logistic; log-logistic.

We also presented several important tradeoffs between J-QPD and L-QPD. L-QPD is more computationally-efficient than J-QPD, due to the simpler functional form of the logistic distribution compared to the normal distribution – computing cumulative probabilities and quantiles for L-QPD is about an order-of-magnitude faster than those

required for J-QPD. Also, L-QPD-S spans a wider area than J-QPD-S in Pearson's (1895, 1901, and 1916) moment-ratio space, which is noteworthy, since this space has become a standard for measuring distribution flexibility – as noted in Chapter 7.

However, while J-QPD has finite moments (like lognormal distributions), L-QPD-S can have finite, infinite, or undefined moments, depending on the parameterization – like log-logistic distributions. Also, L-QPD is slightly less accurate than J-QPD at approximating various commonly-named distributions. For L-QPD-B, examples include the beta distributions. For L-QPD-S, examples include the beta-prime and lognormal distributions. Also, L-QPD less-accurately approximates a normal distribution than J-QPD, since the root distribution in L-QPD is the logistic distribution rather than the Gaussian (normal). Still, L-QPD approximates these commonly-named distributions quite well in an absolute sense.

Finally, it is important to mention that L-QPD-S has log-logistic tails in an asymptotic sense. If thinner tails are desired, then J-QPD-S may be a better modeling alternative, since it has lognormal tails. Conversely, if fatter tails are desired, and finite moments are not required, then the LS-II distributions presented in Table 8.1 may be a more appropriate modeling choice.

Chapter 9 : Modeling Dependence with J-QPDs

If an expert's distribution for some uncertainty, *X*, changes with respect to observed values for another uncertainty, *Y*, then we say that *X* and *Y* are *relevant, correlated,* – or *dependent*. For example, adopting the example from Smith (1993), suppose we want to valuate a prospective drilling venture where *X* denotes the uncertain oil price, and *Y* denotes uncertain production costs. Figure 9.1 shows a partial influence diagram[1] of the problem, where the arrow from Oil Price to Production Costs indicates that the distribution for Production Costs depends on (changes with) the observed value for Oil Price.

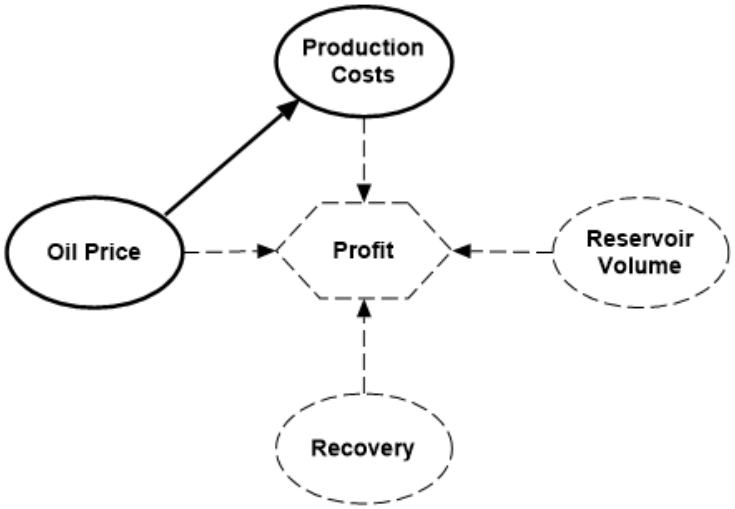

Figure 9.1. Influence Diagram for the Wildcatter Example, adopted from Smith (1993).

When the distributions for dependent uncertainties are discrete, we can depict their relationship quantitatively using a decision tree, and characterize the conditional probabilities using Bayes' equation:

[1] For more on influence diagrams, see Howard and Matheson (1981), and Shachter (1986, 1988).

$$P(A|B) = \frac{P(A \cap B)}{P(B)} = \frac{P(A) \cdot P(B|A)}{P(B)}. \tag{9.1}$$

Returning to the Wildcatter problem, for example, Figure 9.2 shows an event tree for Production Costs (*PC*) and Oil Price (*OP*) for the case in which both *PC* and *OP*|*PC* have a discrete distribution with two possible outcomes: low, high. Notice that Bayes' equation is straightforward in the discrete case, and fully captures the joint distribution between pairs of uncertainties.

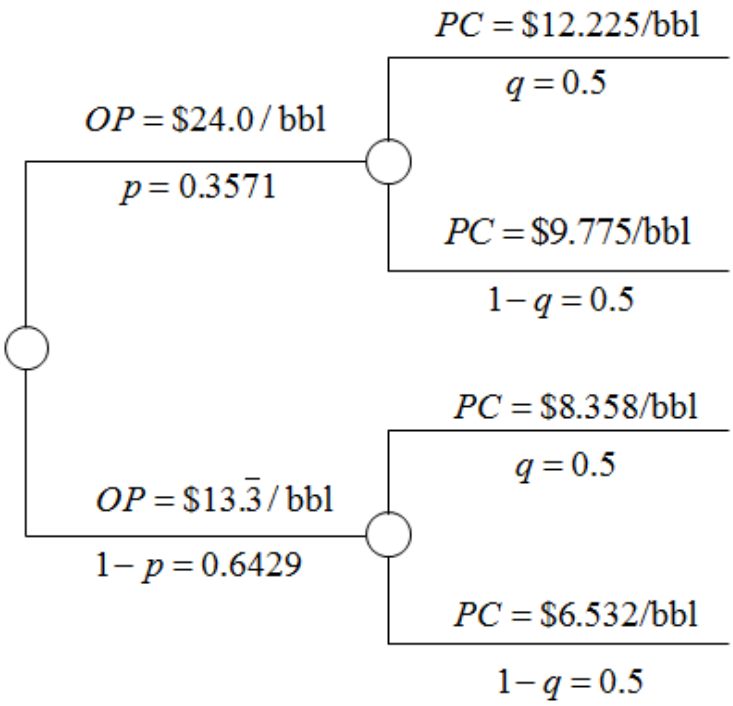

Figure 9.2. Event Tree for the Wildcatter Example.

Difficulty in encoding dependence among uncertainties arises when their joint and marginal distributions are continuous. So far, we have demonstrated the fidelity and efficiency of encoding *marginal* distributions, given QP pairs and specified support bounds, using J-QPD. In this chapter, we use J-QPD to develop efficient, high-fidelity

methods for encoding and sampling from a continuous joint distribution among a set of dependent uncertainties.

INTRODUCTION

Decision and risk analyses often involve the construction of probabilistic models by encoding a joint distribution among a set of uncertainties, and then simulating from this joint distribution. In the context of expert elicitation, two common approaches arise: (1) assess-and-assign marginal distributions, assess pairwise correlations (e.g., "Spearman's rho"), and then couple the marginals with an underlying copula (e.g., normal) consistent with the pairwise correlation assessments. (2) assess-and-assign marginal and conditional distributions. A common way in which analysts carry out Approach (1) is with the following steps:

- Assess quantile-probability (QP) data[2] for the marginal distribution of each uncertainty.
- Construct marginal distributions by fitting a distribution (e.g., by least-squares) from a canonical family (e.g., normal, lognormal, beta, etc.) to the QP assessments for each uncertainty.
- Assess pairwise rank-order correlations between uncertainties[3], and then construct the underlying normal (Gaussian) copula specified by the matrix of assessed rank-order correlations[4].

---

[2] For the rest of this chapter, we assume {10^{th}, 50^{th}, 90^{th}} percentiles for assessed QP data, unless explicitly noted otherwise.

[3] Rank-order correlations commonly refer to "Spearman's ρ" or "Kendall's τ". Clemen, Fischer, and Winkler (2000) present six methods for assessing Spearman's ρ or Kendall's τ.

[4] A normal copula is fully specified by a matrix of rank-order correlations, provided that the corresponding Pearson product-moment correlation matrix is positive-definite. Clemen and Reilly (1999) discuss how to translate a matrix of rank-order correlations into a normal copula, and we touch on this computation in later sections.

Approach (1) applies well when it is relatively easy to directly assess marginal distributions. However, it is sometimes easier to conditionally assess some uncertainties with respect to others, rather than directly assess their marginal distributions, in which case Approach (2) is better suited. A common way in which analysts carry out Approach (2) is with the following steps:

- Assess $\{10^{th}, 50^{th}, 90^{th}\}$ percentiles for marginal distributions that can be directly assessed.
- Construct marginal distributions by fitting a distribution (e.g., by least-squares) from a canonical family (e.g., normal, lognormal, beta, etc.) to the QP assessments for each directly-assessed uncertainty.
- Discretize the fitted distributions for each directly-assessed marginal distribution[5].
- Assess several triplets of $\{10^{th}, 50^{th}, 90^{th}\}$ percentiles for the remaining uncertainties, conditioned on values of the discretized marginal distribution.

Based on the above steps for both methods, Approach (1) and (2) for specifying joint distributions both present several practical issues, as listed in Table 9.1. Regarding 1a., we assume that analysts appropriately pursue Approach (2) for uncertainties that are difficult to assess directly, and thus we do not address 1a. in this chapter. We also do not address issue 2a. in this chapter. For the rest of this chapter, we use J-QPD for the assignment of marginal distributions, thus eliminating issues b., c., and d. in Table 9.1. The primary focus in this chapter is on addressing issues 1e. and 2e. in Table 9.1.

We now elaborate on issue 1e. in more detail by first introducing some notation to streamline the discussion. Suppose we are using Approach (1), as outline above, using a

[5] It is also possible to skip the "curve-fitting" step and just assign a discrete distribution directly to the assessed $\{10^{th}, 50^{th}, 90^{th}\}$ percentiles. See Bickel et al. (2011) and Hammond and Bickel (2013a, b) for a review of discretization methods and recent extensions.

normal copula. Let Φ and Φ^{-1} denote the CDF and quantile function, respectively, for the standard normal distribution. Furthermore, suppose we have n uncertainties, indexed $i = 1, \ldots, n$, and let F_i and Q_i denote the marginal CDF and quantile function (respectively) for uncertainty i. Randomly sampling one vector of observations, $\mathbf{x} = (x_1, x_2, \ldots, x_n)$, from this joint distribution consists of the following steps:

1. Generate a random vector, $\mathbf{z} = (z_1, z_2, \ldots, z_n)$, from a multivariate [standard] normal distribution[6] whose correlation matrix is consistent with the matrix of assessed rank-order correlation coefficients.
2. Generate the corresponding vector of correlated uniform random variates by applying Φ: $\mathbf{u} = \Phi(\mathbf{z}) = (\Phi(z_1), \Phi(z_2), \ldots, \Phi(z_n))$.
3. Generate the vector of observations, $\mathbf{x}$, by applying marginal quantile functions to $\mathbf{u}$: $\mathbf{x} = (Q_1(u_1), Q_2(u_2), \ldots, Q_n(u_n))$.

Steps 2 and 3 can be "computationally-expensive" in many cases. For example, suppose the marginals are beta distributions. Given $\mathbf{z}$, step 2 involves n evaluations using Φ, and worse, step 3 involves n evaluations of the quantile function for a beta distribution, each of which involves computing the inverse of the incomplete beta function. If the marginals are gamma distributions, then step 3 involves n evaluations of the quantile function for a gamma distribution, each of which involve the inverse of the incomplete gamma function. To put this in broader perspective, in a problem with twenty uncertainties, randomly sampling one million observations (vectors) from the joint distribution for the first example would involve a total of twenty-million evaluations using Φ, and twenty-million evaluations of the inverse of the incomplete beta function.

[6] Methods for sampling from a multivariate normal distribution are well-known. For example, see Gentle (2009). Thus, simulation step 1 is not the focus of this chapter.

We develop a marginal procedure (MP) in this chapter for specifying a joint distribution that improves upon Approach (1) by using J-QPD for marginal distributions instead of curve-fitting. As addressed in Chapter 4, using J-QPD for marginal distributions in place of curve-fitting eliminates issues b., c., and d. in Table 9.1. However, as we demonstrate, since J-QPDs amount to simple, closed-form operations applied to a standard normal distribution, our MP approach also replaces simulation steps 2 and 3 described above with these simple, closed-form operations. Thus, by eliminating issues b., c., d., and 1e. in Table 9.1, MP ultimately provides a method for specifying a joint distribution that not only encodes an expert's beliefs with greater fidelity (issues b. and d.) than Approach (1), but that is also more computationally-efficient (issues c. and 1e.) than Approach (1) in many cases.

Approach (1)	Approach (2)
1a. Direct assessment of marginals can be difficult.	**2a**. The number of required assessments grows exponentially with the number of conditioning uncertainties.
b. Curve-fits often never honor the assessed QP pairs.	
c. Curve-fitting often requires nonlinear, nonconvex optimization.	
d. Curve-fits often violate natural support limits[7].	
1e. Simulating from a joint distribution with normal copula can be computationally inefficient.	**2e**. The hybrid discrete-continuous joint distribution may not realistically capture an expert's beliefs.

Table 9.1. Disadvantages of Approach (1) and (2) for Specifying Joint Distributions.

We now elaborate on issue 2e. in Table 9.1, regarding Approach (2) for specifying a joint distribution among uncertainties. As noted by Hadlock and Bickel (2017) and by Keelin (2016), distributions exhibiting discontinuities may not reasonably

[7] For example, if a normal distribution is fitted to market share assessments, then the resulting model can generate negative market shares, or shares that exceed the size of the market, thereby reducing model fidelity.

reflect an expert's beliefs when knowledge of smoothness (continuous derivatives) is present. This applies to Approach (2), since the resultant joint distributions contain a combination of discretized marginal distributions, and continuous conditional distributions, and thus do not reasonably capture an expert's joint distribution when knowledge of smoothness is present.

We develop a conditional procedure (CP) in this chapter for specifying a joint distribution that improves upon Approach (2) in two ways. First, like MP, CP uses J-QPD for marginal distributions instead of curve-fitting. Second, CP uses J-QPD further to specify a smooth correlation structure consistent with all marginal and conditional assessments. Thus, by eliminating issues b., c., d., and 2e. in Table 9.1, CP ultimately provides a method for specifying a joint distribution that not only encodes an expert's beliefs with greater fidelity (issues b., d., and 2e.) than Approach (2), but that is also more computationally-efficient (issue c.) than Approach (2).

The rest of this chapter is organized as follows. In the next section, we develop and discuss MP in more detail, using a simple illustration. In the section that follows, we develop and discuss CP in more detail, using a simple illustration. We then highlight one noteworthy limitation of CP. Finally, the last section provides concluding remarks and recommendations for practice.

A MARGINAL PROCEDURE (MP) FOR ENCODING DEPENDENCE

In this section, we develop our marginal procedure (MP) for specifying a joint distribution among uncertainties, which uses J-QPD to improve upon Approach (1) in terms of model fidelity (issues b. and d. in Table 9.1) and computational efficiency (issues c. and 1e. in Table 9.1). To build context, we walk through the Eagle Airlines example problem presented by Clemen and Reilly (1999), using three approaches: the

traditional approach (Approach (1)) used by Clemen and Reilly (1999), our standard MP approach using J-QPD, a modified MP approach using transformations.

Eagle Airlines

Based on the problem in Clemen and Reilly (1999), involving the decision of whether to purchase a used aircraft, sensitivity analysis suggests modeling four key uncertainties: *Price* (*P*), *Hours Flown* (*H*), *Capacity* (*C*), and *Operating Cost* (*O*). In this section, we model the problem based on Approach (1). Specifically, an expert provides {10^{th}, 50^{th}, 90^{th}} percentiles for all four uncertainties, and pairwise values for Spearman's rank-order correlation coefficients (Spearman's rho). Table 9.2 provides these assessment data, which are the same values used in Clemen and Reilly (1999).

					Spearman's rho Assessments		
Uncertainty	Designation	P10	P50	P90	*P*	*H*	*C*
Price	*P*	\$95	\$100	\$108	-	-	-
Hours Flown	*H*	500	800	1000	-0.5	-	-
Capacity	*C*	40%	50%	60%	-0.25	0.5	-
Operating Cost	*O*	\$230	\$245	\$260	0	0	0.25

Table 9.2. Eagle Airlines – Assessment Data for Key Uncertainties.

Model using Approach (1)

In the original problem, Clemen and Reilly (1999) assign the marginal distributions shown in Table 9.3 to the {10^{th}, 50^{th}, 90^{th}} percentile assessment data, which have approximately the same {P10, P50, P90} values shown in Table 9.2. Now, using Approach (1), a normal copula combined with the data in Table 9.2 and Table 9.3 fully specifies a joint distribution for the four uncertainties. Now, to simulate a random vector from this joint distribution, we first generate a random vector, $\mathbf{z} = (z_p, z_h, z_c, z_o)$ from the multivariate standard normal distribution corresponding to the matrix of Spearman's rho

values given in Table 9.2. From simulation step 2, we then generate the corresponding vector of correlated uniform random variates by applying Φ: $\mathbf{u} = \Phi(\mathbf{z}) = (\Phi(z_p), \Phi(z_h), \Phi(z_c), \Phi(z_o))$. Finally, following simulation step 3, we generate the random vector of observations, $\mathbf{x}$, by applying marginal quantile functions to $\mathbf{u}$: $\mathbf{x} = (Q_p(u_p), Q_h(u_h), Q_c(u_c), Q_o(u_o))$. Since *P*, *H*, and *C* all have beta distribution assignments, Q_p, Q_h, and Q_c each involve one evaluation of the inverse of the incomplete beta function. Alternatively, since *O* has a normal distribution, Q_o involves one evaluation of Φ^{-1}.

Uncertainty	Distribution	Parameters	Bounds
Price (*P*)	Scaled beta	$\alpha = 9, \beta = 15$	\$[81.94, 133.96]
Hours Flown (*H*)	Scaled beta	$\alpha = 4, \beta = 2$	[66.91, 1135.26]
Capacity (*C*)	Beta	$\alpha = 20, \beta = 20$	[0, 1]
Operating Cost (*O*)	Normal	$\mu = 245, \sigma = 11.72$	\$(-∞, ∞)

Table 9.3. Marginal Distribution Assignments for the Original Problem[8].

Model using MP

We now consider our marginal procedure (MP) using J-QPD. Since *C* is a fractional quantity between zero and one, we shall assign a J-QPD-B distribution to *C* parameterized by $\boldsymbol{\theta}_{0.1} = \{x_0, x_{0.1}, x_{0.50}, x_{0.90}, x_1\} = \{0,\ 0.4,\ 0.5,\ 0.6,\ 1\}$. However, suppose that the analyst and expert are not comfortable imposing a hard (finite) upper bound for *P*, *H*, and *O*. Since *P*, *H*, and *O* are inherently nonnegative quantities, we provide J-QPD-S assignments for each of their marginal distributions, each having a lower bound of zero. The quantile functions for the J-QPD assignments for all four uncertainties are shown in Table 9.4.

[8] See Clemen and Reilly (1999).

Uncertainty	Type	Quantile Function[9]	Bounds
Price (*P*)	J-QPD-S	$95 \cdot \exp\left(0.0684 \cdot \sinh\left(0.6934 + \sinh^{-1}\left(0.5855 \cdot z\right)\right)\right)$	$[0, ∞)
Hrs. Flown (*H*)	J-QPD-S	$1000 \cdot \exp\left(0.1878 \cdot \sinh\left(-1.0085 + \sinh^{-1}\left(0.9273 \cdot z\right)\right)\right)$	[0, ∞)
Capacity (*C*)	J-QPD-B[10]	$\Phi(0.1977 \cdot z)$	[0, 1]
Op. Cost (*O*)	J-QPD-S	$260 \cdot \exp\left(0.2345 \cdot \sinh\left(-0.2507 + \sinh^{-1}\left(0.1977 \cdot z\right)\right)\right)$	$[0, ∞)

Table 9.4. Marginal J-QPD Assignments using MP.

Given the J-QPD quantile function assignments in Table 9.4, expressed as transformations applied to the standard normal distribution, we now reconsider our simulation steps using the MP approach for encoding a joint distribution. As in Approach (1), take as given some random vector, $\mathbf{z} = (z_p, z_h, z_c, z_o)$, drawn from the multivariate standard normal distribution. Let $T_i(z)$ denote the transformation function for uncertainty "*i*". Referencing Table 9.4, for example, the transformation function for *P* is:

$$T_P(z) = 95 \cdot \exp\left(0.0684 \cdot \sinh\left(0.6934 + \sinh^{-1}\left(0.5855 \cdot z\right)\right)\right).$$

To generate a random vector of observations, **x**, from our joint distribution using MP, we simply take $\mathbf{x} = (T_p(z_p), T_h(z_h), T_c(z_c), T_o(z_o))$, in place of applying simulation steps 2 and 3. Not counting closed-form operations, given $\mathbf{z} = (z_p, z_h, z_c, z_o)$, generating one **x** vector in this example involves only one evaluation of Φ, in the transformation function using J-QPD-B for Capacity (*C*). By comparison, recall that Approach (1) above involved: four evaluations of Φ, three evaluations of the inverse of the incomplete beta function, and one evaluation of Φ^{-1}. Moreover, in this example, Approach (1) above takes over twenty times as much runtime to generate **x** compared to the MP approach presented here. For example, using MATLAB's built-in functions, generating ten million **x** vectors takes

[9] In each quantile function shown in Table 9.4, $z = \Phi^{-1}(p)$. We express the quantile functions in this way to emphasize that in our multivariate simulation using the normal copula, we will take advantage of the fact that the J-QPDs are direct transformations applied to the standard normal distribution.

[10] This quantile function corresponds to the special case of J-QPD-B given in Chapter 4.

about 70 seconds using modeling Approach (1), and about 3 seconds using the MP approach.

Modified MP Approach using Transformations

It is possible to increase the computational efficiency of MP further by using an appropriate transformation upon J-QPD-S distributions for uncertainties that are inherently bounded (such as market shares) instead of using a J-QPD-B distribution, as we do in Eagle Airlines above for Capacity (*C*). We first provide a generic description of our approach here, and then return to Eagle Airlines for a brief illustration.

Consider some uncertainty, *X*, that is bounded on [0, 1], and having {10th, 50th, 90th} percentiles of $\{x_{0.1}, x_{0.5}, x_{0.9}\}$. Rather than directly assign a J-QPD-B distribution to *X*, we can define a new variable, $Y = X/(1-X)$, which has support on [0, ∞), and assign it a J-QPD-S distribution with quantile function, $Q_Y(p)$, parameterized by:

$$\boldsymbol{\theta}_{0.1} = \left\{0, \frac{x_{0.1}}{1-x_{0.1}}, \frac{x_{0.5}}{1-x_{0.5}}, \frac{x_{0.9}}{1-x_{0.9}}, \infty\right\}.$$

Then, define the quantile function for *X*, denoted $Q_X(p)$, as:

$$Q_X(p) = \frac{Q_Y(p)}{1+Q_Y(p)}.$$

Defining the marginal distribution for *X* in this way instead of directly assigning a J-QPD-B distribution eliminates the need to evaluate Φ in the case of bounded uncertainties when simulating from the joint distribution, given a random vector, **z**, of values drawn from a multivariate standard normal distribution specified by the normal copula – simulation step 1. More generally, if *X* has finite bounds specified by [*l*, *u*], and having {10th, 50th, 90th} percentiles of $\{x_{0.1}, x_{0.5}, x_{0.9}\}$ then take $Y = (X - l)/(u - X)$, which has support on [0, ∞), and assign it a J-QPD-S distribution with quantile function, $Q_Y(p)$, parameterized by:

$$\boldsymbol{\theta}_{0.1} = \left\{0, \frac{x_{0.1} - l}{u - x_{0.1}}, \frac{x_{0.5} - l}{u - x_{0.5}}, \frac{x_{0.9} - l}{u - x_{0.9}}, \infty\right\}.$$

Then, define the quantile function for X, denoted $Q_X(p)$, as:

$$Q_X(p) = l + (u - l) \cdot \frac{Q_Y(p)}{1 + Q_Y(p)}.$$

As an illustration, let X be the *Capacity* (C) uncertainty in the Eagle Airlines example, where $[l, u] = [0, 1]$, and where $\{x_{0.1}, x_{0.5}, x_{0.9}\} = \{0.4, 0.5, 0.6\}$. As above, we define $Y = X/(1–X)$, and assign the J-QPD-S distribution to Y parameterized by:

$$\boldsymbol{\theta}_{0.1} = \left\{0, \frac{x_{0.1}}{1 - x_{0.1}}, \frac{x_{0.5}}{1 - x_{0.5}}, \frac{x_{0.9}}{1 - x_{0.9}}, \infty\right\} = \left\{0, \frac{0.4}{1 - 0.4}, \frac{0.5}{1 - 0.5}, \frac{0.6}{1 - 0.6}, \infty\right\} = \{0, 0.667, 1, 1.5, \infty\}.$$

In this case, the resultant J-QPD-S distribution for Y is a lognormal distribution[11] with $\mu = 0$ and $\sigma = 0.3164$, which has the quantile function: $Q_Y(p) = \exp(0.3164\Phi^{-1}(p))$. Thus, the quantile function that we assign to *Capacity* is:

$$Q_X(p) = \frac{\exp\left(0.3164 \cdot \Phi^{-1}(p)\right)}{1 + \exp\left(0.3164 \cdot \Phi^{-1}(p)\right)} = \frac{1}{1 + \exp\left(-0.3164 \cdot \Phi^{-1}(p)\right)}.$$

Figure 9.3 provides a comparison of the distribution for the previously-assigned J-QPD-B assignment above for Capacity (shown dashed), and this new assignment using transformations (shown solid). Note that the two approaches produce nearly indiscernible distributions. The main point, however, is to demonstrate a more computationally-efficient method for assigning bounded distributions using a transformation upon J-QPD-S, rather than assigning J-QPD-B directly, to eliminate the need to perform evaluations involving Φ when simulating from the joint distribution using a normal copula.

[11] Recall from Chapter 4 that J-QPD-S subsumes the lognormal distributions as a special case.

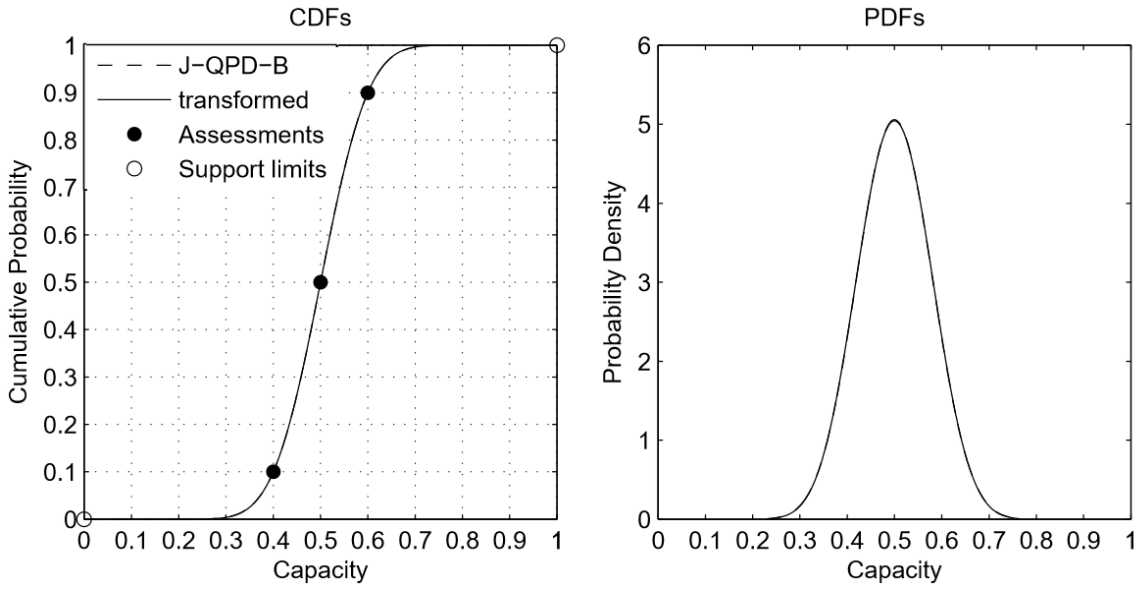

Figure 9.3. J-QPD-B (dashed) and Transformed (solid) Distributions for *Capacity* (*C*).

A CONDITIONAL PROCEDURE (CP) FOR ENCODING DEPENDENCE

In this section, we provide a new conditional procedure (CP) for specifying a joint distribution among uncertainties, improving upon Approach (2), again using the Eagle Airlines example as an illustration. In this case, for the sake of illustration, suppose that the expert gives assessments for *Hours Flown* (*H*), conditional on the {10th, 50th, 90th} percentile assessments for *Capacity* (*C*) given in Table 9.2, yielding the following conditional assessments for *H*|*P*, shown in Figure 9.4[12]:

- $\{H_{10}, H_{50}, H_{90}\} \mid C_{10} = \{405, 645, 885\}$ hours[13].
- $\{H_{10}, H_{50}, H_{90}\} \mid C_{50} = \{540, 800, 980\}$ hours.
- $\{H_{10}, H_{50}, H_{90}\} \mid C_{90} = \{700, 920, 1050\}$ hours.

In this case, we presume that it is easier to assess *H*|*C* than *H* directly. For our example, we already have a J-QPD assignment for the marginal distribution for *C*,

[12] These conditional assessment values are approximately consistent with those in the MP model.
[13] For example, this means that, given that *Capacity* (*C*) is equal to its 10th percentile ($C_{10} = 40\%$), the {10th, 50th, 90th} percentiles for *Hours Flown* (*H*) are {405, 645, 885} hours, respectively.

specified by $\boldsymbol{\theta}_{0.1} = \{x_0, x_{0.1}, x_{0.50}, x_{0.90}, x_1\} = \{0,\ 40,\ 50,\ 60,\ 100\}\%$, and given in Table 9.4. Since our marginal distributions are characterized in quantile function form, we can easily simulate from the marginal distribution for *C* by inverse-transform sampling.

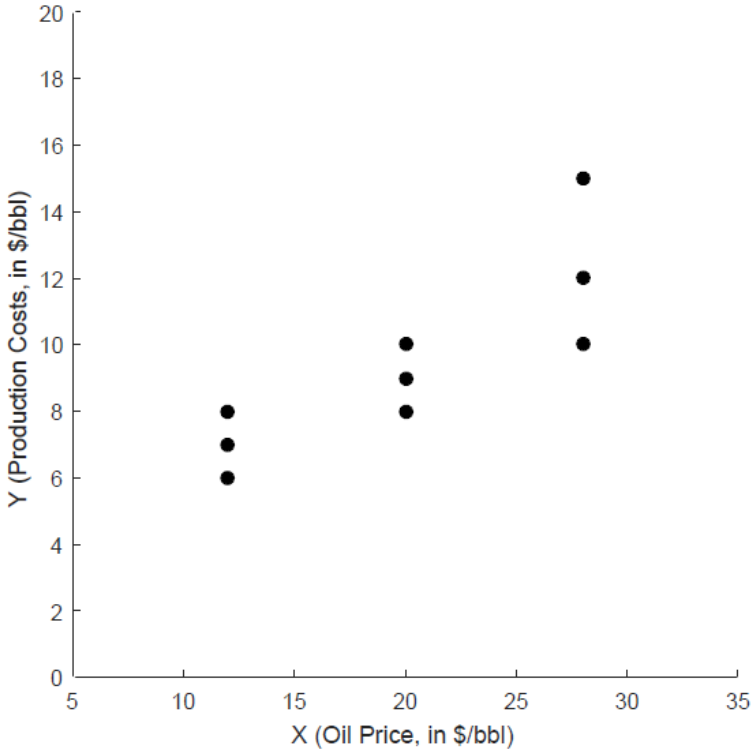

Figure 9.4. Conditional Assessments for *Capacity* (*C*) and *Hours Flown* (*H*).

Suppose we draw the random value, c = 54.13%, for *C* using inverse-transform sampling with its quantile function, Q_c, given in Table 9.4. How can we assign a distribution to $H|\{C = 54.13\%\}$? We have low-base-high assessments for *H* at the {10th, 50th, 90th} percentiles for *C*, but we do not have low-base-high assessments for *H* at any arbitrary value of *C*, such as *C* = 54.13%, in this case. Assume the correlation structure between *C* and *H* is monotonically increasing in this example; i.e., that $H_p|c$ is increasing in c for any fixed value of $p \in (0, 1)$. For example, the 27th percentile for *H*, given the 50th percentile of *C*, is greater than the 27th percentile of *H*, given the 10th percentile for *C*.

Since J-QPD quantile functions are increasing and maximally-feasible (MF), we use them to encode a correlation structure between *C* and *H*.

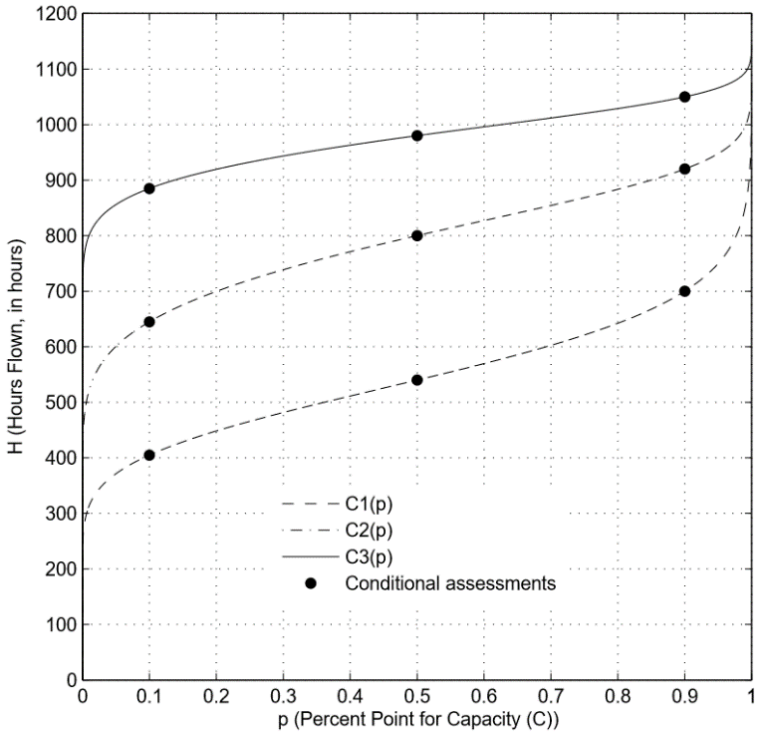

Figure 9.5. Correlation C-Curves for *C* and *H* using Assessment Data.

As before, suppose that the expert and analyst agree that *H* should have support on [0, ∞). Figure 9.5 provides an alternative visualization for Figure 9.4, showing percent points for *C*, (p_c), on the horizontal axis rather than *C*. The solid points represent our conditional assessments. Since $p_c \in [0, 1]$, by our monotonicity assumption, we can construct the following J-QPD-S quantile function assignments to encode a correlation structure between *C* and *H* that precisely honors our conditional assessments and bound requirements. The correlation-curves, or C[14]-curves, shown Figure 9.5 are specified as follows:

[14] Note that the designation "C" here in C-curves refers to correlation, and is not referring to the *Capacity* (*C*) uncertainty in our example.

- $C_{0.1}(p_c)$: $H_{10} \mid p_c$ = J-QPD-S with $\boldsymbol{\theta}_{0.10} = \{0, 405, 540, 700, \infty\}$ hours.
- $C_{0.5}(p_c)$: $H_{50} \mid p_c$ = J-QPD-S with $\boldsymbol{\theta}_{0.10} = \{0, 645, 800, 920, \infty\}$ hours.
- $C_{0.9}(p_c)$: $H_{90} \mid p_c$ = J-QPD-S with $\boldsymbol{\theta}_{0.10} = \{0, 885, 980, 1050, \infty\}$ hours.

Given these C-curves, we have a complete correlation structure between C and H. Given $c = 54.13\%$, construct a J-QPD-S assignment for $H|\{c = 54.13\%\}$ as follows:

(1) From the marginal distribution for C, characterized by Qc, we infer that $c = 54.13\%$ is the 70th percentile for C, meaning that $p_c = 0.7$.

(2) Using our three correlation C-curves with $p_c = 0.7$, we compute:

$H_{10} \mid \{c = 54.13\%\} = Q(0.7;\ \boldsymbol{\theta}_{0.10} = \{0, 405, 540, 700, \infty\}) = 602.51$ hours.

$H_{50} \mid \{c = 54.13\%\} = Q(0.7;\ \boldsymbol{\theta}_{0.10} = \{0, 645, 800, 920, \infty\}) = 854.28$ hours.

$H_{90} \mid \{c = 54.13\%\} = Q(0.7;\ \boldsymbol{\theta}_{0.10} = \{0, 885, 980, 1050, \infty\}) = 1011.82$ hours.

(3) Construct the J-QPD-S assignment for $H \mid \{c = 54.13\%\}$, characterized by:

$$\boldsymbol{\theta}_{0.10} = (0,\ \{H_{10} \mid c = 54.13\%\},\ \{H_{50} \mid c = 54.13\%\},\ \{H_{90} \mid c = 54.13\%\},\ \infty) = \{0, 602.5, 854.3, 1011.8,\ \infty\}.$$

Given this $\boldsymbol{\theta}_{0.10}$ vector, construct the corresponding J-QPD-S quantile function:

$$Q_{H|54.13\%}(p) = 1011.8 \cdot \exp\left(0.146 \cdot \sinh\left(-0.990 + \sinh^{-1}\left(0.906 \cdot \Phi^{-1}(p)\right)\right)\right).$$

Figure 9.6 shows the probability distribution for $H|C = 54.13\%$. We provide generalized steps for CP for the bivariate case, where we directly assess the marginal distribution for one uncertainty, X, and then gather assessments for another uncertainty, Y, conditional on the low-base-high assessments for X.

1. Obtain an SPT of assessments for the marginal distribution for uncertainty, X.
2. Obtain conditional SPTs for: $Y \mid X_{\text{low}}$, $Y \mid X_{\text{base}}$, and $Y \mid X_{\text{high}}$.
3. As a modeling decision, identify appropriate bounds for X and Y.

4. Construct a J-QPD for the marginal distribution for X, denoted Q_X, using the assessed SPT and chosen support bounds. If the support is bounded (semi-bounded), use J-QPD-B (J-QPD-S).
5. Assuming that $Y_p \mid x$ is increasing in x, construct three correlation curves[15]:
   a. $C_{\text{low}}(x)\colon Y_{\text{low}} \mid x = Q\left(F_X(x);\ \boldsymbol{\theta}_{0.10} = \left(Y_0,\ Y_{\text{low}} \mid X_{\text{low}},\ Y_{\text{low}} \mid X_{\text{base}},\ Y_{\text{low}} \mid X_{\text{high}}, Y_{100}\right)\right)$
   b. $C_{\text{base}}(x)\colon Y_{\text{base}} \mid x = Q\left(F_X(x);\ \boldsymbol{\theta}_{0.10} = \left(Y_0,\ Y_{\text{base}} \mid X_{\text{low}},\ Y_{\text{base}} \mid X_{\text{base}},\ Y_{\text{base}} \mid X_{\text{high}}, Y_{100}\right)\right)$
   c. $C_{\text{high}}(x)\colon Y_{\text{high}} \mid x = Q\left(F_X(x);\ \boldsymbol{\theta}_{0.10} = \left(Y_0,\ Y_{\text{high}} \mid X_{\text{low}},\ Y_{\text{high}} \mid X_{\text{base}},\ Y_{\text{high}} \mid X_{\text{high}}, Y_{100}\right)\right)$
6. Simulate an observation of X, x, using inverse-transform sampling with Q_X.
7. Construct a J-QPD for $Y \mid x$, denoted $Q_{Y|x}$, characterized by: $\boldsymbol{\theta}_{0.10} = \left(Y_0,\ C_{\text{low}}(x),\ C_{\text{base}}(x),\ C_{\text{high}}(x), Y_{100}\right)$.
8. Generate an observation for $Y \mid x$ using inverse-transform sampling with $Q_{Y|x}$.
9. If the desired sample size for observations of $\{X,\ Y\}$ is obtained, stop. Otherwise, go to step (6).

[15] If $Y_p \mid x$ is *decreasing* in x (negative correlation), then apply reflected C-curves about the line, $p_x = 0.5$.

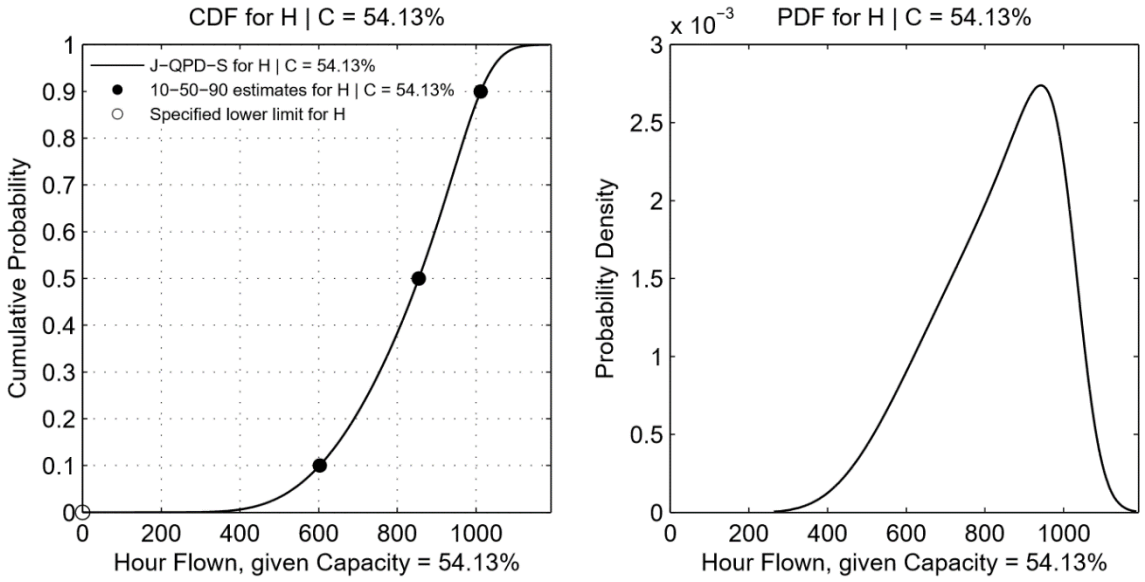

Figure 9.6. J-QPD-S CDF and PDF for *Hours Flown* (*H*), Given *Capacity* (*C*) = 54.13%.

For our example, Figure 9.7 provides a scatterplot of 500 joint observations for {*C*, *H*} using MP and CP, using the same random number seed in both cases, along with density contours using both approaches. We note the similarity of the MP- and CP-based joint distributions for our example, based on a visual comparison of the density contours in Figure 9.7, as well as the closeness of the rank-order correlation coefficients (Kendall and Spearman) and the Pearson product-moment correlation coefficients.

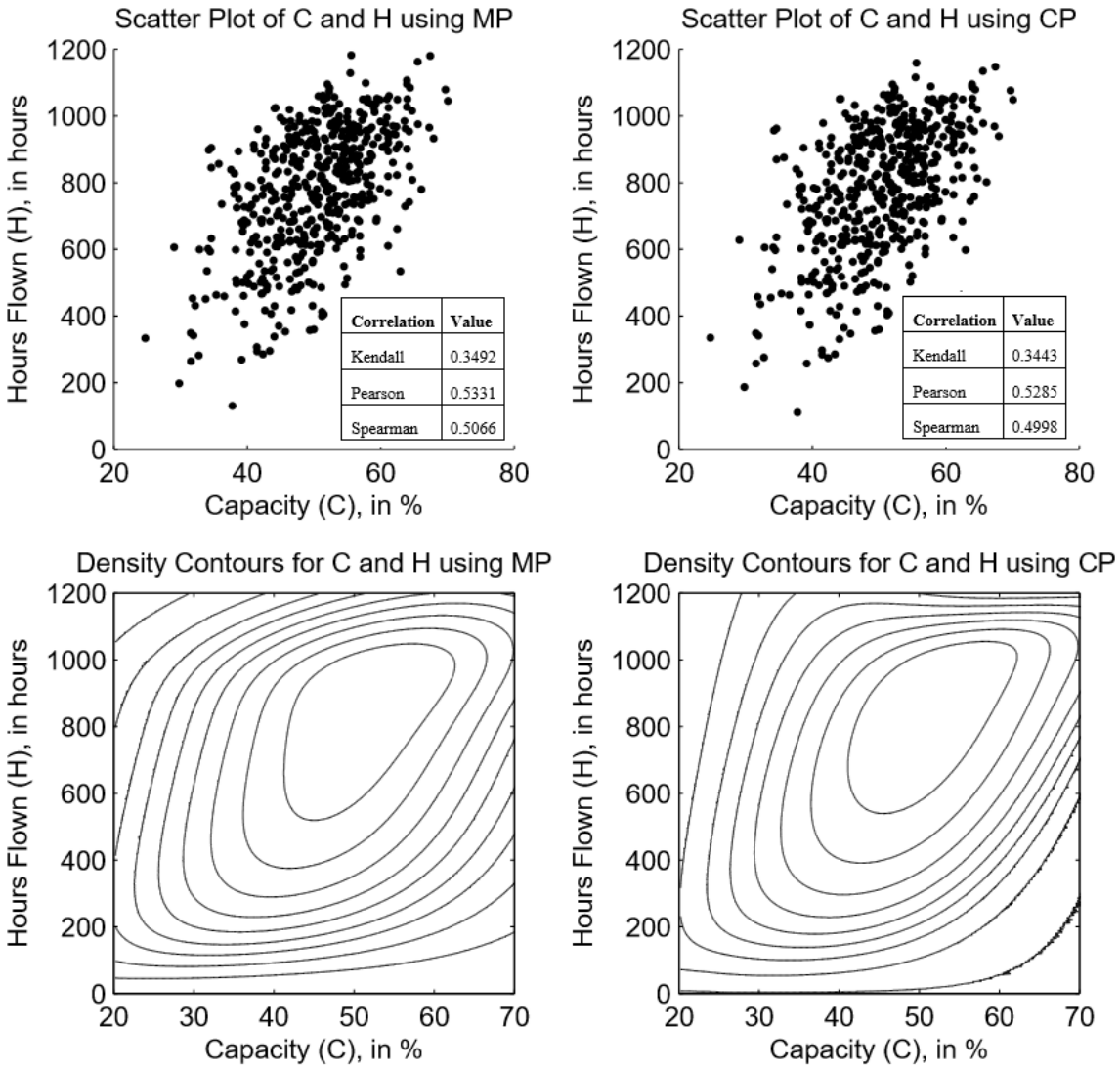

Figure 9.7. Scatterplot and Density Contours for *C* and *H* using MP (left) and CP (right).

Limitation of CP

We conclude this section by pointing out a noteworthy, but generally benign, limitation of encoding correlation CP. Figure 9.8 provides a "skewed" example where the monotonicity requirement is satisfied, but where there is overlap in the *C*-curves, meaning that this example violates coherence. Beyond about $p = 0.95$, for example, $(y_{0.1} \mid p_x) > (y_{0.5} \mid p_x) > (y_{0.9} \mid p_x)$. Although we expect these overlap scenarios to be rare in many

practical applications, we suggest that analysts examine *C*-curves for overlap before going to step (6) of CP.

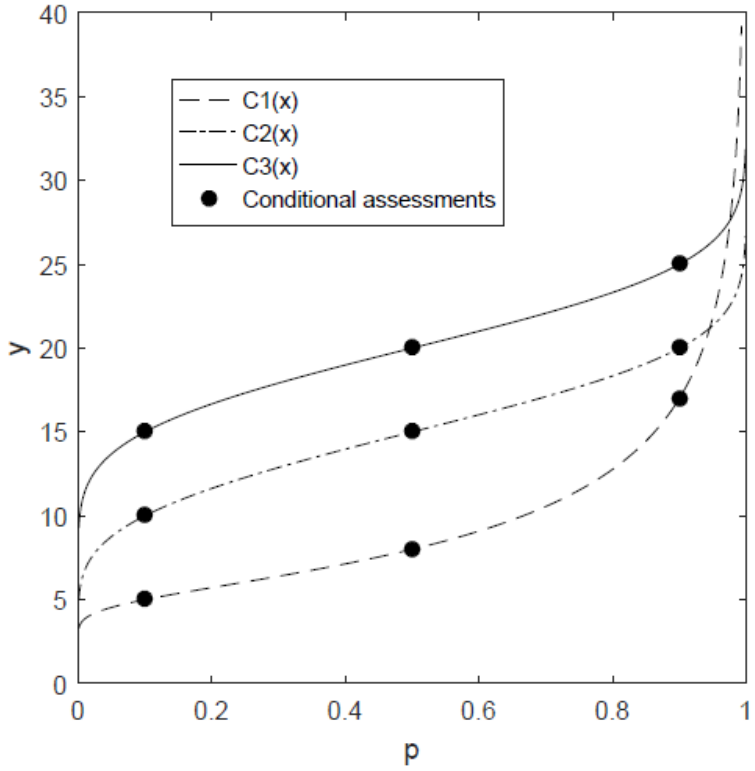

Figure 9.8. Example where CP C-Curves Overlap.

CONCLUSION AND RECOMMENDATIONS FOR PRACTICE

In this chapter, we have provided two methods for specifying joint distributions among uncertainties: the marginal procedure (MP), and the conditional procedure (CP). MP applies to cases where marginal distributions are relatively easy to assess directly, and suggests gathering a set of quantile-probability (QP) pairs of assessments (e.g., 10^{th}-50^{th}-90^{th} percentiles) for each uncertainty, and a matrix of Spearman's rank correlation coefficient ("Spearman's rho") assessments. MP then assigns a J-QPD distribution to each set of marginal assessments, and produces an underlying normal copula between dependent variables, specified by "Spearman's rho" estimates. Compared to the approach

of constructing marginal distributions by fitting a commonly-named distribution (e.g., beta, gamma, etc.) to the marginal QP assessment pairs, and then using these marginal distribution assignments in conjunction with a normal copula, the advantages of MP are:

- MP encodes an expert's beliefs with greater fidelity by providing smooth marginal distribution assignments that honor QP assessments and specified support bounds, unlike curve-fitting.
- MP is more computationally-efficient since its marginal distribution assignments are directly parameterized by assessed QP pairs and bounds, and do not require nonlinear (and possibly nonconvex) optimization to parameterize, unlike many cases of curve-fitting.
- Given marginal distribution assignments and a sample drawn from an underlying standard normal copula, based on assessed values for Spearman's rho, MP is more computationally-efficient since J-QPDs are simple transformations applied to a standard normal distribution.

Alternatively, CP is designed for situations where it is easier to assess QP pairs for a second uncertainty, conditioned on assessments for the first uncertainty (e.g., 10^{th}-50^{th}-90^{th} percentiles). Like MP, CP assumes a monotonic relationship between dependent uncertainties, and uses J-QPDs to capture marginal distributions and correlation structure. CP precisely honors all marginally- and conditionally-assessed QP pairs, and provides a smooth description for the joint distribution for dependent uncertainties, unlike the more traditional approach of conditioning on a discretized marginal distribution.

In practice, we suggest implementing MP by default wherever possible, since assessment of a single Spearman's rho value can be sufficient to describe the correlation structure between two uncertainties in many cases, and since the accuracy for corresponding assessment procedures is well-documented. Alternatively, the number of

conditional assessments required for CP grows exponentially with the number of correlated uncertainties to which CP is applied. Also, since our CP procedure is defined based on the bivariate case, we suggest implementing CP only when necessary. A combination of MP and CP is possible, and might be appropriate in large-scale problems. Nevertheless, both MP and CP offer an improvement to current methods for encoding and simulating from joint distributions for uncertainties based on expert elicitation.

Chapter 10 : A Decision Analysis Using J-QPD

In this chapter, we briefly present the application of J-QPD to two decision analysis problems. The first is a slightly-modified[16] version of the illustrative Eagle Airlines problem presented by Reilly (1998), as an update to the problem introduced by Clemen (1996). The second is a slightly-modified version of a real-estate asset portfolio evaluation problem, based on the real-world application by Keelin (2016). There are two main objectives here:

(1) Demonstrate how to implement J-QPD within a decision context, accounting for both marginal and joint uncertainty.

(2) Show how J-QPD provides a more authentic representation of uncertainty in the context of decision modeling, compared to current practices of quantifying uncertainty.

EAGLE AIRLINES – REVISITED

The problem concerns Dick Carothers' decision on whether to invest his \$9,072 into a money market, or purchase a plane to add to his fleet. The influence diagram, adapted from Clemen and Reilly (1999), is shown in Figure 10.1, and marginal assessment data is presented in Table 10.1. Table 10.2 presents the matrix of assessments for Spearman's rho among the uncertainties. The objective value for the problem is calculated as follows:

$$TR = CR \cdot HF \cdot CP + (1 - CR) \cdot HF \cdot CAP \cdot ns \cdot PL \quad (10.1)$$

$$TC = HF \cdot OC + INS + PP \cdot PF \cdot IR \quad (10.2)$$

$$\text{Profit} = TR - TC \quad (10.3)$$

$$\text{Value} = \text{Profit} - \$9,072. \quad (10.4)$$

CP refers to Charter Price, which is given by 3.25**PL*, and *ns* is the number of seats, which is five. In Figure 10.1, we do not include relevance arrows linking all nine

[16] We have only modified numbers, such as assessments and constants, but not the problem structure.

uncertainties in Table 10.1, since doing so overwhelms the figure with fourteen more arrows, corresponding to Spearman's rho values in Table 10.2.

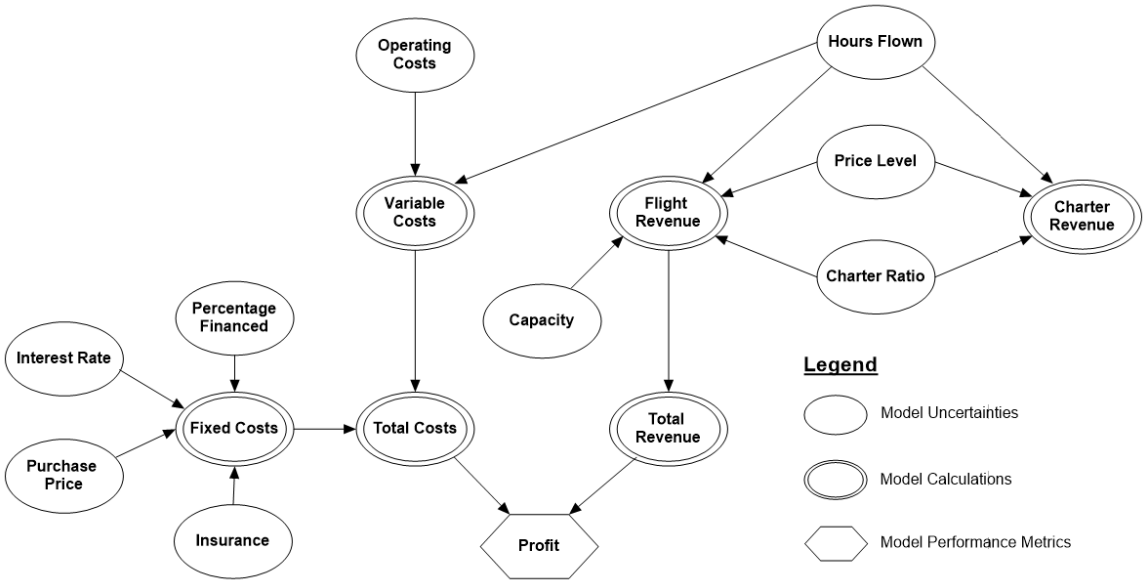

Figure 10.1. Influence Diagram for Eagle Airlines, adopted from Reilly (1998).

Uncertainty	**Tag**	**P10**	**P50**	**P90**
Charter ratio (%)	*CR*	45	50	70
Capacity (%)	*CAP*	40	50	75
Price level ($)	*PL*	190	200	240
Hours flown (hrs)	*HF*	500	700	1000
Operating cost ($/hr)	*OC*	500	520	605
Percentage financed (%)	*PF*	30	50	70
Interest rate (%)	*IR*	10	12	13
Insurance ($)	*INS*	43,200	49,700	54,000
Purchase price ($)	*PP*	183,600	194,400	216,000

Table 10.1. Marginal Low-Base-High Assessment Data.

	CR	***CAP***	***PL***	***HF***	***OC***	***PF***	***IR***	***INS***	***PP***
CR	1.0	-0.5	0.25	0.25	0.25	0	0	0	0
CAP		1.0	-0.5	0.5	0.25	0	0	0	0
PL			1.0	-0.25	0	0	0	0	0
HF				1.0	0	0	0	0.25	0
OC					1.0	0.25	0	0	0
PF						1.0	-0.5	0.5	0.5
IR							1.0	0	-0.25
INS								1.0	0
PP									1.0

Table 10.2. Assessed Values for Spearman's Rho.

Quantifying the Uncertainty

Given both marginal (low-base-high) and joint (Spearman's rho) assessment data, the next step is to encode a complete joint distribution for all uncertainties in the problem. We begin with the marginal distributions.

Encoding Marginal Distributions

To assign a J-QPD for the marginal distribution of each uncertainty, we must first select the J-QPD type in each case (J-QPD-B or J-QPD-S), along with the corresponding bounds. Since *CR*, *CAP*, *PF* and *IR* correspond to fractional quantities (in percentages), we assign J-QPD-B distributions to all four of these uncertainties, each having support on [0, 1], or [0, 100] %. For *PL*, *HF*, *OC*, *INS* and *PP*, the only bound remarks that we can comfortably make are that these quantities are necessarily non-negative. Thus, we assign a J-QPD-S to the marginal distribution for each of these five uncertainties, each having a lower bound of zero. Table 10.3 provides the J-QPD assignments for all nine uncertainties, parameterized by the low-base-high assessments and bounds in all cases,

and Figure 10.2 (Figure 10.3) shows the PDFs (CDFs) for all nine J-QPD distribution assignments in Table 10.3.

Uncertainty	Type	Quantile Function	Bounds
CR	J-QPD-B	$\Phi(-0.1257 + 0.0527 \cdot \sinh(1.2515 \cdot (\Phi^{-1}(p) + 1.2816)))$	[0,100]%
CAP	J-QPD-B	$\Phi(-0.2533 + 0.1652 \cdot \sinh(0.9469 \cdot (\Phi^{-1}(p) + 1.2816)))$	[0,100]%
PL	J-QPD-S	$190 \cdot \exp\left(0.0251 \cdot \sinh\left(1.4640 + \sinh^{-1}\left(1.5965 \cdot \Phi^{-1}(p)\right)\right)\right)$	$[0, \infty)$
HF	J-QPD-S	$500 \cdot \exp\left(1.3630 \cdot \sinh\left(0.2444 + \sinh^{-1}\left(0.1926 \cdot \Phi^{-1}(p)\right)\right)\right)$	$[0, \infty)$
OC	J-QPD-S	$500 \cdot \exp\left(0.0177 \cdot \sinh\left(1.5358 + \sinh^{-1}\left(1.7282 \cdot \Phi^{-1}(p)\right)\right)\right)$	$[0, \infty)$
PF	J-QPD-B	$\Phi(0.5244 + 2.5e7 \cdot \sinh((1.64e-8) \cdot (\Phi^{-1}(p) - 1.2816)))$	[0,100]%
IR	J-QPD-B	$\Phi(-1.1264 + 0.0391 \cdot \sinh(0.8147 \cdot (\Phi^{-1}(p) - 1.2816)))$	[0,100]%
INS	J-QPD-S	$54 \cdot \exp\left(0.0923 \cdot \sinh\left(-0.8080 + \sinh^{-1}\left(0.7014 \cdot \Phi^{-1}(p)\right)\right)\right)$	$[0, \infty)$
PP	J-QPD-S	$183.6 \cdot \exp\left(0.0566 \cdot \sinh\left(0.8888 + \sinh^{-1}\left(0.7885 \cdot \Phi^{-1}(p)\right)\right)\right)$	$[0, \infty)$

Table 10.3. Marginal J-QPD Assignments.

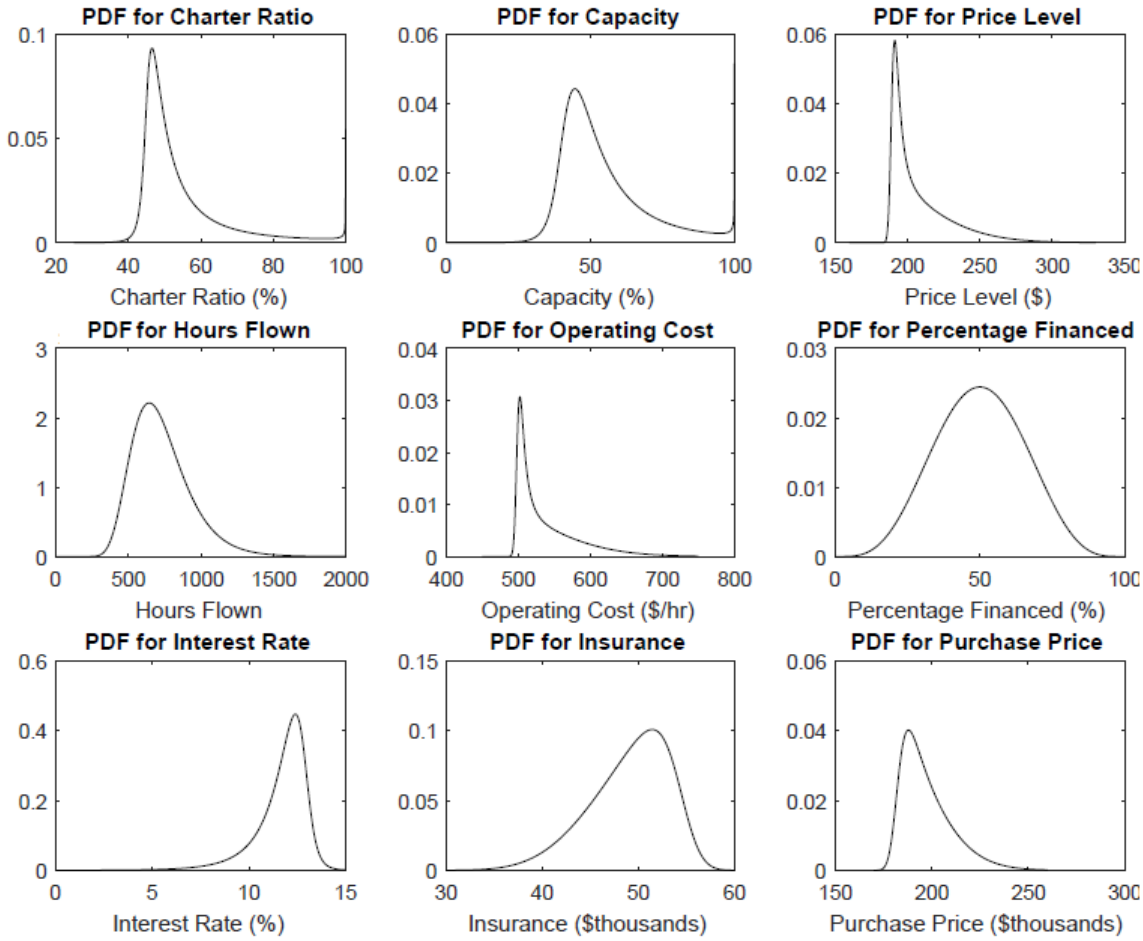

Figure 10.2. PDFs for the Input J-QPD Assignments.

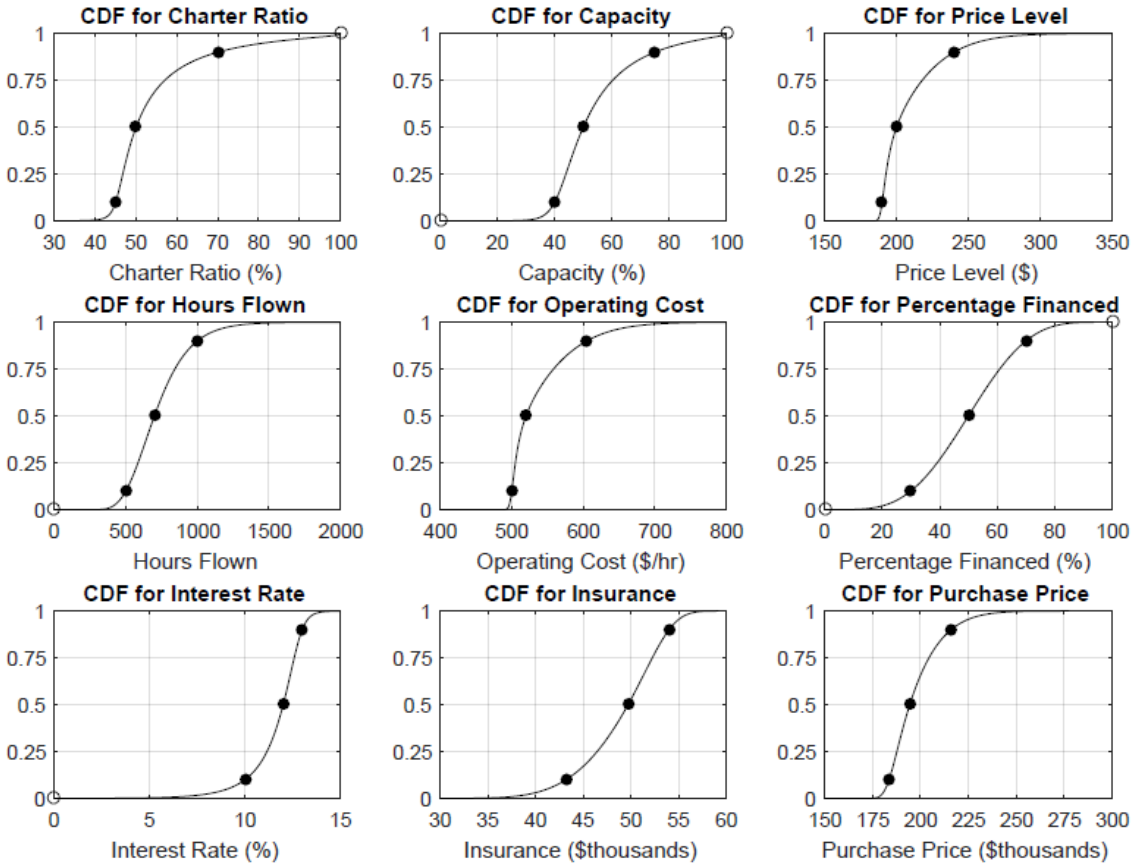

Figure 10.3. CDFs for the Input J-QPD Assignments.

Encoding Joint Distributions

Given marginal distributions for each uncertainty, the next step is to encode a correlation structure between them, using the MP or CP procedure prescribed in Chapter 9. Since we have a matrix of assessed values for Spearman's rho between uncertainty pairs, we use the MP approach. Let $\mathbf{R}_s$ denote the matrix of Spearman's rho values given in Table 10.2. Using the transformation given by Kruskal (1958), we compute the matrix of Pearson's product-moment correlation coefficients, denoted $\mathbf{R}_p$, as:

$$\mathbf{R}_p = 2 \cdot \sin\left(\frac{\pi \mathbf{R}_s}{6}\right) \tag{10.5}$$

where the sine function is applied element-wise to $\mathbf{R}_s$. Table 10.4 gives $\mathbf{R}_p$.

	CR	***CAP***	***PL***	***HF***	***OC***	***PF***	***IR***	***INS***	***PP***
CR	1.0	-0.518	0.261	0.261	0.261	0	0	0	0
CAP		1.0	-0.518	0.518	0.261	0	0	0	0
PL			1.0	-0.261	0	0	0	0	0
HF				1.0	0	0	0	0.261	0
OC					1.0	0.261	0	0	0
PF						1.0	-0.518	0.518	0.518
IR							1.0	0	-0.261
INS								1.0	0
PP									1.0

Table 10.4. Matrix of Pearson Product-Moment Correlation Coefficients, $\mathbf{R}_{p.}$

The Pearson correlation matrix is positive semidefinite in this case, making it amenable for use with the normal copula in MAP. We implement the following simulation procedure to evaluate the expected value of the plane purchase:

(1) Generate a vector of one-hundred million uniform random variates, one for each of the nine uncertainties, using standard Latin hypercube sampling[17].

(2) Pass the vectors of uniform random variates through a multivariate normal distribution with a nine-by-one vector of zeros for the mean vector, and covariance matrix equal to $\mathbf{R}_p$[18]. Let X denote the 100,000,000-by-9 matrix of observations generated from this joint normal distribution.

(3) Generate the matrix of correlated uniform random variates: $U = \Phi(X)$.

(4) For $i = \{1, \ldots, 9\}$, let Q_i denote the J-QPD quantile function for the i^{th} uncertainty in Table 10.3. We generate the vector of observations for uncertainty "i", denoted Y_i, using: $Y_i = Q_i(U_i)$.

[17] For more information, see: Iman et al. (1980 and 1981); McKay et al. (1979); Eglajs and Audze (1977).
[18] This is because we want marginal distributions for this multivariate normal distribution to be standard normal distributions (with a mean of zero, and a variance of one).

(5) For j = {1,…, 100,000,000}, generate the vector of "value" observations, V_j, using Equations (10.1) through (10.4).

Figure 10.4 shows the CDF for 'Value' using MP, compared to that using the MCS discretization shortcut[19], along with the expected value (EV) using both approaches. Notice that whereas MCS predicts an expected *loss* of $3,600 by purchasing the plane, our continuous approach using J-QPD with MP predicts an expected net *gain* of $1,900.

[19] The McNamee-Celona shortcut (MCS) assigns probabilities of {0.25, 0.50, 0.25} to the {10th, 50th, 90th} percentiles, and is popular in practice. For detail, see McNamee and Celona (1990), or Bickel et al. (2011). The simulation procedure is the same here, except for step (4), where Q_i now refers to the MCS quantile function for the i^{th} uncertainty. As an example, the MCS quantile function for *CR* is:

$$Q_{CR}(p) = \begin{cases} 45\%, & 0.00 \le p \le 0.25 \\ 50\%, & 0.25 \le p < 0.75 \\ 70\%, & 0.75 \le p < 1.00 \end{cases}$$

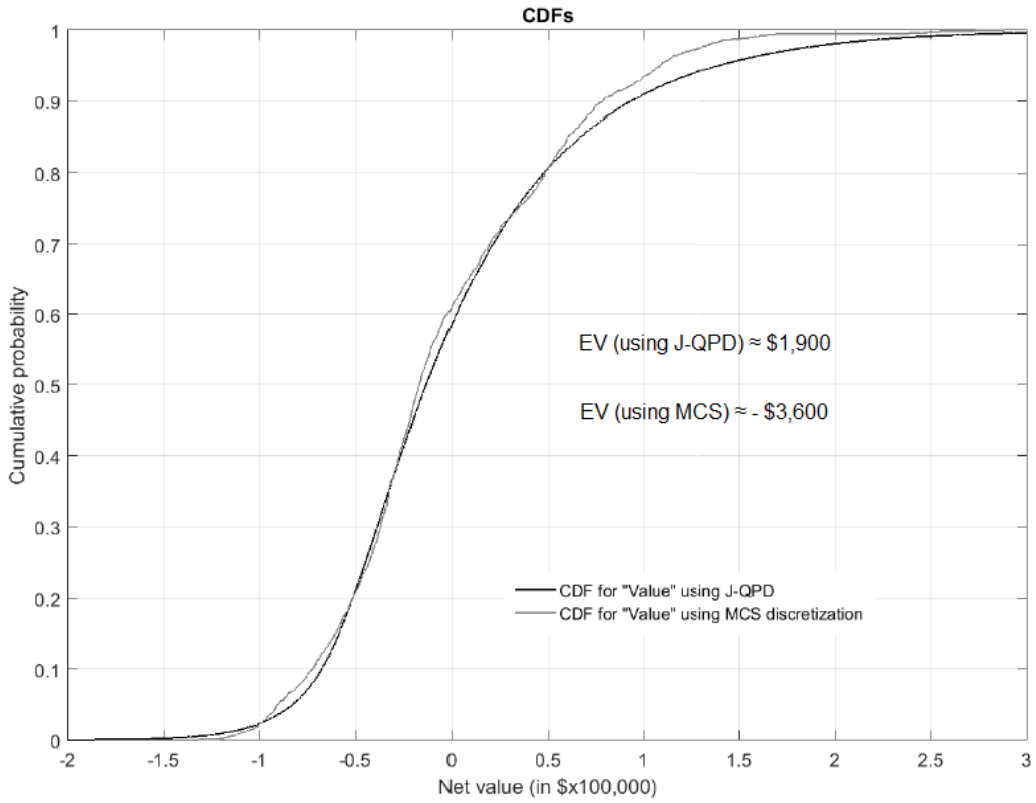

Figure 10.4. CDFs for 'Value' Using J-QPD/MP and MCS.

The Reduced Model

While the original model incorporates uncertainty for all nine input variables in Table 10.1, in this section we only incorporate uncertainty for several of these nine variables. By doing so, the key tradeoff here is a reduction in model fidelity, but increased accuracy due to a reduction in simulation error. In the discretized model, for example, the decision tree for the original problem has 3^9= 19,683 possible outcomes. The number of outcomes decreases exponentially as we reduce the number of uncertain variables. To gain insight into which variables should be locked to their deterministic base values, we first perform a one-way sensitivity analysis, by generating the tornado diagram shown in Figure 10.5.

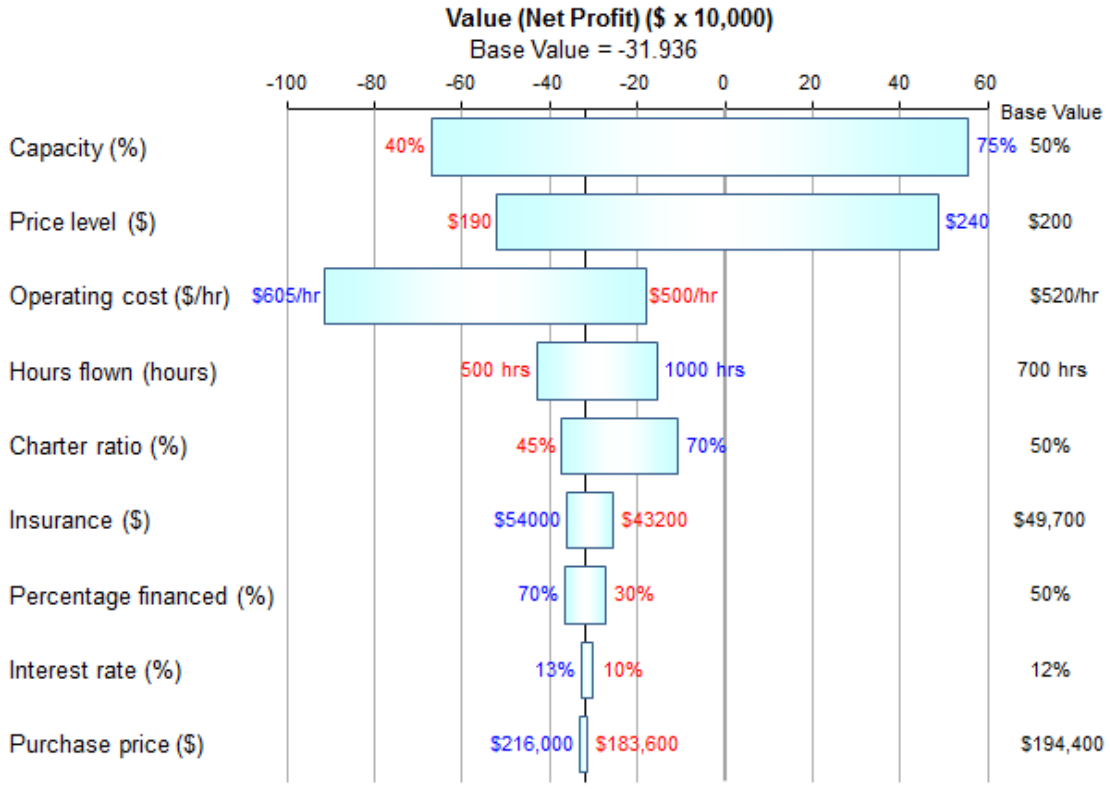

Figure 10.5. Tornado Diagram for Value, in Tens of Thousands of Dollars.

Tornado diagrams measure sensitivity of an output variable with respect to input variables based on low, base and high (e.g., P10, P50 and P90) percentile assessments of each individual input variable (these correspond to the low, base and high assessments of each input variable shown in Table 10.1. The development of the tornado diagram in Figure 10.5 involves adjusting each input parameter one-at-a-time, and then rerunning the model to obtain new values for 'Value' (i.e., net profit)[20].

Loosely speaking, and reading from top to bottom, input parameters are ranked from "most influential" (widest bar) to "least influential" (thinnest bar). However, the wideness of a bar can be due to a combination of two major factors.

[20] For sensitivity analysis methods involving changing more than one variable at a time, see Clemen (2014).

(1) Uncertainty – The difference between high (P90) and low (P10) assessments for each input parameter. If this range is large, we might observe a large change in the output variable even if the input itself is only a moderate driver.

(2) The influence of the input on the output – We are referring to the influence of the input on the output with respect to the actual "physics" of the underlying system.

The argument for ranking key drivers with respect to bar widths, however, is based on the idea that we have "accurate" P10, P50 and P90 assessments for each input parameter; i.e., that these numbers correspond to good expert elicitation. If more information becomes available for these parameters, then practice is to refine these assessments based on updated expert elicitations, and then rerun the analyses. From this point forward, however, we assume that we have good expert assessments.

We note several important insights gained from Figure 10.5. First, deterministically computing value by setting all nine uncertainties to their P50 yields a net *loss* of $31,936, compared to the expected net gain of $1,920 predicted by the stochastic simulation model using J-QPD/MP and shown in Figure 10.4. Interestingly, while *INS* and *PP* have large (P90-P10) ranges in an absolute sense, these variables contribute little (ranging them individually) toward changes in the output variable – 'Value'. Alternatively, adjusting the Price Level (*PL*) from $190 to $240 changes 'Value' from -$52,000 to +$48,600.

Referencing Figure 10.5, we incorporate uncertainty only for the top five variables shown (*CAP*, *PL*, *OC*, *HF*, and *CR*), and we fix the bottom four variables (*INS*, *PF*, *IR*, *PP*) at their base (P50) values. For the discrete case, using MCS, 'Value' now has only $3^5 = 243$ possible outcomes, compared to the 19,683 possible outcomes in the original model – a reduction in outcomes by a factor of 81. We now perform the exact same simulation procedure as in the original model.

Figure 10.6 shows the CDFs for the output ('Value') using our J-QPD/MP approach (solid curve), compared to that using the MCS discretization shortcut, along with the expected value (EV) using both approaches. Again, notice that MCS predicts an expected loss (now of $4,310) by purchasing the plane, and the continuous J-QPD/MP approach estimates a net gain of $1,070. Notice that while the absolute values of the EV have changed significantly compared to the original model, the decision recommendations do not change in either case, lending compelling evidence that Dick Carothers should purchase the plane. This assumes, of course, that all marginal (low-base-high) and correlation (Spearman's rho) values are assessed with perfect accuracy.

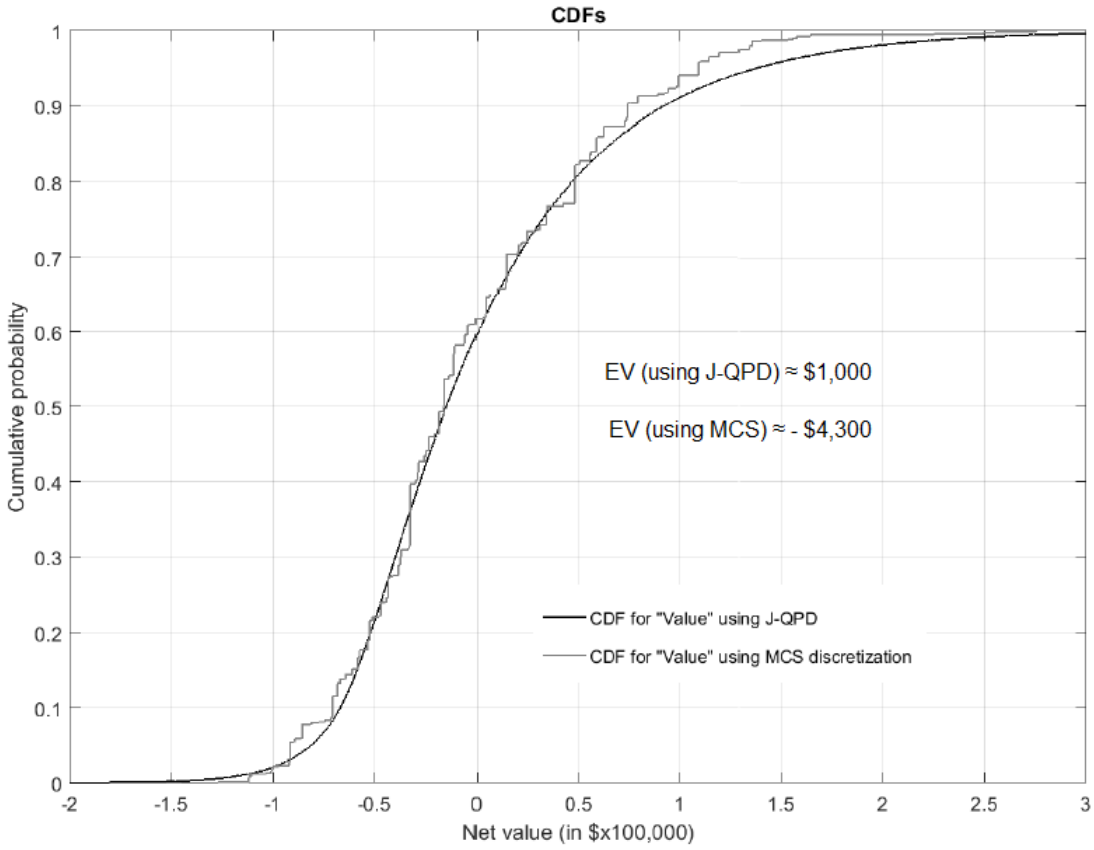

Figure 10.6. CDFs for 'Value' Using J-QPD/MP versus MCS.

ASSET PORTFOLIO EVALUATION PROBLEM

We now briefly present the application of J-QPD to the asset portfolio evaluation problem introduced by Keelin (2016)[21], which involves the decision on how much to bid for a portfolio of 259 real estate assets, offered by a financial institution via public auction. The decision maker in this problem is a potential bidder who engages a team of experts (representing "the analyst" in this case) to assess the value of the portfolio, which is the sum of the uncertain values of each asset. As part of the assessment process, the team extensively evaluated the uncertainty of each asset, ultimately providing the {10^{th},

[21] We modify the numbers only slightly here. Also, while the problem in Keelin (2016) is a real-world application, we treat this modified version as a hypothetical problem.

50^{th}, 90^{th}} percentile assessments shown in Figure 10.7. In addition to the marginal assessments, the team concluded that all assets in the portfolio are positively-correlated. Specifically, the team estimated a Pearson product-moment correlation coefficient of 0.8 between all pairs of assets.

Asset	P10	P50	P90
1	18,150	21,133	22,625
2	10,465	11,362	12,408
3	15,781	16,908	18,260
4	4,234	4,422	4,610
5	2,629	2,979	3,295
6	13,945	14,875	16,176
⋮	⋮	⋮	⋮
259	3,500	4,000	4,500

Figure 10.7. Low-Base-High Assessments by Asset (in $ 000s)

Using the assessment data in Figure 10.7, the team decided to assign a J-QPD-S (semi-bounded) distribution to the {10^{th}, 50^{th}, 90^{th}} percentile assessments for each asset. In the absence of further information, both the team and the potential bidder agreed that the lower bound for each asset should be zero. Obviously, asset values are inherently non-negative. However, the team had no justifiable reason to assign any other non-zero lower bound to any of the assets. Also, both the team and the decision maker felt uncomfortable imposing a finite upper bound on the value of any asset, thus lending them justification for using J-QPD-B.

To capture correlation among all assets, the team used a normal copula consistent with the pairwise correlation values of 0.8, in conjunction with the MP approach for encoding joint distributions. A one-way sensitivity analysis ultimately revealed assets 1 through 20, and asset 259 to be the key contributors of uncertainty in total portfolio value. Thus, the team modeled uncertainty in these assets, and fixed the remaining assets

at their base (median) values. Ultimately, the team constructed a distribution on total portfolio value in two ways: (1) using J-QPD-S in conjunction with the MP approach for the twenty-one key assets (assets 1 through 20, and asset 259); (2) using the traditional Extended Swanson-Megill[22] (ESM) discretization shortcut, which assigns probabilities of {0.3, 0.4, 0.3} to the {10^{th}, 50^{th}, 90^{th}} percentiles for each asset, in conjunction with sampling from the underlying normal copula.

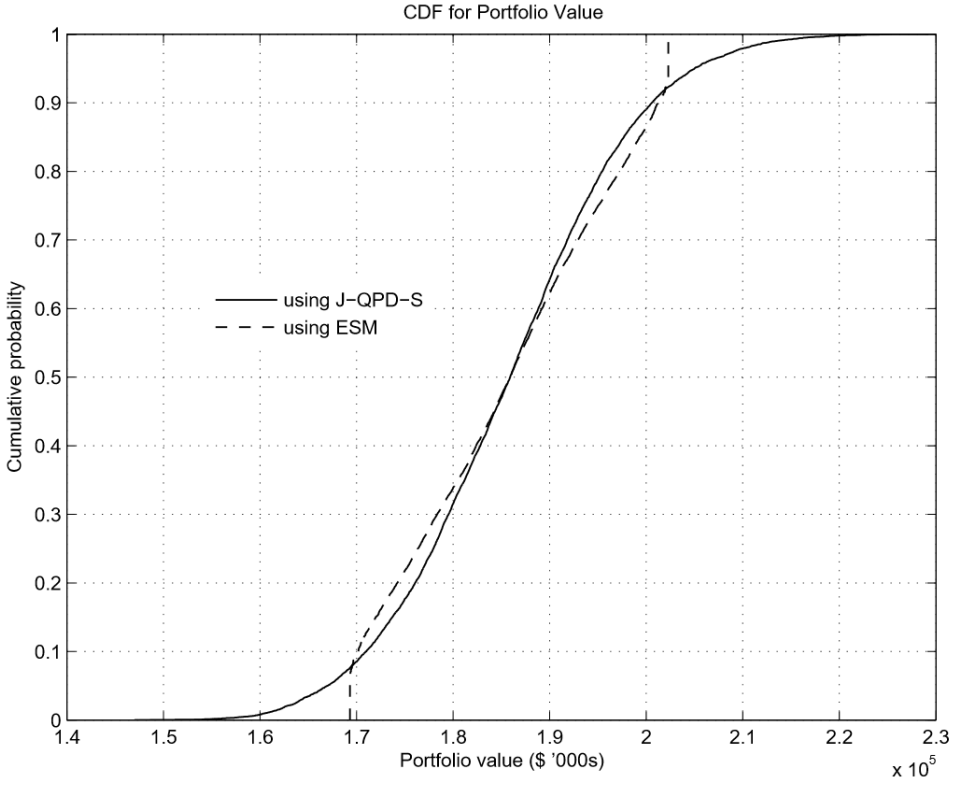

Figure 10.8. Simulation CDFs for Portfolio Value using ESM and J-QPD.

The CDFs for total portfolio value using both methods is shown in Figure 10.8. As clearly shown, the greatest insight from the comparison was the fact that the CDF using discretization with ESM showing a near-zero probability of the portfolio value falling just below $170,000,000, and a near-zero value of it exceeding just over

[22] See Hurst, et al. for more detail.

$200,000,000. Based on experience and judgment, the team concluded that while the CDF based on ESM well-captured portfolio value uncertainty in the body of the distribution, from roughly the 10^{th} percentile to the 90^{th} percentile shown in Figure 10.8, the sharp chop in tails beyond these values seemed unrealistic.

This problem illustrates how conventional approaches to quantifying uncertainty, in this case discretization, can potentially mislead decision making based on inherently continuous uncertainties, compared to using J-QPD. For example, a bid based on the 5^{th} percentile in Figure 10.8 would result in an overbid of between 2 and 3 million dollars using ESM instead of J-QPD.

Chapter 11 : Conclusion

This chapter concludes with a summary of the main contributions and corresponding results presented in this dissertation, recommendations and guidelines for practice, and several avenues for future research.

SUMMARY

In this dissertation, we developed a new probability distribution system, known as J-QPD, by applying well-known transformations to the Johnson SU distribution, followed by strategic re-parameterization. By design, the resulting J-QPD system is parameterized by a set of quantile-probability (QP) pairs, and consists of two sub-families:

- **J-QPD-B** (bounded) distributions.
- **J-QPD-S** (semi-bounded) distributions.

Unlike existing probability distribution systems, J-QPD satisfies all five of our desiderata presented in Chapter 4. Specifically, the J-QPD system is conveniently parameterized by a symmetric percentile triplet (SPT) of low-base-high assessments (e.g., 10^{th}, 50^{th}, 90^{th} percentiles), and specified support bounds, and is maximally-feasible (MF), in the sense that it can honor any valid SPT vector of low-base-high values, along with any compatible pair (lower and upper) of support bounds. Both the quantile function and CDF are readily available. J-QPD distributions have finite moments (like lognormal distributions), but also offer a highly flexible semi-bounded distribution with unbounded moments as a limiting case. J-QPD distributions are highly flexible in the sense of Pearson, and can also closely approximate distributions from a wide array of commonly-named families, when parameterized by the same SPT and support bounds.

For example, J-QPD-S subsumes the lognormal family as a special case, and effectively serves as a two-shape-parameter extension to the lognormal family, but in

quantile-parameterized form. Also, J-QPD-S is highly accurate at approximating Weibull and gamma distributions (including the exponential distribution), and most beta-prime distributions. The J-QPD-B (bounded) distributions approximate nearly all beta distributions with high accuracy, particularly the bell-shaped beta distributions, but also offer infinitely many other distributional forms than beta, due to having one additional shape parameter over beta[23]. Although inherently smooth, J-QPD-B distributions also approximate triangular distributions with reasonable accuracy.

The J-QPD system provides a high-fidelity and efficient means of precisely assigning a smooth probability distribution to a triplet of low-base-high assessments, in conjunction with two possible support scenarios commonly encountered in practice: specified bounded support; semi-bounded support with specified lower bound. No fitting (optimization) is needed, such as with least-squares, and the J-QPD assignments precisely honor the QP pairs. Also, J-QPD quantile functions allow for direct Monte Carlo simulation via direct inverse transform sampling, as a means of generating output value distributions.

We showed that the J-QPD distributions are particularly amenable to encoding dependence in two key ways. The first approach, known as the marginal assessment procedure (MP), uses a normal copula specified by a Spearman's rank correlation coefficient (Spearman's rho), assessed using methods outlined in Clemen, Fischer, and Winkler (2000). MP is a natural choice when marginal distributions are relatively easy to assess. The second approach, known as the conditional procedure (CP), naturally applies to cases where it is more natural to obtain low-base-high assessments of one uncertainty, *conditioned* upon assessed values of another uncertainty. CP uses J-QPD quantile

[23] J-QPD-B distributions also have one additional shape parameter over the Logit- and Probit-normal distributions, among others.

functions for both marginal and conditional distribution assignments, and to encode the underlying correlation structure.

RECOMMENDATIONS AND GUIDELINES FOR PRACTICE

General Remarks on Using J-QPD

Since J-QPD-S has lognormal tails, in the sense of Parzen (1979), we caution against its application when fatter tails, such as those of Pareto distributions, are needed. If a semi-bounded distribution with heavy tails is needed, and finite moments are not required, then we suggest using the J-QPD-S II (or S-II) (limiting distribution) provided in Table 7.1. Both J-QPD-B and J-QPD-S are generally highly accurate at approximating bell-shaped, and modestly-skewed J-shaped distributions, as seen in Chapter 6.

The appropriateness of implementing the J-QPD system should be judged according to the characteristics of the decision being modeled. In situations where there is inherent non-linearity in the value function, as with (e.g.) network investment applications (pipelines, communications, power transmission, etc.), an analyst may choose to implement the smooth J-QPD distribution assignments as a supplement to more conventional approaches – such as using discretization shortcuts. Indeed, Keelin (2016) presents a compelling real-world bidding problem involving a portfolio of real estate assets where use of discretization yields poor decision making. Also, recall the results of our illustrative example in Chapter 10.

In other cases, a decision maker may want an estimate of the probability of incurring a loss (e.g., the probability that NPV is less than zero) in a risky alternative – beyond simply having estimates of expected values. In this case, an analyst may prefer to implement the smooth J-QPD distribution assignments to better capture the shape (e.g., percentiles) of the output distribution.

J-QPD versus Traditional QPDs

A "recommendations and guidelines for practice" section is incomplete without mentioning the tradeoffs between our new J-QPD system and the broader definition of QPDs introduced by Keelin and Powley (2011), discussed in Chapter 3. We begin with a high-level comparison of the advantages of each approach over the other, shown in Table 11.1, and then provide more detailed guidance.

Advantages of J-QPD	**Advantages of QPD**
The Maximally-Feasible Property	Can accept QP pairs of non-SPT form
SPT assessments are common practice	Extendable to more QP pairs
Easier manipulation of support	Includes doubly-unbounded support
More amenable to both MP and CP	More easily handles overdetermined QP pairs
Finiteness of moments more easily managed	
Closer to named distributions	

Table 11.1. Comparing the Advantages of J-QPD to Traditional QPDs.

(1) Since assessing QP pairs in SPT-form is common practice[24], then J-QPD or L-QPD are practical modelling choices among continuous distributions, by default, if at least a finite lower bound of support can be reasonably imposed, such as zero for inherently non-negative quantities (e.g., distance, time, volume, etc.). In these cases, the MF property guarantees a unique J-QPD or L-QPD assignment, obviating the need for coaching an analyst on how to deal with infeasibility.

Also, where a finite lower bound of support can be reasonably specified, "engineering the support" is simply a matter of:

- Choosing J-QPD-S when a finite upper bound cannot be easily specified.
- Choosing J-QPD-B when a finite upper bound can also be specified, as with [0, 1] in the assessment of fractional quantities, such as market share.

[24] For example, see McNamee and Celona (1990), Hammond and Bickel (2013a), and Hurst et al. (2000).

By contrast, traditional QPDs require the choice of an appropriate transformation (such as "Exp") to achieve the desired support. However, as noted in Chapter 3 and Chapter 4, different transformations affect shape differently, and some transformations can yield infinite or undefined moments. This could be problematic if an expert's knowledge presumes finite moments. J-QPD circumvents this issue, since it has finite moments, except for the limiting distribution system: S-II.

(2) Traditional QPDs may be more appropriate if one or more of the following situations is encountered:

a. Assessed points contain incoherent QP pairs; e.g., the 50^{th} percentile is less than the 40^{th} percentile. In this case, Keelin and Powley (2011) offer a straightforward way of performing a least-squares fit for a given QPD type (e.g., SQN or Metalog) to the set of QP pairs, via a closed-form solution, using methods in Boyd and Vandenberghe (2009).

b. The number of assessed QP pairs is greater than that required for J-QPD. Using SQN, for example, if the number of QP pairs is greater than four, then the least-squares approach mentioned in (a) is an option. For larger sets of QP pairs, consider using the Metalog system, since Keelin (2016) prescribes a means of appending an arbitrarily large number of basis functions to meet the number of assessed QP pairs.

c. Assessed QP pairs are of non-SPT form. In this case, a QPD such as Metalog can be constructed having the same number of parameters (and basis functions) as the number of QP pairs. However, as illustrated in Chapter 3 and Chapter 4, there is no guarantee of feasibility.

d. Neither a finite lower nor upper bound of support cannot reasonably be imposed, suggesting use of doubly-unbounded support; e.g., log-returns on risky assets within financial markets. The standard SQN or Metalog distributions are natural candidates, since they have support on $(-\infty, \infty)$.

SUGGESTIONS FOR FUTURE RESEARCH

Reexamining Discretization Using J-QPD

Recently, Hammond and Bickel (2013a and 2013b, henceforth "HB") reexamined the accuracy of three-point discrete approximations to continuous distributions based on preserving the first several moments (mean, variance, skewness, and kurtosis) of the "true" continuous distribution, following earlier examination[25]. They constructed a fine grid of location-scale distributions across the portion of the $\{\beta_1, \beta_2\}$ space shown in Figure 11.1, and for each distribution, computed the error between the moments of the "true" distribution selected from the grid, and the given discrete distribution intended to approximate it. This comparison procedure is like our closeness computations using the APDM and APDV measures in Chapter 6, with several key differences in the case of HB:

- HB's grid of "true" distributions is built upon the region of Pearson's moment-ratio ($\{\beta_1, \beta_2\}$) space shown in Figure 11.1, while the grids built in Chapter 6 involve the beta and beta-prime distributions, as depicted in our new $\{s_\alpha, t_\alpha\}$ space.
- HB's analysis compares several discrete approximation shortcuts, which we discuss in more detail shortly, to each "true" distribution in the $\{\beta_1, \beta_2\}$ space

[25] For examples, see: Pearson and Tukey (1965); Keefer and Bodily (1983); Miller and Rice (1983); Zaino and D'Errico (1989); and McNamee and Celona (1990);

based on error measures with respect to the mean, variance, skewness, and kurtosis of the true distribution.

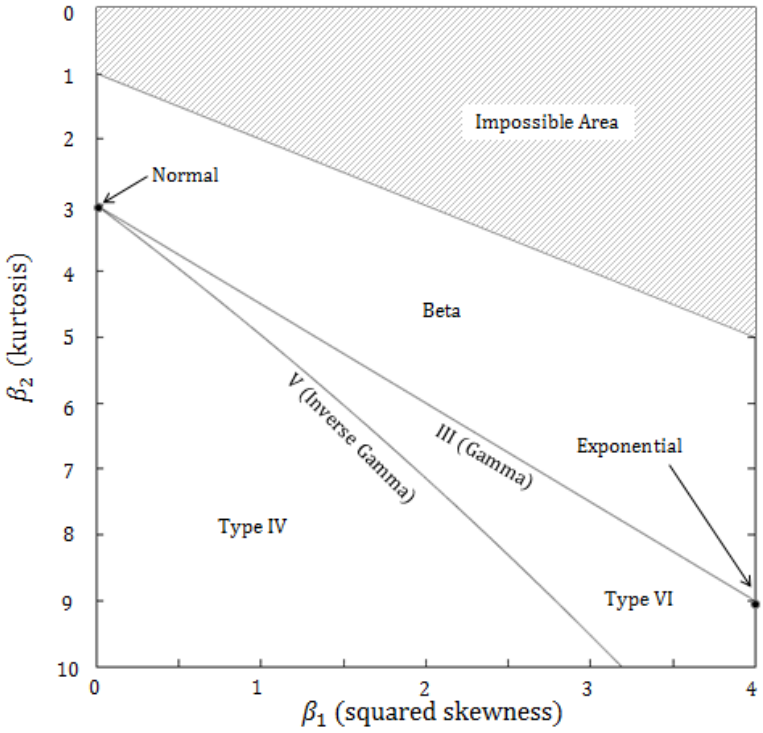

Figure 11.1. The Pearson System in the $\{\beta_1, \beta_2\}$ Space.

For example, suppose that the distribution selected from the $\{\beta_1, \beta_2\}$ grid is beta (3,7), and the discretization under consideration is Extended Swanson-Megill (ESM), which assigns probabilities of {0.3, 0.4, 0.3} to the {10^{th}, 50^{th}, 90^{th}} percentiles. In this case, the corresponding discrete approximation for beta (3,7) is as shown in Figure 11.2. The true mean (μ) and variance (σ^2) for a beta (3,7) distribution are: $\mu = 0.3$; $\sigma^2 = 0.0191$. The mean ($\hat{\mu}$) and variance ($\hat{\sigma}^2$) for the ESM discrete approximation in this case are:

$$\hat{\mu} = 0.3x_{0.1} + 0.4x_{0.5} + 0.3x_{0.9} = 0.3004,$$

$$\hat{\sigma}^2 = 0.3x_{0.1}^2 + 0.4x_{0.5}^2 + 0.3x_{0.9}^2 - \hat{\mu}^2 = 0.0196\,.$$

Using this example as context, using ESM to approximate beta(3,7), several noteworthy error metrics that HB consider are:

APDM based on standard deviation:

$$100\% \cdot \left| \left(\frac{\hat{\mu} - \mu}{\sigma} \right) \right| = 100\% \cdot \left| \left(\frac{0.3004 - 0.3}{0.1382} \right) \right| = 0.2665\ \%$$

APDV:

$$100\% \cdot \left| \left(\frac{\hat{\sigma}^2 - \sigma^2}{\sigma^2} \right) \right| = 100\% \cdot \left| \left(\frac{0.0196 - 0.0191}{0.0191} \right) \right| = 2.8565\ \%$$

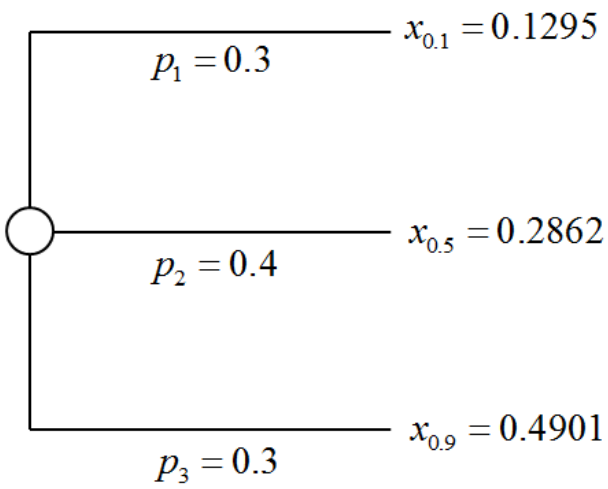

Figure 11.2. Extended Swanson-Megill (ESM) Discretization for Beta (3, 7).

Continuing this process for the entire grid of $\{\beta_1, \beta_2\}$ pairs (distributions) considered, HB then reported summary statistics for the sets of distributions occupying the different sub-regions of Figure 11.1. HB then developed new three-point discrete distributions, tailored to each region, by choosing the percentiles and weights (probabilities) that minimize the mean-squared-error (MSE) with respect to the mean, averaged across all distributions within the given region.

Extending Discretization Analysis with J-QPD

Now that we have an arguably much broader set of distributions in J-QPD, we could naturally use the J-QPD system to extend HB's analysis of discretization. Consider J-QPD-B as an example, since it has three shape parameters, and one degree of freedom more (an additional shape parameter) than the J-QPD-S distributions. We noted in Chapter 7 that due to the presence of three shape parameters for each α, it is possible to have more than one distinct location-scale J-QPD-B distribution for a given point in the $\{\beta_1, \beta_2\}$ space. Therefore, instead of constructing a grid of points across various regions of Pearson's $\{\beta_1, \beta_2\}$ space, we construct a three-dimensional grid of points across the feasible region of $\{10^{th}, 50^{th}, 90^{th}\}$ percentile triplets for J-QPD-B distributions with support on [0, 1] (without loss of generality), corresponding to the tetrahedron shown in Figure 11.3. While Figure 11.3 below provides an illustration of such a grid for points spaced at 0.05 apart, our actual grid used for analysis has points spaced at 0.02 apart, for a total of 18,424 points (distributions) considered in our analysis.

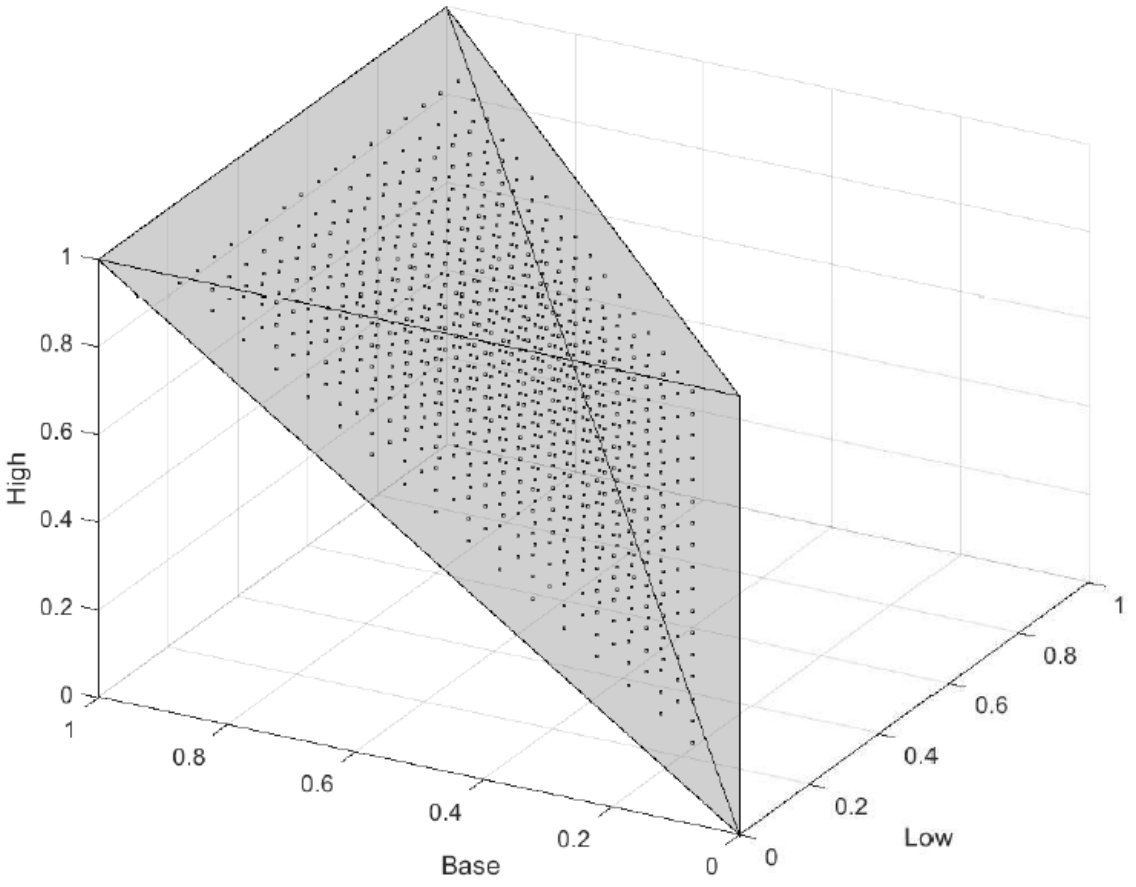

Figure 11.3. Grid of Distributions Uniformly Spaced over the J-QPD-B Feasible Region.

Let n = 18,424 (number of distributions considered), and let $i = \{1, 2, 3, \ldots, n\}$ denote the index for the i^{th} distribution in our set. For each of our 18,424 points considered, we perform the following computations:

(1) Specify the J-QPD-B distribution assignment for the $\boldsymbol{\theta}_{0.1}$ vector corresponding to the given point, by constructing the quantile function, denoted $Q_i(p)$, using the equations given in (4.4).

(2) Compute the mean and variance of this J-QPD-B assignment by numerical integration:

Mean: $\mu_i = \int_0^1 Q_i(p)dp$,

2nd raw moment[26]: $\mu_2^i = \int_0^1 \left(Q_i(p)\right)^2 dp$,

Variance: $v_i = \mu_2^i - \mu_i^2$.

(3) Construct the three-point discrete approximations for this J-QPD-B assignment for ESM, MCS, and EPT. ESM (MCS) uses probabilities of {0.3, 0.4, 0.3} ({0.25, 0.5, 0.25}) on the {10th, 50th, 90th} percentiles, while EPT uses probabilities of {0.185, 0.630, 0.185} on the {5th, 50th, 95th} percentiles. Let l_i, b_i, and h_i denote the {10th, 50th, 90th} percentiles for the i^{th} distribution, and let l_i' and h_i' denote its {5th, 95th} percentiles, respectively.

(4) Compute the mean and variance for ESM, MCS, and EPT.

Mean (ESM): $\mu_{\text{ESM}}^i = 0.3l_i + 0.4b_i + 0.3h_i$,

Mean (MCS): $\mu_{\text{MCS}}^i = 0.25l_i + 0.50b_i + 0.25h_i$,

Mean (EPT): $\mu_{\text{EPT}}^i = 0.185l_i' + 0.63b_i + 0.185h_i'$,

Variance (ESM): $v_{\text{ESM}}^i = 0.3l_i^2 + 0.4b_i^2 + 0.3h_i^2 - \left(\mu_{\text{ESM}}^i\right)^2$,

Variance (MCS): $v_{\text{MCS}}^i = 0.25l_i^2 + 0.50b_i^2 + 0.25h_i^2 - \left(\mu_{\text{MCS}}^i\right)^2$,

Variance (EPT): $v_{\text{EPT}}^i = 0.25l_i'^2 + 0.50b_i^2 + 0.25h_i'^2 - \left(\mu_{\text{EPT}}^i\right)^2$.

(5) Compute APDM and APDV between the J-QPD-B assignment and its discrete approximation for the given point, using expressions from Chapter 6 as follows:

$$APDM_{\text{ESM}}^i = 100 \cdot \left| \frac{\mu_{\text{ESM}}^i - \mu_i}{h_i - l_i} \right|,$$

$$APDM_{\text{MCS}}^i = 100 \cdot \left| \frac{\mu_{\text{MCS}}^i - \mu_i}{h_i - l_i} \right|,$$

$$APDM_{\text{EPT}}^i = 100 \cdot \left| \frac{\mu_{\text{EPT}}^i - \mu_i}{h_i - l_i} \right|,$$

[26] Note the slight abuse of notation. Any presence of "*i*" refers to an index designation, and not an exponent, regardless of whether it appears as a superscript or subscript.

$$APDV^{i}_{\text{ESM}} = 100 \cdot \left| \frac{v^{i}_{\text{ESM}} - v_i}{v_i} \right|,$$

$$APDV^{i}_{\text{MCS}} = 100 \cdot \left| \frac{v^{i}_{\text{MCS}} - v_i}{v_i} \right|.$$

$$APDV^{i}_{\text{EPT}} = 100 \cdot \left| \frac{v^{i}_{\text{EPT}} - v_i}{v_i} \right|.$$

After completing steps (1) to (5) for all 18,424 distributions, we compute the following summary statistics for these distributions:

- $\text{Mean}\left(APDM\right) = \left(\frac{1}{n}\right) \cdot \sum_{i=1}^{n} APDM_i$,
- $\text{P50}\left(APDM\right) = \underset{i}{\text{Med}}\left\{APDM_i\right\}$,
- $\text{Max}\left(APDM\right) = \underset{i}{\text{Max}}\left\{APDM_i\right\}$,
- $\text{Mean}\left(APDV\right) = \left(\frac{1}{n}\right) \cdot \sum_{i=1}^{n} APDV_i$,
- $\text{P50}\left(APDV\right) = \underset{i}{\text{Med}}\left\{APDV_i\right\}$,
- $\text{Max}\left(APDV\right) = \underset{i}{\text{Max}}\left\{APDV_i\right\}$.

The 'Mean(APDM)' ('Mean(APDV') statistics correspond to the *average* of the individual 'APDM_i' ('APDV_i') values, taken over all "*i*"; i.e., over all 18,424 distributions. The 'P50(APDM)' ('P50(APDV') statistics correspond to the median, evaluated over all of the individual 'APDM_i' ('APDV_i') values. Finally, the 'Max(APDM)' ('Max(APDV') statistics correspond to the maximum, evaluated over all individual 'APDM_i' ('APDV_i') values. Note that each value for APDM_i and APDV_i is both distribution-specific, as indexed by "*i*", and dependent upon the discretization under consideration. These statistics are presented in Table 11.2. We include the P50 statistics since in the limiting case, as J-QPD-B distributions approach the S-II distributions, moments diverge upward toward infinity. Thus, the mean and max statistics for MSE are

more sensitive to these extreme cases than the median statistic for MSE, as noted in Table 11.2.

	Mean(APDM)	P50(APDM)	Max(APDM)	Mean(APDV)	P50(APDV)	Max(APDV)
ESM	2.63%	1.86%	11.12%	20.66%	16.16%	78.12%
MCS	1.34%	0.79%	10.78%	18.25%	13.91%	81.00%
EPT	1.50%	0.78%	12.17%	19.92%	12.24%	91.01%

Table 11.2. Summary Statistics for ESM and MCS for all 18,424 Distributions.

Note that our analysis of discretization accuracy with respect to J-QPD-B, while much broader than that performed by HB (since J-QPD-B has three shape parameters), examines the entire feasible region for J-QPD-B; e.g., we do not distinguish between bell- or U-shaped distributions. Thus, this analysis is representative of the situation in which all we know about our distribution is that it is smooth[27], and well-represented by a distribution within the J-QPD-B system, properly shifted and scaled as needed.

Examining the performance of discretization with respect to the mean in Table 11.2, MCS outperforms ESM an all three error metrics, particularly with respect to the mean and median values for APDM, and outperforms EPT on the mean and max values of APDM; it is essentially a tie with respect to P50 (APDM). This suggests that when preserving the mean is important, but that we are not sure whether an expert's distribution is unimodal (e.g., bell-shaped) or multimodal (such as U-shaped) in shape (only that it has a smooth characterization), then MCS might be a relatively safe bet. This result contrasts with HB's examination of the bell-shaped beta distributions, for example, wherein they find that EPT (not counting their own optimal discrete distributions) is the

[27] We mean that the degree to which an expert's knowledge changes over its domain is smooth (continuous derivatives), unlike the TSP distribution proposed by Kotz and Van Dorp (2006), for example.

superior choice in preserving the mean, and ESM is preferred when considering discrete distributions using {10th, 50th, 90th} percentiles.

Alternatively, examining the performance of discretization with respect to the variance in Table 11.2, neither one of these three discrete distributions is generally superior to the others. However, with respect to mean and median values for APDV, MCS and EPT are comparable, and that both are generally superior to ESM. This is also in direct contrast to HB's analysis of the bell-shaped beta distributions, wherein they find that EPT is generally considerably superior to both ESM and MCS at preserving variance.

Constructing New Discrete Distributions with J-QPD

Another natural extension is to follow HB's lead in creating new three-point discrete distributions, optimized (for example) to minimize one or more of our summary statistics over all 18,424 points (distributions). Unlike HB, however, we choose as our objective to minimize the median (rather than the mean) value of mean-squared error (MSE) over all 18,424 distributions, which we define as:

$$MSE_i = 100 \cdot \left(\frac{\mu_i - \mu_i}{h_i - l_i} \right)^2 .$$

The first approach follows that of HB for symmetric discrete approximations, by finding an SPT ($\alpha \in (0, 0.5)$) and probability vector, {p, 1–2p, p}, $p \in (0, 0.5)$, so that MSE is minimized over all 18,424 points (distributions). The second approach, motivated by the results in Table 11.2, differs from the first approach only in that the objective is to minimize the *median* squared error across all points. In both cases, we also consider the variant in which the SPT (α) is specified (in this case, we use {10th, 50th, 90th} percentiles), and the decision variable is simply "p". For the first approach, in which the *mean* squared error is minimized over all distributions, the two formulations are:

$$\min_{p,\alpha} \ \frac{100}{18,424} \cdot \sum_{i=1}^{18,424} \left(\frac{p \cdot Q_i(\alpha) + (1-2p) \cdot Q_i(0.5) + p \cdot Q_i(1-\alpha) - \mu_i}{h_i - l_i} \right)^2$$

$$\text{s.t.} \quad 0 \le p \le 0.5, \qquad 0 \le \alpha \le 0.5 \qquad \text{(GP1)}$$

$$\min_{p} \ \frac{100}{18,424} \cdot \sum_{i=1}^{18,424} \left(\frac{p \cdot l_i + (1-2p) \cdot b_i + p \cdot h_i - \mu_i}{h_i - l_i} \right)^2$$

$$\text{s.t.} \quad 0 \le p \le 0.5, \qquad .$$

(SP1)

For the second approach, in which the *median* squared error is minimized over all distributions, the two formulations are:

$$\min_{p,\alpha} \ 100 \cdot \underset{i}{\text{Med}} \left\{ \left(\frac{p \cdot Q_i(\alpha) + (1-2p) \cdot Q_i(0.5) + p \cdot Q_i(1-\alpha) - \mu_i}{h_i - l_i} \right)^2 \right\}$$

$$\text{s.t.} \quad 0 \le p \le 0.5, \qquad 0 \le \alpha \le 0.5 \qquad \text{(GP2)}$$

$$\min_{p} \ 100 \cdot \underset{i}{\text{Med}} \left\{ \left(\frac{p \cdot l_i + (1-2p) \cdot b_i + p \cdot h_i - \mu_i}{h_i - l_i} \right)^2 \right\}$$

$$\text{s.t.} \quad 0 \le p \le 0.5, \qquad . \qquad \text{(SP2)}$$

The operation, "Med", means that the median value is taken over all $i = \{1, 2, 3, \ldots, n\}$. Problem SP1 is a convex quadratic program with one decision variable (p) and one constraint, and is easily solved[28]. Alternatively, problems GP1, GP2, and SP2 are all non-convex, non-linear programs. However, since these problems involve (at most) two decision variables (p, α), we find solutions that are arbitrarily close to the global optimum

[28] See, for example, Boyd and Vandenberghe (2009) for details.

by constructing a fine grid of (p, α) pairs (e.g., for GP1 and GP2), computing the objective function for all such pairs, and then choosing the pair that minimizes the objective function in each case[29].

Table 11.3 specifies optimal three-point discrete distributions for all four cases. SP refers to the optimizations over p, while fixing points to the standard ($\{10^{th}, 50^{th}, 90^{th}\}$) percentiles (hence the name, "SP"), while GP refers to the optimization in which both p and α are decision variables. The augmented name, "mean" ("median"), means that the objective is to minimize the mean (median) value of MSE over all 18,424 points (distributions). Note the closeness of both SP discrete distributions to MCS, lending credence to MCS when preserving the mean over standard percentiles, and when little is known about distribution shape. Alternatively, GP distributions implement $\{\alpha, p\}$ pairs that are neither close to standard percentiles, nor those used by EPT.

New Discretization	Quantiles to use	Probabilities to use
GP_mean (GP1)	{0.068, 0.500, 0.932}	{0.1896, 0.6208, 0.1896}
GP_median (GP2)	{0.0675, 0.5000, 0.0675}	{0.204, 0.592, 0.204}
SP_mean (SP1)	{0.1, 0.5, 0.9}	{0.245, 0.510, 0.245}
SP_median (SP2)	{0.1, 0.5, 0.9}	{0.24, 0.52, 0.24}

Table 11.3. Optimized Symmetric Three-Point Discrete Distributions.

Table 11.4 is a duplicate of Table 11.2, except that now we have appended the performance metrics for all four optimal discrete distributions to compare their performance across all summary statistics, as compared to the existing discrete approximations. As before, the "winning" discretization for a given performance metric is shown in the highlighted cells. Notice that while the GP discrete distributions are

[29] For GP1 and GP2, using MATLAB, we used a grid of (p, α) pairs, both taken from 0.002 to 0.498, and both spaced in increments of 0.002. For SP2, we simply used a vector of p values, ranging from 0.002 to 0.498, spaced in increments of 0.002.

designed to minimize errors with respect to the mean across our distribution set, they also generally perform slightly better at preserving the variance.

	Mean(|APDM|)	P50(|APDM|)	Max(|APDM|)	Mean(|APDV|)	P50(|APDV|)	Max(|APDV|)
ESM	2.63%	1.86%	11.12%	20.66%	16.16%	78.12%
MCS	1.34%	0.79%	10.78%	18.25%	13.91%	81.00%
EPT	1.50%	0.78%	12.17%	19.92%	12.24%	91.01%
GP1	1.08%	0.74%	7.23%	16.89%	13.41%	68.64%
GP2	1.14%	0.53%	8.24%	16.89%	10.27%	70.54%
SP1	1.31%	0.75%	11.14%	18.76%	14.62%	81.32%
SP2	1.30%	0.72%	11.50%	19.38%	15.39%	81.63%

Table 11.4. Summary Errors for New and Existing Discretization Methods.

Further Discretization

We have extended HB's analysis approach of discretization to J-QPD distributions, but implementing several differences:

- We specify our comprehensive set of J-QPD distributions using the feasibility region, rather than the traditional $\{\beta_1, \beta_2\}$ space introduced by Pearson.
- We used a slightly modified version for errors with respect to the mean, the absolute percent difference in the means (APDM), by dividing the difference in means by the inter-decile range (P90-P10), so that the error measure is indifferent to changes of location or scale.
- Like HB's work, we identified new optimal discrete distributions by minimizing the mean value of APDM over our set of distributions, but also by minimizing the *median* value of APDM over this set.

However, we have only touched the surface in terms of extending discretization using J-QPD. First, we did not perform a similar analysis using J-QPD-S. Second, and similar in spirit to HB's work, we did not yet delineate our results in terms of classes of distribution

shapes; e.g., bell-, U-, J-shaped, etc. An additional step here is to characterize the modality of J-QPD in terms of a $\boldsymbol{\theta}_\alpha$ vector.

Extending J-QPD to Doubly-Unbounded Support

We close by suggesting some natural extensions to our work. The first is to develop a distribution system similar to J-QPD, but with support on $(-\infty, \infty)$. However, more than three assessed points are required in this case, if it is important to characterize location, scale and both infinite tails. Also, the percentile-based flexibility space might need to be redefined in this case, since distributions with doubly-unbounded support all correspond to the point [1, 1] within the $\{s_\alpha, t_\alpha\}$ space presented in Chapter 5. The $\{s, t\}$ space offered by Powley (2013) is a viable approach in the case of *four* assessed points. However, this poses the challenge of extending our SPT and maximally-feasible concept to four assessed points. The mathematical form of the distribution, and the structure (spacing) of the four-point SPT vector needs to be carefully selected to satisfy the five desiderata. Again, the Johnson SU distribution might be a natural candidate. However, no one has identified four percentile points that are both commonly-accepted for assessment (e.g., 5^{th}, 10^{th}, 25^{th}, 50^{th}, 75^{th}, 90^{th}, 95^{th}) *and* spaced so that there is an explicit analytical solution for the four parameters, thus allowing for quantile-parameterized representation.

Extending the Maximally-Feasible Property Beyond SPT Form

We saw in Chapter 5 that the J-QPD systems are maximally-feasible given our SPT/bound structure described in Chapter 4. However, J-QPD is *not* maximally-feasible whenever the low-base-high assessments are *not* of SPT form. For example, suppose we have an inherently non-negative uncertainty, and thus specify zero for the lower support bound. Also, suppose an expert provides $\{20^{th}, 60^{th}, 90^{th}\}$ percentiles of {30, 40, 200}, which are not of SPT form, and suggests using an upper bound of ∞. We face two issues

in this case when trying to implement J-QPD-S. The first issue is that when low-base-high assessments are not of SPT form, Desideratum 1 is immediately violated, and thus we cannot specify a J-QPD-S distribution (by finding an $\alpha \in (0, 0.5)$, and a triplet, $0 < x_\alpha < x_{0.5} < x_{1-\alpha}$) without solving a non-linear system of equations for these values. More importantly, however, for our specific non-SPT example, we face infeasibility; i.e., one can show that there exists no $\alpha \in (0, 0.5)$ and triplet, $0 < x_\alpha < x_{0.5} < x_{1-\alpha}$, satisfying $\{x_{0.2}, x_{0.6}, x_{0.9}\} = \{30, 40, 200\}$.

Removing location and scale in our example, we have: $\frac{x_{0.6}}{x_{0.9}} = 0.2,\ \frac{x_{0.2}}{x_{0.6}} = 0.75.$

Figure 11.4 shows the feasible region of {P60/P90, P20/P60} pairs for J-QPD-S, taken across all possible values for $\alpha \in (0, 0.5)$, and all possible $\{s_\alpha, t_\alpha\}$ pairs, based on a sampling of one million points; i.e., one million $\{\alpha, s_\alpha, t_\alpha\}$ randomly-sampled triplets, each of which corresponds to a unique location-scale J-QPD-S distribution.

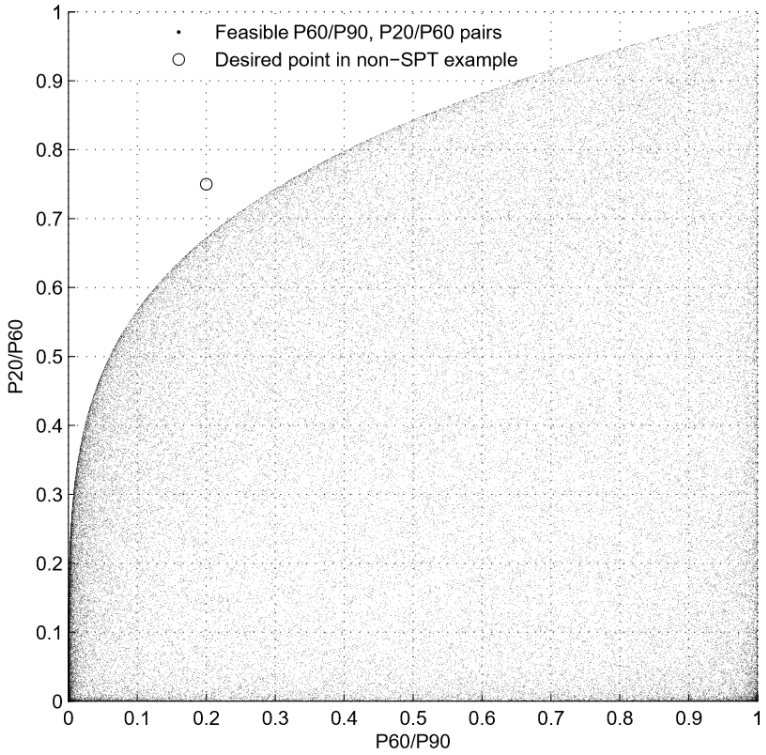

Figure 11.4. Feasible Region of {P60/P90, P20/P60} Pairs for J-QPD-S.

A major ideal is to identify a new probability distribution system that is smooth and meets all five desiderata like J-QPD, but that is also quantile-parameterized by (and maximally-feasible for) any triplet of compatible low-base-high assessments, regardless of whether the triplet of assessments is of SPT form. The QPDs developed by Keelin and Powley can handle vectors of QP pairs of non-SPT form, given the linear relationship between quantile- and probability data vectors, but are not maximally-feasible, as we saw in the example of Figure 3.2.

Fitting J-QPD to an Over-Specified Set of QP Pairs

A second extension to our work is the development of a simple method for fitting J-QPD to an over-specified vector of assessed points. The linear form of the parameters in the SQN system allow Keelin and Powley (2011) to represent the least-squares fit problem as

a simple quadratic program in the four unknown parameters, giving SQN a tractability advantage over J-QPD in the case of an over-specified system. Perhaps it might be possible to develop a five-point version of an SPT, with percent points spaced so as to yield a tractable regression problem in solving for the three unknown parameters.

Appendix A: Proof of Proposition 2

Proposition 2 (MF Property). Consider any compatible $\boldsymbol{\theta}_\alpha = (l, \mathbf{x}_\alpha, u) = (l, x_\alpha, x_{0.50}, x_{1-\alpha}, u)$. There exists a unique quantile function, Q, characterized by (4.4), that satisfies:

- $Q_B(0) = l$,
- $Q_B(\alpha) = x_\alpha$,
- $Q_B(0.5) = x_{0.5}$,
- $Q_B(1-\alpha) = x_{1-\alpha}$,
- $Q_B(1) = u$.

Proof. Since we are given $\boldsymbol{\theta}_\alpha$ as compatible, it follows that $l < x_\alpha < x_{0.50} < x_{1-\alpha} < u$. Since $\boldsymbol{\theta}_\alpha$ is chosen arbitrarily, it suffices to show that the functional representation, $Q(p)$, given in (4.4) corresponds to a quantile function for the given $\boldsymbol{\theta}_\alpha$. The expression, $\lambda \cdot \sinh(\delta \cdot (\Phi^{-1}(p) + n \cdot c)) + \xi$, in (4.4) corresponds to the quantile function for a Johnson SU distribution (by definition), provided that $\lambda > 0$ and $\delta > 0$. Since $\Phi(x)$ is increasing over the real number line, it follows that $Q(p)$ is an increasing quantile function for the given $\boldsymbol{\theta}_\alpha$ if and only if $\lambda > 0$ and $\delta > 0$ in accordance with the parameter expression in (7). There are three cases to consider:

Case 1: $n = -1$.

Referencing the parameter expressions given in (4.4), we have: $n = -1 \Leftrightarrow L + H - 2B < 0 \Leftrightarrow H - B < B - L$, and $\dfrac{H-L}{2(H-B)} > 1$.

This implies that:

$$\delta = \left(\frac{1}{c}\right)\cosh^{-1}\left(\frac{H-L}{2(H-B)}\right) > 0.$$

$$\Rightarrow \lambda = \frac{H-L}{\sinh(2\delta c)} > 0.$$

Case 2: $n = 1$.

Referencing the parameter expressions given in (4.4), we have:

$$n = -1 \Leftrightarrow L + H - 2B > 0 \Leftrightarrow H - B > B - L,$$

and $\dfrac{H - L}{2(B - L)} > 1.$

This implies that:

$$\delta = \left(\frac{1}{c}\right)\cosh^{-1}\left(\frac{H - L}{2(B - L)}\right) > 0.$$

$$\Rightarrow \lambda = \frac{H - L}{\sinh(2\delta c)} > 0.$$

Case 3: $n = 0$.

For the case in which $n = 0$, $Q(p)$ is defined as in (4.6):

$$Q(p) = l + (u - l) \cdot \Phi\left(B + \left(\frac{H - L}{2c}\right) \cdot \Phi^{-1}(p)\right).$$

By inspection, $Q(p)$ is non-decreasing as defined since $(u - l) > 0$, and since $H - L > 0$.

This completes the proof of Proposition 2. ■

Appendix B: Showing that S-II has Unbounded Moments

Consider the following quantile function representation:

$$Q(p) = l + \theta \exp\left(\lambda \sinh(\delta(\Phi^{-1}(p) + \gamma))\right),\ \delta > 0,\ \lambda > 0,\ \theta > 0.$$

We seek to show that all positive moments of $Q(p)$ are infinite. Without loss of generality, we set $l = 0$ and $\theta = 1$, since these correspond to location and scale parameters, respectively. Let μ_k denote the k^{th} raw moment of $Q(p)$, for any $k > 0$. By definition, the quantile representation of μ_k is given by:

$$\mu_k = \int_0^1 Q^k(p)dp = \int_0^1 \exp\left(k \cdot \lambda \cdot \sinh\left(\delta \cdot (\Phi^{-1}(p) + \gamma)\right)\right)dp$$

$$= \frac{1}{\sqrt{2\pi}} \int_{-\infty}^{\infty} \exp\left(-\frac{x^2}{2} + k \cdot \lambda \cdot \sinh\left(\delta \cdot (x + \gamma)\right)\right)dx.$$

The integrand is non-negative, and we note that:

$$\lim_{x \to \infty}\left(\exp\left(-\frac{x^2}{2} + k \cdot \lambda \cdot \sinh\left(\delta \cdot (x + \gamma)\right)\right)\right) = \infty,$$

since $k\lambda > 0$ and $\delta > 0$. Thus, the integral diverges, which implies that μ_k is infinite for $Q(p)$ whenever $k > 0$. ■

Appendix C: Finiteness of J-QPD-S Moments

As defined in (4.7), the quantile function for the J-QPD-S distribution is given by:

$$Q_S(p) = l + \theta \cdot \exp\left(\lambda \cdot \sinh\left(\sinh^{-1}\left(\delta \cdot \Phi^{-1}(p)\right) + \sinh^{-1}(n \cdot c \cdot \delta)\right)\right).$$

We seek to show that all positive moments of $Q_S(p)$ are finite. There are three cases to consider: n = {-1, 0, 1}. For n = 0, recall that we recover a lognormal distribution, which is well-known to have finite positive moments. We now consider n = {-1, 1}. Without loss of generality, we remove location and scale. Consider:

$$Q_S(p) = \exp\left(\lambda \cdot \sinh\left(\sinh^{-1}\left(\delta \cdot \Phi^{-1}(p)\right) + \sinh^{-1}(n \cdot c \cdot \delta)\right)\right),\ \lambda > 0,\ \delta > 0.$$

Let μ_k denote the k^{th} raw moment associated with $Q_S(p)$, for any $k > 0$. By definition, the quantile representation of μ_k is given by:

$$\mu_k = \int_0^1 (Q_S(p))^k dp = \int_0^1 \exp\left(k \cdot \lambda \cdot \sinh\left(\sinh^{-1}\left(\delta \cdot \Phi^{-1}(p)\right) + \sinh^{-1}(n \cdot c \cdot \delta)\right)\right) dp$$

$$\int_0^1 \exp\left(k \cdot \lambda \cdot \left(\delta \cdot \Phi^{-1}(p)\sqrt{1 + (c \cdot \delta)^2} + n \cdot c \cdot \delta \cdot \sqrt{1 + \left(\delta \cdot \Phi^{-1}(p)\right)^2}\right)\right) dp.$$

Now, let us first consider $n = -1$.

Case 1: n = -1.

We have:

$$\mu_k = \int_0^1 \exp\left(k \cdot \lambda \cdot \left(\delta \cdot \Phi^{-1}(p)\sqrt{1 + (c \cdot \delta)^2} - \underbrace{c \cdot \delta \cdot \sqrt{1 + \left(\delta \cdot \Phi^{-1}(p)\right)^2}}_{>0}\right)\right) dp$$

$$\leq \int_0^1 \exp\left(k \cdot \lambda \cdot \left(\delta \cdot \Phi^{-1}(p)\sqrt{1 + (c \cdot \delta)^2}\right)\right) dp$$

$$= \int_0^1 \exp\left(k \cdot \lambda \cdot \delta \cdot \sqrt{1 + (c \cdot \delta)^2} \cdot \Phi^{-1}(p)\right) dp = \exp\left(\left(\frac{1}{2}\right) \cdot k^2 \cdot \lambda^2 \cdot \delta^2 \cdot \left(1 + (c \cdot \delta)^2\right)\right) < \infty.$$

■

Case 2: n = 1.

In this case, we have:

$$\left(Q_S(p)\right)^k = \exp\left(k \cdot \lambda \cdot \left(\delta \cdot \Phi^{-1}(p)\sqrt{1 + (c \cdot \delta)^2} + c \cdot \delta \cdot \sqrt{1 + \left(\delta \cdot \Phi^{-1}(p)\right)^2}\right)\right).$$

We note the following:

$$\mu_k = \int_0^1 \left(Q_S(p)\right)^k dp = \int_0^{1/2} \left(Q_S(p)\right)^k dp + \int_{1/2}^1 \left(Q_S(p)\right)^k dp \le \int_0^{1/2} \left(Q_S(0.5)\right)^k dp + \int_{1/2}^1 \left(Q_S(p)\right)^k dp$$

$$= \left(\frac{1}{2}\right)\exp\left(k\cdot\lambda\cdot c\cdot\delta\right) + \int_{1/2}^1 \exp\left(k\cdot\lambda\cdot\left(\delta\cdot\Phi^{-1}(p)\sqrt{1+(c\cdot\delta)^2} + c\cdot\delta\cdot\sqrt{1+\left(\delta\cdot\Phi^{-1}(p)\right)^2}\right)\right)dp$$

$$\le \left(\frac{1}{2}\right)\exp\left(k\cdot\lambda\cdot c\cdot\delta\right) + \int_{1/2}^1 \exp\left(k\cdot\lambda\cdot\left(\delta\cdot\Phi^{-1}(p)\sqrt{1+(c\cdot\delta)^2} + c\cdot\delta\cdot\left(1+\delta\cdot\Phi^{-1}(p)\right)\right)\right)dp$$

$$\le \left(\frac{1}{2}\right)\exp\left(k\cdot\lambda\cdot c\cdot\delta\right) + \int_0^1 \exp\left(k\cdot\lambda\cdot\left(\delta\cdot\Phi^{-1}(p)\sqrt{1+(c\cdot\delta)^2} + c\cdot\delta\cdot\left(1+\delta\cdot\Phi^{-1}(p)\right)\right)\right)dp$$

$$= \left(\frac{1}{2}\right)\exp\left(k\cdot\lambda\cdot c\cdot\delta\right) + \exp\left(k\cdot\lambda\cdot\delta\cdot\left(c+\left(\frac{1}{2}\right)k\cdot\lambda\cdot\delta\cdot\left(c\cdot\delta+\sqrt{1+(c\cdot\delta)^2}\right)^2\right)\right) < \infty.$$

■

Appendix D: Proof of Proposition 1

Proposition 1 (MF Property). Consider any compatible $\boldsymbol{\theta}_\alpha = (l, \mathbf{x}_\alpha, \infty) = (l, x_\alpha, x_{0.50}, x_{1-\alpha}, \infty)$. There exists a unique quantile function, Q, characterized by (4.7), that satisfies:

- $Q_S(0) = l$,
- $Q_S(\alpha) = x_\alpha$,
- $Q_S(0.5) = x_{0.5}$,
- $Q_S(1-\alpha) = x_{1-\alpha}$,
- $Q_S(1) = \infty$.

Proof. Since we are given $\boldsymbol{\theta}_\alpha$ as compatible, it follows that $l < x_\alpha < x_{0.50} < x_{1-\alpha} < \infty$. Since $\boldsymbol{\theta}_\alpha$ is chosen arbitrarily, it suffices to show that the functional representation, $Q_S(p)$, given in (4.7) corresponds to a quantile function for the given $\boldsymbol{\theta}_\alpha$. Since $\Phi^{-1}(p)$ is increasing over p, and since the "Exp", "sinh", and "$\sinh^{-1}$" operators are all non-decreasing over the real number line, it follows that $Q_S(p)$ is an increasing quantile function for the given $\boldsymbol{\theta}_\alpha$ if and only if $\theta > 0$, $\lambda > 0$ and $\delta > 0$ in accordance with the parameter expression in (4.7). There are three cases to consider:

Case 1: $n = -1$.

Referencing the parameter expressions given in (4.7), we first note that $\theta = x_{1-\alpha} - l > 0$, due to the given compatibility of $\boldsymbol{\theta}_\alpha$. Next, we observe that:

$$n = -1 \Leftrightarrow L + H - 2B < 0 \Leftrightarrow H - B < B - L, \text{ and } \frac{H-L}{2(H-B)} > 1.$$

This implies that:

$$\delta = \left(\frac{1}{c}\right)\sinh\left(\cosh^{-1}\left(\frac{H-L}{2(H-B)}\right)\right) > 0.$$

$$\Rightarrow \lambda = \left(\frac{1}{\delta \cdot c}\right)\cdot(H-B) > 0.$$

Case 2: $n = 1$.

Referencing the parameter expressions given in (4.7), we first note that $\theta = x_\alpha - l > 0$, due to the given compatibility of $\boldsymbol{\theta}_\alpha$. Next, we observe that:

$$n = -1 \Leftrightarrow L + H - 2B > 0 \Leftrightarrow H - B > B - L, \text{ and } \frac{H-L}{2(B-L)} > 1.$$

This implies that:

$$\delta = \left(\frac{1}{c}\right)\sinh\left(\cosh^{-1}\left(\frac{H-L}{2(B-L)}\right)\right) > 0.$$

$$\Rightarrow \lambda = \left(\frac{1}{\delta \cdot c}\right)\cdot(B-L) > 0.$$

Case 3: $n = 0$.

For the case in which $n = 0$, $Q_S(p)$ is given as in (4.8):

$$Q_S(p) = l + \theta\exp\left(\lambda\delta\Phi^{-1}(p)\right), \text{ with}$$

$$\theta = x_{0.5} - l > 0,$$

$$\lambda\delta = \frac{H-B}{c} = \frac{B-L}{c} > 0.$$

Thus, $Q_S(p)$ is non-decreasing over p in this case, and is thus a quantile function. This completes the proof of Proposition 1. ■

Appendix E: Finiteness of L-QPD-S Moments

Consider the quantile function for the L-QPD-S distributions, given by:

$$Q_S(p) = l + \theta \exp\left(\lambda \sinh\left(\sinh^{-1}\left(\delta \Phi^{-1}(p)\right) + \sinh^{-1}(nc\delta)\right)\right),\ \theta > 0,\ \lambda > 0,\ \delta > 0,$$

where $\Phi^{-1}(p) = \log\left(\frac{p}{1-p}\right)$.

For $k > 0$, the k^{th} raw moment associated with Q_s exists if and only if:

$$k\lambda\delta\left(nc\delta + \sqrt{1+(cd)^2}\right) < 1.$$

Proof. Without loss of generality, let $l = 0$, and $\theta = 1$, so that we have:

$$Q_S(p) = \exp\left(\lambda \sinh\left(\sinh^{-1}\left(\delta \Phi^{-1}(p)\right) + \sinh^{-1}(nc\delta)\right)\right), \lambda > 0,\ \delta > 0,$$

which can also be expressed as:

$$Q_S(p) = \exp\left(\lambda\delta\left(\Phi^{-1}(p)\sqrt{1+(c\delta)^2} + nc\sqrt{1+\left(\delta \cdot \Phi^{-1}(p)\right)^2}\right)\right).$$

For this proof, we make use of the following facts:

(1) $|x| \le \sqrt{1+x^2} \le 1 + |x|,\ x \in \mathbb{R}$

(2) For a log-logistic distribution with shape parameter, β, the k^{th} raw moment exists if and only if $k < \beta$[30].

There are three cases to consider:

Case 1: $n = 0$.

In this case, Q_s reduces to:

$$Q_S = \exp\left(\lambda\delta\sqrt{1+(c\delta)^2}\,\Phi^{-1}(p)\right) = \left(\frac{p}{1-p}\right)^{\lambda\delta\sqrt{1+(c\delta)^2}}.$$

This corresponds to a log-logistic distribution with shape parameter: $\beta = \frac{1}{\lambda\delta\sqrt{1+(c\delta)^2}}$, and thus the k^{th} raw moment exists if and only if $k\lambda\delta\sqrt{1+(c\delta)^2} < 1$. Since $n = 0$ in this

[30] For more details, see Tadikamalla and Johnson (1982), and Tadikamalla (1980).

case, it follows that the k^{th} raw moment exists if and only if $k\lambda\delta\left(nc\delta+\sqrt{1+(cd)^2}\right)<1$, thus establishing the proof for Case 1.

Case 2: $n = 1$.

Letting ϕ denote the PDF for the standard logistic distribution, and $M=\sqrt{1+(c\delta)^2}$, we can express the k^{th} raw moment associated with Q_s, denoted μ_k, as:

$$=\int_{-\infty}^{\infty}\phi(x)\cdot\exp\left(k\lambda\delta\left(Mx+c\sqrt{1+(\delta x)^2}\right)\right)dx.$$

Since $c > 0$, $\delta > 0$, and $\lambda > 0$, then if μ_k exists and is finite, we note that:

$$=\underbrace{\int_{-\infty}^{\infty}\phi(x)\cdot\exp\left(k\lambda\delta\left(Mx+c\delta x\right)\right)dx}_{LHS}\le\mu_k\le\underbrace{\int_{-\infty}^{\infty}\phi(x)\cdot\exp\left(k\lambda\delta\left(Mx+c\left(1+\delta|x|\right)\right)\right)dx}_{RHS}.$$

Now,

$$LHS=\int_{-\infty}^{\infty}\phi(x)\cdot\exp\left(k\lambda\delta\left(M+c\delta\right)x\right)dx.$$

Thus, *LHS* is the k^{th} raw moment of a log-logistic distribution with shape parameter: $\beta=\dfrac{1}{\lambda\delta\left(M+c\delta\right)}$, which exists if and only if $k\lambda\delta(M + c\delta) < 1$.

Also,

$$RHS=\int_{-\infty}^{0}\phi(x)\cdot\exp\left(k\lambda\delta\left(Mx+c\left(1-\delta x\right)\right)\right)dx+\int_{0}^{\infty}\phi(x)\cdot\exp\left(k\lambda\delta\left(Mx+c\left(1+\delta x\right)\right)\right)dx$$

$$=\int_{0}^{\infty}\phi(x)\cdot\exp\left(k\lambda\delta\left(-Mx+c\left(1+\delta x\right)\right)\right)dx+\int_{0}^{\infty}\phi(x)\cdot\exp\left(k\lambda\delta\left(Mx+c\left(1+\delta x\right)\right)\right)dx$$

$$\le 2\cdot\int_{0}^{\infty}\phi(x)\cdot\exp\left(k\lambda\delta\left(Mx+c\left(1+\delta x\right)\right)\right)dx\le 2\cdot\int_{-\infty}^{\infty}\phi(x)\cdot\exp\left(k\lambda\delta\left(Mx+c\left(1+\delta x\right)\right)\right)dx$$

$$=2\cdot\exp\left(k\lambda c\delta\right)\cdot\underbrace{\int_{-\infty}^{\infty}\phi(x)\cdot\exp\left(k\lambda\delta\left(M+c\delta\right)x\right)dx}_{RHS'}.$$

Notice that $RHS' = LHS$, and that RHS' is just a constant multiplied by *RHS*. Thus, if *RHS* converges, which is equivalent to the condition that $k\lambda\delta(M + c\delta) < 1$, then μ_k exists.

Conversely, if μ_k exists, then *LHS* converges, which is equivalent to the condition: $k\lambda\delta(M + c\delta) < 1$. This completes the proof for Case 2.

Case 3: $n = -1$.

Letting ϕ denote the PDF for the standard logistic distribution, and $M = \sqrt{1+(c\delta)^2}$, we can express the k^{th} raw moment associated with Q_s, denoted μ_k, as:

$$= \int_{-\infty}^{\infty} \phi(x) \cdot \exp\left(k\lambda\delta\left(Mx - c\sqrt{1+(\delta x)^2} \right) \right) dx.$$

Since $c > 0$, $\delta > 0$, and $\lambda > 0$, then if μ_k exists and is finite, we note that:

$$\underbrace{= \int_{-\infty}^{\infty} \phi(x) \cdot \exp\left(k\lambda\delta\left(Mx - c\left(1+\delta|x|\right)\right)\right) dx}_{LHS} \le \mu_k \le \underbrace{\int_{-\infty}^{\infty} \phi(x) \cdot \exp\left(k\lambda\delta\left(Mx - c\delta x\right)\right) dx}_{RHS}.$$

Now,

$$RHS = \int_{-\infty}^{\infty} \phi(x) \cdot \exp\left(k\lambda\delta\left(M - c\delta\right) x\right) dx.$$

Thus, *RHS* is the k^{th} moment of a log-logistic distribution with shape parameter: $\beta = \dfrac{1}{\lambda\delta\left(M - c\delta\right)}$, which exists if and only if $k\lambda\delta(M - c\delta) < 1$.

Also,

$$LHS = \int_{-\infty}^{0} \phi(x) \cdot \exp\left(k\lambda\delta\left(Mx - c\left(1-\delta x\right)\right)\right) dx + \int_{0}^{\infty} \phi(x) \cdot \exp\left(k\lambda\delta\left(Mx - c\left(1+\delta x\right)\right)\right) dx$$

$$\ge \int_{0}^{\infty} \phi(x) \cdot \exp\left(k\lambda\delta\left(Mx - c\left(1+\delta x\right)\right)\right) dx = \exp\left(-k\lambda\delta c\right) \cdot \int_{0}^{\infty} \phi(x) \cdot \exp\left(k\lambda\delta\left(M - c\delta\right) x\right) dx$$

$$\ge \exp\left(-k\lambda\delta c\right) \cdot \int_{0}^{\infty} \phi(x) \cdot \cosh\left(k\lambda\delta\left(M - c\delta\right) x\right) dx = \frac{\exp\left(-k\lambda\delta c\right)}{2} \cdot \underbrace{\int_{-\infty}^{\infty} \phi(x) \cdot \exp\left(k\lambda\delta\left(M - c\delta\right) x\right) dx}_{LHS'}.$$

Notice that $LHS' = RHS$, and that LHS' is just a constant multiplied by *LHS*. Now, if *RHS* converges, which is equivalent to the condition that $k\lambda\delta(M + c\delta) < 1$, then μ_k exists. Conversely, if μ_k exists, then *LHS* converges, which is equivalent to the condition: $k\lambda\delta(M + c\delta) < 1$. This completes the proof for Case 3, and thus the proof. ■

Appendix F: MATLAB Scripts for J-QPD

This appendix provides the MATLAB function (.m) files for quantile function (QF), cumulative distribution function (CDF), and probability density function (PDF) evaluations for the J-QPD-B, J-QPD-S, and J-QPD-S II distributions. All functions take a $\boldsymbol{\theta}_a$ vector as input, as well as a p (x) value for quantile (CDF and PDF) functions.

J-QPD-B Quantile Function

```
function x = JQPDB(p,low,x50,high,per,lower_bound,upper_bound)
%JQPDB Quantile function of the JQPDB (bounded) distribution.
%   X = JQPDB(p,low,x50,high,per,lower_bound,upper_bound) returns the
%   p-level quantile of the JQPDB distribution with {per,0.5,1-per}-
level
%   quantiles given by {low,x50,high} (respectively) and specified
finite
%   lower and upper bounds given by 'lower_bound' and 'upper_bound'
%   (respectively).
%
%   The size of X is the common size of the input arguments. A scalar
input
%   functions as a constant matrix of the same size as the other
inputs.
%
%   See also JQPDBcdf, JQPDBpdf.
%
%   Reference:
%      [1]     Hadlock, C.C., J.E. Bickel. 2017. Johnson
%      Quantile-Parameterized Distributions. Decision Analysis. 14(1).
%
%   by Christopher C. Hadlock.

T =@(p) norminv(p);
TI =@(x) normcdf(x);

if nargin < 5
    lower_bound=0; % default lower bound is zero
    upper_bound=1; % default upper bound is one
end

% Weed out any out of range parameters or probabilities.
okAB = (lower_bound < low & low < x50 & x50 < high & high < upper_bound
& per > 0 & per < 0.5);
k = (okAB & (0 <= p & p <= 1));
allOK = all(k(:));

% Fill in NaNs for out of range cases.
```

```
if ~allOK
    if isa(p,'single') || isa(low,'single') || isa(x50,'single') ||
isa(high,'single') || isa(per,'single') || isa(lower_bound,'single') ||
isa(upper_bound,'single')
       x = NaN(size(k),'single');
    else
       x = NaN(size(k));
    end

    % Remove the out of range cases.  If there's nothing remaining,
return.
    if any(k(:))
        if numel(p) > 1, p = p(k); end
        if numel(low) > 1, low = low(k); end
        if numel(x50) > 1, x50 = x50(k); end
        if numel(high) > 1, high = high(k); end
        if numel(per) > 1, per = per(k); end
        if numel(lower_bound) > 1, lower_bound = lower_bound(k); end
        if numel(upper_bound) > 1, upper_bound = upper_bound(k); end
    else
        return;
    end
end
%-----JQPDB parameters-----%
lb=lower_bound;
ub=upper_bound;

c=T(1-per); % a constant

L=T((low-lb)./(ub-lb));
B=T((x50-lb)./(ub-lb));
H=T((high-lb)./(ub-lb));

g=sign(L+H-2.*B);
d=(1./c).*acosh((L-H)./(2.*max(B-H,L-B)));
lam=(H-L)./sinh(2.*d.*c);
theta=(1/2).*(L.*(1+g)+H.*(1-g));
%-----Compute x-----%
q=lb+(ub-lb).*TI(lam.*sinh(d.*(T(p)+g.*c))+theta); % general quantile
function
if(g==0) % special case
    q=lb+(ub-lb).*TI(B+((H-L)./(2.*c)).*T(p));
end

if allOK
    x = q;
else
    x(k) = q;
end
```

J-QPD-B CUMULATIVE DISTRIBUTION FUNCTION (CDF)

```
function y = JQPDBcdf(x,low,x50,high,per,lower_bound,upper_bound)
%JQPDBcdf JQPDB (bounded) cumulative distribution function.
%   Y = JQPDBcdf(x,low,x50,high,per,lower_bound,upper_bound) returns
the
%   cumulative probability of the JQPDB distribution with
%   {per,0.5,1-per}-level quantiles given by {low,x50,high}
(respectively)
%   and specified finite lower and upper bounds given by 'lower_bound'
and
%   'upper_bound'(respectively) at "x".
%
%   The size of X is the common size of the input arguments. A scalar
input
%   functions as a constant matrix of the same size as the other
inputs.
%
%   See also JQPDB, JQPDBpdf.
%
%   Reference:
%      [1]     Hadlock, C.C., J.E. Bickel. 2017. Johnson
%      Quantile-Parameterized Distributions. Decision Analysis. 14(1).
%
%   by Christopher C. Hadlock.

T =@(p) norminv(p);
TI =@(x) normcdf(x);

if nargin < 5
    lower_bound=0; % default lower bound is zero
    upper_bound=1; % default upper bound is one
end

% Weed out any out of range parameters or probabilities.
okAB = (lower_bound < low & low < x50 & x50 < high & high < upper_bound
& per > 0 & per < 0.5);
k = (okAB & (lower_bound <= x & x <= upper_bound));
allOK = all(k(:));

% Fill in NaNs for out of range cases.
if ~allOK
    if isa(x,'single') || isa(low,'single') || isa(x50,'single') ||
isa(high,'single') || isa(per,'single') || isa(lower_bound,'single') ||
isa(upper_bound,'single')
       y = NaN(size(k),'single');
    else
       y = NaN(size(k));
    end
    y(okAB & x < lower_bound) = 0;
    y(okAB & x > upper_bound) = 1;
```

```
    % Remove the out of range cases.  If there's nothing remaining,
return.
    if any(k(:))
        if numel(x) > 1, x = x(k); end
        if numel(low) > 1, low = low(k); end
        if numel(x50) > 1, x50 = x50(k); end
        if numel(high) > 1, high = high(k); end
        if numel(per) > 1, per = per(k); end
        if numel(lower_bound) > 1, lower_bound = lower_bound(k); end
        if numel(upper_bound) > 1, upper_bound = upper_bound(k); end
    else
        return;
    end
end
%-----JQPDB parameters-----%
lb=lower_bound;
ub=upper_bound;

c=T(1-per); % a constant

L=T((low-lb)./(ub-lb));
B=T((x50-lb)./(ub-lb));
H=T((high-lb)./(ub-lb));

g=sign(L+H-2.*B);
d=(1./c).*acosh((L-H)./(2.*max(B-H,L-B)));
lam=(H-L)./sinh(2.*d.*c);
theta=(1/2).*(L.*(1+g)+H.*(1-g));
%-----Compute y-----%
f=TI(-g.*c+(1./d).*asinh((1./lam).*(-theta+T((x-lb)./(ub-lb)))));
if(g==0) % special case
    f=TI((2.*c./(H-L)).*(-B+T((x-lb)./(ub-lb))));
end

% Broadcast the values to the correct place if need be.
if allOK
    y = f;
else
    y(k) = f;
end
```

J-QPD-B Probability Density Function (PDF)

```
function y = JQPDBpdf(x,low,x50,high,per,lower_bound,upper_bound)
%%JQPDBpdf JQPDB (bounded) probability density function.
%   Y = JQPDBpdf(x,low,x50,high,per,lower_bound,upper_bound) returns
the
%   probability density of the JQPDB distribution with
%   {per,0.5,1-per}-level quantiles given by {low,x50,high}
(respectively)
%   and specified finite lower and upper bounds given by 'lower_bound'
and
```

```
%   'upper_bound'(respectively) at "x".
%
%   The size of X is the common size of the input arguments. A scalar
input
%   functions as a constant matrix of the same size as the other
inputs.
%
%   See also JQPDB, JQPDBcdf.
%
%   Reference:
%      [1]     Hadlock, C.C., J.E. Bickel. 2017. Johnson
%      Quantile-Parameterized Distributions. Decision Analysis. 14(1).
%
%   by Christopher C. Hadlock.

T =@(p) norminv(p);
ti =@(x) normpdf(x);

if nargin < 5
    lower_bound=0; % default lower bound is zero
    upper_bound=1; % default upper bound is one
end

% Weed out any out of range parameters or probabilities.
okAB = (lower_bound < low & low < x50 & x50 < high & high < upper_bound
& per > 0 & per < 0.5);
k = (okAB & (lower_bound <= x & x <= upper_bound));
allOK = all(k(:));

% Fill in NaNs for out of range cases.
if ~allOK
    if isa(x,'single') || isa(low,'single') || isa(x50,'single') ||
isa(high,'single') || isa(per,'single') || isa(lower_bound,'single') ||
isa(upper_bound,'single')
       y = NaN(size(k),'single');
    else
       y = NaN(size(k));
    end
    y(okAB & x < lower_bound) = 0;
    y(okAB & x > upper_bound) = 0;

    % Remove the out of range cases.  If there's nothing remaining,
return.
    if any(k(:))
        if numel(x) > 1, x = x(k); end
        if numel(low) > 1, low = low(k); end
        if numel(x50) > 1, x50 = x50(k); end
        if numel(high) > 1, high = high(k); end
        if numel(per) > 1, per = per(k); end
        if numel(lower_bound) > 1, lower_bound = lower_bound(k); end
        if numel(upper_bound) > 1, upper_bound = upper_bound(k); end
    else
```

```
        return;
    end
end
%-----JQPDB parameters-----%
lb=lower_bound;
ub=upper_bound;

c=T(1-per); % a constant

L=T((low-lb)./(ub-lb));
B=T((x50-lb)./(ub-lb));
H=T((high-lb)./(ub-lb));

g=sign(L+H-2.*B);
d=(1./c).*acosh((L-H)./(2.*max(B-H,L-B)));
lam=(H-L)./sinh(2.*d.*c);
theta=(1/2).*(L.*(1+g)+H.*(1-g));
%-----Compute y-----%
f=(1./d).*(1./(ub-lb)).*ti(-g.*c+(1./d).*asinh((1./lam).*(-theta+T((x-
lb)./(ub-lb))))).*(1./ti(T((x-lb)./(ub-lb)))./sqrt((lam.^2)+((-
theta+T((x-lb)./(ub-lb))).^2));
if(g==0) % special case
    f=((2.*c)./((H-L).*(ub-lb))).*ti((2.*c./(H-L)).*(-B+T((x-lb)./(ub-
lb)))).*(ti(T((x-lb)./(ub-lb))));
end

% Broadcast the values to the correct place if need be.
if allOK
    y = f;
else
    y(k) = f;
end
```

J-QPD-S Quantile Function

```
function x = JQPDS(p,low,x50,high,per,lower_bound)
%JQPDS Quantile function of the JQPDS (semi-bounded) distribution.
%   X = JQPDS(p,low,x50,high,per,lower_bound,upper_bound) returns the
%   p-level quantile of the JQPDS distribution with {per,0.5,1-per}-
level
%   quantiles given by {low,x50,high} (respectively) and specified
finite
%   lower bound given by 'lower_bound'.
%
%   The size of X is the common size of the input arguments. A scalar
input
%   functions as a constant matrix of the same size as the other
inputs.
%
%   See also JQPDScdf, JQPDSpdf.
%
%   Reference:
```

```
%      [1]     Hadlock, C.C., J.E. Bickel. 2017. Johnson
%      Quantile-Parameterized Distributions. Decision Analysis. 14(1).
%
%   by Christopher C. Hadlock.

if nargin < 5
    lower_bound=0; % default lower bound is zero
end

% Weed out any out of range parameters or probabilities.
okAB = (lower_bound < low & low < x50 & x50 < high & per > 0 & per <
0.5);
k = (okAB & (0 <= p & p <= 1));
allOK = all(k(:));

% Fill in NaNs for out of range cases.
if ~allOK
    if isa(p,'single') || isa(low,'single') || isa(x50,'single') ||
isa(high,'single') || isa(per,'single') || isa(lower_bound,'single')
       x = NaN(size(k),'single');
    else
       x = NaN(size(k));
    end

    % Remove the out of range cases.  If there's nothing remaining,
return.
    if any(k(:))
        if numel(p) > 1, p = p(k); end
        if numel(low) > 1, low = low(k); end
        if numel(x50) > 1, x50 = x50(k); end
        if numel(high) > 1, high = high(k); end
        if numel(per) > 1, per = per(k); end
        if numel(lower_bound) > 1, lower_bound = lower_bound(k); end
    else
        return;
    end
end
%-----JQPDS parameters-----%
lb=lower_bound;
c=norminv(1-per); % a constant

L=log(low-lb);
B=log(x50-lb);
H=log(high-lb);

g=sign(L+H-2.*B);
theta=(1./2).*((low-lb).*(1+g)+(high-lb).*(1-g));
d=(1./c).*sinh(acosh((H-L)./(2.*min(B-L,H-B))));
lam=(1./(d.*c)).*min(H-B,B-L);
%-----Compute x-----%
```

```
q=lb+theta.*exp(lam.*sinh(asinh(d.*norminv(p))+asinh(g.*c.*d))); %
general quantile function
if(g==0) % special case - a lognormal distribution
    q=lb+x50.*(s1.^(-norminv(p)./c));
end

% Broadcast the values to the correct place if need be.
if allOK
    x = q;
else
    x(k) = q;
end
```

J-QPD-S Cumulative Distribution Function (CDF)

```
function y = JQPDScdf(x,low,x50,high,per,lower_bound)
%JQPDScdf JQPDS (semi-bounded) cumulative distribution function.
%   Y = JQPDScdf(x,low,x50,high,per,lower_bound) returns the
%   cumulative probability of the JQPDS distribution with
%   {per,0.5,1-per}-level quantiles given by {low,x50,high}
(respectively)
%   and specified finite lower bound given by 'lower_bound' at "x".
%
%   The size of X is the common size of the input arguments. A scalar
input
%   functions as a constant matrix of the same size as the other
inputs.
%
%   See also JQPDS, JQPDSpdf.
%
%   Reference:
%      [1]     Hadlock, C.C., J.E. Bickel. 2017. Johnson
%      Quantile-Parameterized Distributions. Decision Analysis. 14(1).
%
%   by Christopher C. Hadlock.

if nargin < 5
    lower_bound=0; % default lower bound is zero
end

% Weed out any out of range parameters or probabilities.
okAB = (lower_bound < low & low < x50 & x50 < high & per > 0 & per <
0.5);
k = (okAB & (lower_bound <= x));
allOK = all(k(:));

% Fill in NaNs for out of range cases.
if ~allOK
    if isa(x,'single') || isa(low,'single') || isa(x50,'single') ||
isa(high,'single') || isa(per,'single') || isa(lower_bound,'single')
       y = NaN(size(k),'single');
```

```
    else
       y = NaN(size(k));
    end
    y(okAB & x < lower_bound) = 0;

    % Remove the out of range cases.  If there's nothing remaining,
return.
    if any(k(:))
        if numel(x) > 1, x = x(k); end
        if numel(low) > 1, low = low(k); end
        if numel(x50) > 1, x50 = x50(k); end
        if numel(high) > 1, high = high(k); end
        if numel(per) > 1, per = per(k); end
        if numel(lower_bound) > 1, lower_bound = lower_bound(k); end
    else
        return;
    end
end
%-----JQPDS parameters-----%
lb=lower_bound;
c=norminv(1-per); % a constant
L=log(low-lb);
B=log(x50-lb);
H=log(high-lb);

g=sign(L+H-2.*B);
theta=(1./2).*((low-lb).*(1+g)+(high-lb).*(1-g));
d=(1./c).*sinh(acosh((H-L)./(2.*min(B-L,H-B))));
lam=(1./(d.*c)).*min(H-B,B-L);
%-----Compute y-----%
f=normcdf((1./(lam.*d)).*(sqrt(1+((c.*d).^2)).*log((x-lb)./theta)-
g.*c.*d.*sqrt((lam.^2)+((log((x-lb)./theta)).^2))));
if(g==0) % special case - a lognormal distribution
    f=normcdf((-c./log(s1)).*log((x-lb)./x50));
end
f(x==lb)=0;
f(x==inf)=1;
% Broadcast the values to the correct place if need be.
if allOK
    y = f;
else
    y(k) = f;
end
```

J-QPD-S Probability Density Function (PDF)

```
function y = JQPDSpdf(x,low,x50,high,per,lower_bound)
%%JQPDSpdf JQPDS (semi-bounded) probability density function.
%   Y = JQPDSpdf(x,low,x50,high,per,lower_bound) returns the
%   probability density of the JQPDS distribution with
```

```
%   {per,0.5,1-per}-level quantiles given by {low,x50,high}
(respectively)
%   and specified finite lower bound given by 'lower_bound' at "x".
%
%   The size of X is the common size of the input arguments. A scalar
input
%   functions as a constant matrix of the same size as the other
inputs.
%
%   See also JQPDS, JQPDScdf.
%
%   Reference:
%      [1]     Hadlock, C.C., J.E. Bickel. 2017. Johnson
%      Quantile-Parameterized Distributions. Decision Analysis. 14(1).
%
%   by Christopher C. Hadlock.

if nargin < 5
    lower_bound=0; % default lower bound is zero
end

% Weed out any out of range parameters or probabilities.
okAB = (lower_bound < low & low < x50 & x50 < high & per > 0 & per <
0.5);
k = (okAB & (lower_bound <= x));
allOK = all(k(:));

% Fill in NaNs for out of range cases.
if ~allOK
    if isa(x,'single') || isa(low,'single') || isa(x50,'single') ||
isa(high,'single') || isa(per,'single') || isa(lower_bound,'single')
       y = NaN(size(k),'single');
    else
       y = NaN(size(k));
    end
    y(okAB & x < lower_bound) = 0;

    % Remove the out of range cases.  If there's nothing remaining,
return.
    if any(k(:))
        if numel(x) > 1, x = x(k); end
        if numel(low) > 1, low = low(k); end
        if numel(x50) > 1, x50 = x50(k); end
        if numel(high) > 1, high = high(k); end
        if numel(per) > 1, per = per(k); end
        if numel(lower_bound) > 1, lower_bound = lower_bound(k); end
    else
        return;
    end
end
%-----JQPDS parameters-----%
lb=lower_bound;
```

```
c=norminv(1-per); % a constant
L=log(low-lb);
B=log(x50-lb);
H=log(high-lb);

g=sign(L+H-2.*B);
theta=(1./2).*((low-lb).*(1+g)+(high-lb).*(1-g));
d=(1./c).*sinh(acosh((H-L)./(2.*min(B-L,H-B))));
lam=(1./(d.*c)).*min(H-B,B-L);
%-----Compute y-----%
f=(1./(lam.*d)).*(1./(x-lb)).*(sqrt(1+((c.*d).^2))-g.*c.*d.*log((x-
lb)./theta)./sqrt((lam.^2)+((log((x-
lb)./theta)).^2))).*normpdf((1./(lam.*d)).*(sqrt(1+((c.*d).^2)).*log((x
-lb)./theta)-g.*c.*d.*sqrt((lam.^2)+((log((x-lb)./theta)).^2))));
if(g==0) % special case - a lognormal distribution
    f=normpdf((-c./log(s1)).*log((x-lb)./x50));
end

% Broadcast the values to the correct place if need be.
if allOK
    y = f;
else
    y(k) = f;
end
```

J-QPD-S II Quantile Function

```
function x = JQPDS2(p,low,x50,high,per,lower_bound)
%JQPDS2 Quantile function of the JQPDS2 (semi-bounded) distribution.
%   X = JQPDS2(p,low,x50,high,per,lower_bound,upper_bound) returns the
%   p-level quantile of the JQPDS2 distribution with {per,0.5,1-per}-
level
%   quantiles given by {low,x50,high} (respectively) and specified
finite
%   lower bound given by 'lower_bound'.
%
%   The size of X is the common size of the input arguments. A scalar
input
%   functions as a constant matrix of the same size as the other
inputs.
%
%   See also JQPDS2cdf, JQPDS2pdf.
%
%   Reference:
%      [1]     Hadlock, C.C., J.E. Bickel. 2017. Johnson
%      Quantile-Parameterized Distributions. Decision Analysis. 14(1).
%
%   by Christopher C. Hadlock.

if nargin < 5
    lower_bound=0; % default lower bound is zero
end
```

```
% Weed out any out of range parameters or probabilities.
okAB = (lower_bound < low & low < x50 & x50 < high & per > 0 & per <
0.5);
k = (okAB & (0 <= p & p <= 1));
allOK = all(k(:));

% Fill in NaNs for out of range cases.
if ~allOK
    if isa(p,'single') || isa(low,'single') || isa(x50,'single') ||
isa(high,'single') || isa(per,'single') || isa(lower_bound,'single')
       x = NaN(size(k),'single');
    else
       x = NaN(size(k));
    end

    % Remove the out of range cases.  If there's nothing remaining,
return.
    if any(k(:))
        if numel(p) > 1, p = p(k); end
        if numel(low) > 1, low = low(k); end
        if numel(x50) > 1, x50 = x50(k); end
        if numel(high) > 1, high = high(k); end
        if numel(per) > 1, per = per(k); end
        if numel(lower_bound) > 1, lower_bound = lower_bound(k); end
    else
        return;
    end
end
%-----JQPDS2 parameters-----%
lb=lower_bound;
c=norminv(1-per); % a constant

low=low-lb; % re-locate the lower bound to zero
x50=x50-lb; % re-locate the lower bound to zero
high=high-lb; % re-locate the lower bound to zero
s1=x50./high; % first quantile-based shape parameter
s2=low./x50; % second quantile-based shape parameter

g=sign(log(s2./s1));
theta=(1/2).*(low.*(1+g)+high.*(1-g));
d=(1./c).*acosh(log(s1.*s2)./(2.*log(max(s1,s2))));
lam=-log(max(s1,s2))./sinh(d.*c);
%-----Compute x-----%
q=lb+theta.*exp(lam.*sinh(d.*(norminv(p)+g.*c))); % general quantile
function
if(g==0) % special case - a lognormal distribution
    q=lb+x50.*(s1.^(-norminv(p)./c));
end

% Broadcast the values to the correct place if need be.
```

```
if allOK
    x = q;
else
    x(k) = q;
end
```

J-QPD-S II Cumulative Distribution Function (CDF)

```
function y = JQPDS2cdf(x,low,x50,high,per,lower_bound)
%JQPDS2cdf JQPDS2 (semi-bounded) cumulative distribution function.
%   Y = JQPDS2cdf(x,low,x50,high,per,lower_bound) returns the
%   cumulative probability of the JQPDS2 distribution with
%   {per,0.5,1-per}-level quantiles given by {low,x50,high}
(respectively)
%   and specified finite lower bound given by 'lower_bound' at "x".
%
%   The size of X is the common size of the input arguments. A scalar
input
%   functions as a constant matrix of the same size as the other
inputs.
%
%   See also JQPDS2, JQPDS2pdf.
%
%   Reference:
%      [1]     Hadlock, C.C., J.E. Bickel. 2017. Johnson
%      Quantile-Parameterized Distributions. Decision Analysis. 14(1).
%
%   by Christopher C. Hadlock.

if nargin < 5
    lower_bound=0; % default lower bound is zero
end

% Weed out any out of range parameters or probabilities.
okAB = (lower_bound < low & low < x50 & x50 < high & per > 0 & per <
0.5);
k = (okAB & (lower_bound <= x));
allOK = all(k(:));

% Fill in NaNs for out of range cases.
if ~allOK
    if isa(x,'single') || isa(low,'single') || isa(x50,'single') ||
isa(high,'single') || isa(per,'single') || isa(lower_bound,'single')
       y = NaN(size(k),'single');
    else
       y = NaN(size(k));
    end
    y(okAB & x < lower_bound) = 0;

    % Remove the out of range cases.  If there's nothing remaining,
return.
    if any(k(:))
```

```
        if numel(x) > 1, x = x(k); end
        if numel(low) > 1, low = low(k); end
        if numel(x50) > 1, x50 = x50(k); end
        if numel(high) > 1, high = high(k); end
        if numel(per) > 1, per = per(k); end
        if numel(lower_bound) > 1, lower_bound = lower_bound(k); end
    else
        return;
    end
end
%-----JQPDS2 parameters-----%
lb=lower_bound;
c=norminv(1-per); % a constant
low=low-lb; % re-locate the lower bound to zero
x50=x50-lb; % re-locate the lower bound to zero
high=high-lb; % re-locate the lower bound to zero
s1=x50./high; % first quantile-based shape parameter
s2=low./x50; % second quantile-based shape parameter
g=sign(log(s2./s1));
theta=(1./2).*(low.*(1+g)+high.*(1-g));
d=(1./c).*acosh(log(s1.*s2)./(2.*log(max(s1,s2))));
lam=-log(max(s1,s2))./sinh(d.*c);
%-----Compute y-----%
f=normcdf((1./d).*asinh((1./lam).*log((x-lb)./theta))-g.*c);
if(g==0) % special case - a lognormal distribution
    f=normcdf((-c./log(s1)).*log((x-lb)./x50));
end
f(x==lb)=0;
% Broadcast the values to the correct place if need be.
if allOK
    y = f;
else
    y(k) = f;
end
```

J-QPD-S II Probability Density Function (PDF)

```
function y = JQPDS2pdf(x,low,x50,high,per,lower_bound)
%%JQPDS2pdf JQPDS2 (semi-bounded) probability density function.
%   Y = JQPDS2pdf(x,low,x50,high,per,lower_bound) returns the
%   probability density of the JQPDS2 distribution with
%   {per,0.5,1-per}-level quantiles given by {low,x50,high}
(respectively)
%   and specified finite lower bound given by 'lower_bound' at "x".
%
%   The size of X is the common size of the input arguments. A scalar
input
%   functions as a constant matrix of the same size as the other
inputs.
%
%   See also JQPDS2, JQPDS2cdf.
%
%   Reference:
```

```
%       [1]     Hadlock, C.C., J.E. Bickel. 2017. Johnson
%       Quantile-Parameterized Distributions. Decision Analysis. 14(1).
%
%   by Christopher C. Hadlock.

if nargin < 5
    lower_bound=0; % default lower bound is zero
end

% Weed out any out of range parameters or probabilities.
okAB = (lower_bound < low & low < x50 & x50 < high & per > 0 & per <
0.5);
k = (okAB & (lower_bound <= x));
allOK = all(k(:));

% Fill in NaNs for out of range cases.
if ~allOK
    if isa(x,'single') || isa(low,'single') || isa(x50,'single') ||
isa(high,'single') || isa(per,'single') || isa(lower_bound,'single')
       y = NaN(size(k),'single');
    else
       y = NaN(size(k));
    end
    y(okAB & x < lower_bound) = 0;

    % Remove the out of range cases.  If there's nothing remaining,
return.
    if any(k(:))
        if numel(x) > 1, x = x(k); end
        if numel(low) > 1, low = low(k); end
        if numel(x50) > 1, x50 = x50(k); end
        if numel(high) > 1, high = high(k); end
        if numel(per) > 1, per = per(k); end
        if numel(lower_bound) > 1, lower_bound = lower_bound(k); end
    else
        return;
    end
end
%-----JQPDS2 parameters-----%
lb=lower_bound;
c=norminv(1-per); % a constant
low=low-lb; % re-locate the lower bound to zero
x50=x50-lb; % re-locate the lower bound to zero
high=high-lb; % re-locate the lower bound to zero
s1=x50./high; % first quantile-based shape parameter
s2=low./x50; % second quantile-based shape parameter
g=sign(log(s2./s1));
theta=(1/2).*(low.*(1+g)+high.*(1-g));
d=(1./c).*acosh(log(s1.*s2)./(2.*log(max(s1,s2))));
lam=-log(max(s1,s2))/sinh(d.*c);
%-----Compute y-----%
```

```
f=(1./d).*normpdf((1./d).*asinh((1./lam).*log((x-lb)./theta))-
g.*c).*(((((1./lam).*log((x-lb)./theta)).^2)+1).^(-0.5)).*(1./((x-
lb).*lam));
if(g==0) % special case - a lognormal distribution
    f=normpdf((-c./log(s1)).*log((x-lb)./x50));
end

% Broadcast the values to the correct place if need be.
if allOK
    y = f;
else
    y(k) = f;
end
```

References

Abbas, A.E. 2003a. Entropy Methods for Univariate Distributions in Decision Analysis. *Bayesian Inference and Maximum Entropy Methods in Science and Engineering: 22nd International Workshop*, edited by C.J. Williams, American Institute of Physics, College Park, MD, 339 – 349.

Abbas, A.E., D.V. Budescu, H. Yu, R. Haggerty. 2008. A Comparison of Two Probability Encoding Methods: Fixed Probability vs. Fixed Variable Values. *Decision Analysis* **54**(4) 190-202.

Abbas, A.E. 2003b. Entropy Methods in Decision Analysis. Ph.D. dissertation, Stanford University.

Aitchison, J., S.M. Shen. 1980. Logistic-Normal Distributions: Some Properties and Uses. *Biometrika* **67**(2) 261-272.

Balakrishnan, N. 1992. *Handbook of the Logistic Distribution*. Marcel Dekker, New York.

Bickel, J. E., L. W. Lake, J. Lehman. 2011. Discretization, Simulation, and Swanson's (Inaccurate) Mean. *SPE Economics and Management* **3**(3) 128-140.

Boyd, S., L. Vandenberghe. 2009. *Convex Optimization*. Cambridge University Press, Cambridge, UK.

Bukac, J.L. 1972. Fitting SB Curves Using Symmetrical Percentile Points. *Biometrika*. **59** 688-690.

Burr, I. 1973. Parameters for a General System of Distributions to Match a Grid of α_3 and α_4. *Communications in Statistics* **2**(1) 1-21.

Clemen, Robert T. 2014. *Making Hard Decisions with Decision Tools*, *3rd Edition*. Cengage Learning, 2014. [CengageBrain Bookshelf].

Clemen, R.T., G.W. Fischer, R.L. Winkler. 2000. Assessing Dependence: Some Experimental Results. *Management Science*, **46**(8) 1100-1115.

Clemen, R.T., T. Reilly. 1999. Correlations and Copulas for Decision and Risk Analysis. *Management Science*, **45**(2) 208-224.

Cody, W.J. 1969. Rational Chebyshev Approximations for the Error Function. *Mathematics of Computation*, **23**(107) 631-637.

Dagum, C. 1977. A New Model of Personal Income Distribution: Specification and Estimation. *Economie Appliquees* **30** 413-437.

Darling, D.A. 1957. The Kolmogorov-Smirnov, Cramer-von Mises Tests. *The Annals of Mathematical Statistics*, 28(4) 823-1098.

Eglajs, V., P. Audze. 1977. New Approach to the Design of Multifactor Experiments. Problems of Dynamics and Strengths. Riga: Zinatne Publishing House: 35 104-107.

Garthwaite, P.H., J.B. Kadane, A. O'Hagan. 2005. Statistical Methods for Eliciting Probability Distributions. *Journal of the American Statistical Association* **100**(470) 680-701.

Gentle, J.E. *Computational Statistics*. New York: Springer, 2009.

Gilchrist, W. *Statistical Modelling with Quantile Functions.* CRC Press, 2000.

Hadlock, C.C., J.E. Bickel. 2017. Johnson Quantile-Parameterized Distributions. *Decision Analysis* **14**(1) 35-64.

Hammond, R.K., J.E. Bickel. 2017. Discretization Precision and Assessment Error. *Decision Analysis* **14**(1) 21-34.

Hammond, R.K., J. E. Bickel. 2013a. Reexamining Discrete Approximations to Continuous Distributions. *Decision Analysis* **10**(1) 6-25.

Hammond, R.K., J. E. Bickel. 2013b. Approximating Continuous Probability Distributions Using the 10th, 50th, and 90th Percentiles. *The Engineering Economist* **58**(3) 189-208.

Hammond, R.K. 2014. Discrete Approximations to Continuous Distributions in Decision Analysis. Ph.D. dissertation, The University of Texas at Austin.

Herrerias-Velasco, J.M., R. Herrerias-Pleguezuelo, J.R. Van Dorp. 2009. The Generalized Two-Sided Power Distribution. *Journal of Applied Statistics* **36**(5) 573-587.

Howard, R.A. 1988a. Decision Analysis: Practice and Promise. *Management Science*, **34**(6) 679-695.

Howard, R.A. 1988b. Uncertainty about Probability: A Decision Analysis Perspective. *Risk Analysis*, **8**(1) 91-98.

Howard, R.A., J.E. Matheson. 1981. "Influence diagrams", in Readings on the Principles and Applications of Decision Analysis, eds. R.A. Howard and J.E. Matheson, Vol. II (1984), Menlo Park CA: Strategic Decisions Group.

Hurst, A., G.C. Brown, R.I. Swanson. 2000. Swanson's 30-40-30 Rule. *AAPG Bulletin* **84**(12) 1883-1891.

Iman, R.L., J.M. Davenport, D.K. Zeigler. 1980. Latin Hypercube Sampling (A Program User's Guide). Technical Report. Sandia National Laboratories, Albuquerque, New Mexico.

Iman, R.L., J.C. Helton, J.E. Campbell. 1981. An Approach to Sensitivity Analysis of Computer Models, Part 1. Introduction, Input Variable Selection and Preliminary Variable Assessment. *Journal of Quality Technology*. **13**(3) 174-183.

Jaynes, E.T. 1968. Prior Probabilities. *IEEE Transactions on Systems Science and Cybernetics,* **4**(3) 227-241.

Johnson, N. L. 1949. Systems of Frequency Curves Generated by Methods of Translation. *Biometrika* **36**(149) 78-82.

Johnson, N.L., S. Kotz, N. Balakrishnan. 1994. Continuous Univariate Distributions. Volume 1, Volume 2. John Wiley & Sons. New York.

Jones, M. C., A. Pewsey. 2009. Sinh-arcsinh Distributions. *Biometrika* **96**, 761-780.

Keefer, D.L. 1995. Facilities Evaluation Under Uncertainty: Pricing a Refinery. *Interfaces*. **25**(6) 57-66.

Keefer, D.L., S.E. Bodily. 1983. Three-Point Approximations for Continuous Random Variables. *Management Science*. **29**(5) 595-609.

Keelin, T. W., B. W. Powley. 2011. Quantile-Parameterized Distributions. *Decision Analysis* **8**(3) 206-219.

Keelin, T.W. 2016. The Metalog Distributions. *Decision Analysis* **13**(4) 243-277.

Keeney, R.L. 1987. An Analysis of the Portfolio of Sites to Characterize for Selecting a Nuclear Repository. *Risk Analysis* **7**(2) 195-218.

Kotz, S., J.R. Van Dorp. 2006. A Novel Method for Fitting Unimodal Continuous Distributions on a Bounded Domain Utilizing Expert Judgment Estimates. *IIE Transactions*. **38**(5) 421-436.

Kruskal, W. 1958. Ordinal Measures of Association. *Journal of the American Statistical Association*. 53 814-861.

Kullback, S., R.A. Leibler. 1951. On Information and Sufficiency. *Annals of Mathematical Statistics* **22**(1) 79-86.

Kullback, S. 1959. *Information Theory and Statistics*. John Wiley & Sons.

Kumaraswamy, P. 1980. A Generalized Probability Density Function for Double-Bounded Random Processes. Journal of Hydrology, **46**(1-2) 79-88.

Mage, D.T. 1980. An Explicit Solution for SB Parameters Using Four Percentile Points. *Technometrics*, **22** 247-251.

Matheson, J.E., R.L. Winkler. 1976. Scoring Rules for Continuous Probability Distributions. *Management Science*, **22**(10) 1087-1096.

Matheson, J.E., R.A. Howard. 1968. *An Introduction to Decision Analysis*, Stanford Research Institute, Menlo Park, California.

McKay, M.D., R.J. Beckman, W.J. Conover. 1979. A Comparison of Three Methods for Selecting Values of Input Variables in the Analysis of Output from a Computer Code. *Technometrics*, **21**(2) 239-245.

McNamee, P., J, Celona. 1990. Decision Analysis with Supertree, 2nd Edition. (The Scientific Press, South San Francisco).

Mead, R. 1965. A Generalised Logit-Normal Distribution. *Biometrics*. **21**(3) 721-732.

Merkhofer, M.W. 1987. Quantifying Judgmental Uncertainty: Methodology, Experiences, and Insights. *IEEE Transactions on Systems, Man, and Cybernetics* **17**(5) 741-752.

Miller, A., T, Rice. 1983. Discrete Approximations of Probability Distributions. *Management Science*, **29**(3) 352-362.

Moors, J.J.A. 1988. A Quantile Alternative for Kurtosis. *The Statistician* **37** 25-32.

Moors, J.J.A., R. Th. A. Wagemakers, V.M.J. Coenen, R.M.J. Heuts, M.J.B.T. Janssens. 1996. Characterizing Systems of Distributions by Quantile Measures. *Statistica Neerlandica* **50**(3) 417-430.

Mudholkar, G.S., D.K. Srivastava. 1993. Exponentiated Weibull Family for Analyzing Bathtub Failure-Rate Data. *IEEE Transactions on Reliability* **42**(2) 299-302.

Ord, J.K. 1972. *Families of Frequency Distributions*. Volume 30.

Parzen, E. 1979. Nonparametric Statistical Data Modeling. *Philosophical Journal of the American Statistical Association* **74**(365) 105-121.

Pearson, E., J.W. Tukey. 1965. Approximate Means and Standard Deviations Based on Distances between Percentage Points of Frequency Curves. *Biometrika*, **52**(3) 533-546.

Pearson, K. 1895. Contributions to the Mathematical Theory of Evolution, II: Skew Variation in Homogeneous Material. *Philosophical Transactions of the Royal Society of London* **186** 343-414.

Pearson, K. 1901. Mathematical Contributions to the Theory of Evolution. X. Supplement to a Memoir on Skew Variation. *Philosophical Transactions of the Royal Society of London* **197** 443-459.

Pearson, K. 1916. Mathematical Contributions to the Theory of Evolution. XIX. Second Supplement to a Memoir on Skew Variation. *Philosophical Transactions of the Royal Society of London* **216** 429-457.

Pflug, G.C. 2001. Scenario Tree Generation for Multi-Period Financial Optimization by Optimal Discretization. *Mathematical Programming* **89**(2) 251-271.

Powley, B.W. 2013. Quantile Function Methods for Decision Analysis. Ph.D. dissertation, Stanford University.

Reilly, T. 1998. Sensitivity Analysis for Dependent Variables. Draft, Babson College.

Runde, A.S. 1997. Estimating Distributions, Moments, and Discrete Approximations of a Continuous Random Variable Using Hermite Tension Splines. Ph.D. dissertation, University of Oregon.

Selvidge, J.E. 1980. Assessing the Extremes of Probability Distributions by the Fractile Method. *Decision Sci.* **11**(3) 493-502.

Singh, S., G. Maddala. 1976. A Function for the Size Distribution of Incomes. *Econometrica.* **44**(5) 963-970.

Smith, J.E. 1990. Moment Methods for Decision Analysis. Ph.D. dissertation, Stanford University.

Smith, J.E. 1993. Moment Methods for Decision Analysis. *Management Science*, **39**(3) 340-358.

Shachter, R.D. 1986. "Evaluating influence diagrams". *Operations Research*. **34**(6): 871–882.

Shachter, R.D. 1988. "Probabilistic inference and influence diagrams". *Operations Research*. **36**(4): 589–604.

Spetzler, C., C.A.S. Staël von Holstein. 1975. Probability Encoding in Decision Analysis. *Management Science*, **22**(3) 340-358.

Stonebraker, J.S. 2002. How Bayer Makes Decisions to Develop New Drugs. *Interfaces* 32(6) 77-90.

Stonebraker, J.S., D.L. Keefer. 2009. Modeling Potential Demand for Supply-Constrained Drugs: A New Hemophilia Drug at Bayer Biological Products. *Operations Research*. **57**(1) 19-31.

Tadikamalla, P.R., N.L. Johnson. 1982. Systems of Frequency Curves Generated by Transformations of Logistic Variables. *Biometrika* **69**(2) 461-465.

Tadikamalla, P.R. 1980. A Look at the Burr and Related Distributions. *International Statistical Review* **48**(3) 337-344.

Tauchen, G., R. Hussey. 1991. Quadrature-based Methods for Obtaining Approximate Solutions to Nonlinear Asset Pricing Models. *Econometrics* **59**(2) 371-396.

Tversky, A., D. Kahneman. 1974. Judgment Under Uncertainty: Heuristics and Biases. *Science*. **185**(4157) 1124-1131.

Upadhyay, R.R., O.A. Ezekoye. 2008. Treatment of Design Fire Uncertainty Using Quadrature Method of Moments. Fire Safety Journal **43**(2) 127-139.

Van Dorp, J.R., S. Kotz. 2002a. A Novel Extension of the Triangular Distribution and its Parameter Estimation. *The Statistician* **51**(1) 63-79.

Van Dorp, J.R., S. Kotz. 2002b. The Standard Two-Sided Power Distribution and its Properties: with Applications in Financial Engineering. *The American Statistician* **56**(2) 90-99.

Vander Wielen, M.J., R.J. Vander Wielen. 2015. The General Segmented Distribution. *Communications in Statistics – Theory and Methods* **44**(10) 1994-2009.

Wallsten, T.S., D.V. Budescu. 1983. State of the Art Encoding Subjective Probabilities: A Psychological and Psychometric Review. *Management Science*, **29**(2) 151-173.

Wang, T., J.S. Dyer. 2012. A Copula-Based Approach to Modeling Dependence in Decision Trees. *Operations Research* **60**(1) 225-242.

Williger, B.J.A. 2009. Practical Portfolio Simulation: Determining the Precision of a Probability Distribution of a Large Asset Portfolio when the Underlying Project Economics are Captured by a Small Number of Discrete Scenarios, SPE Annual Technical Conference and Exhibition. Society of Petroleum Engineers, New Orleans, LA.

Zaino, N.A., J.R. D'Errico. 1989. Optimal Discrete Approximations for Continuous Outcomes with Applications in Decision and Risk Analysis. *Journal of the Operational Research Society*. **40**(4) 379-388.